Title
Extracellular iron acquisition and iron-regulated protein expression in mycobacteria

Permalink
https://escholarship.org/uc/item/4b13s6j8

Author
Wong, Diane Kristin

Publication Date
1998

Peer reviewed|Thesis/dissertation

Extracellular Iron Acquisition and Iron-Regulated Protein

Expression in Mycobacteria

by

Diane Kristin Wong

DISSERTATION

Submitted in partial satisfaction of the requirements for the degree of
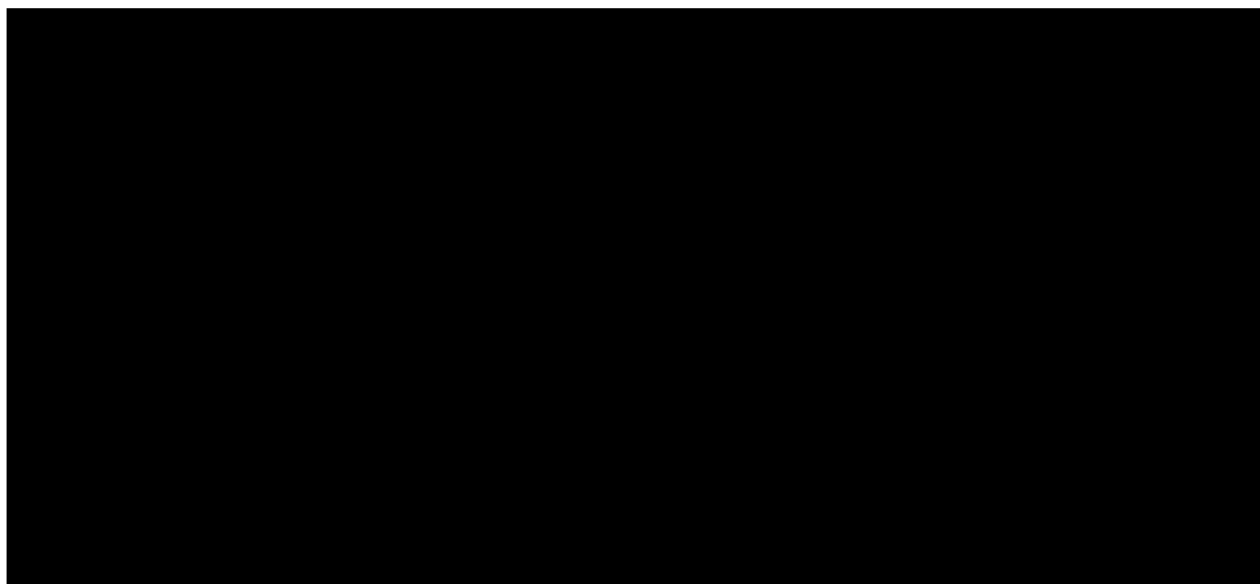
DOCTOR OF PHILOSOPHY

in

Pharmaceutical Chemistry

in the

GRADUATE DIVISION

of the

UNIVERSITY OF CALIFORNIA SAN FRANCISCO

Acknowledgements

I would like to thank my advisor Professor Bradford Gibson for his advice and support that he gave me throughout my graduate career. I also want to extend a special thanks to Dr. Nancy Phillips for her help, support, and patience throughout the years, showing me by example how to be a good scientist. I would also like to thank Dr. Michael Tullius, Nicole Samuels, Jeffrey Engstrom, and Dr. Willie Melaugh for their friendship and support over the last 5 years.

I would also like to thank our collaborators, Dr. Marcus Horwitz, Dr. Jovana Gobin, and Dr. Bai-yu Lee. I am indebted to Jovana and Bai-yu for providing the many samples over the years and to Marcus for his advice and guidance throughout this research project.

I would like to thank the members of the UCSF Mass Spectrometry Facility. I am especially grateful to Fred Walls for the endless hours that we have spent analyzing samples on the Concept mass spectrometer and to Dave Maltby for his help and expertise in running the instruments. I would also like to acknowledge Perseptive Biosystems for the generous loan of the Voyager and Voyager-DE mass spectrometers and to thank Dr. Arnold Falick for his many helpful discussions.

Lastly I would like to thank my parents for their unending love and support.

Collaborations

Chapter 2 is largely based on the following papers: Gobin, J., Moore, C.H., Reeves, J. Jr., Wong, D.K., Gibson, B.W., and Horwitz, M.A. (1995) Iron acquisition by *Mycobacterium tuberculosis*: Isolation and characterization of a family of iron-binding exochelins. *Proc. Natl. Acad. Sci. USA* 92:5189-5193; Wong, D.K., Gobin, J., Horwitz, M.A., and Gibson, B.W. (1996) Characterization of exochelins of *Mycobacterium avium*: evidence for saturated and unsaturated and for acid and ester forms. *J. Bacteriol.* 178(21): 6394-6398; and Gobin, J., Wong, D.K., Gibson, B.W., and Horwitz, M.A. (1998) Characterization of exochelins of *Mycobacterium bovis* and *M. bovis* BCG (submitted). The isolation and purification of the exochelins from *M. tuberculosis*, *M. avium*, and *M. bovis* were performed at UCLA by Dr. Jovana Gobin. The preliminary mass spectrometric characterization of the *M. tuberculosis* exochelins was carried out by Dr. Chris Moore, while on sabbatical in Professor Gibson's laboratory. The mass spectrometric characterization of the *M. tuberculosis* exochelin R_1 alkyl chain and the *M. avium* and *M. bovis* exochelins was performed by myself.

The NMR work performed in Chapter 3 was done with the aid of Dr. Nancy Phillips in my laboratory. The synthetic desferri-exochelin sample was generously provided by Dr. Marcus Horwitz.

Chapter 4 is work being done in collaboration with Dr. Mark Grillo. Dr. Grillo performed the isolation of the rat liver microsomes and rat hepatocytes and was also instrumental in the experimental design. The HPLC analysis and mass spectrometric analysis was performed by myself.

Chapter 5 is based largely on a paper that has been submitted for publication to Infection and Immunity: Wong, D.K., Lee, B.Y., Horwitz, M.A., and Gibson, B.W. Identification of Fur, aconitase, and other proteins expressed by *Mycobacterium tuberculosis* under conditions of low and high iron by combined two dimensional gel

electrophoresis and mass spectrometry. Dr. Bai-Yu Lee grew the *M. tuberculsois* and performed the 2-D gel electrophoresis at UCLA. The in-gel digestions, mass spectrometric analysis, and protein identification were carried out at UCSF by myself.

ABSTRACT

Mycobacterium tuberculosis is the primary causative agent of tuberculosis. The capacity of mycobacteria to infect the host appears to be closely related to its ability to acquire iron since serum containing poorly saturated transferrin, such as human serum, is tuberculostatic. This tuberculostatic effect is neutralized by the addition of iron (Kochan 1969, Kochan et al 1971).

Mycobacteria have been shown to produce small water-soluble siderophores called exochelins which are thought to bind iron in the extracellular aqueous environment and deliver it back to the mycobacteria. In an effort to learn more about the mycobacterial iron acquisition system, the exochelins from numerous species of mycobacteria (including *M. tuberculosis*, *M. avium*, and *M. bovis*) have been isolated, purified, and characterized by mass spectrometry. The exochelins were found to be a family of iron-binding molecules which all share a common core structure – including 3 amino acid moieties (2 N-hydroxylysines and 1 serine or threonine). The structure of the *M. tuberculosis* exochelins was confirmed by nuclear magnetic resonance studies. In addition, in an effort to learn more about the biotransformation of exochelins *in vivo*, the metabolism of exochelins in an *in vitro* model was investigated. Several dufferent hydroxylated forms of exochelins were identified.

To learn more about the role of iron in the physiology of *M. tuberculosis*, we have been investigating iron-regulated proteins in *M. tuberculosis* grown under conditions of high and low iron. Proteins in cellular extracts from *M. tuberculosis* Erdman strain grown under low (1 mM) and high (70 mM) iron conditions were separated by 2-D polyacrylamide gel electrophoresis, which allowed high resolution separation of several hundred proteins, as visualized by Coomassie staining. The expression of at least 15 proteins was induced and 12 proteins decreased by low iron. In-gel trypsin digestion , mass spectrometric analysis, and database searching on these proteins allowed for the

identification of 10 iron-regulated proteins, including Fur and aconitase proteins, both of which are known to be regulated by iron in other bacterial systems.

List of Abbreviations

BCG	Bacille Calmette-Guérin
CID	collision-induced dissociation
COSY	2-D J-correlated spectroscopy
1-D	one-dimensional
2-D	two-dimensional
Da	daltons
DMSO	dimelthyl sulfoxide
DQF-COSY	double-quantum filtered COSY
EDTA	ethylenediaminetetraacetic acid
EF-Tu	elongation factor Tu
ESI-MS	electrospray ionization mass spectrometry
exochelin MN	*Mycobacterium neoaurum* exochelin
exochelin MS	*Mycobacterium smegmatis* exochelin
Fur	ferric - uptake regulator
GC/MS	gas chromatography/mass spectrometry
HOHAHA	2-D homonuclear Hartmann-Hahn spectroscopy
HPLC	high-performance liquid chromatography
HSPs	heat shock proteins
IRE-BP	iron-responsive element binding protein
IREPs	iron-regulated envelope proteins
keV	kilo electron volts
LAM	lipoarabinomannans
LSIMS	liquid secondary ion mass spectrometry
M	molar
$(M+nH)^{n+}$	multiply charged protonated ion
m/z	mass to charge ratio
MALDI	matrix-assisted laser desorption/ionization mass spectrometry
MDR	multidrug-resistant
M_r	molar mass
MS	mass spectrometry
MS/MS	tandem mass spectrometry
NMR	nuclear magnetic resonance spectroscopy
NOE	nuclear Overhauser effect
NOESY	2-D nuclear Overhauser effect spectroscopy
OAA	oxaloacetate
PEP	phosphoenolpyruvate
PEPCK	phosphoenolpyruvate carboxykinase

PPIase	peptidyl-prolyl cis-trans isomerase
PSD	post-source decay
ROESY	2-D rotating-frame Overhauser effect spectroscopy
SCAD	short – chain alcohol dehydrogenase
SDS-PAGE	sodium dodecyl sulfate - polyacrylamide gel electrophoresis
TB	tuberculosis
TDM	trehalose 6,6' - dimycolates
TFA	trifluoroacetic acid
TNF-α	tumor necrosis factor - α
TOF	time-of-flight
UDPGA	uridine 5'-diphosphoglucuronic acid
UTR	untranslated region
UV	ultraviolet light

Table of Contents

List of Tables

List of Figures

Chapter 3

Chapter 4

Chapter 5

Chapter 1: Overview of *M. tuberculosis* pathogenesis and the role of iron in pathogenesis

1.1 History of tuberculosis

The organisms from the genus *Mycobacterium* have plagued populations throughout history. The mycobacterial infections, leprosy and tuberculosis, have been major factors in the morbidity and mortality of the human race since ancient times. Evidence of mycobacterial infection has been found as far back as 4000 B.C. as lesions suggestive of Pott's disease (tuberculosis of the spine) were found in the skeletons of a neolithic man (c. 4000 B.C.) and in Egyptian mummies (3700-1000 B.C.) (Morse et al. 1964; Grange 1989). Skin diseases which are suggestive of leprosy have also been described in ancient medical writings from China (c. 250 B.C.) and India (between 600 and 400 B.C.) (Gupta 1909; Wong and Wu 1932; Grange 1989).

In more recent times, as public health and economic environments improved, mycobacterial diseases have been on the decline. The dramatic decrease of cases from the 1950s to the 1980s was hastened by the development of effective chemotherapeutic agents. However, a resurgence in the number of tuberculosis cases in the late 1980s through the early 1990s has once again brought tuberculosis into the spotlight, since it has reached epidemic proportions in many regions throughout the world, including several American cities. There are many possible reasons for this resurgence. These include a reduction in the amount of mycobacterial research funding, a change in the treatment policies of tuberculosis patients from institutionalization to out-patient treatment which often results in poor patient drug compliance, the subsequent emergence of multidrug-resistant tuberculosis, and the increased risk of mycobacterial infections in HIV-infected individuals.

Tuberculosis is the leading cause of death due to a single infectious agent among adults throughout the world, with more than 3 million deaths attributed to the disease in 1995 (Dolin et al. 1994; WHO 1996). It has been estimated that one-third of the world is infected with *M. tuberculosis* (Bloom and Murray 1992; Young and Duncan 1995). If the present rising trend continues, the incidence of tuberculosis will rise by an additional one-third in the next decade (Dolin et al. 1994; Young and Duncan 1995). As a result of these alarming statistics, the WHO declared tuberculosis to be a global health emergency in 1993 (Dolin et al. 1994; WHO 1996).

In recent years, a third serious disease attributed to mycobacteria has emerged, AIDS-associated disseminated *Mycobacterium avium* infection. Although *M. avium* is a common environmental saprophyte found in soil and groundwater throughout the world (Inderlied et al. 1993; Falkinham 1996), infections due to *M. avium* were rare prior to the early 1980s (Collins 1989). However, *M. avium* infections are currently the most common systemic bacterial infections that occur in AIDS patients in developed nations (Collins 1989; Masur et al. 1989; Inderlied et al. 1993).

1.1.2 The organisms

Mycobacteria are aerobic, gram-positive, acid-fast, non-motile, and nonspore-forming bacillli. They are commonly of environmental origin and include pathogenic, nonpathogenic, and saprophytic species (Carter 1975; Roberts et al. 1991; Hines et al. 1995). The mycobacteria are small, ranging in size from 0.2 to 0.6 x 1.0 to 10.0 μm, with a very high lipid content in their cell walls (Roberts et al. 1991). They have long generation times when compared to more commonly studied bacteria, like *Escherichia coli*. Fast growing species, like *M. smegmatis* and *M. phlei*, form colonies in less than a week. *M. flavescens*, which grows at an intermediate rate, takes 1 to 2 weeks to form colonies. *The slow* growers, including *M. tuberuclosis* which has a doubling time of 16-18 hrs

(Wayne 1977), require 2 to 8 weeks to grow (Hines et al. 1995). The complete *M. tuberculosis* genome has recently been sequenced and found to contain over 4,000 genes (Cole et al. 1998).

1.1.3 Chemotherapy

1.1.3.1 History

Although tuberculosis has been around since ancient times, effective chemotherapy was only discovered in the 1940s and 1950s. The discovery of anti-tuberculosis drugs contributed to a progressive decline in tuberculosis cases until recently. The discovery of streptomycin in 1943 marked the beginning of modern tuberculosis chemotherapy. However, the biggest advance was the introduction of isoniazid in 1952. In the 1950s, the combination of isoniazid, streptomycin, and para-aminosalicylic acid (later replaced by ethambutol) was able to cure 90% of TB patients (Committee 1952). The addition of rifampin (1971) to tuberculosis chemotherapy allowed for a shorter treatment period and increased cure rate (Newman et al. 1974). Collazos *et al.* (Collazos et al. 1995) provides an excellent review of past and present treatment regimens.

1.1.3.2 Current Chemotherapy

Today, the most widely accepted drug regimen for immunocompetent individuals consists of a combination of isoniazid, rifampin, and pyrazinamide daily for 2 months, followed by isoniazid and rifampin daily over the next 4 months (Collazos et al. 1995). The mechainisms of action of some of these drugs are summarized below (Davidson and Hanh 1986; Alford 1990; Van Scoy and Wilkowske 1992). Isoniazid inhibits the biosynthesis of mycolic acids, long chain fatty acids located in the mycobacterial cell wall (Collazos et al. 1995; Johnsson et al. 1995). Rifampin appears to block proteins synthesis

3

by acting on the β-subunit of the DNA-dependent RNA polymerase. Pyrazinamide, a pyrazine analog of nicotinamide, exerts its bactericidal activity only in the intracellular, acidic environment where it can be converted to its active metabolite.

1.1.4 Multidrug-resistant tuberculosis

The emergence of multidrug-resistant (MDR) tuberculosis in the last few years has brought a new urgency to the race for new chemotherapies. It has been reported that MDR tuberculosis, defined as tuberculosis resistant to at least isoniazid and rifampin, was found in 3-19% of all patients (National action plan to combat multidrug- resistant tuberculosis 1992; Frieden et al. 1993; Advisory Council for the Elimination of Tuberculosis 1993; Bloch et al. 1994). MDR tuberculosis has a very poor response to available treatment. In immunocompetent individuals, only 56-88% show a consistent response to chemotherapy and the relative risk of failure of therapy is much greater (80 x) than in other tuberculosis cases (Mitchison and Nunn 1986; Goble et al. 1993; Iseman 1993). The overall mortality rate for these individuals is 37%, with a mortality directly attributable to tuberculosis of 22% (Goble et al. 1993). The pandemic of HIV infection in recent decades has added to the tuberculosis epidemic, as it is strongly associated with MDR tuberculosis. In the early 1990s, it was found that in AIDS patients who are coninfected with MDR tuberculosis, there was a 72-89% mortality rate, with a median survival time of only 4-16 weeks (Edlin et al. 1992; Fischl et al. 1992; Pearson et al. 1992; Barnes and Barrows 1993; Ellner et al. 1993; Frieden et al. 1993; Advisory Council for the Elimination of Tuberculosis 1993).

1.1.5 Mycobacterial infections - pathogenesis

1.1.5.1 Route of entry

The interaction between *M. tuberculosis* and the host's immune response can be thought of as a complex system of positive and negative signaling pathways (Boom 1996). *M. tuberculosis* is a facultative intracellular pathogen which can multiply both intra- and extracellularly. It primarily infects humans, entering the body via inhalation of aerosols, where it then preferentially infects and multiplies within mononuclear phagocytes (Clark-Curtiss 1998). Following inhalation of the aerosolized droplet nuclei (containing between 1-3 bacilli), *M. tuberculosis* enters the alveoli of the lung (Riley et al. 1962; Lurie 1964; Dannenberg and Rook 1994). The bacilli are phagocytized by alveolar macrophages located in the lung tissue. The majority of these bacilli are killed since many of these macrophages are partially activated as a result of constant exposure to inhaled particulate (Dannenberg and Rook 1994; Young and Duncan 1995). However, some bacilli are able to multiply in the alveolar macrophages. When these bacilli are released by the macrophages, they are then phagocytized by other nonactivated macrophages, presumed to be derived from the peripheral blood. The mycobacteria are thought to be ingested by the peripheral blood-derived mononuclear cells via complement receptor and complement component C3-mediated phagocytosis (Schlesinger et al. 1990; Bermudez et al. 1991; Schlesinger and Horwitz 1991). There is additional evidence that *M. avium* and *M. tuberculosis* also bind to the mannosyl-fucosyl and fibronectin receptors on macrophage surfaces and that these receptors also facilitate phagocytosis (Bermudez and Young 1989; Schlesinger et al. 1994). In addition to giving *M. tuberculosis* greater flexibility for cell entry, this ability to use a variety of receptors to mediate entry may also influence the host cell's responses during and immediately after entry (Dannenberg and Rook 1994; Young and Duncan 1995; Schlesinger 1996).

1.1.5.2 Intracellular fate of the mycobacteria - macrophage response

A symbiotic relationship eventually develops between the mycobacteria and the macrophages. If the alveolar macrophages allow the phagosomally enclosed bacilli to grow unrestricted, the bacteria will eventually lyse the macrophage and be taken up by other alveolar macrophages or non-activated macrophages from the peripheral blood (Dannenberg and Rook 1994). These incoming immature and non-activated macrophages readily take up the mycobacteria, but are incapable of inhibiting their growth and the bacilli continue to multiply. The macrophages are not injured by the mycobacteria since the host hasn't yet developed a hypersensivity response. As a result, the number of the bacilli and macrophages in the lesion increases at a logarithmic rate (Dannenberg and Rook 1994). However, this symbiotic relationship ends when the host develops a hypersensitivity or tissue-damaging response and the lesion progresses to caseous necrosis. In this stage, the lesions (tubercles) develop necrotic centers where the host cells have been destroyed by the immune response. The bacteria are subsequently released into the extracellular environment. The bacilli are able to survive in the solid caseous material, but cannot actively multiply in this nonpermissive extracellular environment. It is thought that the anoxic conditions, low pH, and the presence of inhibitory fatty acids contribute to the inhibition of mycobacterial growth (Dannenberg and Rook 1994). If there is a high bacterial load, the lesions can grow increasingly larger. However, if the lesions remain small and the number of bacilli are low, then the tubercles usually regress and the infection is resolved.

In those people with strong cell-mediated, macrophage-activating response, the primary tubercle is walled off and the activated macrophages are able to ingest and destroy any escaping bacilli, arresting the infection. However, in those individuals who do not have a strong macrophage-activating response or if their tissue-damaging response is too strong, the tubercles liquefy and cavities are formed. This liquefied caseous lesion

6

becomes a rich growth medium for the mycobacteria and the bacilli are able to multiply extensively in the extracellular space. The strong tissue-damaging response resulting from the large antigenic load can often result in the rupture of the bronchi walls of the lung, releasing the bacilli and liquefied caseous material into the airways. The bacilli are then transported to other parts of the body and to the environment (Dannenberg and Rook 1994).

In addition, in some infected individuals, even though the infection is arrested, not all of the bacilli are eliminated in the cell-mediated response. In many cases, these individuals may remain disease-free for the rest of their lives. However, if a breakdown in their immune system occurs, the tubercle bacilli may be reactivated and begin to multiply, causing active disease. This breakdown could be the result of many causes, including the natural aging process, stress, and the development of immunosuppressive disease (Clark-Curtiss 1998).

1.1.6 Virulence Determinants of *M. tuberculosis*

In Webster's dictionary, virulence is defined as "the relative infectiousness of a microorganism causing disease." However, virulence is not dependent solely on the pathogen. The genetic and immunologic make-up of the host must also be considered. Virulence is determined by numerous traits that enable the pathogen to exploit host weaknesses and allow it to overcome the host's immune system (Jacobs and Bloom 1994). *M. tuberculosis* is a facultative intracellular pathogen which can infect and multiply within both professional and non-professional phagocytic cells. Little information exists about how the bacilli enters the cells or which virulence factors enable the mycobacteria to survive and multiply within the host cells. These virulence factors can have direct effects on the host cells, including attachment, invasion, and intracellular multiplication. They can also have indirect interactions with the host cells through secreted factors like hemolysin and

7

cytotoxin, which can cause cell lysis (King et al. 1993; Leao et al. 1995; McDonough and Kress 1995). In addition, other mycobacterial products like lipoarabinomannans (LAMs) and heat shock proteins (HSP) can stimulate a host cell immune response (Quinn et al. 1996).

1.1.6.1 Resistance to oxidizing agents

1.1.6.1.1 Resistance to hydrogen peroxide

Studies which compared *M. tuberculosis* strains of high and low virulence showed a strong correlation between virulence and susceptibility to killing by hydrogen peroxide (Mitchison et al. 1963; Nair et al. 1964). This was supported by studies showing peroxide-sensitive *M. tuberculosis* mutants were not able to survive as well as the peroxide-resistant *M. tuberculosis* in infected guinea pigs (Jackett et al. 1981). *katG*, the gene encoding an *M. tuberculosis* catalase has also been shown to be important to virulence. Zhang *et al.* (Zhang et al. 1992) found that deletion of *katG* resulted in peroxide sensitivity in some strains of *M. tuberculosis*. In addition, *katG*, along with *inhA* (a gene involved in the biosynthesis of mycolic acids) were both found to be involved in isoniazid-sensitivity.

1.1.6.1.2 Resistance to other oxidizing agents

Although no clear relationship was detected between virulence and superoxide anion and low pH resistance (Jackett et al. 1978), a mutation in the superoxide dismutase gene has been found in one avirulent strain (Zhang et al. 1992). Nitric oxide (NO) has also been found to be lethal to many microorganisms as it can react with superoxide anion, forming peroxynitrite, eventually producing other bactericidal molecules like singlet oxygen, nitrogen dioxide radical, and hydroxyl radical (Noronha-Dutra et al. 1993).

Although the mycobacterial target of NO is not presently known, studies have shown that virulence of *M. avium* in the mouse (Doi et al. 1993) and *M. tuberculosis* in the guinea pig (O'Brien et al. 1994) coincide with resistance to the bactericidal effects of NO.

1.1.6.2 Attachment and Invasion

There are clear differences between virulent and less virulent strains of *M. tuberculosis* when examining mycobacterial entry and survival in the macrophages. This suggests the involvement of strain-specific factors. Macrophages are able to phagocytize both live and killed *M. tuberculosis*. However, only live bacilli are able to enter the nonprofessional phagocytic cells, like cultured fibroblast and epithelial cells (Filley and Rook 1991; Filley et al. 1992; Mehta et al. 1996). In the nonprofessional phagocytes, many other intracellular pathogens are thought to trigger a signal transduction pathway, enabling the uptake of foreign particles (Bliska et al. 1993). The hypothesis that *M. tuberculosis* contains similar cell entry factors was supported by the discovery of an *M. tuberculosis* open reading frame that was found to be slightly homologous to several proteins known to be involved in mammalian cell entry of other intracellular parasites. When cloned into *E. coli*, it resulted in their entry into HeLa cells while also enhancing their survival inside human macrophages (Arruda et al. 1993).

Many different receptors have been implicated in the entry of *M. tuberculosis* into phagocytic cells. A gene encoding a fibronectin binding protein was also discovered in the *M. tuberculosis* genome. In a manner similar to the way that *M. bovis* BCG was found to adhere to fibronectin-coated surfaces (Ratliff et al. 1987), *M. tuberculosis* may bind to the fibronetin receptors on mucosal surfaces and macrophages (Abou-Zeid et al. 1988). It has also been demonstrated that complement receptor CR4 was the major receptor involved in the uptake of a less virulent strain of *M. tuberculosis* in human alveolar macrophages. However, in human blood monocytes, complement receptors CR1 and CR3 were found to

be more important (Hirsch et al. 1994). Studies showed that although the bacilli were able to multiply in both alveolar macrophages and blood monocytes, it was found that the macrophages were better able to inhibit growth. This could be attributed to the increased production of tumor necrosis factor-α which is associated with CR4-mediated phagocytosis in the alveolar macrophages (Quinn et al. 1996).

1.1.6.3 Interactions with phagosomes and lysosomes

Once inside the cells, the mycobacteria are thought to avoid the antibacterial attacks of the phagocytic cell using numerous mechanisms. Early studies by Armstrong and Hart (Armstrong and Hart 1971) found that fusion of lysosomes with phagosomes containing live *M. tuberculosis* H37Rv was inhibited, presumably due to restricted lysosomal movement in the infected cell (Hart et al. 1987). This is supported by more recent studies in which Clemens and Horwitz (Clemens and Horwitz 1995) demonstrated that *M. tuberculosis* exists in an endosome-like vacuole, where the majority of the phagosomes didn't fully mature into phagolysosomes. Cyclic AMP (Lowrie et al. 1975), ammonia (Gordon et al. 1980), and polyanionic cell wall components like sulpholipids (Goren et al. 1976) have all been associated with the inhibition of phagosome-lysosome fusion.

Ammonia production would result in a higher pH in the phagosome. This is consistent with the findings that phagosomes containing live *M. tuberculosis* and *M. avium* were not at acidic pH, while dead bacillli were found in acidic vesicles (Crowle et al. 1991; Sturgill-Koszycki et al. 1994). A urease gene in *M. tuberculosis* has been cloned and characterized (Reyrat et al. 1995) and is thought to generate ammonia, resulting in the inhibition of phagosome-lysosome fusion and acidification of the lysosomes (Clemens and Horwitz 1995).

McDonough *et al.* (McDonough et al. 1993) have suggested an alternative mechanism. They found that extensive fusion between phagosomes and lysosomes in mouse and human phagocytes was detected within 2 hours of infection. In addition, they reported the appearance of budding of the virulent H37Rv strain from the phagolysosome into a new, distinctive vesicle between 2 and 7 days post-infection. The vaccine strain *M. bovis* BCG did not appear to share this budding phenomenon. Although the avirulent H37Ra strain was also capable of budding from the original phagolysosome, it was not able to multiply in the new vesicles. These findings suggest that the small amount of fused phagosomes detected in previous studies may not reflect the ability of *M. tuberculosis* to inhibit fusion, but rather may be a result of its ability to escape from the fused phagosome (McDonough et al. 1993; Bloom et al. 1994). This mechanism may be similar to the mechanisms utilized by *Listeria monocytogenes* and *Shigella flexneri*, where the bacteria were also found to escape the phagosome through this budding phenomenon (Portnoy et al. 1988; Sansonetti 1991). These parasites produce hemolysins and phospholipases that dissolve the phagosomal membrane, enabling their escape. They are then able to infect other cells by budding from the cytoplasm of the infected cell into the adjacent cell (Quinn et al. 1996).

It has also been observed that some *M. tuberculosis* H37Rv apppeared to be able to escape the vesicles into the cytoplasm, whereas *M. bovis* BCG is not found to escape (McDonough et al. 1993). This supports earlier findings that H37Rv, and not the avirulent strain H37Ra, was able to escape into the cytoplasm in the alveolar macrophages of rabbits (Myrvik et al. 1984). It has been shown that *M. tuberculosis* possesses hemolytic activity (King et al. 1993; Udou 1994; Fischer et al. 1996). Leao *et al.* (Leao et al. 1995) has cloned a *M. tuberculosis* phospholipase gene which demonstrated hemolytic activity when expressed in *E. coli*. In addition, King *et al.* (King et al. 1993) found the virulent *M. tuberculosis* H37Rv strain to produce much more hemolytic activity than the avirulent *M.*

bovis BCG strain. This suggests that the presence of this phospholipase activity may play a significant role in the release of the bacteria into the cytoplasm. It is also possible that this hemolytic activity may play a role in the tissue destruction observed in the disease state since cytotoxicity was observed in the absence of human host factors thought to be involved in tissue destruction (like TNF-α) (Rook and Bloom 1994) for the virulent *M. tuberculosis* H37Rv strain, but not for the avirulent *M. bovis* BCG.

1.1.6.4 Mycobacterial cell envelope components

The *M. tuberculosis* cell envelope is a very unique structure, with components that are known to stimulate excessive release of TNF-α (Gordon and Andrew 1996). This is important since much of the obeserved tuberculosis pathogenecity is thought the be attributed to the unregulated release of this cytokine.

1.1.6.4.1 Lipoarabinomannans

Brennan and Nikaido (Brennan and Nikaido 1995) have reported LAM, the major arabinose- and mannose-containing phosphorylated lipopolysaccharide in mycobacterial cell walls (Britton et al. 1994), to be associated with *M. tuberculosis* virulence. It was found that the more virulent *M. tuberculosis* strains didn't induce as much TNF-α production as other less virulent strains (Adams et al. 1993; Roach et al. 1993). This may be a result of structural differences at their nonreducing termini (Chatterjee et al. 1992). LAM is able to decrease microbicidal activity and downregulate macrophage effector function since treatment with LAM resulted in the inhibition of both macrophage activation by interferon-γ and the induction of nitric oxide, resulting in a decrease in microbicidal activity (Sibley et al. 1988; Chan et al. 1991; Roach et al. 1995). LAM can also act as a

potent oxygen radical scavenger and may inactivate both the neutrophil and macrophage-activated activity (Chan et al. 1991).

1.1.6.4.2 Trehalose 6,6'-dimycolates (TDM)

Trehalose 6,6'-dimycolates (TDM) or cord factor, another component of the mycobacterial cell envelope, was one of the first virulence factors associated with *M. tuberculosis* (Middlebrook et al. 1947; Bloch 1950). Silva *et al.* (Silva et al. 1985) showed that removal of TDM from *M. bovis* BCG reduces its ability to survive in the lungs of mice, while additiion of TDM to BCG-infected mice enhances infection (Bloch and Noll 1953). However, others have argued against TDM being a virulence factor since it is also present in the non-pathogenic mycobacteria and the amount was not found to correlate with the organism's pathogenicity (Goren and Brennan 1979).

1.1.6.4.3 Sulfolipids

Sulfolipids, acidic lipids isolated from virulent *M. tuberculosis* strains, were also thought to be associated with mycobacterial virulence (Goren et al. 1974). They can prime neutrophils to produce superoxide (Zhang et al. 1991) and also induce inflammatory proteins that can cause host cell damage (Zhang et al. 1988). In addition, due to its polyanionic nature, sulfolipids are also thought to inhibit phagosome-lysosome fusion in *M. tuberculosis*-infected cells (Goren et al. 1976). Even though initial studies showed a strong correlation between virulent *M. tuberculosis* strains and high levels of sulfolipids (Goren et al. 1974; Goren et al. 1974), later studies, which found low amounts in fully virulent strains, discounted them as a determinant of virulence (Grange et al. 1978; Goren et al. 1982)

1.1.6.5 Heat Shock Proteins

Heat shock proteins are constitutively expressed under normal conditions and their synthesis is increased under conditions of stress. They are members of families of proteins classified according to molecular weight. A high degree of homology was found between the bacterial and human HSPs (Jindal et al. 1989; Quinn et al. 1996). This suggests a role for HSPs in autoimmunity since recognition of cross-reacting epitopes of self-HSPs by T-cells primed against bacterial HSPs, may trigger a pathological autoimmune response (Quinn et al. 1996). The mycobacterial HSPs may also induce the expression of cytokines, like IL-1α, Il-1β, IL-6, and TNF-α, that may play a part in host tissue damage (Retzlaff et al. 1994; Quinn et al. 1996).

1.1.6.6 Mycobacterial metabolism

Once the mycobacteria have successfully evaded the host defense mechanisms, the virulent strains must adapt to the environment in the host. Many studies investigating the permeability of the mycobacterial cell envelope to small nutrients have been performed, as reviewed by Connell *et al.* (Connell and Nikaido 1994). Iron and oxygen are two essential elements required by the bacteria which will be very limited *in vivo*. It has been suggested that oxygen may be a growth-limiting factor since Wayne *et al.* (Wayne 1976; Wayne and Lin 1982) have found that *in vivo* and *in vitro* grown *M. tuberculosis* and virulent and avirulent strains all have different respiration rates.

The capacity of *M. tuberculosis* to infect the host also appears to be closely related to its ability to acquire iron. Serum containing poorly saturated transferrin, such as human serum, is tuberulostatic, and its tuberculostatic effect is neutralized by the addition of iron (Kochan 1969; Kochan et al. 1971). Free iron is very limited in the host, particularly in extracellular sites owing to the high affinity with which it is bound by host iron-binding

proteins (chiefly transferrin and lactoferrin). Many pathogens produce high-affinity iron-binding molecules known as siderophores to help acquire this essential element in the iron-limiting host environment by removing it from the host proteins. Mycobacteria have been shown to produce small water-soluble siderophores called exochelins (Macham and Ratledge 1975; Macham et al. 1975; Barclay and Ratledge 1988). This will be discussed in more detail in the next section.

1.2 Iron Acquisition and Microbial Pathogenesis

1.2.1 General iron acquisition

Iron is an essential component of many cellular processes, ranging from catalyst in electron transport processes to oxygen transporters. It plays a huge role in the life of the cell as both protector and destroyer; a lack of iron can depress oxidative defenses in cells while an excess can damage cells by promoting the Fenton reaction, resulting in the production of highly reactive hydroxyl radical (Byers and Arceneaux 1998). All microorganisms, except lactobacilli (Archibald 1983), require iron for survival. In order to acquire this necessary element, the microorganisms must overcome the insolubility of iron. Even though it is the fourth most abundant element in the earth's crust, it is generally found as a constituent of insoluble oxohydroxide polymers (FeOOOH). These Fe(III) oxides are very stable. Therefore, at neutral pH, Fe(III) has a solubility of approximately 10^{-18} M (Wheeler and Ratledge 1994). This concentration is far below the 10^{-8} to 10^{-6} M Fe levels that are optimal for microbe growth conditions. As a result of these environmental limitations and biological necessities, the microorganisms must find a way to solubilize the iron and make it available for consumption. In addition, they must carefully regulate its uptake since both Fe(II) and Fe(III) can act as catalysts in the generation of hydroxyl radicals, some of the most potent known oxidizing agents (Guerinot and Yi 1994).

15

In addition, most of the iron in the host is complexed in iron-binding proteins, leaving very little free iron to support bacterial growth. The majority of iron is intracellular, occurring mainly in heme, iron-sulfur proteins, and ferritin. The small quantities of extracellular iron are tightly bound to iron-storage proteins like transferrin and lactoferrin. It is believed that the host is able to modulate its iron levels as a defense mechanism against infection by the microorganisms (Payne 1993). Therefore, pathogens have developed a variety of iron acquisition systems to acquire iron in the host, as the ability to compete with the host for this necessary element appears to be an important determinant of their virulence.

1.2.1.1. Direct utilization of host iron sources

Some microbes are able to utilize host iron sources by binding transferrin and/or lactoferrin directly and then removing the iron from the proteins. The organisms of this type include pathogenic *Neisseria* (Cornelissen et al. 1992), *Haemophilus influenzae* (Schryvers 1988), and *Trichomonas vaginalis* (Lehker and Alderete 1992). Other microbes, like *Vibrio cholerae* (Stoebner and Payne 1988), are able to utilize heme as their iron source. In addition to expressing membrane transport for hemes (Henderson and Payne 1993), *V. cholerae* also synthesizes a hemolytic cytotoxin which may aid the cellular release of the heme and hemoglobin (Stoebner and Payne 1988).

1.2.1.2 Indirect utilization of host iron sources

Many microbes use an indirect method to acquire iron in which they produce compounds or enzymes to acquire the iron from the host complexes, making it available for incorporation by the pathogen. *L. monocytogenes* synthesizes and secretes a reductase which reduces the iron while bound to transferrin, effecting its release (Cowart and Foster

16

1985). However, the more common method utilized by pathogens is the production of siderophores (Greek for iron bearers). These are low-molecular weight (typically less than 1000 Da) iron chelators which facilitate the solubilization and removal of iron from the host iron-binding proteins and transport it back to the microorganism. Typically produced under conditions of low iron stress, these siderophores have very high Fe(III)-binding constants. They can differ greatly in chemical structure, but all chelate Fe(III) in 6-coordinate octahedral complexes. The formation constants of siderophores for Fe(III) are typically 10^{30} or greater (Neilands 1995), which is very strong in comparison to EDTA's Fe(III) stability constant of 10^{24} (Wheeler and Ratledge 1994). Unlike heme, which can bind iron in both the (+2) and (+3) states and serve as an effective electron shuttle, siderophores only show a high affinity for Fe(III). The weaker complexation of siderophores for Fe(II) allows for an efficient means of release of the siderophore-bound Fe(III) inside the cell via reduction. Siderophores have been isolated from numerous different pathogens, including *Histoplasma capsulatum* (Holzberg and Artis 1983), *Candida albicans* (Holzberg and Artis 1983), and several species of *Salmonella* (Neilands 1981) and *Vibrio* (Payne and Lawlor 1990). It is believed that mycobacteria utilize host iron stores indirectly through the use of siderophores (to be discussed later).

1.2.1.3 Intracellular vs. extracellular iron acquisition

Intracellular and extracellular pathogens face very different environments during infection. Septicemic pathogens, which multiply in the blood and extracellular spaces of the host, must synthesize siderophores that are able to remove iron from transferrin or uptake systems specific for transferrin. Extracellular pathogens which inhabit other portions of the host, like mucosal surfaces, need to be capable of acquiring iron from lactoferrin (Payne 1993). In contrast, intracellular pathogens have access to the intracellular milieu. This contains numerous other iron sources like heme and heme

proteins, ferritin (iron storage protein), and iron-sulfur proteins. Although these stores wouldn't be readily accessible to microbes enclosed in vesicles, they would be available to those residing in the cytoplasm. Due to the large amount of reducing factors in the cell, there may also be a very small intracellular pool of free Fe(III). However, the majority of the iron will still be complexed in host proteins.

1.2.2 Regulation of iron gene expression

Due to problems associated with both insufficient and excess supplies of iron, the synthesis of the numerous systems involving iron acquisition, distribution, and storage must be under tight regulation. In the majority of microbes, low-iron conditions induce the expression of components of iron acquisition systems. In numerous gram-negative (and some gram-positive) bacteria, this expression is under the control of the *fur* (ferric uptake regulation) gene, which acts as a negative repressor of the uptake systems (Bagg and Neilands 1987; Neilands 1995). The Fur protein is thought to chelate Fe(II) and polymerize around the "iron box", or "fur box," a consensus sequence (GATAATGATAATCATTATC) located in the operator regions of genes under Fur control (de Lorenzo et al. 1988; Le Cam et al. 1994). Many of the genes that are regulated by Fur are unrelated to iron uptake. In gram-negative bacteria, many of these genes encode virulence determinants (Hantke 1981; Hantke 1984; Litwin and Calderwood 1993). Fur has also found to be a positive regulator of genes in *E. coli* (Niederhoffer et al. 1990) and *Pseudomonas aeruginosa* (Hassett et al. 1996). In some organisms, other proteins have been found that also activate the expression of some of the iron-uptake genes. In some cases, these proteins are also under the regulation of fur, providing an additional level of control (Byers and Arceneaux 1998). In *P. aeruginosa*, the expression of the siderophore (enterobactin) receptor is under the control of a two-component signal transduction system (Dean and Poole 1993).

18

In addition to Fur, a second iron-responsive element has been found to act as a negative repressor. *dtxR* (diptheria toxin regulation), also known as *ideR* (iron-dependent regulation), was discovered in *Corynebacterium diphtheriae* where it controls the expression of both toxin and siderophore biosynthesis (Boyd et al. 1990; Schmitt and Holmes 1991). The regulatory protein encoded by *dtxR* does not share high homology with Fur proteins and appears to bind a very different consensus sequence than that of the *fur* box. The discovery of functional homologs in several species of mycobacteria (Doukhan et al. 1995; Dussurget et al. 1996), including *M. tuberculosis* (Schmitt et al. 1995)), *Brevibacterium lactofermentum* (Oguiza et al. 1996), and *Streptomyces pilosus* (Gunter-Seeboth and Schupp 1995) suggests the existence of a new family of regulators.

1.2.3 Iron acquisition in mycobacteria

Mycobacteria have been shown by Macham, Ratledge, Barclay, and colleagues (Macham and Ratledge 1975; Macham et al. 1975; Barclay and Ratledge 1988) to produce small water-soluble siderophores called exochelins. As depicted in figure 1.1 (modified from Wheeler and Ratledge (Wheeler and Ratledge 1994)), they proposed that the exochelins bind iron in the extracellular aqueous environment and transport the metal back to another high-affinity iron binding molecule associated with the cell wall of the mycobacteria - the mycobactin (Macham et al. 1975).

1.2.3.1 Mycobactins

Both exochelins and mycobactins are induced by low concentrations of iron in broth medium (Snow 1970; Macham and Ratledge 1975). Mycobactin is a highly lipophilic molecule thought to facilitate the transport of iron across the cell wall to the interior of the bacterium (Marshall and Ratledge 1972). It was originally thought that
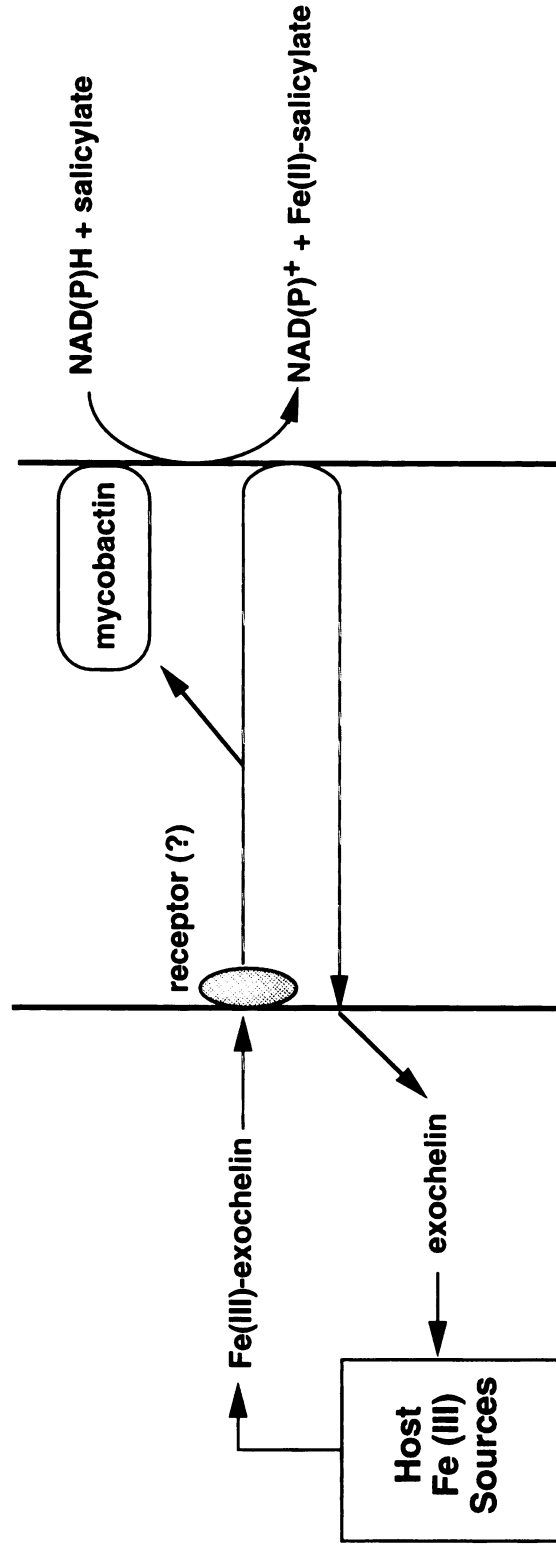
Figure 1.1. Hypothesis for siderophore-mediated iron uptake in mycobacteria. It is proposed that exochelins bind iron in the extracellular aqueous environment and deliver the metal back to the bacterial cell where the iron can either be reduced to Fe(II) by cytoplasmic reductases or it can be transferred to the mycobactin, a cell-envelope associated molecule thought to be involved in iron storage, modified from Wheeler and Ratledge (Wheeler and Ratledge 1994).

20

mycobactin was the extracellular siderophore produced by mycobacteria since it has a very high affinity for Fe(III) (K_s of ca. 10^{35}) (Wheeler and Ratledge 1994). The molecule was found to contain 3 amino acid moieties - 2 N-hydroxylysines and 1 serine or threonine (see Fig 1.2) (Greatbanks and Bedford 1969). The presence of a very long alkyl chain (R_1 in Fig 1.2) makes the molecule very lipophilic, ensuring that it remains within the cell envelope and that it is not secreted (Ratledge et al. 1982). The next candidate for the mycobacterial siderophore was salicylic acid, which can be found in increased amounts in the culture filtrates of some mycobacterial species (Ratledge and Winder 1962). However, this idea was discarded when it was discovered that salicylate was unable to mediate iron uptake in the presence of phosphate ions, instead forming insoluble ferric phosphate (Ratledge et al. 1974). Macham and Ratledge (Macham et al. 1975) later discovered iron-solubilizing factors in *M. smegmatis* and *M. bovis* BCG culture filtrates that were still able to function in the presence of phosphate ions. These factors, named "exochelins," were thought to be the extracellular siderophores secreted by the mycobacteria (Macham and Ratledge 1975; Macham et al. 1975). The detection of exochelins in numerous other mycobacterial species, including *M. tuberculosis*, *M. africanium*, *M. avium*, and *M. paratuberculosis* (Barclay and Ratledge 1983; Barclay and Ratledge 1988) provided more evidence that these were indeed the mycobacterial siderophores.

1.2.3.2 Exochelins

There are two general types of exochelins, classified according to their extractability into organic solvents (Ratledge 1984). The chloroform-insoluble exochelins produced by saprophytic mycobacteria are not extractable into organic solvent. The chloroform-soluble exochelins, produced by the slow-growing pathogenic mycobacteria, including *M. tuberculosis*, *M. avium*, and *M. bovis*, are extractable into organic solvents (Barclay and Ratledge 1988). In contrast to mycobactins, which have been extensively studied and their

21
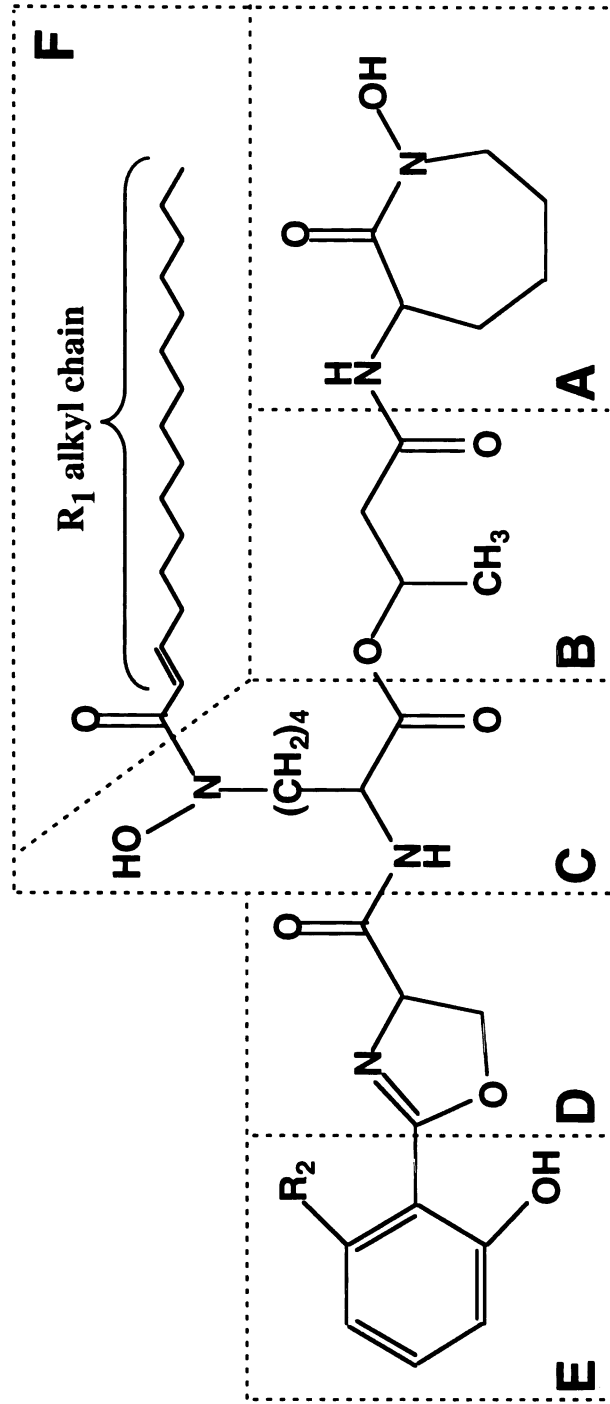
Figure 1.2. Structure of mycobactin, an intracellular, high-affinity iron-binding molecule. The mycobactin can be divided into 6 structural units (A - F), resulting from hydrolytic cleavages of internal amide or ester bonds. These structural elements likely correlate to separate biosynthetic precursor components, such as N-hydroxylysine (A and C), β-hydroxybutyric acid (B), serine or threonine (D), and salicylic acid (E). The R_1 group is a very long (saturated or unsaturated) alkyl chain which accounts for its high degree of lipophilicity and association with the mycobacterial cell envelope.

structures delineated (Snow 1970), individual exochelins had not been purified and characterized until recently (Gobin et al. 1995; Lane et al. 1995; Sharman et al. 1995; Sharman et al. 1995; Wong et al. 1996; Gobin et al. 1998).

1.2.3.2.1 Exochelins from saprophytic mycobacteria

Recently, the exochelins produced by saprophytic mycobacteria *M. smegmatis* (Sharman et al. 1995) and *M. neoaurum* (Sharman et al. 1995) were purified and characterized by Sharman and colleagues. The exochelin produced by *M. smegmatis* (exochelin MS) was isolated from mycobacteria grown in iron-deficient media and purified to greater than 98% by ion-exchange chromatograohy and high-performance liquid chromatography (HPLC). A combination of nuclear magnetic resonance (NMR) and mass spectrometric experiments allowed for the identification of exochelin MS to be a formylated pentapeptide: N-(δN-formyl,δN-hydroxy-R-ornithinyl)-β-alaninyl-δN-hydroxy-R-ornithinyl-R-allo-threoninyl-δN-hydroxy-S-ornithine (see Fig 1.3A).

Exochelin MN, the siderophore produced by *Mycobacterium neoaurum*, was also studied through a combination of NMR, mass spectrometry, derivatization, and gas chromatography (Sharman et al. 1995). This exochelin is a hexapeptide containing two δ-N-hydroxyornithines and a β-hydroxyhistidine (see Fig 1.3B). Although the hydroxamates are a common motif in siderophore chemistry, the β-hydroxyhistidine has only been found in one other siderophore (Hancock et al. 1993). This unique amino acid may account for the novel metal-bound structure of this exochelin. Exochelin MN was not only capable of delivering iron to *M. neoaurum*, but was also able to transport iron into *M. leprae* cells. Exochelins from other species (*M. smegmatis*, *M. vaccae*, and *M. bovis* BCG) were unable to mediate iron transport in *M. leprae* (Sharman et al. 1995). This suggests that the siderophores from *M. leprae* and *M. neoaurum* may have many similarities. This is very helpful considering all efforts to isolate exochelins from *M. leprae*

(A) Exochelin MS
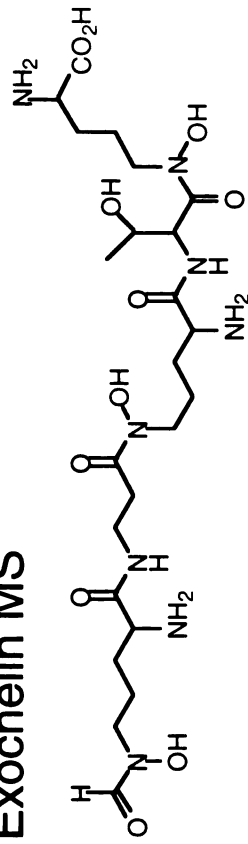
(B) Exochelin MN
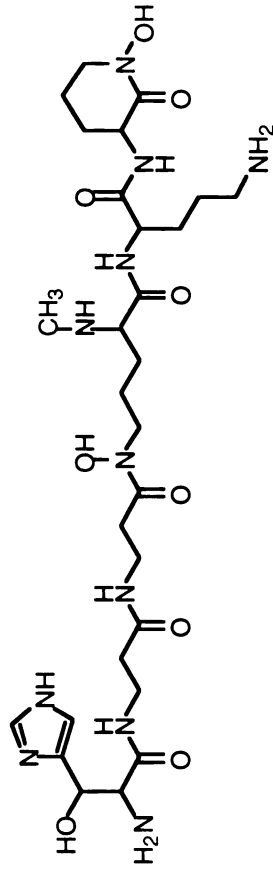
Figure 1.3. The structures of exochelins produced by (A) *M. smegmatis* (Sharman et al. 1995) and (B) *M. neoaurum* (Sharman et al. 1995).

24

have failed since *M. leprae* cannot be grown in laboratory cultures (Hall and Ratledge 1987).

The iron acquisition systems in these saprophytic mycobacteria are receptor-mediated. Proteins located on the surface of the microbial cells mediate the uptake of the ferri-siderophore complexes (Postle 1990; Nikaido and Saier 1992; Wooldridge et al. 1992; Nikaido 1993; Zhou and van der Helm 1993). Like the other components of the acquisition system, the expression of these receptors is increased in low-iron conditions. These mycobacterial proteins were visualized by SDS-PAGE and are referred to as iron-regulated envelope proteins (IREPs) (Hall et al. 1987; Sritharan and Ratledge 1989; Sritharan and Ratledge 1990). Antibodies were raised to many of the *M. smegmatis* IREPs (180, 84, 29, and 25 kD). However, only the antibodies raised against the 29 kD IREP prevented iron uptake in the cells in the presence of ferri-exochelins (Hall et al. 1987). This implies that the 29 kD IREP has a high specificity for the ferri-siderophore complex (Wheeler and Ratledge 1994), suggesting a role as possible exochelin receptor.

1.2.3.2.2 Exochelins from slow-growing, pathogenic mycobacteria

As part of this thesis work, the exochelins from the slow-growing pathogenic mycobacteria, *M. tuberculosis*, *M. avium*, and *M. bovis*, were isolated and characterized and found to share the same core structure as the mycobactins (to be discussed in Chapter 2).

It is not known whether or not the uptake of the ferri-siderophores in the slow-growing mycobacteria is receptor mediated. Alternatively, the iron could be directly transferred into the mycobactin located in the cell wall. However, studies by Barclay and Ratledge (Barclay and Ratledge 1986) suggest the existence of cell surface receptors. They demonstrated that the relief of the bacteriostatic effect of serum on *M. avium* and *M.*

paratuberculosis not only required the presence of exochelins (and/or mycobactins), but also that the mycobacteria be pre-grown in low iron media. Under these conditions, the synthesis of the IREPs would be increased and the receptors would presumably be able to function simultaneously with the added exochelins. If this uptake process was not receptor-mediated and the exochelin was able to transfer the iron directly to the mycobactin through the cell envelope, the mycobacteria should not have to be pre-grown in the low iron media.

1.2.3.3 Release of Fe from exochelin/mycobactin

Despite the high stability constants of the exochelins and mycobactins with Fe(III) (approximately 10^{25} and 10^{35}, respectively) (Wheeler and Ratledge 1994), reduction of Fe(III) to Fe(II) allows for the easy release of the iron from the complexes. NADPH-dependent reductases have been found that can readily reduce ferri-exochelin and ferri-mycobactin (Brown and Ratledge 1975; McCready and Ratledge 1979). Initial studies attempting to characterize a specific reductase for siderophore reduction (McCready and Ratledge 1979) concluded that it probably wasn't a specific protein since ferri-mycobactin could be reduced by cell extracts from numerous other organisms (*E. coli* and *Candida utilis*). Although never experimentally proven, it has been suggested that salicylate was the intracellular Fe(II) acceptor and that Fe(II)-salicylate was the correct Fe precursor prior to insertion into porphyrins and apoproteins (Wheeler and Ratledge 1994).

Chapter 2.   Isolation, Purification, and Characterization of Exochelins of Slow-Growing, Pathogenic Mycobacteria

2.1 *M. tuberculosis* Exochelins

2.1.1 INTRODUCTION

There are two general types of exochelins classified according to their extractability into organic solvents (Ratledge 1984). The chloroform-insoluble exochelins, produced by saprophytic mycobacteria, are not extractable into any organic solvent. The chloroform-soluble exochelins, produced by slow-growing pathogenic mycobacteria, including *M. tuberculosis*, *M. avium*, and *M. bovis*, are extractable into chloroform (Barclay and Ratledge 1988).

Due to purification problems, physiological and structural studies of exochelins have only recently been performed. The structures of chloroform-insoluble exochelins from the non-pathogens *M. smegmatis* (Sharman et al. 1995) and *M. neoaurum* (Sharman et al. 1995) have recently been reported. These structures differ greatly from the chloroform-soluble exochelins isolated from the pathogens *M. tuberculosis* (Gobin et al. 1995) and *M. avium* (Lane et al. 1995; Wong et al. 1996). More precisely, the exochelins of the non-pathogens are peptides, whereas the exochelins from the pathogenic mycobacteria resemble mycobactins and contain both amino acid and non-amino acid moieties. In this first section, I describe the purification and characterization by mass spectrometry (MS) of exochelins of *M. tuberculosis* [from both a virulent (Erdman) and an avirulent (H37a) strain].

2.1.2 MATERIALS AND METHODS

2.1.2.1 Materials

2.1.2.1.1 *Medium and Reagents*

Modified iron-deficient Sauton's broth medium (Eidus and Hamilton 1964) was prepared with 1-10 μM Fe^{+3} and without Tween. Mycobactin J was purchased from Allied Monitor (Fayette, MO).

2.1.2.1.2 *Bacteria*

M. tuberculosis Erdman (ATCC no. 35801) and H37Ra (ATCC no. 25177) strains were grown on Middlebrook 7H11 agar plates (Pal and Horwitz 1992), suspended in modified Sauton's medium at A_{540} = 0.05, and cultured in 225-cm^3 culture flasks (Costar) at 150 ml per flask and at 37°C in 5% CO_2/ 95% air for 3, 6, or 8 weeks.

2.1.2.2 *Methods*

2.1.2.2.1 *Purification of Exochelins*

The culture supernatant fluid was filtered successively through 0.8- and 0.2 μm low-protein-binding filters and saturated with iron (150 mg of ferric chloride per liter). Ferri-exochelins were extracted into chloroform by shaking 1 vol of culture filtrate with 1.5 vol chloroform. The chloroform layer (containing the exochelins) was removed, dehydrated overnight with anhydrous magnesium sulfate (2 g/l), filtered through a fritted

glass filter, and evaporated by rotary evaporation, yielding a brown compound. The brown extract was suspended in buffer A [100% H_2O/ 0.1% trifluoroacetic acid (TFA)] and exochelins were prepurified on a C_{18} Sep-Pak cartridge (Waters, Millipore). Visible as a brown band at the top of the column, exochelins were eluted with buffer B (50% acetonitrile/ 0.1% TFA). This partially purified material was loaded onto a C_{18} column in buffer A and subjected to reverse-phase high-performance liquid chromatography (HPLC) with a 0-100% buffer B gradient at a flow rate of 1 ml/min on a Rainin HPXL system (Woburn, MA), monitoring at 220 and 450 nm on a dual-wavelength detector. All peaks exhibiting high 450-nm absorbance, tentatively identified as exochelins, were hand collected and subjected to a final purification on a reverse-phase alkyl phenyl column.

2.1.2.2.2 *Purification of Mycobactins*

The bacterial cells from cultures described above were suspended in 6 ml of 95% ethanol per gram of wet cells and stirred for 24 hr at 24°C. The ethanol extract containing mycobactins was then filtered, and the filtrate was saturated with 600 mg of ferric chloride per liter and diluted 1:1 with distilled water. Ferrimycobactins were extracted into chloroform by shaking 1 vol of the ethanol extract with 0.5 vol of chloroform. Mycobactins were purified successively on a C_{18} Sep-Pak cartridge, C_{18} column, and alkyl phenyl column using the same procedures used to purify exochelins except that buffer B consisted of 95% acetonitrile/ 0.1% TFA.

2.1.2.2.3 *Mass Spectrometric Analysis*

Peaks isolated from the HPLC and identified as potential exochelins on the basis of their strong 450 nm absorbance were first subjected to mass analysis by liquid secondary ion mass spectrometry (LSIMS) on a Kratos Analytical Instruments MS50S mass

spectrometer. Samples were concentrated under vacuum and small aliquots (1-5 µl) were transferred to the LSIMS probe along with 1 µl thioglycerol/glycerol (1:1, vol/vol) matrix. A Cs^+ beam energy of 10 keV was used to bombard the sample and the resulting secondary ions were accelerated to 8 keV. Scans were taken in the positive ion mode at 100 sec per decade and recorded with a Gould (Cleveland) ES-1000 electrostatic recorder. Mass assignments were made to an accuracy of less than or equal to ± 0.2 Da by manual calibration using Ultramark 1621 as an external reference. For exact mass measurements, the peptide YSPTSPS, with an exact ^{12}C monoisotopic mass of m/z 738.331 for the (M + H)$^+$ ion, was added to the LSIMS probe along with the exochelin samples and used as the internal reference mass under peak matching conditions. The resolving power of the spectrometry was ≈ 7000 (M/ΔM).

Electrospray ionization mass spectrometry (ESI-MS) was conducted in the positive ion mode using a VG/Fison (Manchester, U.K.) BioQ triple quadrupole mass spectrometer and a Vydac (Hesperia, CA) narrow bore C_{18} reverse-phase HPLC column (1 mm x 10 cm). Conditions for HPLC separation were similar to that described for the analytical separation of exochelins with the exception of a lower rate of 70 µl/min and a postcolumn split ratio of ≈ 20:1.

Tandem MS was performed on a four-sector mass spectrometer (Kratos Concept II HH, Kratos Analytical, Manchester, England). The collision cell was filled with He and floated at 2 keV for a collision energy of 6 keV. Samples were ionized using a LSIMS source operating with Cs^+ in the positive-ion mode, and all spectra were recorded and mass assigned using an array detector and Mach3 data system (Walls et al. 1990).

2.1.3 RESULTS

2.1.3.1 *The M. tuberculosis Exochelin Family*

We purified the exochelins of *M. tuberculosis* from culture filtrates by chloroform extraction and reverse-phase HPLC. To enhance the production of exochelins, the bacteria were cultured in iron-deficient medium. To allow their ready detection during the purification procedure, the exochelins were first loaded with iron. Preliminary studies using $^{59}FeCl_3$-saturated culture filtrates demonstrated efficient extraction of the label into chloroform (J. Gobin, unpublished data). Iron-binding compounds were subsequently detected in the HPLC eluate by simultaneously monitoring the UV absorbance at 450 nm, a wavelength at which iron compounds generally exhibit relatively high absorbance, and at 220 nm, a wavelength at which amide and aromatic groups absorb. There were approximately 5 major and 10 minor peaks exhibiting a high 450 nm absorbance eluting off a C_{18} column (see Fig 2.1A). We tentatively identified all of these peaks as exochelins and subsequently confirmed their identities as exochelins by MS. Virtually all of the exochelins in the culture filtrate were extracted with a single chloroform extraction. After the culture filtrates were extracted twice with chloroform and the 5 major exochelin peaks in each extract were quantitated, the amount of each peak in the second extract was < 5% of the amount in the first extract.

All major exochelin peaks were purified further by a second reverse-phase HPLC run on an alkyl phenyl column. The final products were highly pure, as evidenced by elution off the column of a single major absorbance peak (see Fig 2.1B) and by the finding of a single mass species of exochelin during subsequent mass analysis.

The HPLC pattern of exochelins released into the culture medium by *M. tuberculosis* Erdman strain was very similar after 3, 6 (see Fig. 2.3), and 8 weeks of

31

Figure 2.1 (A) Elution profile of a 6-week culture filtrate from *M. tuberculosis* Erdman strain (chloroform extract of 100-ml culture filtrate) on a C_{18} reverse-phase HPLC column. Iron-binding compounds were monitored at 220 and 450 nm. Dashed line represents concentration of buffer B. (B) Elution profile of major exochelin peak on an alkyl phenyl column. The major exochelin peak eluting at 77 min on the C_{18} reverse-phase HPLC column in (A) was rechromatographed on an alkyl phenyl column. Dashed line represents concentration of buffer B.

33
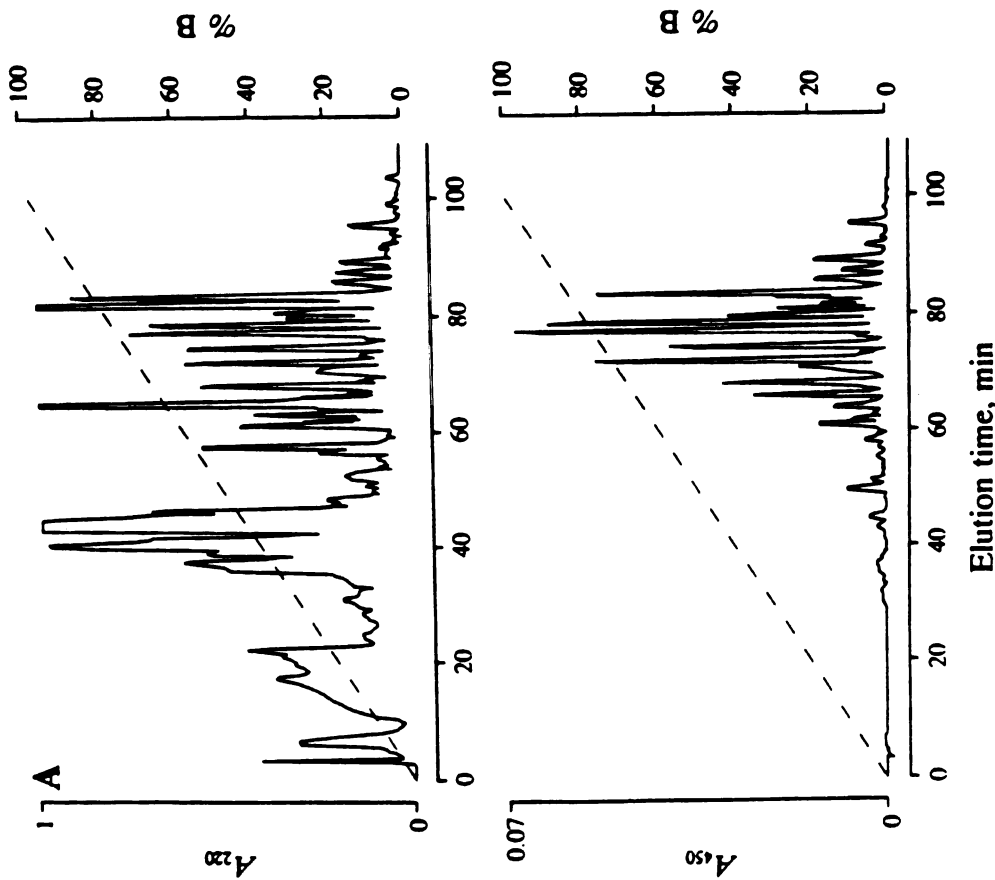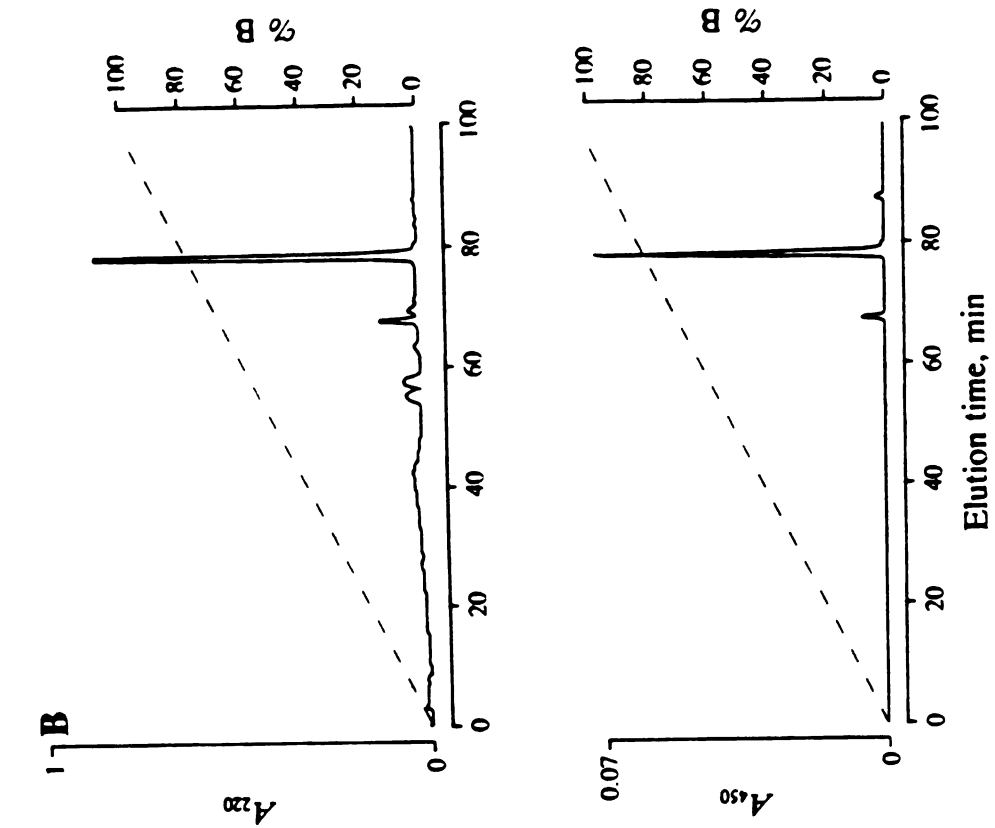
incubation. Subsequent LSIMS analysis of the major peaks revealed that exochelins of the same mass were released at each of those times. Quantitatively, the highest amount of exochelins was recovered from 6-week cultures, which had 6.7 and 1.5 times the amount of exochelins in 3- and 8-week cultures, respectively. The decline in quantity after 6 weeks likely reflects a decreased rate of production of exochelins by stationary-phase organisms, whose metabolism is slowed, and degradation of exochelins, which degrade slowly even at 4°C in the purified state. The set of exochelins produced by the highly virulent Erdman strain of *M. tuberculosis* was similar to that produced by the avirulent H37Ra strain on the basis of the HPLC elution pattern and mass determination.

2.1.3.2 *Characterization of Exochelins of M. tuberculosis*

MS analysis confirmed that all peaks exhibiting a high 450 nm absorbance were exochelins. LSIMS of each peak revealed an ion pair differing in mass by 53 Da (see Fig 2.2), corresponding to protonated $(M + H)^+$ and iron $(M - 2H + Fe^{III})^+$ adducts of the same molecular ion species. Consistent with this, ESI-MS of each exochelin revealed only one ion for each exochelin species representing the Fe^{+3} adduct $(M - 2H + Fe^{III})^+$. This indicated that the protonated form seen during LSIMS is an artifact of that technique and that all the exochelins are most likely Fe^{+3} loaded in solution. On LSIMS analysis, the major exochelin had peaks at m/z 773 (iron adduct) and 720 (protonated adduct). Similar desferri artifacts for bacterial siderophores have been previously reported by LSIMS (or FAB) in the case of acaligin, a siderophore produced by *Bordatella pertussis* and *B. bronchiseptica* (Moore et al. 1995).

High-resolution peak matching of exochelins with $(M + H)^+$ at m/z 720 and 748 yielded exact m/z values of 720.345 (M_{Exp} = 710.337) and 748.373 (M_{Exp} = 747.365) for their corresponding isotopically pure ^{12}C-containing molecular ions. These exact masses are within ± 3-5 ppm for an elemental composition of neutral non-iron-containing

Figure 2.2 Positive-ion LSIMS spectrum of serine-containing exochelin.

The two most prominent ions at m/z 773.3 and 720.3 correspond to the singly charged

molecular ion for the iron-bound state and iron-free state, respectively. Both of these ion

species can undergo loss of oxygen and are further substituted with sodium and/or

magnesium. A peak at m/z 744 may represent the addition of trivalent aluminum - i.e., (M-

$2H+Al^{III})^+$.
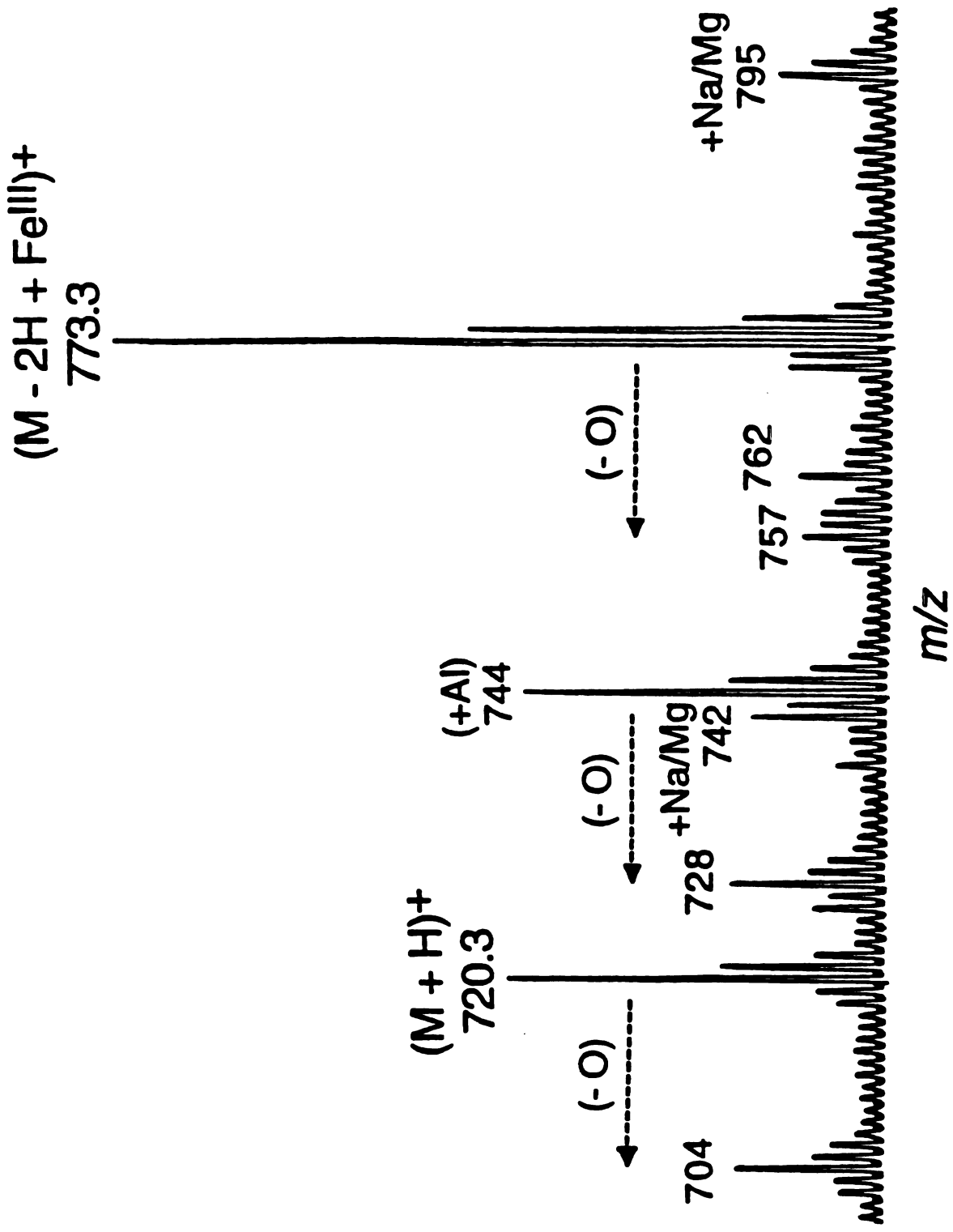
exochelins of M = $C_{34}H_{49}N_5O_{12}$ (M_{Calc} = 719.3378) and M = $C_{36}H_{53}N_5O_{12}$ (M_{Calc} = 747.3691), respectively (Barclay et al. 1985).

Exochelins comprised a large family of molecules (see Fig 2.3). The major species ranged in mass from 745 to 801 Da for the protonated Fe^{+3} adduct, $(M - 2H + Fe^{III})^+$, based on LSIMS and ESI-MS analysis (see Table 2.1). Exochelins differed from each other in mass by multiples of 14 Da, reflecting different numbers of CH_2 groups, and/or by 2 Da, reflecting the likely presence of a double bond in some exochelins. Thus, on the basis of mass alone, exochelins formed two 14-Da-increment series, one saturated [masses $(M - 2H + Fe^{III})^+$ 731-829 Da] and one unsaturated [masses $(M - 2H + Fe^{III})^+$ of 771-813 Da]. The exact location of the double bond in the unsaturated series remains to be determined but is clearly contained in the R_1 alkyl side chain on the basis of tandem MS analysis (see below). However, nuclear magnetic resonance studies performed by Lane et al. on the exochelins produced by *M. avium* showed the R_1 alkyl chain to be α/β-unsaturated (Lane et al. 1995).

The different numbers of CH_2 groups are located primarily on the R_1 alkyl side chain. In addition, the presence or absence of a methyl group at R_3 further subdivides exochelins into two other families according to whether or not they are serine-containing (R_3 = H) or threonine-containing (R_3 = CH_3) species (as confirmed by amino acid analysis). Therefore, we propose a nomenclature for exochelins that identifies them as members serine (S) or threonine series (T) and whether they terminate in a free carboxylic acid (C) or a methyl ester (M). For example, an exochelin with $(M-2H+Fe^{III})^+$ 773 which contains a threonine and terminates in a methyl ester would 773TM.

2.1.3.3 *Structure of Exochelins and Mycobactins of M. tuberculosis*

As noted above, *M. tuberculosis* produces two high-affinity iron-binding molecules - exochelins and mycobactins. To compare these molecules, we isolated both from the
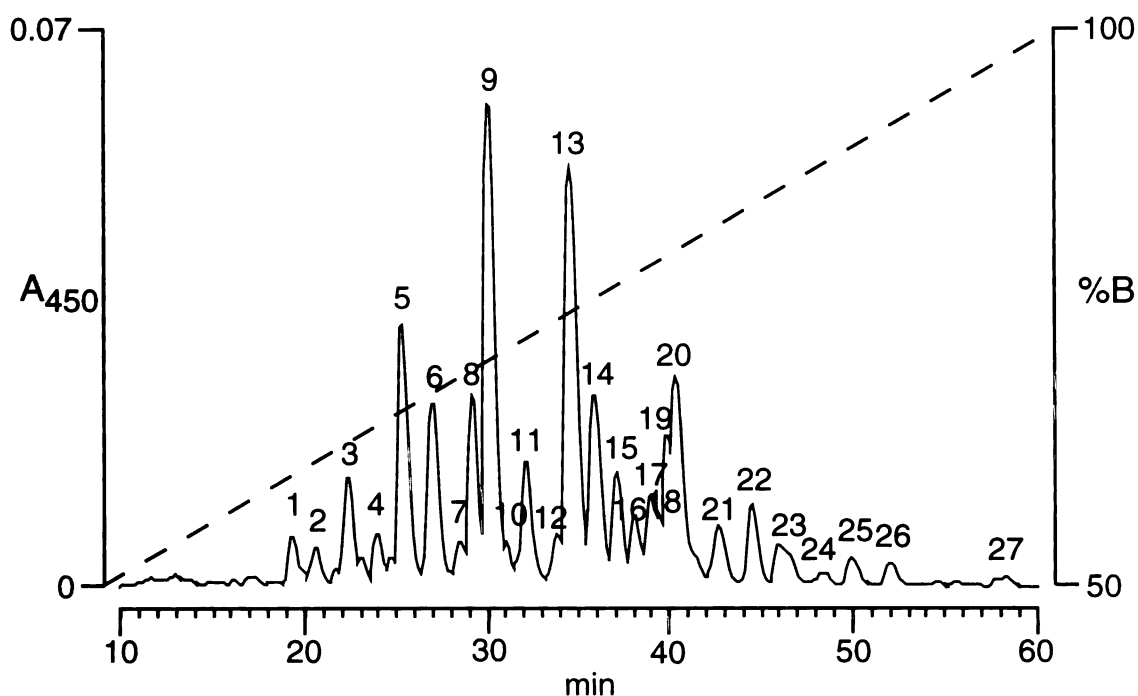
Figure 2.3 Elution profile of 6-week culture filtrate from the *M. tuberculosis* Erdman strain. The preparation was obtained by chloroform extraction of a 100 ml culture filtrate and separated on a C_{18} reverse-phase HPLC column. Iron-binding molecules were monitored at 450 nm. Peaks are numbered in the order of their elution off the HPLC column and are further characterized in Table 2.1.

TABLE 2.1. Molecular Masses (Da) of *M. tuberculosis* Exochelins in HPLC Peaks

| HPLC Fraction Number[a] | $R_1 = (CH_2)_n COOR$ | | | | $R_1 = CH=CH(CH_2)_n COOR$ | | | |
| | $R_3 = H$ | | $R_3 = CH_3$ | | $R_3 = H$ | | $R_3 = CH_3$ | |
	$R = H$	$R = CH_3$	$R = H$	$R = CH_3$	$R = H$	$R = CH_3$	$R = H$	$R = CH_3$
1	731[b], n=3							
2	745, n=4		731, n=2					
3	759, n=5	745, n=3	745, n=3					
4		759, n=4	759, n=4					
5		759, n=4						
6	773, n=6							
7		773, n=5				771, n=3	771, n=3	
8								
9								
10								
11			787, n=6	773, n=4				
12	787, n=7			787, n=5				
13		787, n=6						
14						785, n=4		785, n=3
15								
16						799, n=5		
17	801, n=8							799, n=4
18					799, n=6			
19					799, n=6			
20								
21								813, n=5
22	815, n=9							
23								
24								
25								
26		815, n=8						
27		829, n=9						

$(M - 2H + Fe^{III})^+$

a see Figure 2.3 for HPLC elution positions of peaks 1-27

b masses of iron-loaded exochelins are reported as their molecular ions as observed under positive-ion LSIMS conditions (see text). Each exochelin peak was observed as an ion-pair, $(M+H)^+$ and $(M-2H+Fe^{III})^+$, differing in mass by 53 Da. Assignments were confirmed by tandem MS analysis (as shown in Fig 5).

same strain of *M. tuberculosis* (Erdman strain) and obtained their UV absorbance spectra (see Fig 2.4). The spectra were very similar, with a major peak of absorbance at 220 nm in addition to a peak at 450 nm.

To characterize the structure of exochelins of *M. tuberculosis* further, we studied individual exochelins by high-energy tandem MS (see Fig 2.5A) and compared their structures with mycobactins produced by *M. tuberculosis* and with a commercially available mycobactin J from *Mycobacterium paratuberculosis* (see Fig 2.5B), whose structure has been studied (McCullough and Merkal 1982; Barclay et al. 1985). This analysis revealed that exochelins have a core structure similar to that of mycobactins, a conclusion evident from the similarity of the fragmentation pattern of the two molecules. Fragment ions of both molecules were assigned to one of six structural moieties (**A-F**) within the compounds arising from one or more cleavages about the amides or ester bonds (see Fig 2.5 *Upper*). Some lower mass peaks were identical for the two compounds, such as *m/z* 100, 145, and 171 which are derived from conserved structural units **A** and **C**. For the most part, however, analogous fragment ions were generated for both compounds but were shifted in mass between the two compounds based primarily on differences in alkyl substituents present in the **B**, **E**, and/or **F** moieties. For example, the phenolic group in mycobactin contained a meta-substituted methyl group and peaks containing this residue were shifted 14 Da higher in mass relative to the exochelins, which did not contain this methyl group [e.g., (**DE** - CO)$^+$ at *m/z* 176 vs. 162]. Likewise, peaks containing **B** and **F** in the mycobactin tandem MS/MS spectrum were shifted up in mass relative to the exochelin spectrum by 28 ($\Delta M = C_2H_4$) and 80 ($\Delta M = C_8H_{16}$, -O_2) Da, respectively.

In addition to the saturated serine-containing exochelin shown in Fig 2.5A, 28 other exochelins were analyzed by tandem MS and shown to belong to the saturated serine series [(M - 2H + Fe^{III})$^+$ = 731-829], saturated threonine series [(M - 2H + Fe^{III})$^+$ = 731-787],

41
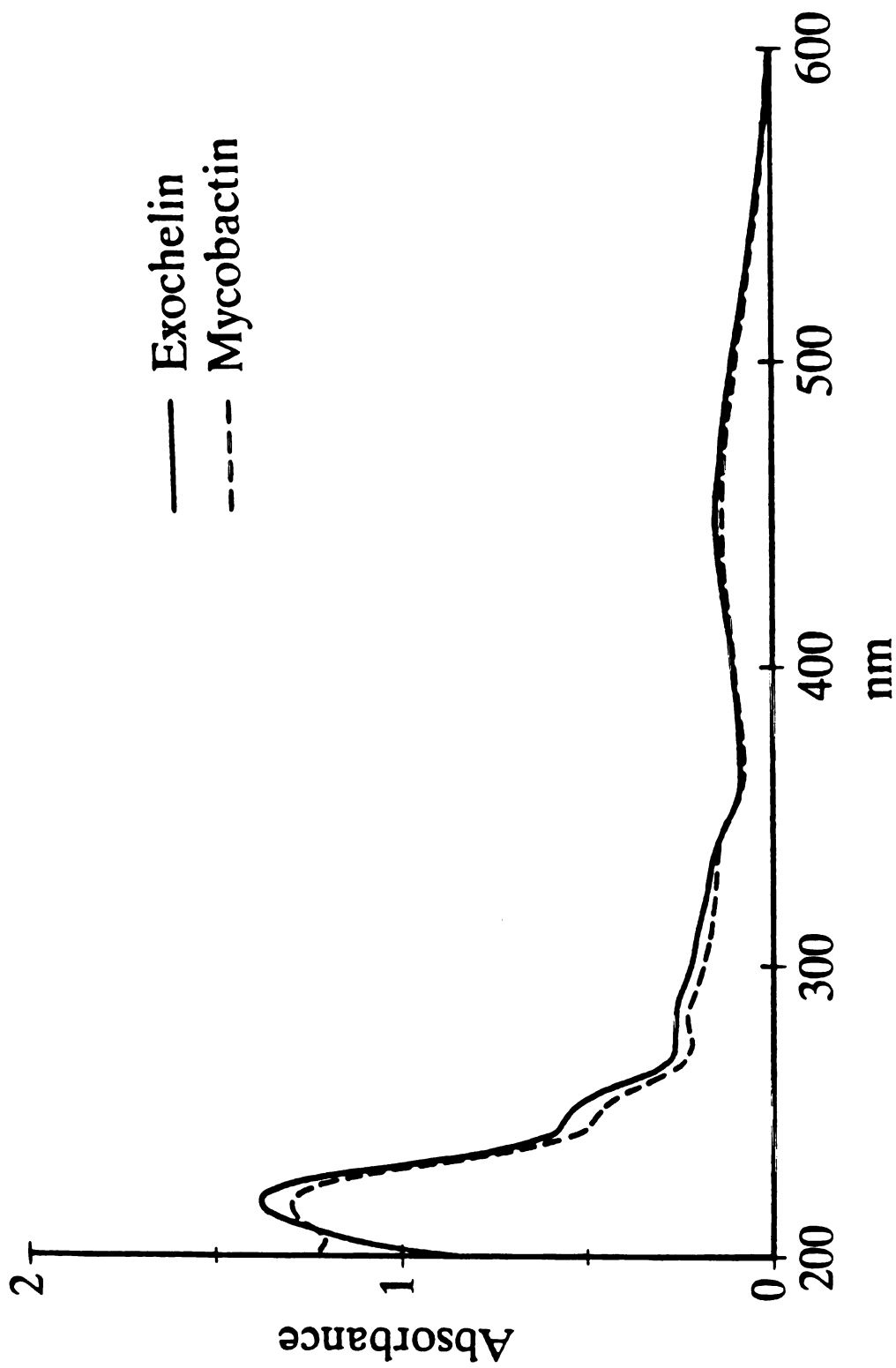
Figure 2.4 Absorbance spectra of the major exochelin [(M-2H+Fe^{III})$^+$ = 773] and major mycobactin from *M. tuberculosis* Erdman strain.

Figure 2.5 Tandem MS under collision-induced dissociatioon of the major saturated serine-containing exochelin with (A) (M+H)$^+$ at m/z 720.3 and (B) commercial mycobactin J. (*Upper*) Fragment ions of both the exochelin and mycobactin are assigned to one of six structural moieties (**A-F**) within these two compounds as described in the test. (*Lower*) On the mass spectra, hydrogen transfers relative to the neutral molecule are indicated by +1, +2, or +3.

(A) Exochelin M$_r$ 719.3 Methyl Ester

$(M+H)^+$ = 720.3

x2

100

C - CO, - OH + 2H

DE - CO

162

A + CO

171

DE + NH + 2H

207

121

C + 2H

145

AB - O

213

AB + 2H

231

CDE - CO, -NOH + H

273

277

DE

190

CDE + O + 3H

352

CDE + H

334

BCDE + H

420

BCDE + NH + 2H

437

CDEF - CO + H

463

CDEF

490

CDEF + O +2H

508

ABCF + 2H

531

ABCDE + 2H

563
564

ABCDEF - (CH$_2$)$_n$COOCH$_3$

ABCDEF - COOCH$_3$

661

MH - CH$_3$OH

MH - H$_2$O

Mass

44

(B) Mycobactin J

$(M+H)^+ = 842.5$

45
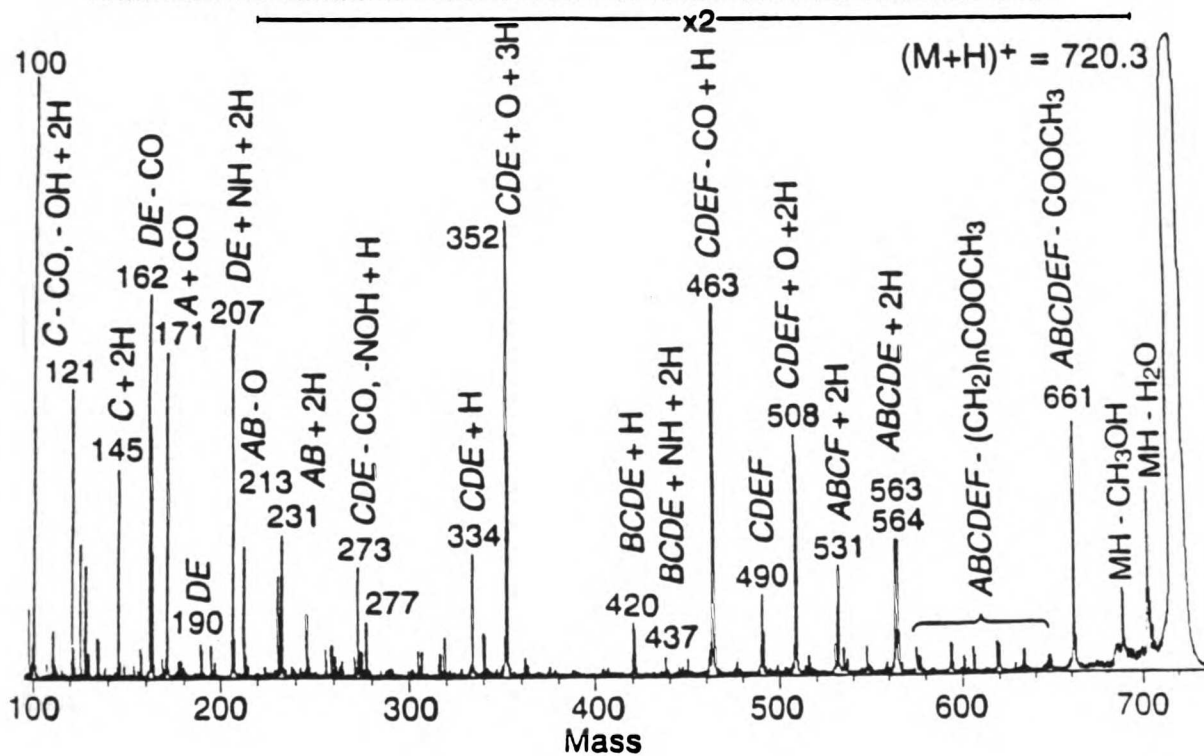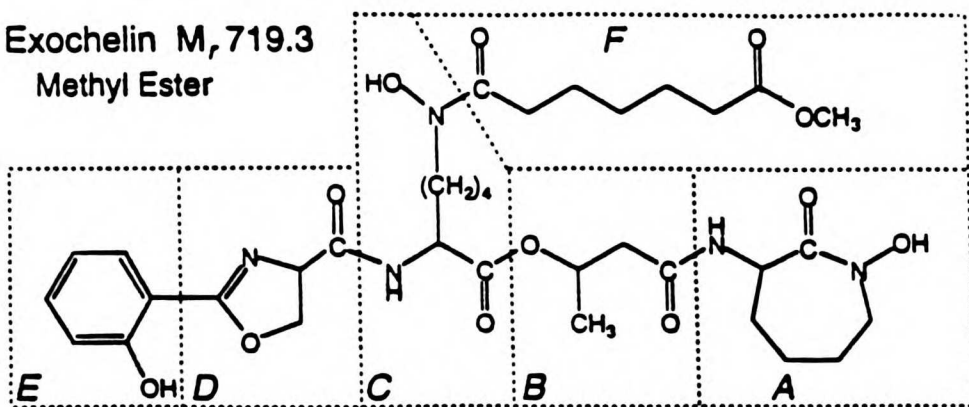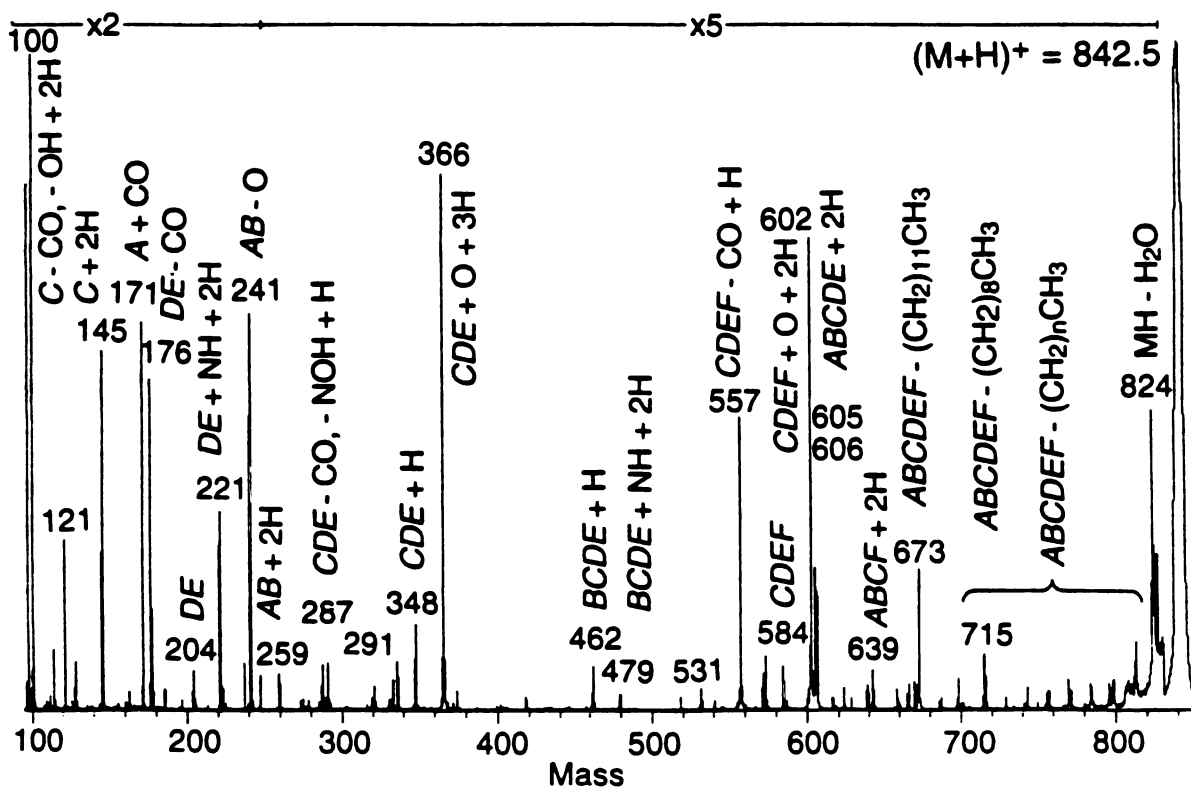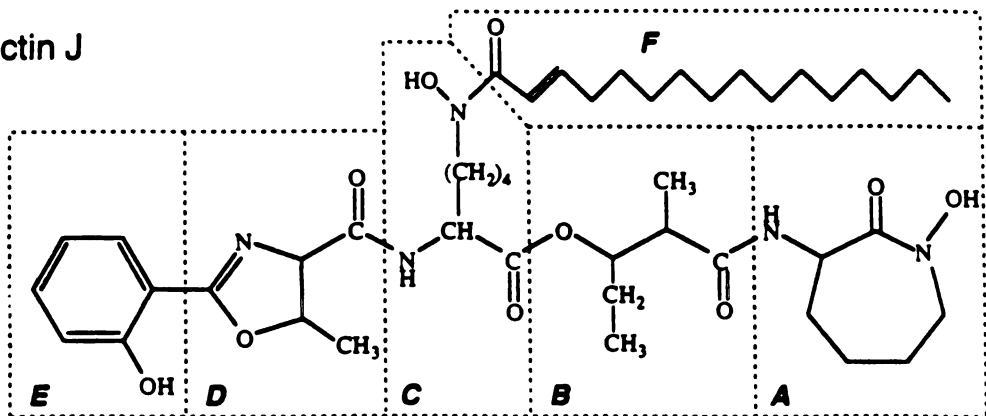
unsaturated serine series [(M - 2H + Fe^{III})$^+$ = 771-799], and unsaturated threonine series [(M - 2H + Fe^{III})$^+$ = 771-813] (see Table 2.1).

Acid hydrolysis of mycobactin J and the exochelin described in Fig 2.5A followed by methylation with diazomethane resulted in the formation of salicylic acid and 2-hexadecanoic acid (mycobactin J), and salicylic acid and pimelic acid (*M. tuberculosis* exochelin), which were identified as their corresponding methyl esters by GC/MS analysis. This provided further proof of the structures of moieties **E** and **F** in both compounds. Furthermore, it was clear from the tandem mass spectrum of the exochelin that pimelic acid is present as a methyl ester, a fact that is supported by the peaks at *m/z* 699 (MH - CH_3OH)$^+$ and 661 (MH - $COOCH_3$)$^+$ and also by the series of alkyl chain cleavages at *m/z* 647, 633, 619, and 605 [MH - (CH_2)$_{1-4}COOCH_3$]$^+$.

Thorough comparisons of the tandem mass spectra obtained from individual exochelins and mycobactins provided tentative structure assignments for exochelins as shown for the non-iron-bound saturated serine-containing exochelin (M_r 719) in Fig 2.5A. The precise substitution pattern of the two linker carbons in the **B** group of the exochelin, which could not be determined from the MS/MS data, was determined by GC/MS analysis. Acid hydrolysis of the exochelin, followed by trimethylsilyl derivatization allowed for the detection of 3-hydroxybutyric acid as moiety **B**, along with confirming **E** as benzoic acid.

The general structure for the exochelins and mycobactins of *M. tuberculosis* is shown in Figure 2.6. The core molecule is circular with iron in the center. It contains 3 amino acid moieties - two N-hydroxylysines and one serine or threonine depending on whether R_3 is a hydrogen or a methyl group. However, the two types of molecules differ from each other in two significant respects. First, exochelins (M_r 730-828 for the neutral Fe^{+3} adducts) are smaller than mycobactins (M_r 882-924 for the neutral Fe^{+3} adducts) owing to a longer alkyl side group at R_1. Second, the shorter R_1 alkyl chains in the exochelins terminate in methyl ester or free carboxylic acid moieties.

$$\text{[Chemical structure: Fe chelate complex with substituents } R_1, R_2, R_3, R_4, R_5 \text{]}$$
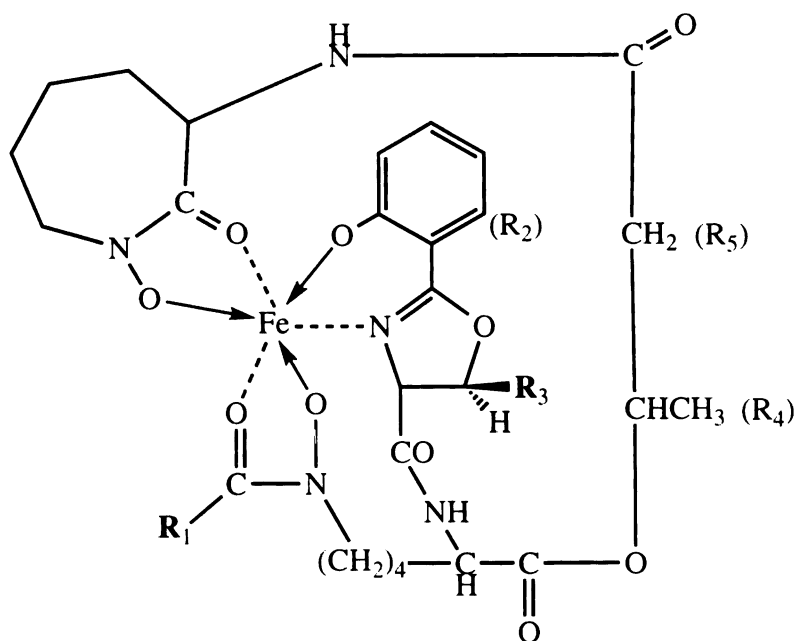
R_1		R_3	M_r
M. tuberculosis Exochelins:			
$(CH_2)_nCOOCH_3$	n = 3-9	H, CH_3	744-828
$(CH_2)_nCOOH$	n = 2-9	H, CH_3	730-814
$CH=CH(CH_2)_nCOOCH_3$	n = 3-5	H, CH_3	770-812
$CH=CH(CH_2)_nCOOH$	n = 3,6	H, CH_3	770,798
M. tuberculosis Mycobactins:			
$(CH_2)_nCH_3$	n = 16-19	H	882-924
$CH=CH(CH_2)_nCH_3$	n = 13-16	H	880-922

Figure 2.6 General structure of exochelins and mycobactins of

M. tuberculosis. Major structural difference betweeen exochelins and mycobactins of *M. tuberculosis* is at R_1, as detailed. In the case of exochelins, R_1 exists as either a saturated methyl ester [$R_1 = (CH_2)COOCH_3$] or a singly unsaturated alkyl methyl ester [$R_1 = (CH_2)_x(CH=CH(CH_2)_yCOOCH_3]$. R_1 is contained in fragment **F** in Figure 2.5. In the case of mycobactins, R_1 exists as either a saturated or an unsaturated alkyl group (Snow 1970).

2.1.4 DISCUSSION

Exochelins and mycobactins, the two high-affinity iron-binding molecules of *M. tuberculosis*, share a common core structure (see Fig 2.6). However, exochelins are smaller than mycobactins owing to a shorter alkyl side chain which terminates in a methyl ester or free acid. These differences render exochelins more polar than mycobactins and likely explain their water solubility. The less polar mycobactins, in contrast, are virtually insoluble in water. The water solubility of exochelins allows these molecules to function as iron-binding molecules in the extracellular milieu of the organism in the host.

That exochelins and mycobactins are so closely related suggests that their core structure is synthesized by a common set of enzymes and that subsequent reactions at R_1 determine whether the final product is an exochelin or a mycobactin. Possibly, one of the molecules is derived from the other or even readily exchangeable through a simple fatty acyl exchange reaction.

Our ability to purify exochelins allows analysis not only of their composition and structures but also of their role in the physiology of *M. tuberculosis* and the pathogenesis of tuberculosis. Among other issues, the role of exochelins in the infected host remains to be clarified. It seems likely that exochelins are required for multiplication of *M. tuberculosis* in extracellular sites of the host such as lung cavities where free iron is undoubtedly very limited. Consequently, the organism must scavenge iron from high-affinity host iron-binding compounds. In support of this concept, our collaborators at UCLA (M. Horwitz) have recently determined that desferri-exochelins rapidly remove iron from human transferrin, whether it is 95% iron saturated or 40% iron saturated, as in human serum. Moreover, they have demonstrated that desferri-exochelins acquire iron from iron-saturated lactoferrin and ferritin. Studies in this laboratory indicate that ferri-exochelins donate iron to desferri-mycobactins in the cell wall of live *M. tuberculosis* organisms. These studies provide evidence for the concept that exochelins may function by

48

transferring iron from human iron-binding proteins to mycobactins in the *M. tuberculosis* cell wall (Gobin and Horwitz 1996).

Whether exochelins are required for intracellular multiplication of *M. tuberculosis* in host mononuclear phagocytes is less certain. *Legionella pneumophila*, another intracellular bacterial parasite and lung pathogen, evidently lack siderophores and yet multiplies in its phagosome in mononuclear phagocytes (Byrd and Horwitz 1989). *L. pneumophila* derives its iron from the intermediate labile iron pool of the mononuclear phagocyte, which in turn obtains iron from iron-transferrin via transferrin receptors, and intracellular ferritin, which recycles iron to the pool (Byrd and Horwitz 1989; Byrd and Horwitz 1991; Byrd and Horwitz 1993). It is possible that *M. tuberculosis*, which has a relatively low requirement for iron for optimal multiplication on artificial medium in comparison with *L. pneumophila* (1 vs. 20 mM), also obtains iron intracellularly without the need for a siderophore. However, *L. pneumophila* and *M. tuberculosis* reside in markedly different phagosomes within the host cell (Clemens and Horwitz 1995) and the availability of iron in these two compartments may differ.

2.2 *M. avium* Exochelins

2.2.1 INTRODUCTION

Mycobacterium avium is a slow-growing mycobacterium and an important human pathogen. Because *M. avium* is one of the most common opportunistic pathogens in AIDS, the prevalence of *M. avium* infection has skyrocketed in recent years (Inderlied et al. 1993). Like many pathogens, *M. avium* produces high-affinity iron-binding molecules known as siderophores to help it acquire iron in the host (Matzanke 1991). Although both our group and Lane *et al.* (Lane et al. 1995) found that the core structure of the exochelins

of *M. avium* resemble the mycobactins, the results of our two groups differ with respect to the R_1 alkyl side chain, which critically influences the water solubility of exochelins and allows them to function in the extracellular environment. Whereas we previously had reported that the R_1 alkyl side chain of the exochelins of *M. tuberculosis* exists in both a saturated and unsaturated form that terminates predominantly as a methyl ester but additionally as a free carboxylic acid (Gobin et al. 1995), Lane *et al.* reported that the R_1 group of the *M. avium* exochelins exists exclusively in unsaturated forms terminating with a carboxylic acid moiety (Lane et al. 1995). Here, we describe the purification of exochelins from a type strain of *M. avium* (ATCC no. 25291) and their characterizations by mass spectrometry. We show them to exist in both saturated and unsaturated forms that terminate in either a free carboxylate or methyl ester, but otherwise to be identical to the mycobactins produced in the same strain. In addition, we demonstrate the ready conversion of exochelins from the methyl ester to carboxylic acid form by esterase treatment.

2.2.2 MATERIALS AND METHODS

2.2.2.1 *Medium and Reagents*

Modified iron-deficient Sauton's broth medium (Eidus and Hamilton 1964) was prepared (1 µM iron, no Tween).

2.2.2.2 *Bacteria*

The *Mycobacterium avium* type strain (ATCC no. 25291) used in this study was cultured in modified Sauton's medium in 1.9 L tissue culture flasks, 300 ml per flask.

without shaking at 37°C in 5% CO_2/95% air for 3, 6, 8, or 10 weeks (Gobin et al. 1995).

The bacteria were grown in iron-deficient broth to enhance exochelin production.

2.2.2.3 Purification of Exochelins

Exochelins and mycobactins were purified as previously described (Gobin et al.

1995). For exochelins, the culture supernatant fluid (final pH 6.5) was saturated with iron,

and ferri-exochelins were extracted into chloroform at the same pH, unless otherwise

specified. The chloroform extract was dried and the exochelins were dissolved in 100%

H_2O/ 0.1% TFA and purified by reverse-phase HPLC on a Vydac C_{18} column (4.6 mm x

25 cm; Western Analytical, Temecula, CA) with a 50-100% buffer B gradient at a flow rate

of 1 ml/min (buffer B = 50% acetonitrile/0.1% TFA). Individual exochelins were further

purified on an alkyl phenyl column (Waters, Bedford, MA). Ferri-exochelins were

identified in the HPLC eluate by their high 450 nm absorbance, and confirmed by MS.

2.2.2.4 Mass Spectrometric Analysis

For structural characterization, peaks isolated from the HPLC were first subjected

to mass analysis by LSIMS using MS-1 on a four-sector mass spectrometer (Kratos

Concept II HH, Kratos Analytical, Manchester, England) as described in detail elsewhere

(Gobin et al. 1995). Tandem MS was performed on the desferri molecular ion forms,

$(M+H)^+$, of exochelins, as well as mycobactins from the same strain, using both MS-1 and

MS-2 of a four-sector Kratos mass spectrometer. All spectra were recorded and mass

assigned using a scanning array detector and Mach3 data system.

ESI-MS was conducted in the positive-ion mode using a VG Platform II

(Manchester, England) quadrupole mass spectrometer. HPLC fractions containing

exochelins were dried down under vacuum, dissolved in the running buffer (50%

acetonitrile/ 1% acetic acid), and a 4 μl sample was injected via a Rheodyne injector into a

constant stream of running buffer flowing at a rate of 20 μl/min.

2.2.2.5 *Esterase Reaction*

The presence of methyl ester forms of exochelins was confirmed by treating them

with rabbit liver esterase (Aldrich). For these experiments, exochelins ($\approx$ 100 μg) were

dissolved in 50 μl of 50% acetonitrile followed by the addition of 0.5 ml of 50 mM Tris

(pH 8.5). Rabbit liver esterase (6.8 mg protein, 0.74 units) was added and the mixture

was incubated for 2 hr at 37°C. Additional rabbit liver esterase (6.8 mg protein, 0.74 units)

was added for an additional 3 hr. The reaction mixture was pre-purified on a C_{18} Sep-Pak

cartridge (Waters, Millipore). Exochelins eluted with 50% acetonitrile/ 0.1% TFA. The

sample was concentrated under vacuum and then loaded onto a Vydac C_{18} column and

separated by HPLC with a 15-70% buffer B (70% acetonitrile/ 0.08% TFA) gradient at a

flow rate of 4 ml/min.

2.2.3 RESULTS

2.2.3.1 *The M. avium Exochelin Family*

Reverse-phase HPLC analysis revealed a large family of *M. avium* exochelins in

the chloroform extracts of culture filtrates. The approximately 20 peaks that eluted off the

C_{18} column with a high 450 nm absorbance (see Fig 2.7) were tentatively identified as

exochelins from their absorbance spectra. As with the exochelins of *M. tuberculosis*,

LSIMS analysis of each peak revealed an ion pair differing in mass by 53 Da,

corresponding to protonated $(M+H)^+$ and iron $(M-2H+Fe^{III})^+$ adducts of the same molecular

species. The exochelins can be grouped into two distinct saturated and unsaturated series.

52
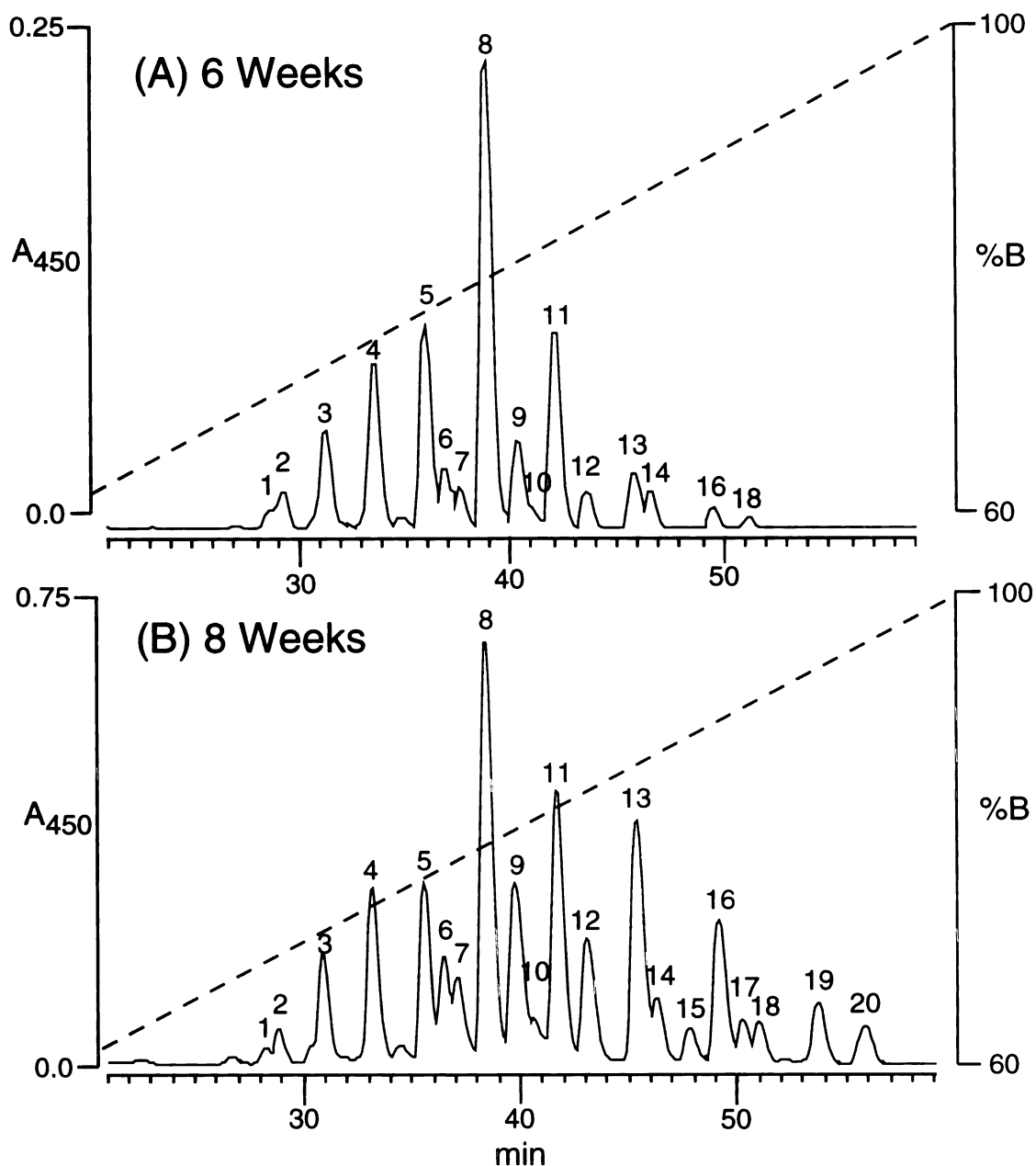
Figure 2.7 **Elution profile of (A) 6-week and (B) 8-week culture filtrate from *M.***
***avium* type strain ATCC no. 25291.** Each preparation was obtained by chloroform

extraction of a 400-ml culture filtrate and separated on a C_{18} HPLC column. Iron-

binding molecules were monitored at 450 nm. The dashed line represents the

concentration of buffer B. Peaks are numbered in the order of their elution off the

HPLC column and are further characterized in Table 2.2.

further subdivided into acid and methyl ester forms, based on their masses, HPLC retention times, and tandem MS spectra (to be discussed later). Within a series, exochelins differed from one another in mass by 14 Da (ΔCH_2) and between series, saturated and unsaturated exochelins of the same form and side chain length differed from one another in mass by 2 Da (CH_2-CH_2 vs. CH=CH) (see Table 2.2).

2.2.3.2 *Characterization of exochelins of M. avium*

Culture filtrates were extracted under both neutral and acidic conditions (pH 7 and 4) to evaluate the possibility that exochelins might undergo degradation or preferential extraction under these different pH regimens. However, no significant differences were found in the chromatogram patterns of exochelins extracted under the two different pH conditions (data not shown). The HPLC pattern of exochelins released into the culture medium changed significantly between 6 and 8 weeks of incubation (see Fig 2.7). The major change was a relative increase in the quantity of later eluting exochelins. Subsequent mass spectrometric analysis of the HPLC peaks from each harvest revealed a significant increase in the amount of exochelins terminating in methyl esters. Quantitatively, more exochelins were recovered from the 8-week (8.3 mg/l) than the 6-week culture (1.2 mg/l).

To characterize their structures further, I analyzed individual exochelins by tandem MS (see Fig 2.8). The similar fragmentation patterns of the *M. avium* and *M. tuberculosis* exochelins confirmed that they share a common core structure, similar to the core structure of mycobactins (see Fig 2.9). The fragment ions resulted from cleavages about the amide or ester bonds and were assigned to the structural moieties A-F (see Fig 2.8). The main differences between the exochelins of *M. avium* and *M. tuberculosis* are in the alkyl substituents present in the β-hydroxy acid (B), oxazoline (D), and acylalkyl acid or methyl ester (F) moieties. As a result, the various exochelins had analogous fragment ions, with those ions containing different alkyl moieties shifted in mass. Unlike *M. tuberculosis*,

TABLE 2.2. Molecular Masses (Da) of *M. avium* Exochelins in HPLC Peaks

HPLC Fraction Number[a]	$R_1 = (CH_2)_nCOOR$		$R_1 = CH=CH(CH_2)_nCOOR$	
	R = H	R = CH$_3$	R = H	R = CH$_3$
1	745[b], n=1			
2	759, n=2			
3	773, n=4			
4	787, n=4			
5			785, n=2	
6	801, n=5			
7		773, n=2		
8			799, n=3	
9		787, n=3		
10	815, n=6			
11			813, n=4	
12		801, n=4		
13				799, n=2
14			827, n=5	
15		815, n=5		
16				813, n=3
17	843, n=8			
18			841, n=6	
19				827, n=4
20	857, n=9		855, n=7	

The column spanner over all four data columns reads: $(M - 2H + Fe^{III})^+$

[a] see Figure 2.7 for HPLC elution positions of peaks 1-20

[b] masses of iron-loaded exochelins are reported as their molecular ions as observed under positive-ion LSIMS conditions (see text).

Each exochelin peak was observed as an ion-pair, $(M+H)^+$ and $(M-2H+Fe^{III})^+$, differing in mass by 53 Da. Assignments were confirmed by tandem MS analysis (as shown in Fig 2.8).

55

Figure 2.8 Tandem mass spectrometry under collision-induced dissociation conditions of isobaric *M. avium* exochelins with (M+H)⁺ at *m/z* 734.3 terminating in a (A) carboxylic acid and (B) methyl ester form. These exochelins correspond to peaks 4 and 9 (Table 2.2). *(upper)* Fragment ions of the exochelins are assigned to one of six structural moieties (**A-F**) within these two compounds as described in the text. *(lower)* On the mass spectra, hydrogen transfers relative to the neutral molecule are indicated by +1, +2, or +3.

(A) Exochelin M$_r$ 733.3
Carboxylic Acid

(M+H)$^+$ = 734.3

57

(B) Exochelin M, 733.3
Methyl Ester

$(M+H)^+ = 734.3$

R₁		R₃	M_r
M. avium Type strain Exochelins:			
$(CH_2)_nCOOCH_3$	n = 2-5	CH_3	772-814
$(CH_2)_nCOOH$	n = 1-9	CH_3	744-856
$CH=CH(CH_2)_nCOOCH_3$	n = 2-4	CH_3	798-826
$CH=CH(CH_2)_nCOOH$	n = 2-7	CH_3	784-854
M. avium Type strain Mycobactins:			
$(CH_2)_nCH_3$	n = 14,18	CH_3	896,924
$CH=CH(CH_2)_nCH_3$	n = 11-14	CH_3	880,894,922
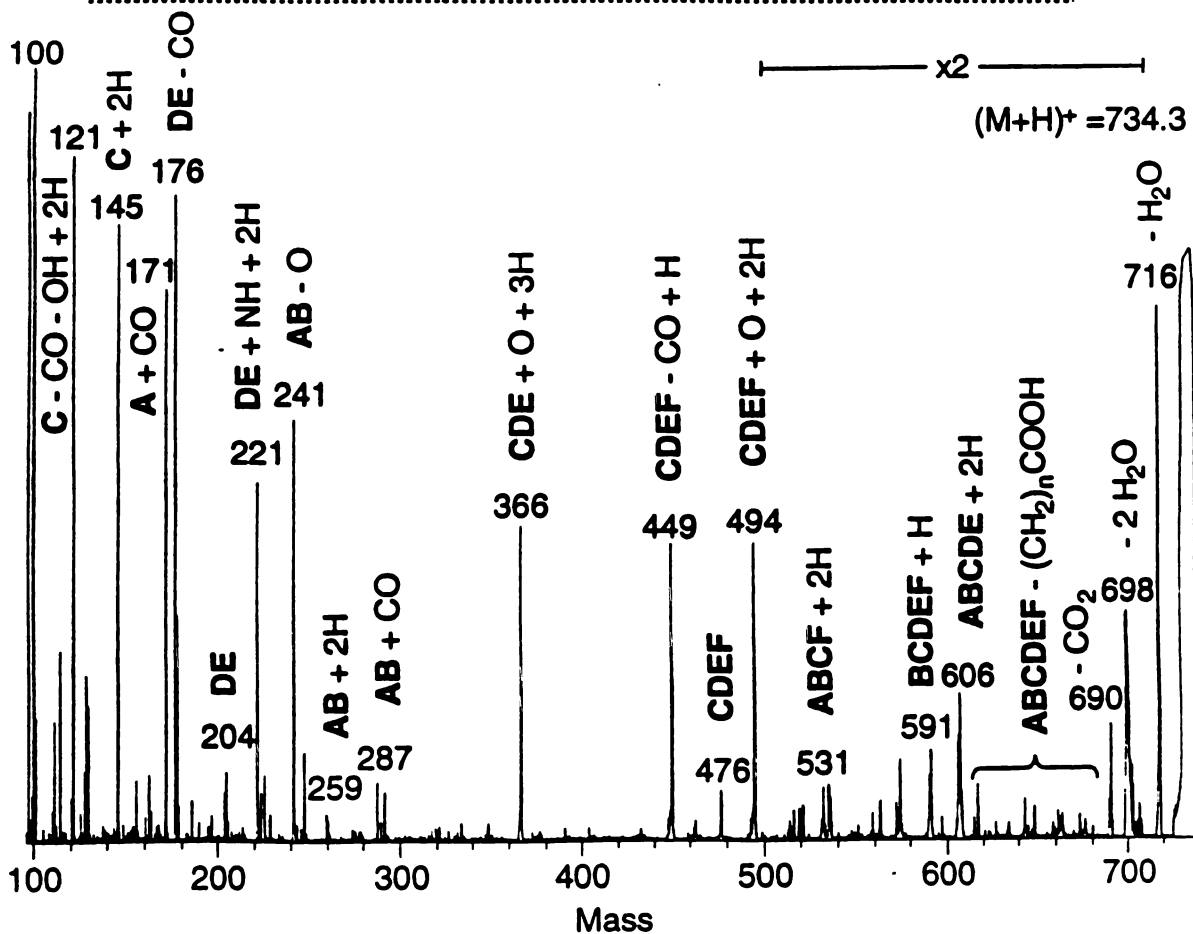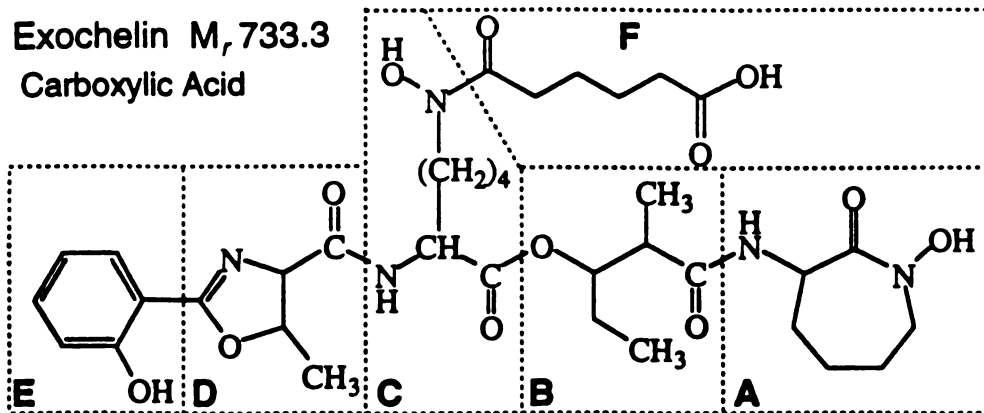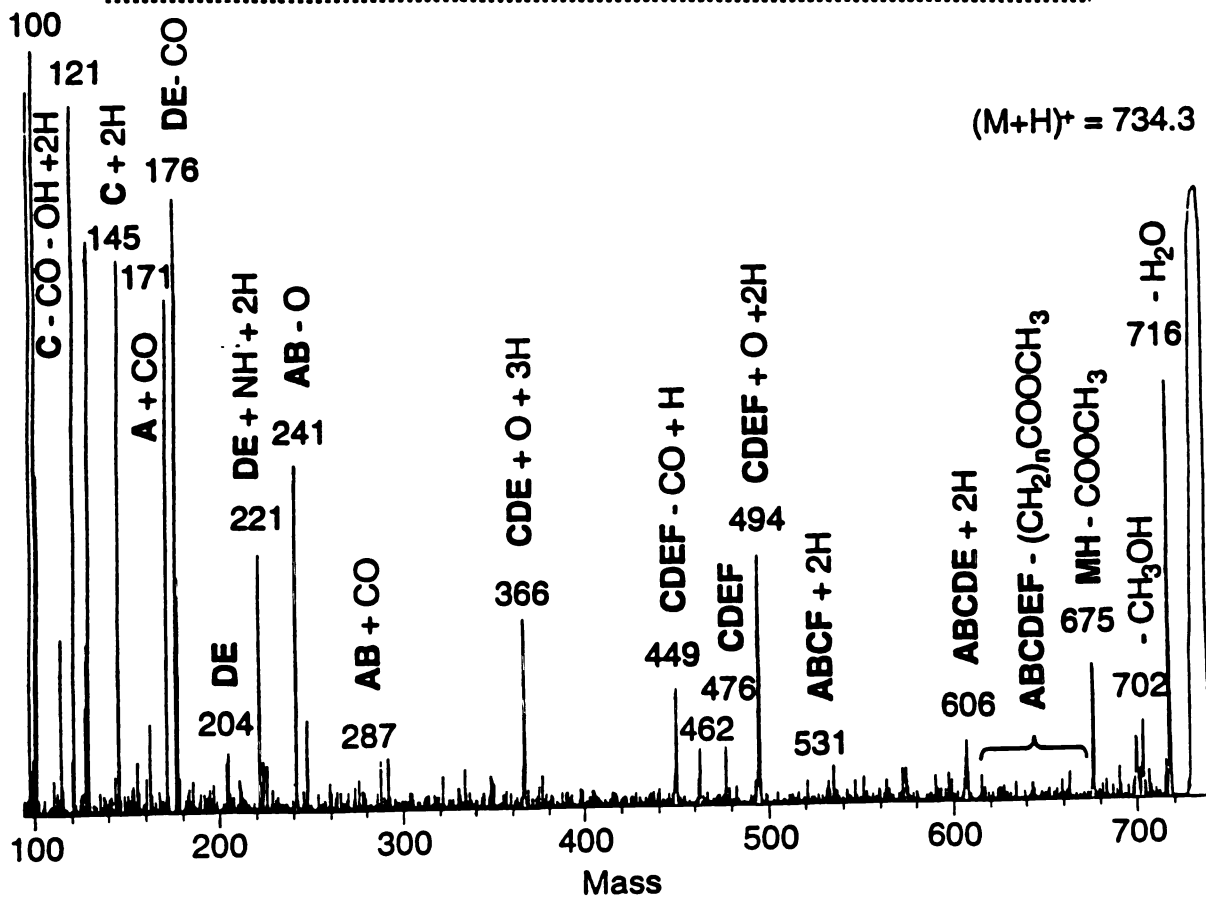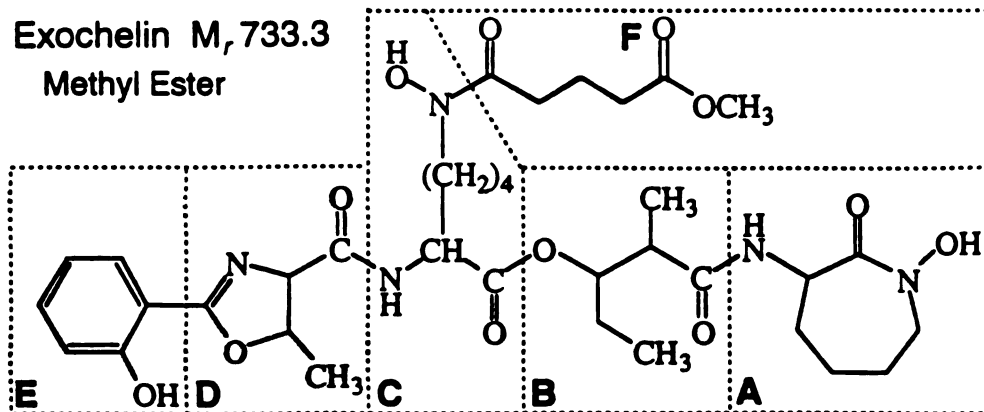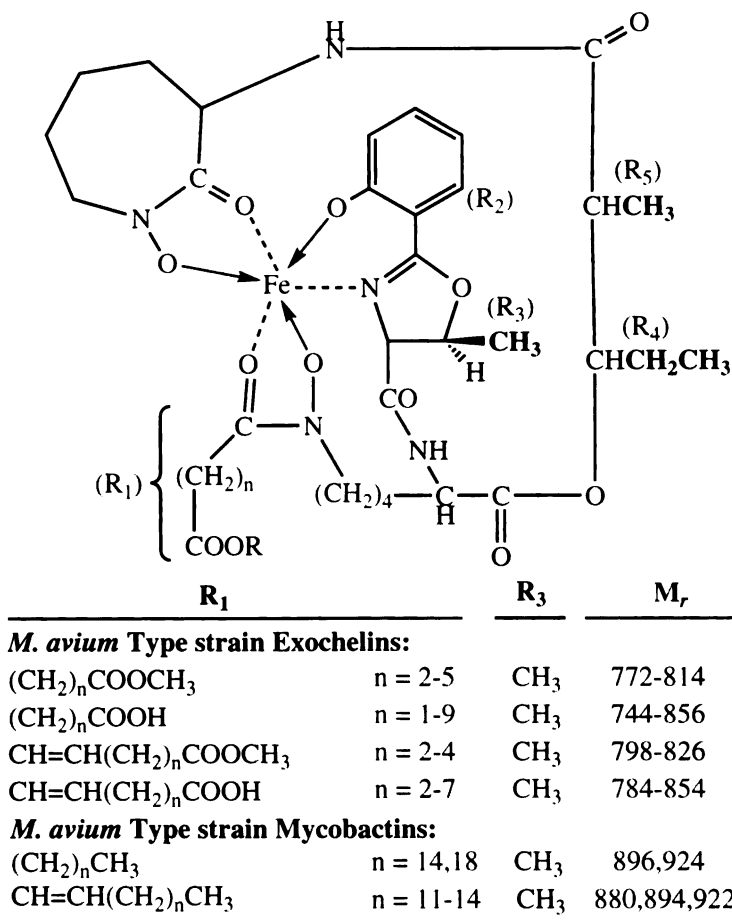
Figure 2.9 General structure of exochelins and mycobactins from M. avium Type strain (ATCC no. 25291). Exochelins contain an R_1 moiety that is either a saturated alkyl methyl ester or free acid, or singly unsaturated alkyl methyl ester or free acid. In a report on exochelins of M. avium strain CR1/69, Lane et al. (Lane et al. 1995) found only the unsaturated, free acid form with n = 3-9 and M_r = 798-882. Tandem MS data of the exochelins of the M. avium Type strain is consistent with R_4 = ethyl and R_5 = methyl, as reported for M. avium CR1/69 (Lane et al. 1995). The preliminary structures of M. avium mycobactins from the Type strain are listed based on tandem MS data. In an earlier report on M. avium mycobactins, Barclay et al. (Barclay et al. 1985) found R_2, R_4, and R_5 to be the same as noted in the figure, but R_3 = H and R_1 is an unsaturated straight chain fatty acid of undetermined length. M. tuberculosis exochelins contain a similarly short R_1 group that also terminates in a carboxylic acid or methyl ester, but differ from M. avium exochelins in the distribution and length of the R_1 group, the oxazoline substituents (R_3 = H or CH_3), and the substituted β-hydroxy acid (R_4 = CH_3 and R_5 = H) (Gobin et al. 1995).

59

which has both serine and threonine containing exochelins (R_3 = H or CH_3), the exochelins from *M. avium* contain only threonine in the oxazoline ring state (R_3 = CH_3), an observation confirmed by amino acid analysis. Similarly, the peaks containing the ester linked **B** moieties were shifted up in mass by 28 Da ($\Delta M = C_2H_4$).

Although tandem mass spectrometric analysis of the $(M + H)^+$ peak yielded information only about the intact salicylic acid substituted oxazoline moiety (**DE**), tandem MS analysis of the $(MH + H_2O)^+$ peak, corresponding to the exochelin with the oxazoline ring hydrolyzed, yielded information about the individual **D** and **E** moieties. The loss of 121 Da, corresponding to salicylic acid (**E** + carbonyl), confirmed the structure of fragment **E** as a phenolic group and **D** as a cyclized threonine, eliminating the possibility that the **D** moiety was a cyclized serine and the **E** moiety a phenolic group with a meta-substituted methyl, as seen in some previously studied mycobactins (Snow 1970).

From the tandem MS analysis, the exochelins could be further categorized as acids or esters. Exochelins with a R_1 chain terminating in a methyl ester always demonstrated a characteristic loss of 32 Da, $(MH - CH_3OH)^+$, and a loss of 59 Da, $(MH - COOCH_3)^+$. In contrast, exochelins with a R_1 chain terminating in a free acid showed a loss of 44 Da, $(MH - CO_2)^+$. Within each of these classes, the exochelins differed in mass by multiples of 14 Da, reflecting different numbers of CH_2 groups on the R_1 alkyl side chain of the molecule. Tandem MS spectra of the two exochelins shown in Figure 2.8 have the same mass and differ only in that one has a terminal acid and the other an ester R_1 side chain.

The existence of exochelins with R_1 chains terminating in methyl esters was confirmed upon treatment of several of those exochelins with rabbit liver esterase. Over a period of several hours, the conversion of an ester-containing exochelin to a free acid form was monitored by HPLC (see Fig 2.10). Mass analysis revealed a mass difference of 14 Da between the original iron-loaded exochelin and esterase-treated form, i.e., $(M - 2H + Fe^{III})^+$ at *m/z* 798 and 784, respectively (see Fig 2.11). Tandem MS spectra of the desferri
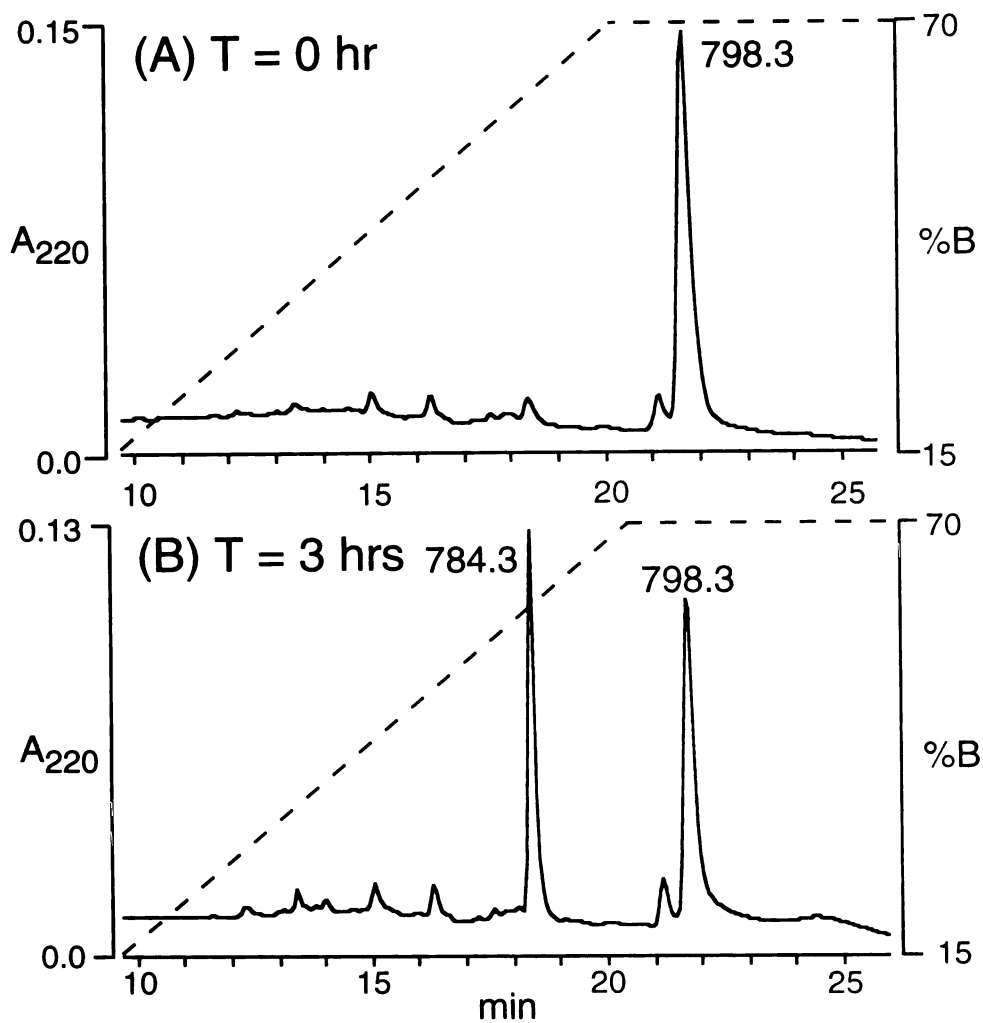
Figure 2.10 Esterase treatment of an *M. avium* exochelin. An exochelin of
mass 798 Da (peak 13, Table 2.2) was treated with rabbit liver esterase for 5
hrs. Progress of the reaction was monitored at 220 nm by reverse-phase
HPLC; (A) T= 0 hr, (B) T = 3 hrs. The conversion of the exochelin from the
methyl ester to free acid was confirmed by mass spectrometry (see text).
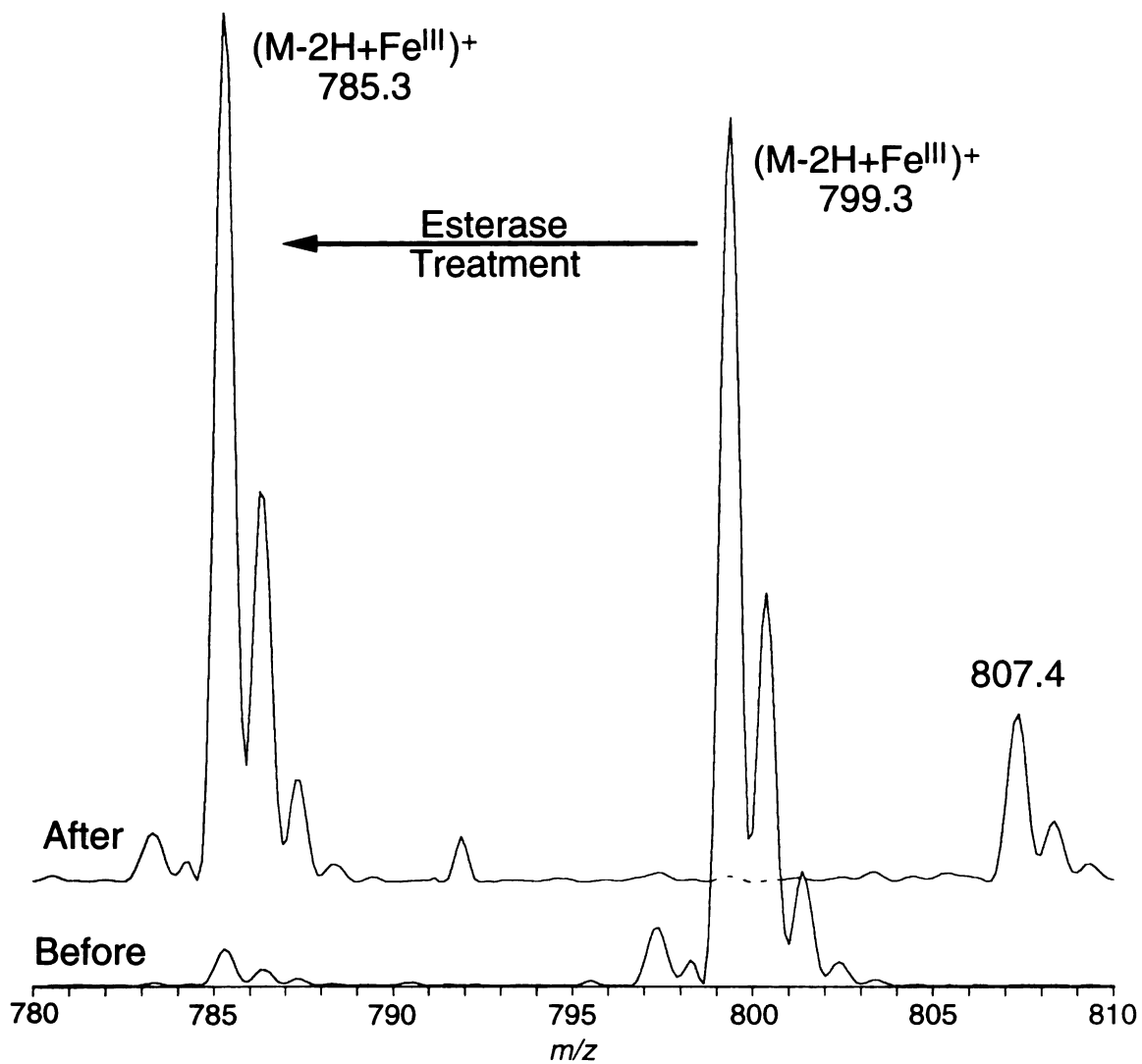
Figure 2.11 Positive-ion electrospray spectra of *M. avium* exochelin treated with rabbit liver esterase. (A) Exochelin before treatment with esterase has a $(M-2H+FeIII)^+$ at m/z 799.3. (B) After incubation with esterase for 5 hours, the loss of the methyl ester is evident in the 14 Da shift to $(M-2H+FeIII)^+$ at m/z 785.3.

molecular ions of these two forms showed a distinct difference in the high mass neutral fragments associated with the R_1 group, loss of methanol and $COOCH_3$ for the original ester and loss of CO_2 for the lower mass esterase-generated form. This confirmed that the 14 Da loss was due to the conversion of the R_1 methyl ester to the free carboxylate.

2.2.4 DISCUSSION

As determined from these studies, the exochelins of *M. avium* are a complex group of siderophores whose structures are clearly related to the mycobactins (see Fig 2.9 and legend). This similarity strongly suggests a common biosynthetic pathway for the exochelins and mycobactins. As we have previously shown for *M. tuberculosis* (Gobin et al. 1995), the major structural difference between the exochelins and mycobactins of *M. avium* is the chemical composition of the R_1 group that is attached to ε-nitrogen of the ε-N-hydroxylysine. In mycobactins, the R_1 group consists of a simple long chain fatty acid that is saturated or unsaturated. An examination by tandem MS of the mycobactins produced by this same *M. avium* strain indicates that R_1 is a mixture of saturated and unsaturated fatty acids containing 14-19 carbons (see Fig 2.9). In exochelins, the R_1 group is a shorter chain fatty acid that similarly terminates in either a free acid or the corresponding methyl ester. Thus, in the two cases where structural data have been obtained on both exochelins and mycobactins isolated from the same strain (this study and our previous study on the exochelins of *M. tuberculosis* (Gobin et al. 1995)), the only difference between the exochelins and mycobactins is in their R_1 moieties.

Previously, Lane *et al.* isolated exochelins from *M. avium* strain CR1/69 under acidic conditions and found that the R_1 group terminates exclusively in a free carboxylic acid (Lane et al. 1995). These investigators suggested the name 'carboxymycobactins' to describe this group of exochelin compounds. Our data, however, clearly show that the R_1 group of *M. avium* exochelins exists in both saturated and unsaturated forms that terminate

63

as both free acids and methyl esters, analogous to the exochelins of *M. tuberculosis* (Gobin et al. 1995). Therefore, we propose that the original exochelin name remain the sole descriptor of these compounds and that they simply be referred to as saturated or unsaturated, or free acid or methyl ester forms.

The question of whether the free-acid forms of exochelins exist only as degradative products of the methyl ester analogs is still unclear, although we have observed that methyl ester hydrolysis occurs less readily than the hydrolysis of the oxazoline moiety (**D**), which we have not observed under neutral extraction conditions. When we extracted the exochelins under the acidic conditions used by Lane *et al.* (Lane et al. 1995), we did not observe a change in the relative proportion of free acid to ester forms. Nonetheless, the methyl ester forms of exochelins will convert to their carboxylic acid analogs during prolonged storage (Gobin et al. 1995), or after brief treatment with esterases. The biological significance of the ester-to-acid conversion, and whether both forms are present during disease remain an intriguing but unanswered question.

2.3 *M. bovis* and *M. bovis* BCG Exochelins

2.3.1 INTRODUCTION

The exochelins of *Mycobacterium bovis* and its attenuated descendant Bacille Calmette-Guérin (BCG) have not been previously characterized. Given that *M. bovis* is less pathogenic in humans than *M. tuberculosis* and *M. avium*, a question could be posed as to whether or not exochelin and/or mycobactin production may be in some way related to this decrease in virulence. Therefore, in this study, we sought to isolate and characterize the exochelins of *M. bovis* and *M. bovis* BCG by mass spectrometry.

M. bovis is a slow-growing mycobacterium that belongs to the *Mycobacterium tuberculosis* complex (*M. africanum*, *M. bovis*, *M. microti*, *M. tuberculosis*, and *M. ulcerans*). *M. bovis* is highly related to *M. tuberculosis* on the basis of DNA homology (Wayne 1984). *M. bovis* derives its importance from several factors. First, as the primary causative agent of bovine tuberculosis, it is of major commercial importance to the cattle and dairy industry. Second, it can cause human tuberculosis. However, with the advent of pasteurization, such cases in immunocompetent individuals are now rare. However, HIV-infected persons appear to be at increased risk for such disease (Bouvet et al. 1993; Organization 1994; van Soolingen et al. 1994; Samper et al. 1997). Third, *M. bovis* strain BCG remains the only currently available vaccine against tuberculosis. Although its efficacy has been questioned, the live vaccine has been administered to nearly 3 billion people since 1945 (Colditz et al. 1994). BCG is also administered intravesicularly in the treatment of bladder cancer. In rare cases, BCG can cause serious and sometimes fatal disseminated disease in immunocompromised persons (Lotte et al. 1984; Colditz et al. 1994; Gobin et al. 1995; Casanova et al. 1996; Gobin and Horwitz 1996).

2.3.2 MATERIALS AND METHODS

2.3.2.1 *Medium and Reagents*

Modified iron-deficient Sauton's broth medium was prepared with 1 μM Fe^{+3} and without Tween.

2.3.2.2 *Bacteria*

We selected for study the *M. bovis* type strain (ATCC no. 19210) and 5 BCG substrains of different geographic origin that are currently being used by pharmaceutical

companies in vaccines or for research purposes: Copenhagen (ATCC no. 27290), Glaxo (ATCC no. 35741), Japanese (ATCC no. 35737), Pasteur (ATCC no. 35734), and Tice (ATCC no. 35743). We cultured them in 1.9 liter tissue culture flasks, 300 ml per flask, without shaking at 37°C in 5% CO_2-95% air for 3 to 8 weeks (Gobin et al. 1995). The bacteria were grown in iron-deficient medium to enhance exochelin production.

2.3.2.3 Purification of Exochelins

We purified the exochelins as previously described (Gobin et al. 1995). Briefly, the supernatant fluid was saturated with iron, and ferri-exochelins were extracted into chloroform. The chloroform extract was dried and the exochelins were purified by reverse-phase HPLC on a C_{18} column (Vydac, Western Analytical, Temecula, CA) with a 50-100% gradient of buffer B (50% acetonitrile/ 0.1% TFA) at a flow rate of 1 ml/min. Individual exochelins were further purified on an alkyl phenyl column (Waters, Bedford, MA) using the same buffers and flow rate.

2.3.2.4 Mass spectrometric analysis

Peaks isolated from the HPLC and identified as potential exochelins were first subjected to mass analysis by MALDI MS. For these experiments, a Voyager linear time-of-flight mass spectrometer (Perseptive Biosystems, Framington, MA) equipped with a 337 nm N_2 laser was used. *M. bovis* exochelins were analyzed using delayed extraction conditions as described by Vestal *et al.* (Vestal et al. 1995). The improved optics of delayed extraction allowed for increased resolving power (1500 M/ΔM) and isotopic resolution of the exochelin molecular ions. Data was recorded with a 500 MHz Tektronix digitizer. Samples were concentrated under vacuum and small aliquots (1 µl) were mixed 1:1 with the matrix (saturated solution of α-cyano-4-hydroxycinnamic acid (Aldrich) in

70% acetonitrile/ 0.1% TFA). The instrument was externally calibrated using a mixture of standard peptides consisting of angiotensin II and bombesin with monoisotopic molecular ions of 1046.54 and 1619.82 Da, respectively.

The exochelins of *M. bovis* were further analyzed by collision-induced dissociation (CID) on a Micromass Autospec orthogonal acceleration time-of-flight (TOF) mass spectrometer (Micromass Inc., Manchester, UK) equipped with a N_2 laser (337 nm). After the MS-1 is tuned manually to transmit the ^{12}C-monoisotopic ion of the precursor mass, a two stage deceleration electrostatic lens focuses the ions into an approximately parallel beam before they enter the gas collision cell. The collision cell is filled with Xe gas with a collision energy of 800 eV. Voltage applied periodically from a "push-out" electrode extracts the precursor and product ions into a linear TOF mass analyser. All spectra were recorded with a microchannel plate detector using a time-to-digital converter (TDC) (Precision Instruments, Knoxville, TN) (Medzihradszky et al. 1997). Small aliquots of sample (1 µl) were mixed 1:1 with the matrix [saturated solution of 2,5-dihydroxybenzoic acid (Aldrich) in acetone]. Calibration of the CID spectra was accomplished using the fragment ions formed from a standard peptide (Renin).

The exochelins of *M. bovis* BCG were also analyzed by tandem mass spectrometry but in this case, using LSIMS with a four-sector Kratos mass spectrometer spectrometer (Kratos Concept II HH, Kratos Analytical, Manchester, England) as previously described (Gobin et al. 1995). The collision cell was filled with He and floated at 2 keV for a collision energy of 6 keV. Samples were ionized using a LSIMS source operating with Cs^+ in the positive-ion mode. Small aliquots of the sample (1-5 µl) were transferred to the LSIMS probe along with 1 µl of thioglycerol/glycerol (1:1, vol/vol) matrix. All spectra were recorded and mass assigned using a scanning array detector and Mach3 data system (Walls et al. 1990).

2.3.3 RESULTS

2.3.3.1 *Characterization of the exochelins of M. bovis*

As with *M. tuberculosis*, the chloroform filtrate of cultures of the *M. bovis* type strain contained a large family of exochelins. Over 20 peaks exhibiting a high 450 nm absorbance eluted from a C_{18} reverse-phase HPLC column (see Figure 2.12). Based on the similarity of their elution pattern to exochelins from *M. tuberculosis* (Gobin et al. 1995), we tentatively identified 18 of these peaks as ferri-exochelins and subsequently confirmed that they were exochelins by mass spectrometric analysis (only the major peaks were analyzed). These results are summarized in Table 2.3. The pattern of elution was very similar at 3, 6, and 8 weeks of culture (data not shown). The yield was highest at 8 weeks (750 μg/l).

2.3.3.2 *Characterization of the exochelins of M. bovis BCG*

All 5 substrains of *M. bovis* BCG produced the same set of exochelins (see Fig 2.13). The overall yields of exochelins from the BCG strains were comparatively low - 75 μg/l for BCG Glaxo, 140 μg/l for BCG Copenhagen, 150 μg/l for BCG Japanese, 345 μg/l for BCG Pasteur, and 390 μg/l for BCG Tice vs. 750 μg/l for *M. bovis* type strain and 2-4 mg/l for *M. tuberculosis*. Furthermore, there was great variation in the relative quantities of individual exochelins. However, exochelins 773TM, 801SC, and 815SC were major species of all BCG strains. As discussed in section 2.1.3.2, these exochelins are named according to (a) their mass in daltons in the iron-loaded form, (b) whether R_3 is H (serine) (S) or CH_3 (threonine) (T), and (c) whether R_1 terminates in a methyl ester (M) or a carboxylate (C) moiety.

68
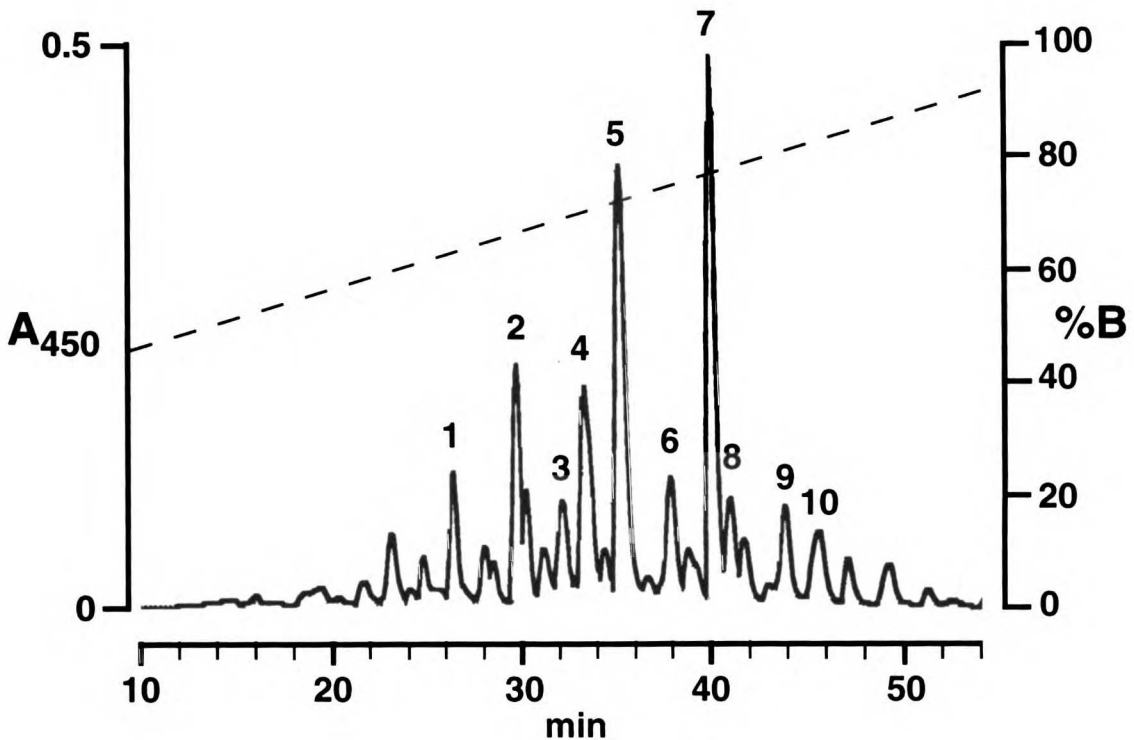
Figure 2.12 Elution profile of an 8-week culture filtrate from *M. bovis* type strain on a C$_{18}$ reverse-phase HPLC column. The chloroform extract of 1l of the *M. bovis* culture filtrate was loaded onto the column. Iron-binding molecules were monitored at 450 nm. The dashed line represents the concentration of buffer B. Each labeled peak was analyzed by mass spectrometry and shown to contain an exochelin (see Table 2.3).

TABLE 2.3. Molecular Masses (Da) of *M. bovis* Exochelins in HPLC peaks

$(M - 2H + Fe^{III})^+$

HPLC Fraction Number [a]	$R_1 = (CH_2)_n COOR$				$R_1 = CH=CH(CH_2)_n COOR$			
	$R_3 = H$		$R_3 = CH_3$		$R_3 = H$		$R_3 = CH_3$	
	$R = H$	$R = CH_3$	$R = H$	$R = CH_3$	$R = H$	$R = CH_3$	$R = H$	$R = CH_3$
1			745, n=3 / 759, n=4 / 773, n=5					
2								
3	773[b], n=6			759, n=3				
4		759, n=4	787, n=6					
5				773, n=4				
6		773, n=5						
7				787, n=5				
8								785, n=3
9			815, n=8			785, n=4		
10				801, n=6				799, n=4

[a] see Figure 2.12 for HPLC elution positions of peaks 1-10

[b] masses of iron-loaded exochelins are reported as their molecular ions as observed by MALDI mass spectrometry (see text). Each exochelin peak was observed as an ion-pair, $(M+H)^+$ and $(M-2H+Fe^{III})^+$, differing in mass by 53 Da. Assignments were confirmed by tandem MS analysis.

70

Figure 2.13   Elution profiles of 8-week culture filtrates from *M. bovis* substrains Copenhagen, Glaxo, Japanese, Pasteur, and Tice on a C_{18} reverse-phase HPLC column. The chloroform extract of 250 ml of each culture filtrate was loaded onto the column. Iron-binding molucules were monitored at 450 nm. Peaks 1, 2, and 3 correspond to exochelins 772TM, 800SC, and 814SC, respectively.
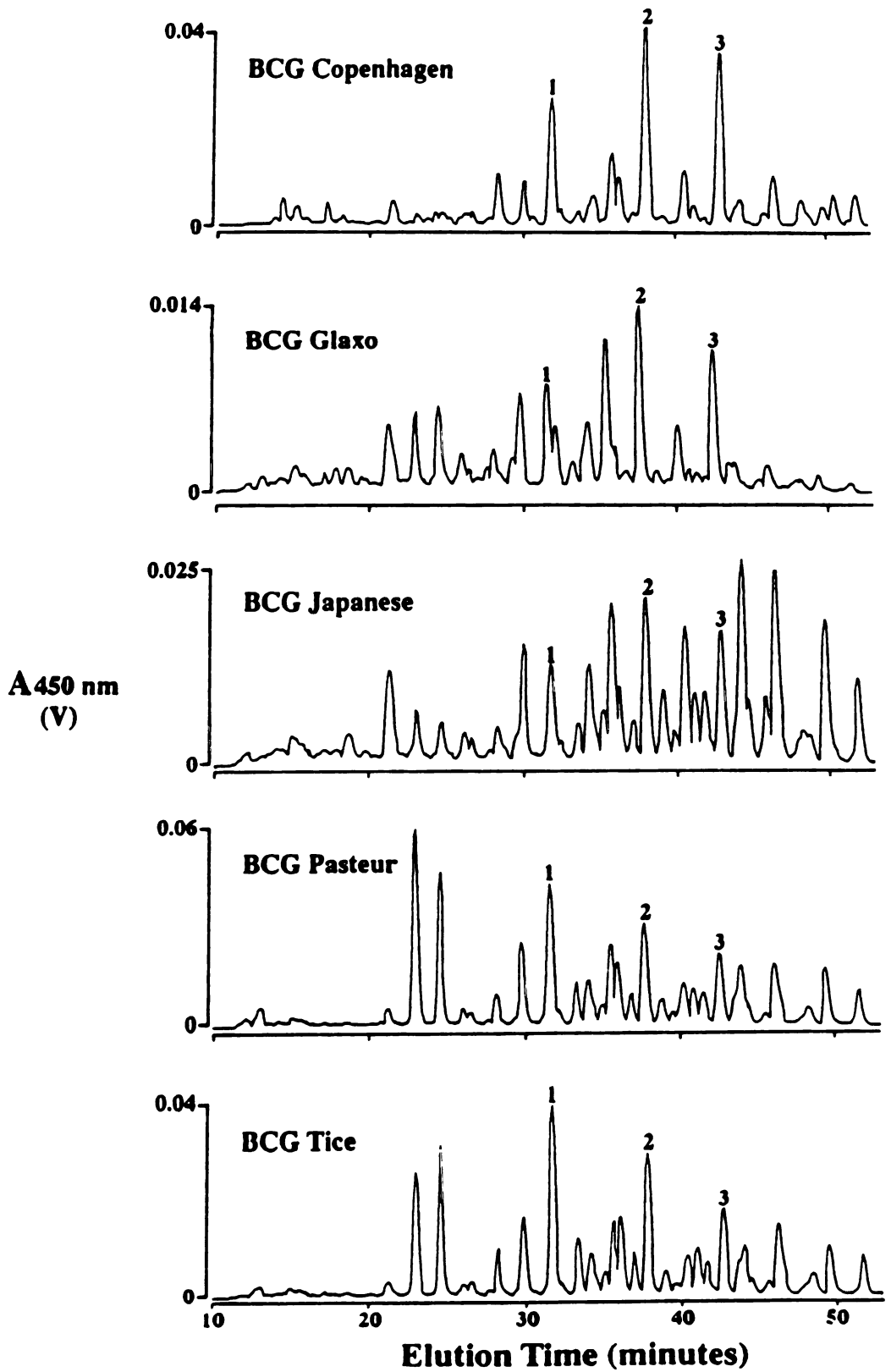
2.3.4 DISCUSSION

Mass spectrometric analysis confirmed that *M. bovis*, *M. bovis* BCG, and *M. tuberculosis* exochelins eluting at the same concentration of acetonitrile are structurally identical. As in the case of *M. tuberculosis*, the core structure of the exochelins of *M. bovis* and *M. bovis* BCG is identical to that of the mycobactins of the same species and contains 3 amino acid moieties - two N-hydroxylysines and either one serine or a threonine depending upon the absence or the presence of a methyl group at R_3 (see Fig 2.14). This core contains the functional groups that bind the iron atom. As in the case of *M. tuberculosis* and *M. avium*, the difference between the exochelins and mycobactins of *M. bovis* resides exclusively in the R_1 side group. The R_1 side chain of the *M. bovis* exochelins is either saturated or unsaturated and terminates with either a methyl or a carboxylic acid, as previously described for *M. tuberculosis* (Gobin et al. 1995) *and M. avium* (Wong et al. 1996).

This study demonstrates that the pathogenic mycobacteria *M. tuberculosis* and *M. bovis* produce the same set of iron-binding exochelins. Moreover, BCG, an attenuated strain of *M. bovis*, produces the same set of exochelins as the pathogenic mycobacteria *M. tuberculosis* and *M. bovis*. There are only two major differences between the exochelins of *M. tuberculosis* and *M. bovis*. One is in the overall amount of exochelins produced which correlates roughly with pathogenicity: *M. tuberculosis* > *M. bovis* > *M. bovis* BCG. The second is in the relative amounts of specific exochelin species produced, as each mycobacterial species and strain has its own unique pattern of exochelin production.

2.4 SUMMARY

The exochelins produced by the slow-growing, pathogenic strains *M. tuberculosis*, *M. avium*, and *M. bovis* were isolated, purified, and characterized. The exochelins
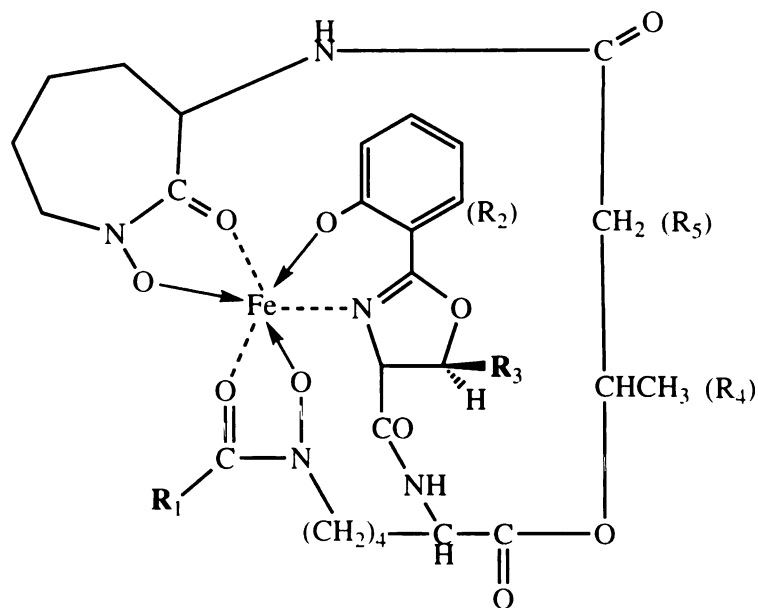
R$_1$		R$_3$	M$_r$
M. bovis Exochelins:			
(CH$_2$)$_n$COOCH$_3$	n = 3-6	H,CH$_3$	758-800
(CH$_2$)$_n$COOH	n = 3-8	H,CH$_3$	744-814
CH=CH(CH$_2$)$_n$COOCH$_3$	n = 3-4	H,CH$_3$	784-798

Figure 2.14 General structure of exochelins of *M. bovis* type strain. The exochelins of *M. bovis* differ from each other at R$_1$ and R$_3$. R$_1$ is either saturated or singly unsaturated and terminates with either a methyl ester (COOCH$_3$) or a carboxylic acid (COOH) moiety. R$_3$ is either H or CH$_3$. The exochelins of *M. bovis* and *M. tuberculosis* display the same variations at R$_1$ and R$_3$ and also are identical at R$_4$ and R$_5$. The exochelins of *M. avium* display the same variations at R$_1$ as *M. bovis* and *M. tuberculosis* but R$_3$ is always CH$_3$. In addition, *M. avium* differs from the other 2 species at R$_4$, which is CHCH$_2$CH$_3$, and R$_5$, which is CHCH$_3$.

produced by each species were found to be a family of iron-binding molecules ranging in mass from 730-828 Da, 744-856 Da, 744-800 Da for the iron-loaded species. Analysis of the exochelins by mass spectrometry revealed that all shared a common core structure with the mycobactins produced by their respective species, consisting of 3 amino acid moieties - 2 N-hydroxylysines and 1 serine/threonine. This suggests a common biosynthetic pathway for the exochelins and mycobactins. The main source of heterogeneity within each family lies in the R_1 alkyl chain. This is the only source of heterogeneity between the mycobactins and exochelins within the same strain. In the mycobactins, it exists as a very long fatty acid chain, accounting for its increased lipophilicity and association with the mycobacterial cell envelope. In contrast, the R_1 alkyl chain in the exochelins is a shorter alkyl chain (either saturated or unsaturated) which terminates in either a free acid or methyl ester. The core structure of the exochelins produced by *M. tuberculosis*, *M. bovis*, and *M. bovis* BCG were identical, containing both serine and threonine in moiety D. The *M. avium* exochelins were slightly different. Only threonine-exochelins were detected in the culture filtrate. In addition, the β-hyroxy acid of the *M. avium* exochelin contains an additional ethyl group (3-hydroxy-2-methyl-pentanoic acid), in comparison with the *M. tuberculosis* (3-hydroxybutyric acid) exochelins.

Knowledge of the composition and structure of exochelins may point to new strategies for interfering with their iron-acquiring function and hence growth of pathogenic mycobacteria in the host. This may in turn provide a rational basis for the design of drugs to combat tuberculosis.

Chapter 3. NMR Characterization of an exochelin from
M. tuberculosis

3.1 INTRODUCTION

The uptake of ferri-siderophore complexes of different organisms is known to be mediated by specific proteins located on the outer cell surface which are found in increased amounts when cells are grown under iron-deficient conditions. Proteins have been recently identified in several species of mycobacteria, designated as iron-regulated envelope proteins (IREPs), that may function as ferri-exochelin receptors (Barclay and Ratledge 1986; Wheeler and Ratledge 1994). Antibodies raised to the 29 kD IREP of *M. smegmatis* were shown to interfere with iron uptake into the cells. In addition, a possible receptor protein for exochelin uptake in *M. avium* recovered from animal infections was also discovered (Sritharan and Ratledge 1990).

From studies of siderophore transport systems in other bacteria, it has been found that the recognition of the structure of the ferri-siderophore complex is very important. Therefore, we performed NMR experiments on the *M. tuberculosis* exochelin in an attempt to construct a three-dimensional (3-D) model of the metal-bound structure. The direct analysis of ferri-exochelins by NMR is not possible since Fe^{+3} is paramagnetic (high spin d^5). The unpaired e^- causes fast-relaxation resulting in changes in chemical shift and severe line broadening. Therefore, a gallium-exochelin analog was used in these NMR studies since Ga^{+3} is similar in size to Fe^{+3} but is not paramagnetic. Although the solvent of choice for these studies is water due to its biological relevance, previous NMR structural studies on the exochelins produced by *M. smegmatis* reported problems in obtaining nuclear Overhauser enhancements (NOEs) in this solvent (Sharman et al. 1995). In this study, we report the complete NMR assignments of the desferri- and gallium-exochelins in DMSO-d$_6$.

3.2 MATERIALS AND METHODS

3.2.1 *Materials*

Synthetic desferri-exochelin

A desferri-exochelin sample was synthesized by SERES Laboratories, Inc. (Santa Rosa, CA). The synthetic scheme was modeled after that of Maurer *et al.* for the synthesis of mycobactin S2 (Maurer and Miller 1983).

3.2.2 *Methods*

3.2.2.1 *Preparation of gallium exochelin*

The gallium-exochelin analog was synthesized according to the procedure given by Snow *et al.* (Snow 1969). Excess $GaCl_3$ (Aldrich) was added to a solution of synthetic desferri-exochelin [2 mg (2.5 μmol) dissolved in 100 μl ethanol]. After 2.5 hrs at room temperature, the solvent was evaporated under a stream of nitrogen. The residue was redissolved in chloroform and washed several times with water (until the washings reached approximately pH 4). The chloroform solution was dried under a stream of nitrogen. The identity of the gallium-exochelin analog was confirmed by mass spectrometry.

3.2.2.2 *Nuclear magnetic resonance spectroscopy*

NMR tubes were prepared by washing with 50% HNO_3, 50 mM EDTA, and distilled water to rid them of iron. All one-dimensional (1-D) and two-dimensional (2-D) experiments were performed on an Omega 500 spectrometer at 35°C. The synthetic desferri-exochelin (1.4 μmol) and gallium-exochelin (2.5 μmol) were each dissolved in 0.4 mL of DMSO-d_6 (Sigma). The 1-D experiments were recorded with 16K data points (32 scans). The spectra were acquired while the desferri- and gallium-exochelin samples were

spinning and non-spinning, respectively. All spectra were referenced to the DMSO peak at 2.49 ppm. The large peak at 3.27 and 3.30 ppm in the desferri- and gallium-exochelin spectra, respectively, corresponds to the HOD peak.

The phase-sensitive double-quantum filtered COSY (DQF-COSY) spectrum (Rance et al. 1983) was acquired with time-proportional phase incrementation of the first pulse (Redfield and Kuntz 1975; Marion and Wuthrich 1983). The data matrices for the desferri- and gallium-exochelin spectra consisted of 512×4096 data points, acquired with 16 scans per t_1 value and a spectral width of 6514.66 Hz. The data matrices were apodized with a 45°-shifted sine-bell wave function in both dimensions and zero-filled in the second dimension to produce a 1024×4096 real data matrix.

The 2-D homonuclear Hartmann-Hahn (HOHAHA) spectra were obtained using the MLEV-17 sequence (Bax and Davis 1985a) and quadrature detection (States et al. 1982). A spectral width of 6514.66 Hz was used with mixing times of 100 ms for both the desferri-exochelin (spinning) and gallium-exochelin (non-spinning) experiments. Data matrices of 512×4096 were acquired for both samples. Both spectra were recorded with 16 scans per t_1 increments, and the matrices were apodized with Gaussian window functions in both dimensions and zero-filled in the second dimension to give final 1024×4096 matrices.

The rotating-frame Overhauser effect spectroscopy experiments (ROESY) were acquired non-spinning in the phase-sensitive mode (Bothner-By et al. 1984; Bax and Davis 1985b). For the desferri-exochelin, a 175 ms mixing time and 3.8 s interscan delay was used. For the gallium-exochelin, mixing times of 100 and 175 ms were used with a 3.7 s interscan delay. The spectral width was 6514.66 Hz and the data matrices contained 512×4096 data points with 32 scans per t_1 value. The matrices were apodized with Gaussian window functions in both dimensions and zero-filled in the second dimension to give final 1024×4096 matrices.

All data was processed using Striker software and displayed using Sparky software. Both programs were developed by the NMR facility at the University of California, San Francisco (Basus et al. 1988; Day and Kuntz 1993; Kneller and Kuntz 1993).

3.3 RESULTS

3.3.1 *Synthetic desferri-exochelin sample*

Previous studies have shown that the exochelins produced by *M. tuberculosis* are actually a family of iron-binding molecules which share the same core structure (Gobin et al. 1995). The exochelin can be divided into 6 structural moieties, including 2 N-hydroxylysines and 1 serine or threonine, depending on the presence or absence of a methyl group in the oxazoline moiety (D) (see Fig 3.1). As previously described in Chapter 1, we have devised a nomenclature to describe the structural elements of the exochelins that divide into 6 parts, A - F. This scheme is summarized in Figure 3.1. Most of the structural heterogeneity lies in the N-hydroxyl-substituted fatty acyl group (F) of the exochelin. Moiety F, which will also be referred to as the R_1 alkyl chain, is a long aliphatic chain (saturated or unsaturated) which terminates in either a free acid or methyl ester. In the beginning of our studies, it proved difficult to purify a significant amount of a single *M. tuberculosis* exochelin in its iron-free form. In addition to problems with co-eluting exochelins during the HPLC purification, a significant amount was being lost in the iron removal process (to be discussed later). Therefore, a synthetic desferri-exochelin was procided by Keystone Biomed Inc. (Los Angeles, CA). The synthetic desferri-exochelin used in this study was serine containing, with a neutral desferri average mass of 719.4 Da. It has a saturated R_1 alkyl chain which terminates in a methyl ester (see Fig 3.1).
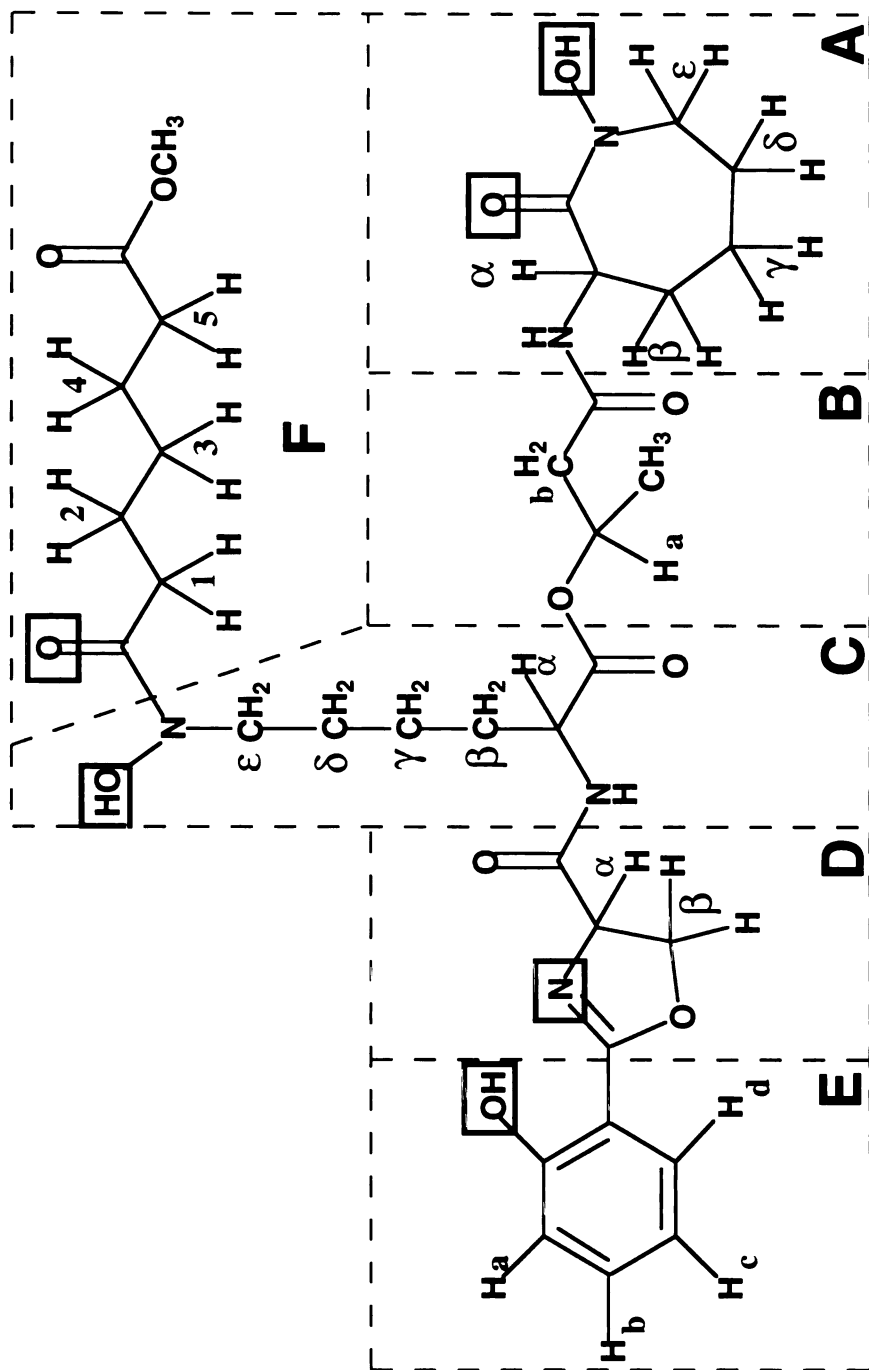
Figure 3.1 Structure of the synthetic desferri-exochelin. The exochelin can be divided into 6 structural moieties (A-F), as indicated by the dashed lines. It contains 3 amino acid moieties - 2 N-hydroxylysines (A and C) and 1 serine (D). Moiety F is a saturated alkyl chain which terminates with a methyl ester. The 6 atoms involved in metal binding are indicated with boxes.

Prior to beginning the NMR experiments, the synthetic desferri-exochelin sample was characterized by HPLC and mass spectrometry. The HPLC retention times for the synthetic exochelin (M_r 719) and the corresponding exochelin isolated from *M. tuberculosis* (M_r 719) gave identical values. Analysis of the synthetic exochelin by tandem mass spectrometry also yielded a spectrum identical to that of the native exochelin (data not shown). Initial synthetic attempts, however, had used the incorrect enantiomer of 3-hydroxybutyric acid (R instead of S). In this case, the resulting exochelin had an identical tandem mass spectrum to the native *M. tuberculosis* exochelin, but the HPLC retention times did not coincide, as might be expected for a diastereomer which differed from the native exochelin at only 1 of the 3 chiral centers.

3.3.2 *Desferri-exochelin NMR assignments*

After the identity of the synthetic exochelin was shown to match that of the native *M. tuberculosis* exochelin, a combination of 1-D and 2-D ^{1}H NMR experiments were performed. The 1-D ^{1}H spectrum of the desferri-exochelin was very complex and revealed only a few basic features of the molecule, such as the presence of a phenyl ring (see Fig 3.2). Additional 2-D experiments (DQF-COSY, HOHAHA, and ROESY) enabled the complete assignment of the protons of the desferri-exochelin (see Table 3.1) and many of their coupling constants (see Table 3.2).

In the case of the two N-hydroxylysines (A and C), the HOHAHA experiment was very useful. The HOHAHA experiment, which employs a spin-lock sequence to allow magnetization transfer between all nuclei within the same coupling network, allowed for the easy identification of both lysine spin systems since the amide protons showed cross-peaks to all but the N-hydroxyl protons (see Fig 3.3). The cyclized N-hydroxylysine (A), with an amide proton at 8.00 ppm, showed separate chemical shifts for each of the protons, implying a certain rigidity to the ring such that the methylene protons were not equivalent. In addition to the HOHAHA spectrum, the DQF-COSY spectrum, which showed coupling

81
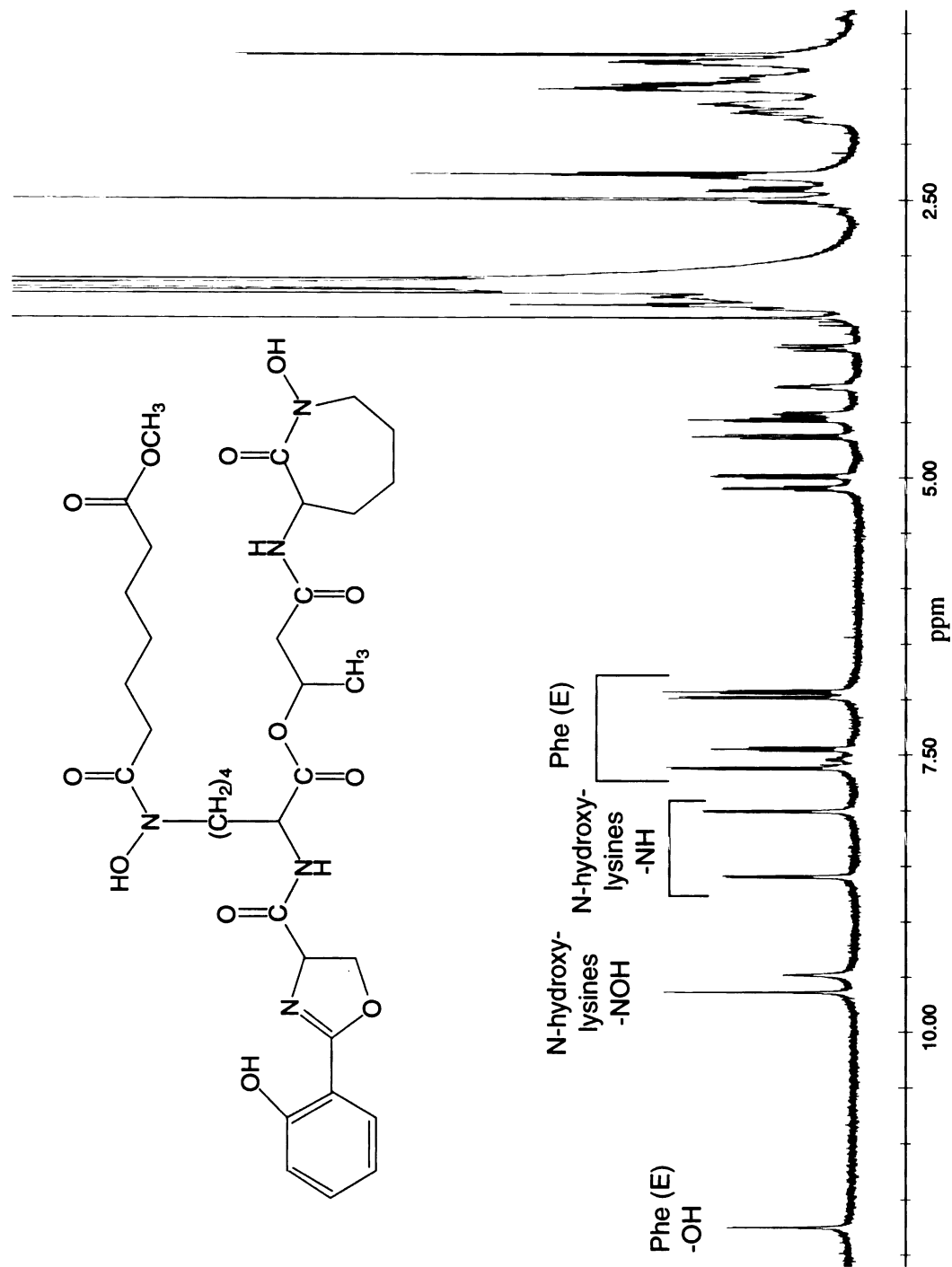
Figure 3.2 One-dimensional ^1H NMR spectrum of the desferri-exochelin taken at 308 K in DMSO. The peaks corresponding to the phenyl ring (E) protons and the lysine amide and N-hydroxyl protons are indicated.

Table 3.1 NMR assignments of desferri-exochelin

Residue	H	Shift	COSY	HOHAHA	ROESY[a]
N-Hydroxy-lysine (A)	NH	8.00	α	α, β1, β2, γ1, γ2, δ1, δ2, ε1, ε2	a(3HB), b1(3HB), b2(3HB), CH$_3$(3HB), b1(3HB), b2(3HB), a(3HB)(w[b])
	α	4.43	NH, β1, β2	NH, β1, β2, γ1, γ2, δ1, δ2, ε1, ε2	
	β1	1.42	α, β2, γ1	NH, α, β2, γ1, γ2, δ1, δ2, ε1, ε2	
	β2	1.74	α, β1, γ2	NH, α, β1, γ1, γ2, δ1, δ2, ε1, ε2	
	γ1	1.63	β1, γ2, δ1	NH, α, β1, β2, γ2, δ1, δ2, ε1, ε2	
	γ2	1.81	β2, γ1	NH, α, β1, β2, γ1, δ1, δ2, ε1, ε2	
	δ1	1.43	δ2, ε2, γ1	NH, α, β1, β2, γ1, γ2, δ2, ε1, ε2	
	δ2	1.67	δ1, ε1	NH, α, β1, β2, γ1, γ2, δ1, ε1, ε2	
	ε1	3.47	δ2, ε2	NH, α, β1, β2, γ1, γ2, δ1, δ2, ε2	
	ε2	3.84	δ1, ε1	NH, α, β1, β2, γ1, γ2, δ1, δ2, ε1	
	NOH	9.64			ε1(LysA), ε2(LysA)
3-Hydroxy-butyric acid (B)	a	5.11	CH$_3$, b1, b2	CH$_3$, b1, b2	NH(LysA)
	CH$_3$	1.22	a	a, b1, b2	NH(LysA)
	b1	2.43	a, b2	a, CH$_3$, b2	NH(LysA)
	b2	2.53	a, b1	a, CH$_3$, b1	NH(LysA)
N-Hydroxy-lysine (C)	NH	8.60	α	α, β1, γ, δ, ε	α(Ser), β1(Ser), β2(Ser) CH$_3$(3HB)(w)
	α	4.19	NH, β1, β2		
	β1	1.74	α, β2, γ	NH, α, β2, γ, δ, ε	
	β2	1.68	α, β1, γ	NH, α, β1, γ, δ, ε	
	γ	1.30	β1, β2, δ	NH, α, β1, β2, δ, ε	
	δ	1.53	γ, ε	NH, α, β1, β2, γ, ε	
	ε	3.44	δ	NH, α, β1, β2, γ, δ	
	NOH	9.48			γ(LysC), δ(LysC), ε(LysC), H1(F)

Serine (D)	α	4.50	β1, β2	β1, β2	NH(LysC)
	β1	4.64	α, β2	α, β2	NH(LysC)
	β2	5.01	α, β1	α, β1	
Phenyl (E)	a	6.98	b, c(w)	b, c, d	
	b	7.46	a, c, d (w)	a, c, d	
	c	6.94	a(w), b, d	a, b, d	
	d	7.63	b(w), c	a, b, c	OH(Phe)
	OH	11.75			a(Phe)
R₁ alkyl chain (F)	1	2.29	H2	H2, H3, H4, H5	
	2	1.49	H1, H3	H1, H3, H4, H5	
	3	1.25	H2, H4	H1, H2, H4, H5	
	4	1.45	H3, H5	H1, H2, H3, H5	
	5	2.26	H4	H1, H2, H3, H4	
	OCH$_3$	3.56			

[a] Only cross-peaks which aided in sequence determination are listed. Cross-peaks within the same spins system (similar to the HOHAHA spectrum) were not included in the table.

[b] 'w' indicates weak interactions

Table 3.2 Coupling constants for desferri- and gallium-exochelin

Residue	H	Desferri-exochelin Shift	Desferri-exochelin J	Gallium-exochelin Shift	Gallium-exochelin J
	NH	8.00	$J_{NH,\alpha} = 7$	7.57	$J_{NH,\alpha} = 6.5$
	α	4.43	$J_{\alpha,NH} = 7$, $J_{\alpha,\beta1} = 12\text{-}13$	4.66	$J_{\alpha,NH} = 6.5$, $J_{\alpha,\beta1} = 10\text{-}12$, $J_{\alpha,\beta2} = 3$
	$\beta1$	1.42	$J_{\beta1,\alpha} = 12\text{-}13$, $J_{\beta1,\beta2} = 13\text{-}15$	1.29	$J_{\beta1,\alpha} = 10\text{-}12$, $J_{\beta1,\beta2} = 14\text{-}15$
	$\beta2$	1.74	$J_{\beta2,\beta1} = 13\text{-}15$	1.84	$J_{\beta2,\alpha} = 5\text{-}6$, $J_{\beta2,\beta1} = 13\text{-}15$
N-Hydroxy-lysine (A)	$\gamma1$	1.63		1.72	
	$\gamma2$	1.81		1.91	
	$\delta1$	1.43	$J_{\delta1,\delta2} = 20\text{-}22$, $J_{\delta1,\varepsilon2} = 11.3$	1.50	$J_{\delta1,\delta2} = 15\text{-}17$, $J_{\delta1,\varepsilon2} = 11\text{-}12$
	$\delta2$	1.67	$J_{\delta2,\delta1} = 20\text{-}22$, $J_{\delta2,\varepsilon1} = 6\text{-}8$	1.75	$J_{\delta2,\delta1} = 15\text{-}17$, $J_{\delta2,\varepsilon1} = 5\text{-}6$
	$\varepsilon1$	3.47	$J_{\varepsilon1,\varepsilon2} = 15.8$, $J_{\varepsilon1,\delta2} = 6\text{-}8$	3.71	$J_{\varepsilon1,\varepsilon2} = 15.5$, $J_{\varepsilon1,\delta2} = 5\text{-}6$
	$\varepsilon2$	3.84	$J_{\varepsilon2,\varepsilon1} = 15.8$, $J_{\varepsilon2,\delta1} = 11.3$	3.94	$J_{\varepsilon2,\varepsilon1} = 15.5$
3-Hydroxybutyric acid (B)	a	5.11	$J_{a,CH3} = 6.6$, $J_{a,b1} = 6.5$, $J_{a,b2} = 7$	5.18	$J_{a,CH3} = 6$, $J_{a,b1} = 2.5$, $J_{a,b2} = 4.8$
	CH_3	1.22	$J_{CH3,a} = 6.6$	1.17	$J_{CH3,a} = 6$
	b1	2.43	$J_{b1,a} = 6.5$, $J_{b1,b2} = 14$	2.22	$J_{b1,a} = 2.5$, $J_{b1,b2} = 14.7$
	b2	2.53	$J_{b2,a} = 7$, $J_{b2,b1} = 14$	2.61	$J_{b2,a} = 4.8$, $J_{b2,b1} = 14.7$
	NH	8.60	$J_{NH,\alpha} = 7$	9.17	$J_{NH,\alpha} = 4$
	α	4.19	$J_{\alpha,NH} = 7$	4.15	$J_{\alpha,NH} = 4$, $J_{\alpha,\beta1} = 7\text{-}8$, $J_{\alpha,\beta2} = 5\text{-}6$
	$\beta1$	1.74	$J_{\beta1,\gamma} = 15\text{-}17$	1.80	$J_{\beta1,\alpha} = 7\text{-}8$, $J_{\beta1,\beta2} = 22\text{-}24$
	$\beta2$	1.68	$J_{\beta2,\gamma} = 14\text{-}16$	1.98	$J_{\beta2,\alpha} = 7\text{-}8$, $J_{\beta2,\beta1} = 22\text{-}24$
N-Hydroxy-	$\gamma1$	1.30	$J_{\gamma,\beta1} = 15\text{-}17$, $J_{\gamma,\beta2} = 14\text{-}16$	1.44	

Group	Atom	δ (1-D)	J (1-D)	δ (2-D)	J (2-D, italic)
lysine (C)	γ2	1.53		1.91	
	δ1		$J_{\delta,\varepsilon} = 6.8$	1.39	$J_{\delta1,\delta2} = 13,\ J_{\delta1,\varepsilon1} = 4\text{-}5$
	δ2			1.82	$J_{\delta2,\delta1} = 13,\ J_{\delta2,\varepsilon1} = 10\text{-}12,\ J_{\delta2,\varepsilon2} = 7\text{-}8$
	ε1	3.44	$J_{\varepsilon,\delta} = 6.8$	3.60	$J_{\varepsilon1,\delta1} = 4\text{-}5,\ J_{\varepsilon1,\delta2} = 10\text{-}12,\ J_{\varepsilon1,\varepsilon2} = 15\text{-}17$
	ε2			4.07	$J_{\varepsilon2,\delta2} = 7\text{-}8,\ J_{\varepsilon2,\varepsilon1} = 15\text{-}17$
Serine (D)	α	4.50	$J_{\alpha,\beta1} = 7.5,\ J_{\alpha,\beta2} = 7.5$	4.48	
	β1	4.64	$J_{\beta1,\alpha} = 7.5,\ J_{\beta1,\beta2} = 10$	4.64	$J_{\beta1,\beta2} = 14\text{-}15$
	β2	5.01	$J_{\beta2,\alpha} = 7.5,\ J_{\beta2,\beta1} = 10$	4.82	$J_{\beta2,\beta1} = 14\text{-}15$
Phenyl (E)	a	6.98	$J_{a,b} = 7.5,\ J_{a,c} = 1$	6.65	$J_{a,b} = 8.2,\ J_{a,c} = 5$
	b	7.46	$J_{b,a} = 7.5,\ J_{b,c} = 7.5,\ J_{b,d} = 2$	7.32	$J_{b,a} = 8.2,\ J_{b,c} = 7.6,\ J_{b,d} = 1.8$
	c	6.94	$J_{c,a} = 1,\ J_{c,b} = 7.5,\ J_{c,d} = 7.8$	6.57	$J_{c,a} = 5,\ J_{c,b} = 7.6,\ J_{c,d} = 7.7$
	d	7.63	$J_{d,b} = 2,\ J_{d,c} = 7.8$	7.53	$J_{d,b} = 1.8,\ J_{d,c} = 7.7$
R₁ alkyl chain (F)	1a	2.29	$J_{1,2} = 7.3$	2.37	$J_{1a,1b} = 8.8,\ J_{1a,2} = 6.3$
	1b			2.51	$J_{1b,1a} = 8.8$
	2	1.49	$J_{2,1} = 7.3$	1.61	$J_{2,1a} = 6.3,\ J_{2,3} = 13\text{-}15$
	3	1.25	$J_{3,4} = 7.4$	1.35	$J_{3,2} = 13\text{-}15$
	4	1.45	$J_{4,3} = 7.4$	1.55	$J_{4,5} = 7.5$
	5			2.31	$J_{5,4} = 7.5$
	OCH_3	3.56		3.58	

Coupling constants (J) in *italics* are apparent coupling constants measured from the 2-D DQF-COSY spectra. All other coupling constants were measured from the 1-D spectra.

**Figure 3.3. Section of the 500 MHz HOHAHA spectrum of the *M*.
tuberculosis desferri-exochelin.** Cross peaks corresponding to the cyclized (A) and
linear (C) N-hydroxylysines are indicated with dashed and solid lines, respectively. The
spin systems of the 2 N-hydroxylysines were easily identified since the amide protons
showed cross-peaks to all but the N-hydroxyl protons in each of their respective spin
systems. Some of the cross-peaks corresponding to the 3-hydroxybutyric acid spic system
are indicated with a dotted line.
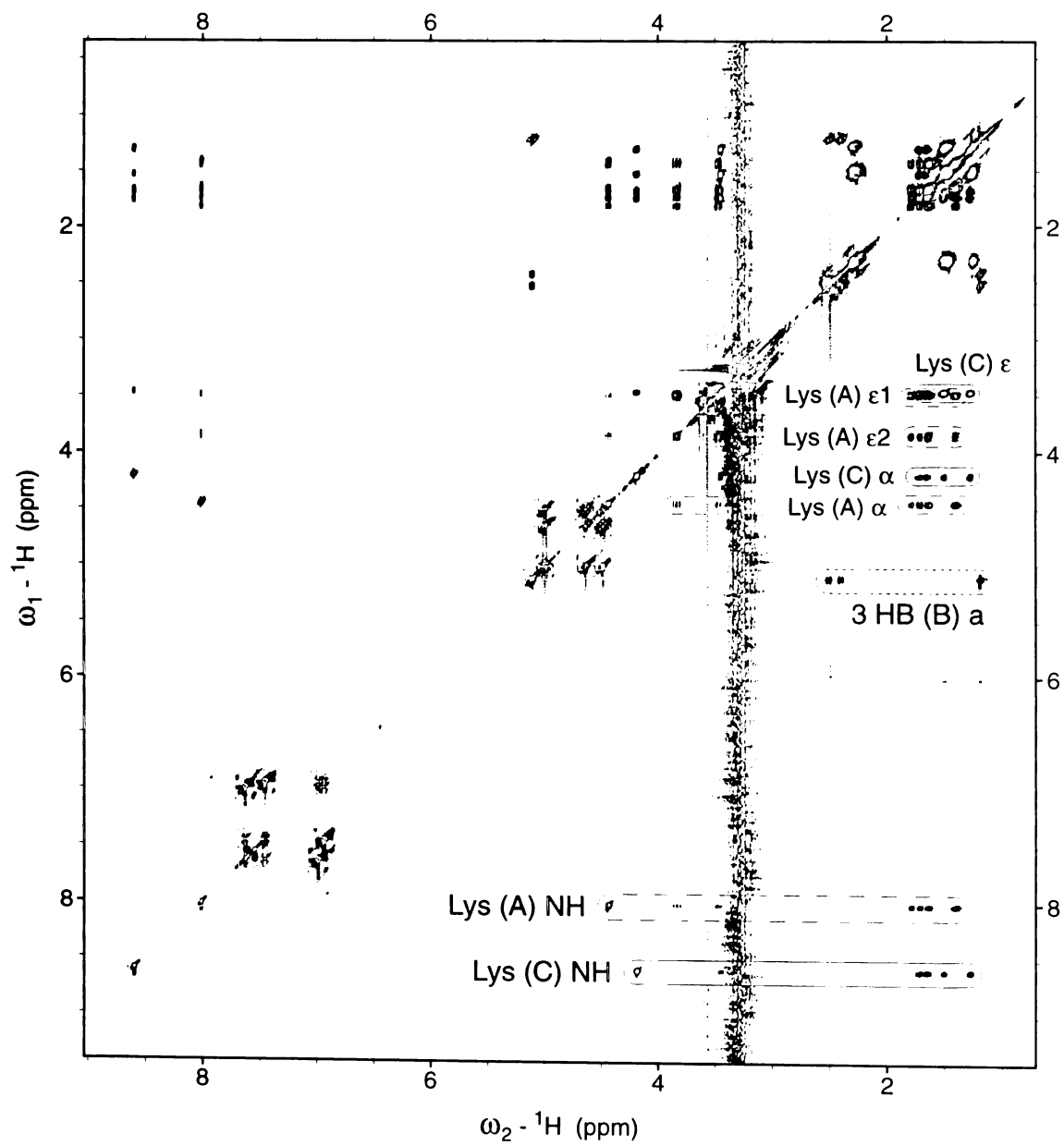
connectivities between directly coupled nuclei, was also integral to assigning the chemical shifts (see Fig 3.4). Starting with the amide proton, it was possible to walk sequentially through the lysine spin system by following the coupling pattern. As depicted in Figure 3.4, the amide proton coupled to the α proton (4.43 ppm, $J_{NH,\alpha} = 7$ Hz), which also showed coupling to both β protons [1.42 (β1) $J_{\alpha,\beta1} = 12$-13 Hz, 1.74 (β2) ppm]. However, the ROESY experiment, which shows through-space interactions (dipolar coupling), was needed to assign the correct resonance of the N-hydroxyl proton (9.64 ppm), as it did not show cross-peaks in either the DQF-COSY or HOHAHA spectra. In the ROESY spectrum, the N-hydroxyl proton exhibited coupling to both of the protons on the ϵ carbon of the lysine [3.47 (ϵ1), 3.84 (ϵ2) ppm]. In addition, ROESY cross-peaks existed between the amide proton of the cyclized N-hydroxylysine (A) and all of the protons in the 3-hydroxybutyric acid (B) spin system, confirming that the lysine spin system with the amide proton at 8.00 ppm is cyclized (A) and not linear (C).

The linear N-hydroxylysine (C) spin system showed both similarities and differences to the cyclized N-hydroxylysine. As in the cyclized N-hydroxylysine (A), in the DQF-COSY spectrum (see Fig 3.4), coupling could be seen from the amide proton (8.60 ppm) to the proton on the α carbon (4.19 ppm, $J_{NH,\alpha} = 7$ Hz). This α proton also shows cross-peaks to both protons on the β carbon [1.74 (β1), 1.68 (β2) ppm]. However, unlike that in N-hydroxylysine (A), the protons on the γ, δ, and ϵ carbons were equivalent. In contrast to the non-equivalent ϵ protons of N-hydroxylysine (A), the portion of the HOHAHA spectrum displayed in Figure 3.5A shows several of the cross-peaks observed to the diastereotopic protons on the ϵ carbon of lysine C. This is understandable since more freedom of motion would be expected in the linear vs. the cyclized lysine. The ROESY spectrum was needed to complete the assignment of this amino acid. The N-hydroxyl proton (9.48 ppm) showed ROESY cross-peaks to the protons on the γ, δ, and ϵ carbons. In addition, ROESY cross-peaks between the amide proton and the α and β protons of the cyclized serine (D) confirmed the assignment of this spin system as the linear

Figure 3.4. Section of the 500 Mhz phase sensitive DQF-COSY spectrum of the *M. tuberculosis* desferri-exochelin and the corresponding region of the 1-D ¹H NMR spectrum. Portions of the N-hydroxylysine spin systems are indicated with a dashed line (cyclized N-hydroxylysine A) or solid line (linear N-hydroxylysine C). A portion of the 3-hydroxybutyric acid spin system is indicated by the dotted line. The spin systems for the phenyl ring (E) and the cyclized serine (D) are outlined with boxes.
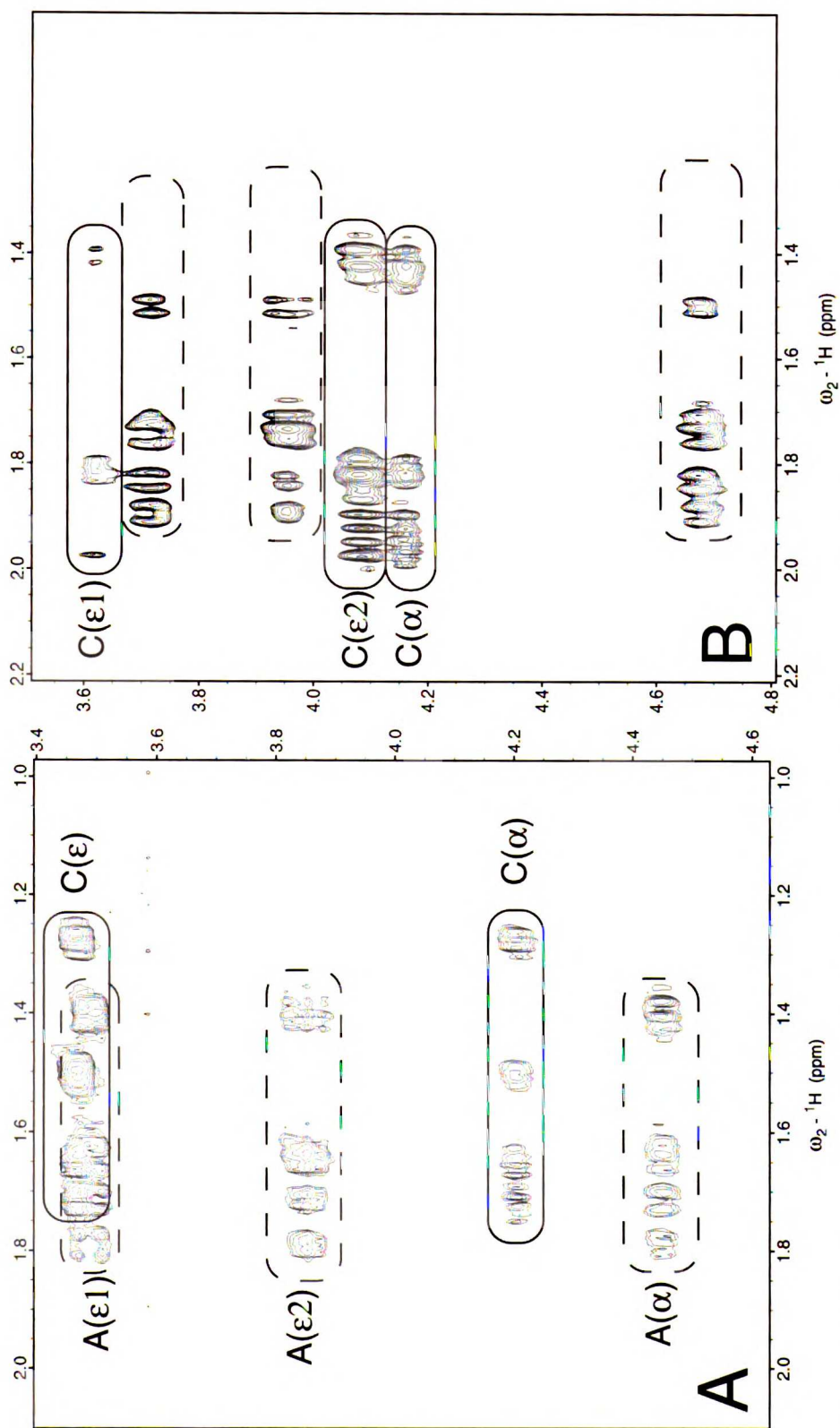
Figure 3.5 Selected regions of 2-D HOHAHA spectra of the (A) desferri- and (B) gallium-exochelin. The two protons on the ε carbon of the linear N-hydroxylysine C are equivalent in the desferri-exochelin (3.44 ppm) but become non-equivalent in the gallium-exochelin (3.60 and 4.07 ppm).

lysine (C). There was also coupling between the N-hydroxyl proton and the protons on the C-1 carbon of moiety F.

The spin system of the 3-hydroxybutyric acid (B) was also relatively easy to differentiate with the aid of the DQF-COSY (see Fig 3.4) and HOHAHA (see Fig 3.3) spectra. The HOHAHA spectrum showed coupling from the H_a proton to the H_b and the methyl protons. The DQF-COSY spectrum enabled the assignment of the protons since H_a showed coupling to both the methyl ($J_{a,CH3}$ = 6.6 Hz) and Hb ($J_{a,b1}$ = 6.5 Hz, $J_{a,b2}$ = 7 Hz) protons (see Fig 3.3), while the methyl protons only coupled to H_a and not to the H_b protons.

In the case of the serine, there was no amide proton to examine since it is a cyclized residue. In both the DQF-COSY and HOHAHA spectra, the α proton (4.50 ppm) couples to both β protons [4.64 (β1), 5.01 (β2)], with coupling constants of $J_{\alpha,\beta1}$ = $J_{\alpha,\beta2}$ = 7.5 Hz. The β protons also exhibit geminal coupling to each other ($J_{\beta1,\beta2}$ = 10 Hz). In addition, as stated before, the α proton and one of the β protons had ROESY cross-peaks with the amide proton from N-hydroxylysine C.

The protons of the salicylic acid moiety (E) had an easily identifiable spin system which fell within the expected chemical shift range for aromatic protons (see Fig 3.3). Proton assignments were made after careful examination of the DQF-COSY spectrum. In the HOHAHA spectrum, all protons (except the hydroxyl) coupled to each other. However, in the DQF-COSY spectrum, the number and intensities of the different cross-peaks gave valuable clues for the assignments (see Fig 3.6). The protons with chemical shifts at 6.98 (Ha) and 7.63 (Hd) ppm each only showed intense cross-peaks to one other proton, protons with chemical shifts at 7.46 (Hb, $J_{a,b}$ = 7.5 Hz) and 6.94 ppm (Hc, $J_{d,c}$ = 7.8 Hz), respectively. This indicated that these protons (a and d) are in the two outer positions of the spin system (see Fig 3.1). Hd showed a strong cross-peak with Hc and only a weak (long-range) coupling to Hb ($J_{d,b}$ = 2 Hz), indicating that Hd was ortho to Hc in the ring and meta to Hb. This is consistent with the 1-D spectrum which shows Ha and
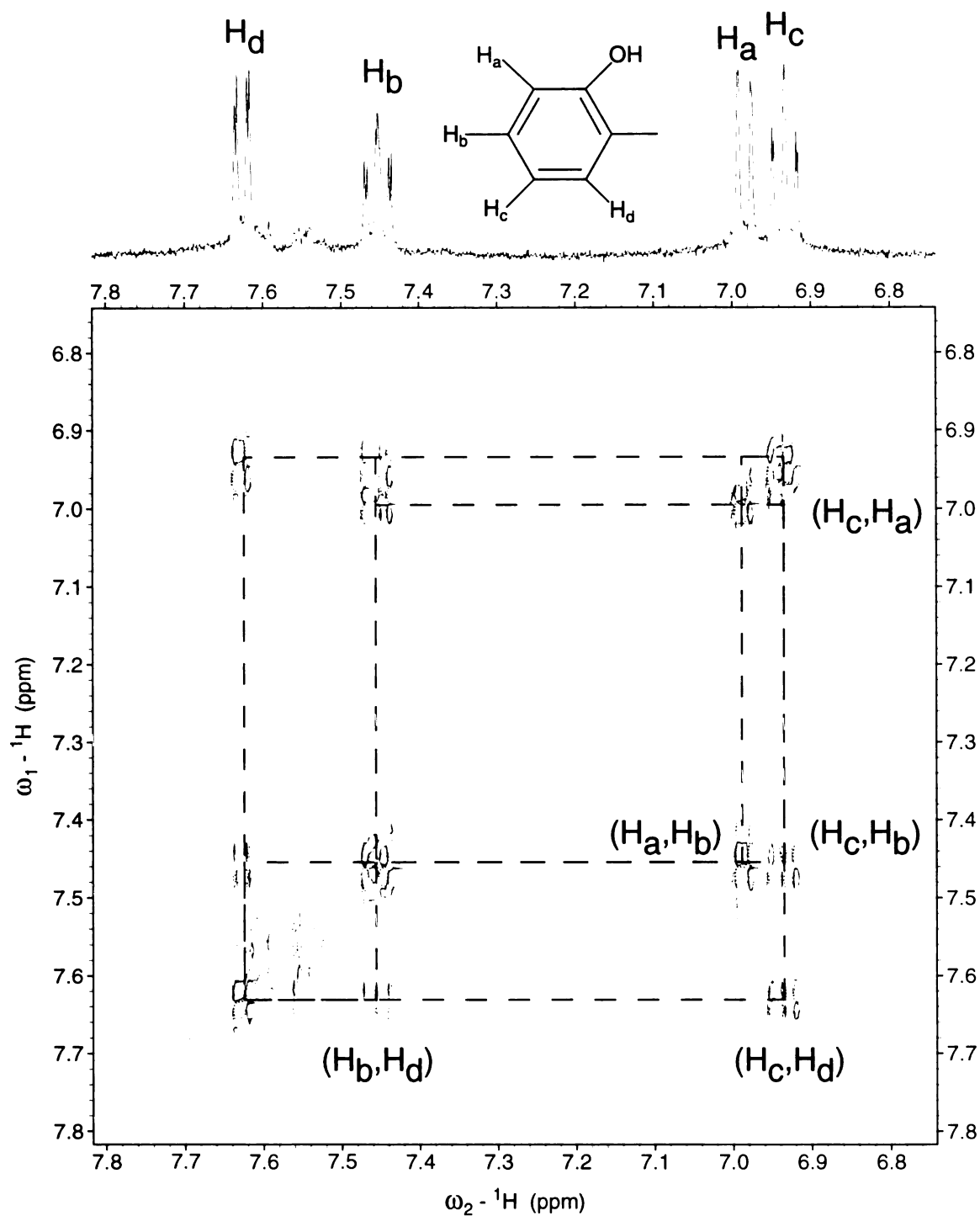
Figure 3.6 **Aromatic region of the 500 MHz phase-sensitive DQF-COSY spectrum of the** *M. tuberculosis* **exochelin and the corresponding region of the 1-D ^{1}H NMR spectrum.** The phenyl protons are labeled as indicated in Figure 3.1. Cross-peaks are connected with dashed lines.

Hd as doublets. In contrast, Hb and Hc appear as triplets as they are split by the protons on both sides. Hc showed strong cross-peaks to Hb ($J_{c,b}$ = 7.5 Hz) and Hd ($J_{c,d}$ = 7.8) and weaker coupling to Ha ($J_{c,a}$ = 1 Hz). Likewise, Hb coupled to Ha ($J_{b,a}$ = 7.5) and Hc ($J_{b,c}$ = 7.5 Hz) and only showed a weak cross-peak to Hd ($J_{b,d}$ = 2 Hz). Only the relative order of the protons around the ring could be determined from the DQF-COSY coupling pattern. However, evidence of weak coupling between the hydroxyl proton on the phenyl ring and Ha suggested that they were adjacent to each other in the ring system. This assignment of the protons around the ring is consistent with the previously reported NMR assignments of the mycobactin by Greatbanks et al. (Greatbanks and Bedford 1969) which placed the ^{1}H with 7.62 ppm meta to the phenolic hydroxyl (position d on the ring).

The additional peaks evident in the aromatic region of the spectrum are due to a contaminating form of the exochelin (see Fig 3.6). Previous characterization by mass spectrometry has shown this minor structure to be a hydrolyzed form of the exochelin where the oxazoline ring [moiety (D)] is opened (see Fig 3.7). This hydrolysis of oxazoline ring systems has been previously observed in other NMR studies of siderophores, including the *M. avium* exochelin (Lane et al. 1995) (where it was the dominant form) and the spermidine siderophores (agrobactin from *Agrobacterium tumefaciens* and parabactin from *Paracoccus denitrificans*) (Peterson et al. 1980). In our own NMR studies, the conversion to the hydrolyzed form continued over time. This was apparent by the increase in intensity of the contaminating aromatic signals. Protons of spin systems remote from the oxazoline ring did not show any noticeable changes in chemical shifts in the hydrolyzed vs. unhydrolyzed form of the exochelins.

The spin system of the long alkyl side chain which terminates in a methyl ester (F) was the most difficult to discern, due in large part to the crowded upfield regions of the spectra. The HOHAHA spectrum showed coupling between all of the protons in the spin system, except for the terminal methyl ester protons. All of the methylene protons were equivalent, with only one chemical shift being found for each pair of protons on carbons 1-
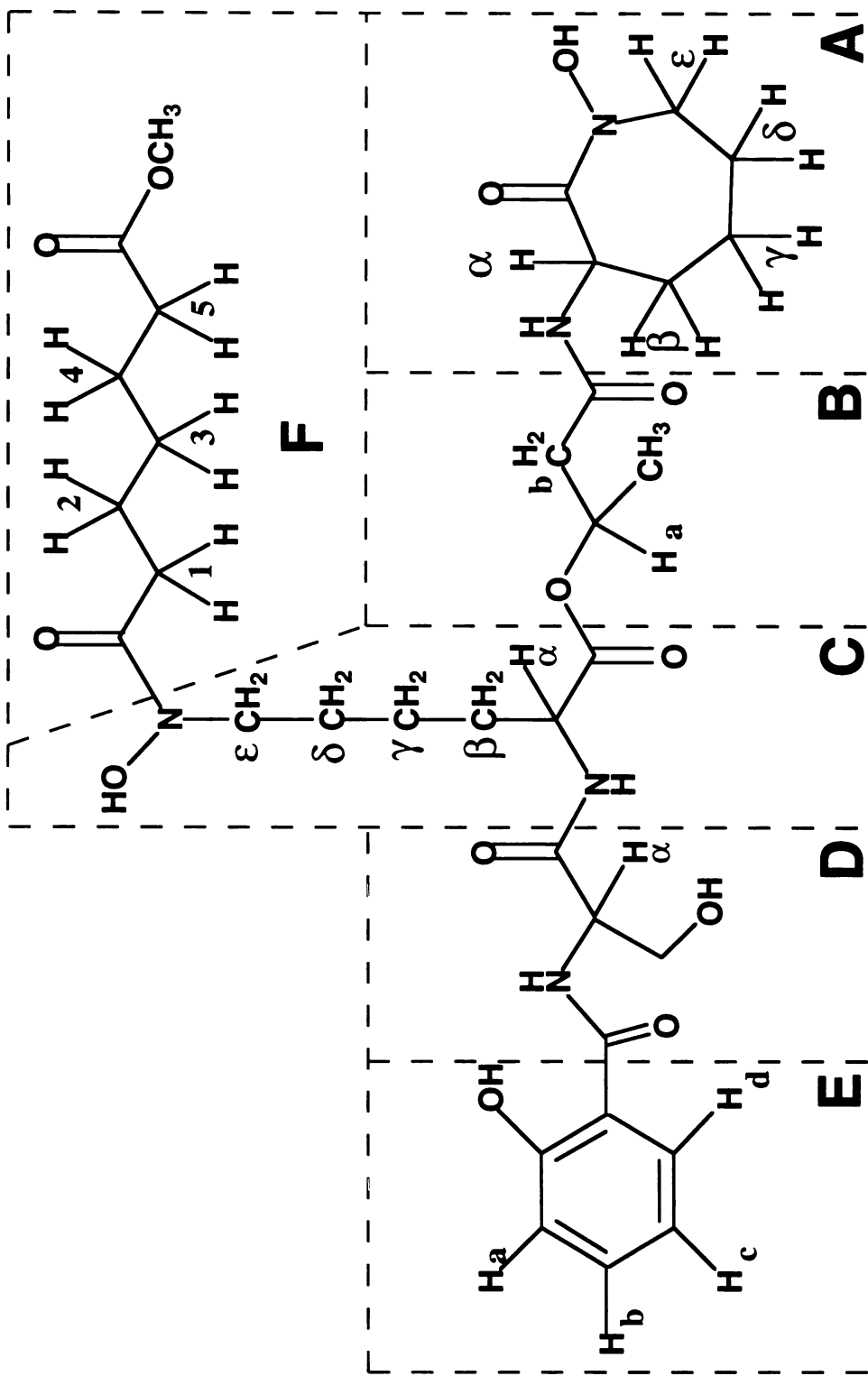
Figure 3.7 Structure of the hydrolyzed exochelin. This ring-open form of the exochelin, where the serine is no longer cyclized (moiety D), appears as a contaminating form in the NMR studies.

5. The protons on C-1 and C-5 were deshielded by the adjacent carbonyls, shifting their proton resonances downfield to 2.29 and 2.26 ppm, respectively. As in the case of the two N-hydroxylysine residues, the DQF-COSY spectrum enabled us to walk down the alkyl chain. For instance, H1 is coupled to H2 ($J_{1,2}$ = 7.3 Hz), which in turn showed cross-peaks to both the H1 and H3 protons. As with the phenyl ring, only the relative order of these protons could be assigned from the DQF-COSY spectrum. The protons of the methlyl ester (3.56 ppm) did not show an observable ROESY peak to any of the protons on the alkyl chain. However, a ROESY cross-peak for H1 to NOH of N-hydroxylysine C fixed the assignment of the alkyl chain.

3.3.3 Gallium-exochelin NMR assignments

Since it is not possible to study the ferri-exochelin complex directly by NMR, the gallium-exochelin analog is being used in our studies of the metal-bound structure. Exochelins are thought to chelate the metal cations (+3) in an octahedral coordination, with the 6 atoms involved in metal binding indicated with boxes in Figure 3.1. The gallium-exochelin analog was made by reacting the single desferri-exochelin with $GaCl_3$ in ethanol over a period of several hours. Analysis by matrix-assisted laser desorption ionization (MALDI) mass spectrometry confirmed that the exochelin was chelating the gallium (see Fig 3.8). The MALDI mass spectrum of the gallium-exochelin showed two main parent peaks at m/z 787 and 789. The relative intensities of these peaks are in agreement with the natural abundance of the two gallium isotopes. Therefore, the existence of the gallium-exochelin analog was not only demonstrated by the correct molecular weight, but also by the distinctive isotope pattern characteristic of gallium-containing molecules.

The proton assignments for the gallium-exochelin molecule were made following the same strategy used in the case of the desferri-exochelin (see Table 3.3), with some of the coupling constants listed in table 3.2. As in the case of the desferri-exochelin, the 1-D spectrum of the gallium analog was also very complex (see Fig 3.9). Numerous

Figure 3.8. MALDI mass spectrum of the gallium-exochelin. The ion cluster at m/z 787.0 corresponds to the singly charged molecular ion for the gallium-bound state. The distinctive isotope pattern is characteristic of gallium-containing molecules since Ga^{69} and Ga^{71} have abundancies of 60.2% and 39.8%, respectively. The contaminating peak cluster at m/z 801 is the result of a transesterification reaction at low pH between the methyl ester of the exochelin (R-OCH_3) and the ethanol solvent used in the reaction to give a gallium-exochelin ethyl ester (R-OCH_2CH_3).
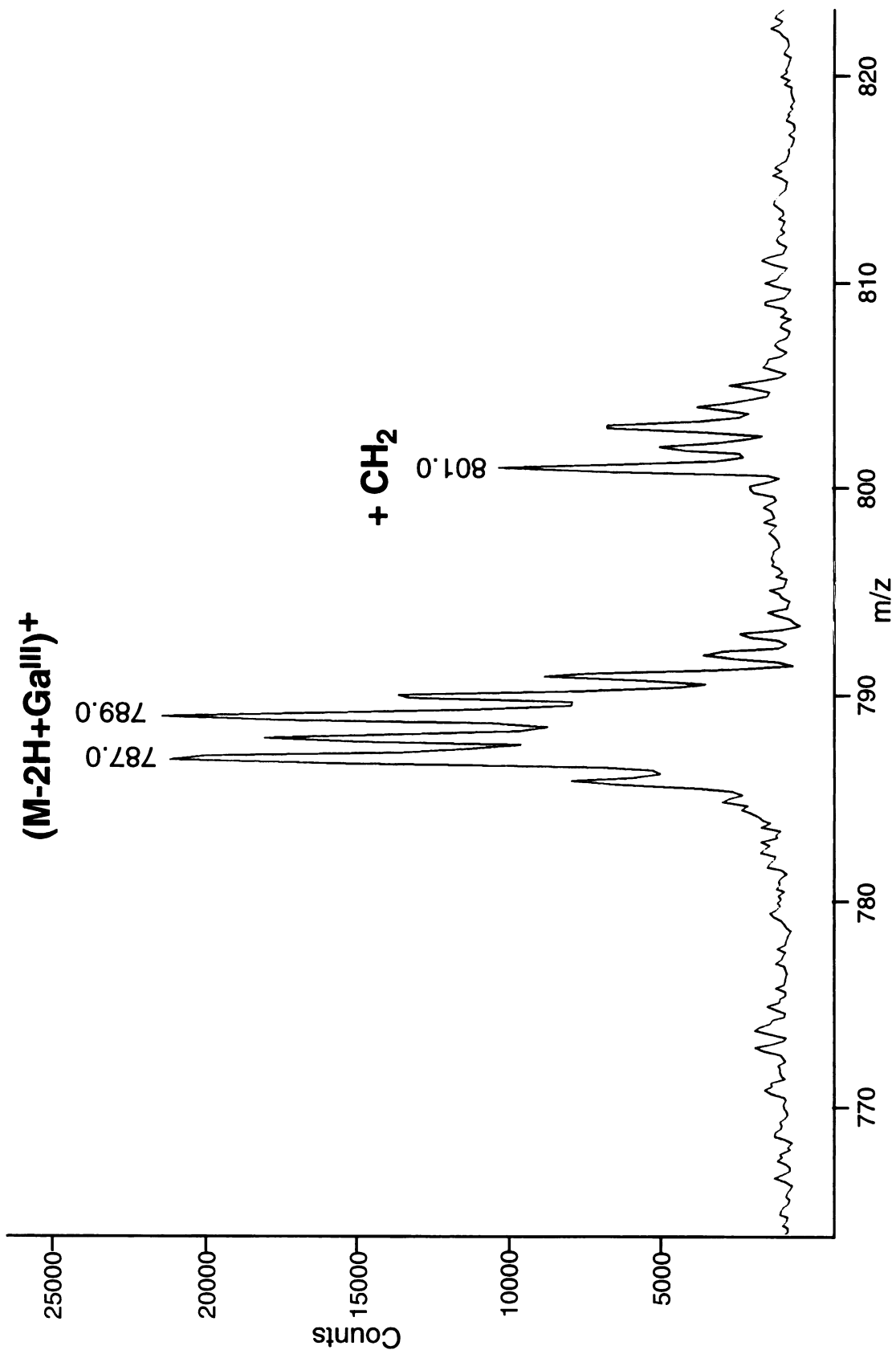
Table 3.3 NMR assignments of gallium-exochelin

Residue	H	Shift	COSY	HOHAHA	ROESY[a]
	NH	7.57	α	α, β1, β2, γ1, γ2, δ1, δ2, ε1, ε2	(a, b1, b2)(3HB)
	α	4.66	NH, β1, β2(w[b])	NH, β1, β2, γ1, γ2, δ1, δ2, ε1(w), ε2(w)	ε1(LysA), ε2 (LysA)
	β1	1.29	α, β2, γ1, γ2(w)	NH, α, β2, γ1, γ2, δ1, δ2, ε1, ε2	
	β2	1.84	α(w), β1, γ1	NH, α, β1, γ1, γ2, δ1, δ2, ε1, ε2	
N-Hydroxy-	γ1	1.72	β1, β2, γ2, δ1	NH, α, β1, β2, γ2, δ1, δ2, ε1, ε2	
lysine (A)	γ2	1.91	β1(w), γ1, δ1(w), δ2	NH, α, β1, β2, γ1, δ1, δ2, ε1, ε2	
	δ1	1.50	γ1, γ2(w), δ2, ε1(w), ε2	NH, α, β1, β2, γ1, γ2, δ2, ε1, ε2	
	δ2	1.75	γ2, δ1, ε1	NH, α, β1, β2, γ1, γ2, δ1, ε1, ε2	
	ε1	3.71	δ1(w), δ2, ε2	NH, α(w), β1, β2, γ1, γ2, δ1, δ2, ε2	α (LysA)
	ε2	3.94	ε1, δ1	NH, α(w), β1, β2, γ1, γ2, δ1, δ2, ε1	α (LysA)
3-Hydroxy-	a	5.18	CH3, b1, b2	CH3, b1, b2	NH (LysA)
butyric	CH3	1.17	a	a, b1, b2	β1(Ser), β2 (Ser)
acid	b1	2.22	a, b2	a, CH3, b2	NH (LysA)
(B)	b2	2.61	a, b1	a, CH3, b1	NH (LysA)
	NH	9.17	α	α, β1, β2, γ1, γ2, δ1, δ2, ε1	b1(Ser), b2(Ser)
	α	4.15	NH, β1, β2	NH, β1, β2, γ1, γ2, δ1, δ2, ε1, ε2	
	β1	1.80	α, β2	NH, α, β2, γ1, γ2, δ1, δ2, ε1, ε2	
	β2	1.98	α, β1, γ1	NH, α, β1, γ1, γ2, δ1, δ2, ε1, ε2	
N-Hydroxy-	γ1	1.44	β2	NH, α, β1, β2, γ2, δ1, δ2, ε1, ε2	
lysine (C)	γ2	1.91		NH, α, β1, β2, γ1, δ1, δ2, ε1, ε2	
	δ1	1.39	δ2, ε1, ε2	NH, α, β1, β2, γ1, γ2, δ2, ε1, ε2	
	δ2	1.82	δ1, ε1(w), ε2	NH, α, β1, β2, γ1, γ2, δ1, ε1, ε2	H1a(F), H1b(F)
	ε1	3.60	ε2, δ1, δ2(w)	β1, β2, γ1, γ2, δ1, δ2, ε2	
	ε2	4.07	ε1, δ1, δ2	β1, β2, γ1, γ2, δ1, δ2, ε1	H1a(F), H1b(F), H2(F)

Residue		δ (ppm)			
Serine (D)	α	4.48		β1(w)	
	β1	4.64	β2	β2	Hd(E), CH$_3$(3HB), NH(LysC)
	β2	4.82	β1	α(w), β1	Hd(E), CH$_3$(3HB), NH(LysC)
Phenyl (E)	a	6.65	b, c(w)	c, b, d	
	b	7.32	a, c, d(w)	a, c, d	
	c	6.57	a(w), b, d	b, c, d	
	d	7.53	b(w), c	a, b, c	β1(Ser), β2(Ser)
R$_1$ alkyl chain (F)	1a	2.37	1b, 2	1b, 2, 3, 4, 5	δ2 (LysC), ε2 (LysC)
	1b	2.51	1a, 2	1a, 2, 3, 4, 5	δ2 (LysC), ε2 (LysC)
	2	1.61	1a, 1b, 3	1a, 1b, 3, 4, 5	ε1(LysC)
	3	1.35	2, 4	1a, 1b, 2, 4, 5	
	4	1.55	3, 5	1a, 1b, 2, 3, 5	
	5	2.31	4	1a, 1b, 2, 3, 4	
	OCH$_3$	3.58			

[a] Only cross-peaks which aided in the determination of the exochelin sequence or solution conformation are listed. Cross-peaks within the same spin system (similar to the HOHAHA spectrum) were not included in the table.

[b] 'w' indicates weak interactions

101
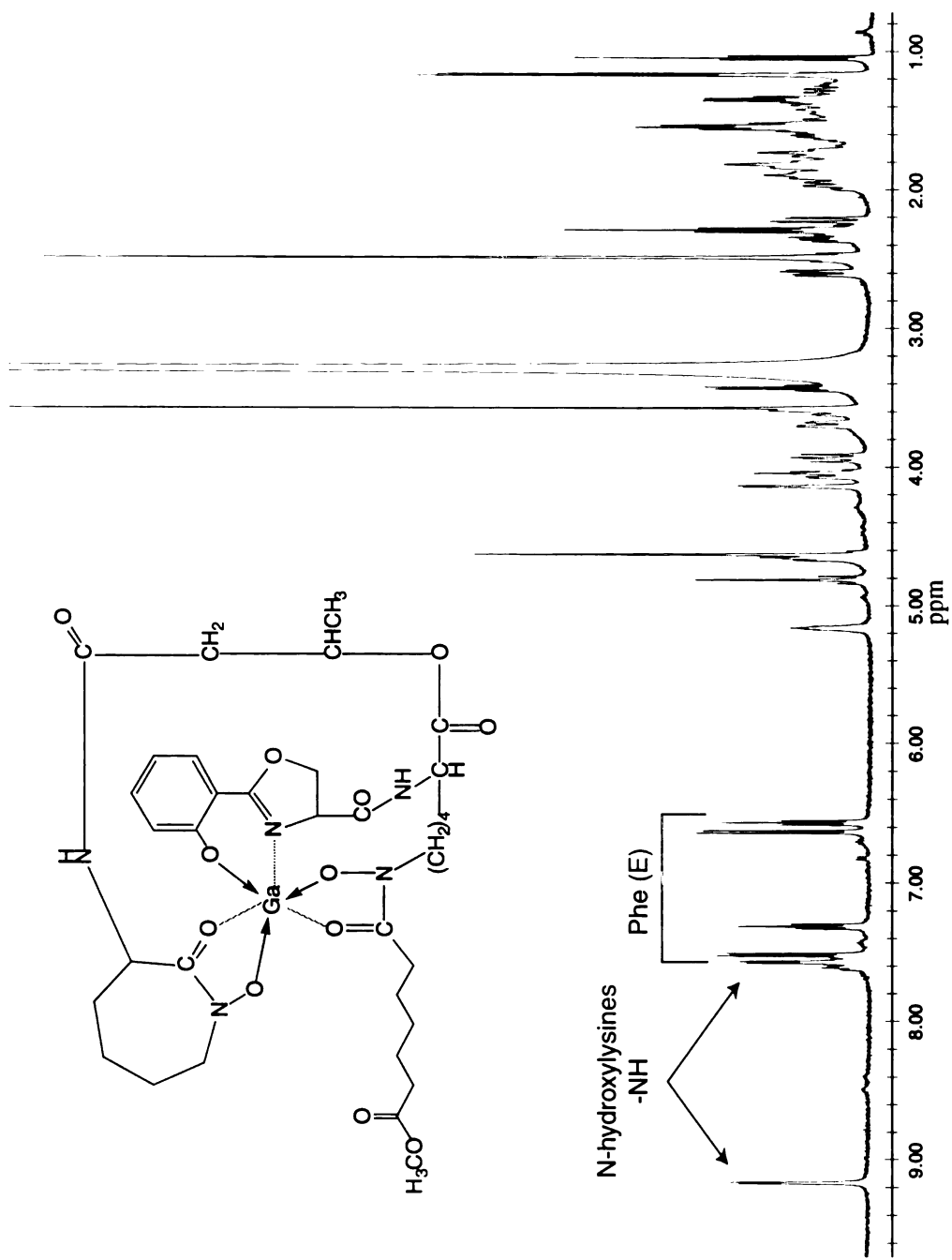
Figure 3.9 One-dimensional ^{1}H NMR spectrum of the gallium-exochelin at 308 K in DMSO. In comparison with the spectrum of the desferri-exochelin (see Fig 3.2), the downfield peaks corresponding to the NOH and OH protons (δ 9.64, 9.48, and 11.75 ppm) are noticeably absent.

observable differences between the desferri- and gallium-exochelin spectra were found. Peaks corresponding to the NOH and OH protons were noticeably absent in the gallium-exochelin spectra since the hydroxyls are presumably ionized, with the oxygens involved in metal binding. As in the case of the desferri-exochelin, using the DQF-COSY (see Fig 3.10) and HOHAHA spectra, it was possible to "walk through" the amino acids, beginning with the amide proton and ending with the two protons on the ε carbon.

In the case of the linear N-hydroxylysine (C), there were many significant changes. The diastereotopic protons of the linear N-hydroxylysine, which were equivalent in the desferri-exochelin spectra, became non-equivalent in the gallium-exochelin spectra (see Fig 3.5). Some of these observed changes were large. The amide proton shifted downfield from 8.60 to 9.17 ppm. The two equivalent protons on the ε carbon of N-hydroxylysine (C) (3.44 ppm) shifted to 3.60 and 4.07 ppm (see Fig 3.5). In addition, the diastereotopic δ protons of N-hydroxylysine (C), which appeared at 1.53 ppm in the desferri-exochelin, shifted to 1.39 and 1.82 ppm ($J_{\delta 1, \delta 2}$ = 13 Hz) in the gallium-exochelin spectrum. The DQF-COSY spectrum revealed strong cross-peaks for geminal coupling between these and other diastereotopic protons.

The most notable difference in the two sets of experiments was the increased number of NOEs observed in the ROESY spectra of the gallium-exochelin in comparison to the desferri-exochelin spectrum. In addition to the ROESY cross-peaks seen in the desferri-exochelin spectrum, which were similar to the peaks seen in the HOHAHA spectrum with some additional sequence information, there were numerous other cross-peaks between protons from different residues which gave valuable insights into the possible conformation of the molecule. These NOEs are indicated in figure 3.11 by the dashed lines.

As with the desferri-exochelin, ROESY cross-peaks helped to confirm the overall sequence of the molecule. Analysis of interresidue coupling enabled the identification of the two N-hydroxylysine spin systems. In the ROESY spectrum, the amide proton of N-

Figure 3.10. Section of the 500 MHz phase sensitive DQF-COSY spectrum of the *M. tuberculosis* gallium-exochelin and the corresponding region of the 1-D ^{1}H NMR spectrum. Portions of the N-hydroxylysine spin systems are indicated with a dashed (cyclized N-hydroxylysine A) or solid (linear N-hydroxylysine C) line. A portion of the 3-hydroxybutyric acid spin system is indicated by the dotted line. The spin systems for the phenyl ring (E) and the cyclized serine (D) are outlined with boxes. There were many observable changes in the linear N-hydroxylysine (C) between the desferri (see Fig 3.4) and gallium spectra, including the downfield shift of the NH and the non-equivalent ε protons in the gallium-exochelin spectrum.

Figure 3.11 Structure of the *M. tuberculosis* exochelin with observed NOEs. The NOEs (indicated by the dashed lines) give information on the solution conformation of the exochelin.

106
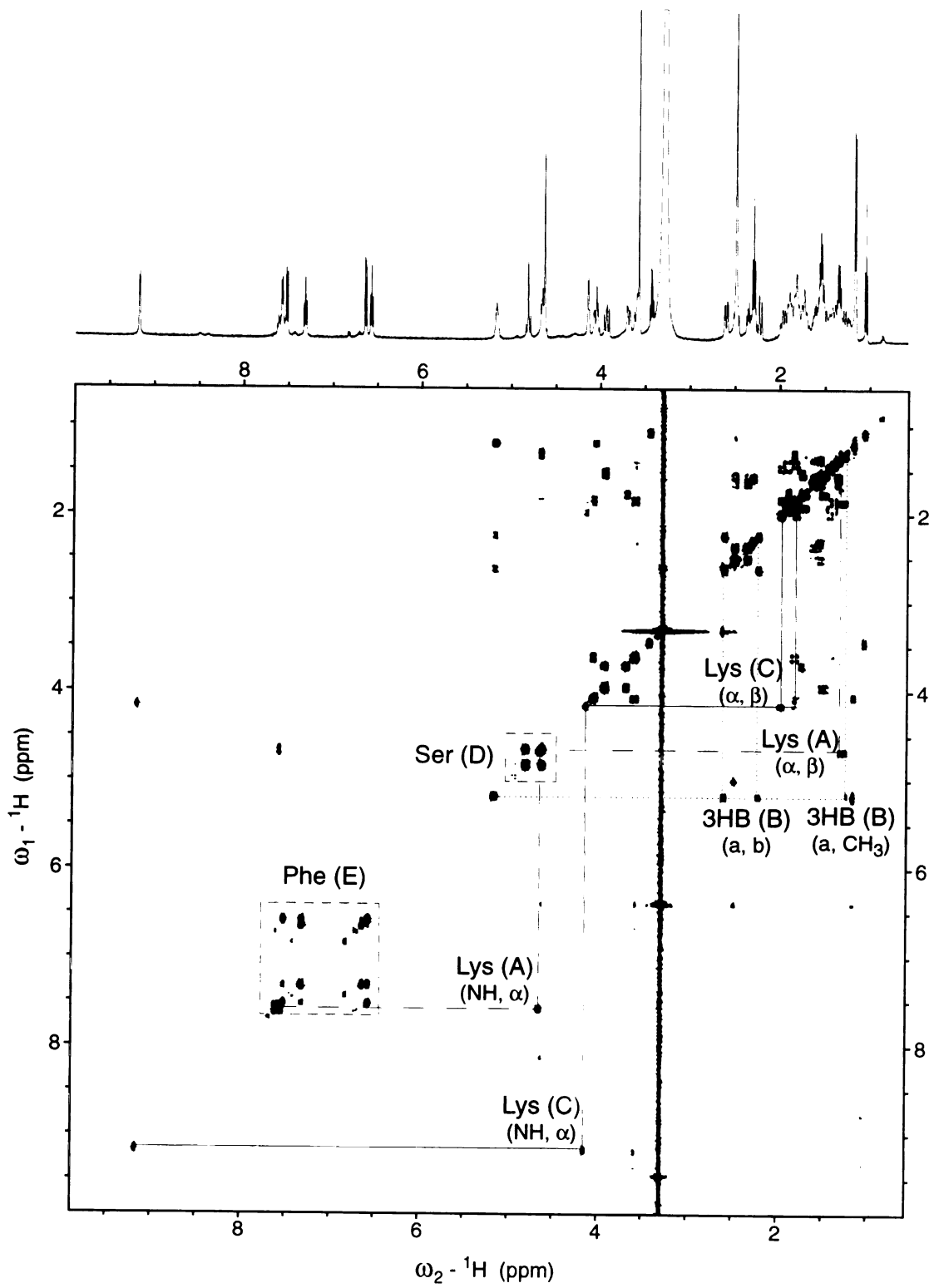
hydroxylysine (C) (9.17 ppm) showed coupling to both β protons [4.64 (β1), 4.82 (β2) ppm] of the cyclized serine (D). In addition, one of the δ protons (1.82 ppm) showed cross-peaks to the two protons on C-1, the carbon adjacent to the carbonyl in moiety F. One of the ε protons (4.07 ppm) not only coupled to the two protons on C-1, but also to the diastereotopic protons on C-2.

These ROESY cross-peaks also enabled the complete assignment of the protons on the R_1 alkyl chain (F). As stated previously in the discussion of the desferri-exochelin assignments, the DQF-COSY and HOHAHA spectra only allow for the relative assignments of the R_1 alkyl chain and phenyl ring. For the phenyl ring (E), Hd showed ROESY cross-peaks to the β protons [4.64 (β1), 4.82 (β2) ppm] of the cyclized serine (D). These NOEs are understandable since the hydroxyl oxygen and the nitrogen of the serine are both thought to be involved in metal binding, positioning Hd closer to the serine β protons in space than Ha. It confirmed that Hd is meta and Ha is ortho to the hydroxyl on the phenyl ring.

In the case of the R_1 alkyl chain in the gallium-exochelin complex, it would be expected that the alkyl chain would have more constraints on its freedom of motion than in the desferri-exochelin since the nearby N-hydroxyl and carbonyl oxygen are both involved in metal complexation. This increased order is apparent when examining the two protons on C-1. In the desferri-exochelin, the H1 protons are equivalent (2.29 ppm). However, in the more-ordered gallium-exochelin structure, the H1 protons are no longer equivalent [2.37 (H1a), 2.51 (H1b) ppm, $J_{1a,1b} = 8.8$ Hz]. These non-equivalent protons would most likely be at the C-1 carbon, rather than at the C-5 carbon, which would have virtually unlimited freedom of motion. The ROESY cross-peaks between the linear N-hydroxylysine (C) δ and ε protons to the H1 and H2 protons of the R_1 alkyl chain also confirmed the order of the protons on the R_1 chain.

Many other NOEs, besides those aiding in sequence determination, were seen in the ROESY spectra, giving information on the solution conformation of the metal-bound

107

exochelin (see Table 3.3). In addition to those interactions described in the previous section, interresidue coupling was observed between both β protons of the serine [4.64 (β1), 4.82 (β2) ppm] and the methyl protons of the 3-hydroxybutyric acid linker (B) and the amide proton of N-hydroxylysine C (see Fig 3.11). ROESY cross-peaks were also observed between the amide proton of N-hydroxylysine (A) and the H_a, H_{b1}, and H_{b2} protons of the 3-hydroxybutyric acid (B). The α proton of N-hydroxylysine (A) also exhibited coupling to both of the ε protons of this same residue.

3.4 DISCUSSION

The one-dimensional ^1H NMR spectrum of the desferri- (see Fig 3.2) and gallium-exochelin (see Fig 3.9) analogs were very complex and additional 2-D NMR experiments were required to assign the molecules completely. DQF-COSY, HOHAHA, and ROESY experiments were performed on the desferri- and gallium-exochelin in DMSO-d_6 at 308 K. The full ^1H assignments for each analog are given in Tables 3.1 and 3.3, respectively.

In our initial NMR experiments using the native exochelins isolated from *M. tuberculosis*, the contaminating aromatic spin system that was discussed earlier was apparent in the DQF-COSY (see Fig 3.6) and HOHAHA spectra. This minor hydrolyzed exochelin structure was thought to have formed in the iron removal process during the sample preparation. During this procedure, the exochelin is incubated for several hours in 50 mM EDTA at pH 4.0. Under these conditions, we had previously found that hydrolysis of the oxazoline ring (moiety D) occurs readily, resulting in a ring open form of the molecule (see Fig 3.7). As stated before, this same observation was seen in the NMR studies performed by Lane *et al.* (Lane et al. 1995) on the *M. avium* exochelin. Therefore, rather than beginning our studies on this mixture of exochelins, I waited for a pure synthetic desferri-exochelin sample to be prepared to begin the NMR studies.

There were numerous observable differences between the desferri- and gallium-exochelin spectra. The diastereotopic protons of the linear N-hydroxylysine (C), which

were equivalent in the desferri-exochelin spectra, became nonequivalent in the gallium-exochelin spectra (see Fig 3.5). In addition, peaks corresponding to the lysine NOH and phenolic OH protons were noticeably absent in the gallium-exochelin spectra since the hydroxyls are presumably ionized and involved in metal binding.

In the cases of both the desferri- and gallium-exochelin, the DQF-COSY and HOHAHA spectra enabled the assignment of the proton spin systems while the ROESY spectra allowed for the determination of the sequence and possible conformation by providing information about interresidue coupling. NOESY experiments were initially performed but failed to yield useful information. This was not surprising since the molecular weight of the exochelin analog places it in the range where NOEs reach a zero point and change from positive to negative (Sharman et al. 1995). There were no ROESY cross-peaks in the desferri-exochelin spectrum indicative of coupling between physically distant protons in the molecule that would imply an ordered structure. However, the ROESY experiments with the gallium-exochelin revealed numerous interactions that were not present in the desferri-exochelin molecule (see Fig 3.11). These interactions will provide valuable distance constraints when a 3-D model of the metal-bound exochelin is constructed. In addition, distances noted in the crystal structure of the mycobactin reported by Hough et al. (Hough and Rogers 1974) will be used to refine the exochelin model.

Knowledge of the 3-D structure of the metal-bound exochelin will hopefully provide a better understanding of its interactions at the mycobacterial cell surface. A complete picture of the mycobacterial iron acquisition system may reveal a likely step to interrupt the process, providing a possible lead in the search for new antimycobacterials.

Chapter 4: *In vitro* metabolism of the exochelin, a siderophore of

M. tuberculosis, as a predictor of its metabolism *in vivo*

4.1 INTRODUCTION

Efforts to detect mycobactins from mycobacteria grown *in vivo* have proven

difficult. Despite the fact that *M. avium* was known to produce large amounts of

mycobactin when grown in iron-deficient media in the laboratory, McCready and Ratledge

failed to detect any mycobactin in *M. avium* recovered from rabbit (Wheeler and Ratledge

1994). In addition, experiments attempting to detect mycobactin in *M. leprae* from

armadillo liver (Kato 1985), *M. tuberculosis* from mouse spleen, *M. avium* from flamingo

liver and spleen, and *M. paratuberculosis* from bovine ileum (Lambrecht and Collins 1993)

have also failed. Efforts in our laboratories to detect exochelins and/or mycobactins in

lungs from guinea pigs infected with *M. tuberculosis* also met with little success

(unpublished data).

The failure to detect exochelins and mycobactins *in vivo* does not necessarily mean

that they are not components of the mycobacterial iron acquisition system *in vivo*. When

the mycobacteria are grown in low iron media in the laboratory, there is likely an

exaggerated response to the stress conditions since there is not any iron present that would

eventually signal the cells to terminate synthesis of the components of the iron uptake

process. In the *in vivo* model, when the mycobacteria encounter similar conditions of iron

deprivation during the initial stages of infection, the mycobacteria would synthesize

components of its iron acquisition system. Consequently, the invading bacteria will

acquire iron, eventually repressing the synthesis of the iron acquisition system

components. It is probable that the *in vivo* mycobacteria would exist on a delicate balance

between iron deficiency and sufficiency and that the synthesis of components of the

acquisition system (i.e., exochelins and mycobactins) will only be sufficient to obtain

enough iron for the cells to sustain growth and would probably not reach the high amounts

that are found in the laboratory setting.

Therefore, in an effort to learn more about the biotransformation of exochelins *in*

vivo, we investigated the metabolism of exochelins in an *in vitro* model. The results from

this study can then serve as predictors for their metabolites *in vivo* (Thummel et al. 1994;

Iwatsubo et al. 1997; Iwatsubo et al. 1997; Obach et al. 1997). In this study, we report on

the metabolism of the exochelin using two *in vitro* models, rat liver microsomes and freshly

isolated hepatocytes, systems which have been shown to be good models for the

characterization of drug metabolites.

4.2 MATERIALS AND METHODS

4.2.1 *Materials*

4.2.1.1 *Synthetic exochelin*

A synthetic desferri-exochelin with a neutral mass of 719 Da was provided by

Keystone Biomed Inc (Los Angeles, CA).

4.2.1.2 *Animals*

The liver microsomes and hepatocytes were isolated from male Sprague-Dawley

rats (B and K Universal, Inc., Fremont, CA).

4.2.2 *Methods*

4.2.2.1 *Preparation of rat liver microsomes*

The microsomes were prepared from rat liver according to the methods of

Guengerich (Guengerich 1989). Thus, three male Sprague-Dawley rats (200-300 g) were

lightly anesthetized with diethyl ether and decapitated. Their livers were removed immediately and placed in ice-cold pH 7.4 buffer containing 0.25 M KH_2PO_4 and 0.15 M KCl (30 ml buffer per liver). The livers were then minced into small pieces and homogenized (on ice) with a glass mortar and teflon pestle (5 strokes, 20 seconds per stroke). This homogenate was centrifuged at 9,000 x g at 4°C for 20 min with a Beckman JA-20 rotor and a Beckman J2-21 centrifuge. The supernate was decanted into a fresh centrifuge tube and centrifuged once again as above. The resulting supernate was re-centrifuged at 100,000 x g for 60 min at 4°C in a Beckman L7-55 high speed centrifuge equipped with a Beckman Ti-45 rotor. The resulting supernate (cytosol) was decanted and the microsomal pellet resuspended in ice-cold buffer and again centrifuged at 100,000 x g for 60 min. The final microsomal pellet was resuspended in buffer (50 ml) containing 150 mM KCl, 1.5 mM EDTA, and 100 mM KH_2PO_4 (pH 7.4). Incubations of the exochelins (in water) with the microsomes were conducted at 37°C with a 60 μg microsomal protein concentration in 0.1 M Na_2HPO_4 buffer (pH 7.4). After pre-incubation with the exochelin for 5 min, reactions were initiated by addition of nicotinamide adenine dinucleotide phosphate (NADPH) in buffer to a final concentration of 1 mM (1 ml total volume). At indicated times (0, 15 min, 30 min, 1 hr, and 2 hr), small aliquots of the incubations were removed, and reactions were stopped by addition of 1 volume of acetonitrile.

4.2.2.2 *Preparation of hepatocytes*

Hepatocytes were prepared from male Sprague-Dawley rats (350-400g) according to the method of Moldéus *et al.* (Moldéus et al. 1978), and greater than 90% cell viability was achieved, as assessed by trypan blue exclusion. Experiments were performed by incubating the exochelin (1.9 mM) with freshly isolated hepatocytes (3 million cells/ml, 2 ml total volume) in Krebs Hensleit buffer (pH 7.4) supplemented with 25 mM HEPES and 1% BSA (w/v). The cells were rotated continuously in 5-ml round-bottom flasks at 37°C

under an atmsophere of 95% oxygen and 5% carbon dioxide. At indicated times (0, 30 min, 1 hr, 2 hrs), 200 µl aliquots were quenched with 200 µl acetonitrile.

4.2.2.3 *Sample analysis*

All of the samples were analyzed for exochelin metabolites by reverse-phase high performance liquid chromatography (HPLC). The samples were vortexed for approximately 2 min and centrifuged for 5 min at 3,500 rpm. A small aliquot (50 µl) of the supernatant was taken, passed through a 0.45 µm microcentrifuge filter (Rainin; Woburn, MA), and diluted to a 500 µl total volume with HPLC buffer A [100 %H_2O/ 0.1 % trifluoroacetic acid (TFA)]. The filtered material was loaded onto a C_{18} column and subjected to reverse-phase HPLC separation using a 15-70% buffer B gradient (70% acetonitrile/0.08% TFA) at a flow rate of 250 µl/min on a Rainin HPXL gradient system (Woburn, MA), monitoring at 220 nm on an ABI 1000S Diode Array Detector.

4.2.2.4 *Mass spectrometric analysis*

For the rat hepatocyte incubations, peaks isolated from the HPLC and identified as potential exochelins were first subjected to mass analysis by matrix-assisted laser desorption ionization (MALDI) mass spectrometry. For these experiments, a Voyager Elite reflectron time-of-flight (TOF) mass spectrometer (Perseptive Biosystems; Framingham, MA) equipped with a 337 nm N_2 laser was used under delayed extraction conditions as described by Vestal *et al.* (Vestal et al. 1995). The improved optics of delayed extraction allowed for increased resolving power (2000 M/ΔM). Data was recorded with a 2 GHz Tektronix TDS 744A digitizer. Samples were concentrated under vacuum and small aliquots (1 µl) were mixed 1:1 with the α-cyano-4-hydroxycinnamic acid matrix (Hewlett Packard). The instrument was externally calibrated using a mixture of standard peptides consisting of angiotensin II and bombesin with monoisotopic masses of 1045.5 and 1618.8 Da, respectively. Post-source decay (PSD) sequencing (Kaufmann et al. 1993) of

selected metabolites involved gating a precursor ion, $(M + H)^+$, to transmit selectively an individual exochelin and its metastable fragment ions. The PSD experiments were carried out varying the reflectron (mirror ratio) and guide wire voltage in 7 steps. The complete PSD spectrum was produced by stitching the segments from individual steps together. Calibration in PSD mode was also performed externally, using a mixture of standard peptides consisting of angiostensin II and bombesin (1045.5 and 1618.8 Da, respectively].

In the analysis of the rat liver microsome incubations, the samples were prepared in the same manner as in the hepatocyte incubations, but were analyzed on a ToFSpec SE (Micromass Inc., Manchester, UK) MALDI-TOF mass spectrometer with a nitrogen laser and operated in reflectron mode (Karas et al. 1991). A standard peptide mixture was used to externally calibrate all mass spectra. PSD sequencing (Kaufmann et al. 1993) involved gating a precursor ion, $(M + H)^+$, to selectively transmit an individual peptide and its metastable fragment ions to the reflectron. The PSD experiments were carried out varying the reflectron voltage in 9 - 11 steps, with the voltage at each step being reduced to 75% of the previous step. The complete PSD spectrum was produced by stitching the segments from individual steps together. Calibration in PSD mode was done using the fragment ions generated from a standard peptide, ACTH 18-39 $[MH^+ = 2466.2$ (monoisotopic)].

4.3 RESULTS

4.3.1 Rat liver microsome incubations

Synthetic exochelin (see Fig 4.1) was incubated with rat liver microsomes over a period of two hours. HPLC analysis of time points (0, 15 min, 30 min, 1 hr, 2 hrs) from the rat liver microsome incubations with synthetic exochelin and NADPH revealed two major metabolites (see Fig 4.2). Analysis of the isolated metabolites using MALDI mass spectrometry showed HPLC peaks A, B, and C to be iron-binding molecules, revealed by an ion pair differing in mass by 53 Da. These peaks correspond to protonated or desferri
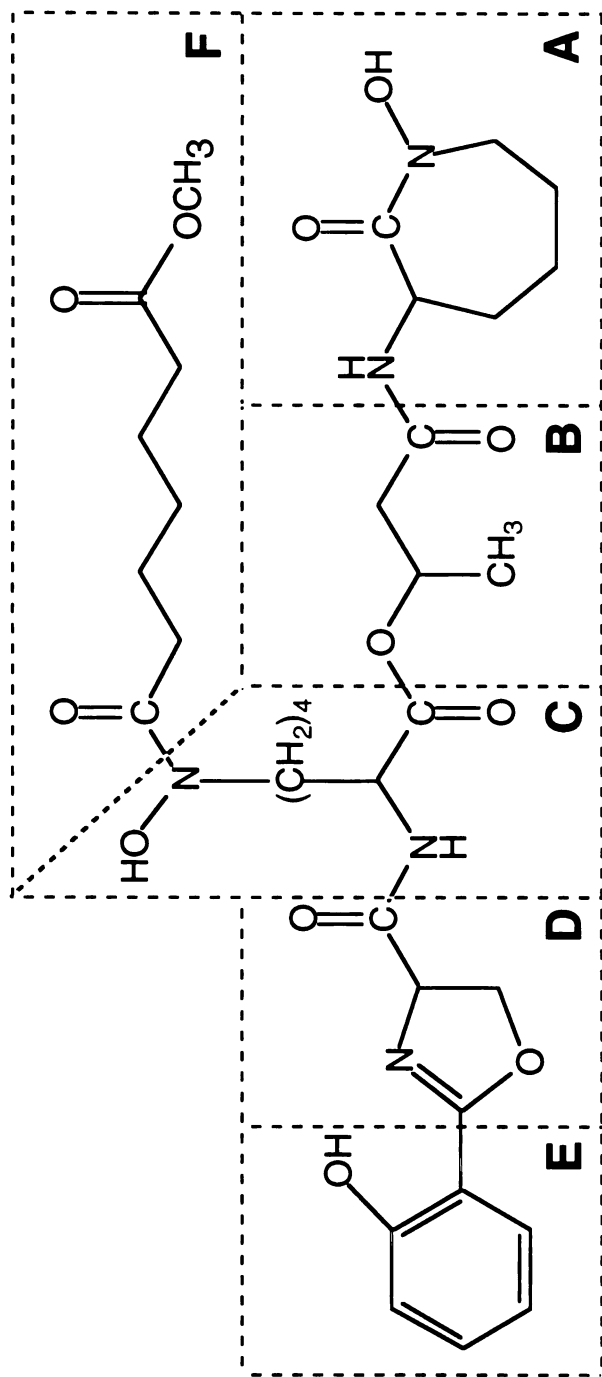
Figure 4.1 Sructure of synthetic exochelin with M$_r$ 719. The exochelin can be divided into 6 structural moieties (A - F), as indicated by the dashed lines. These moieties likely correspond to separate biosynthetic elements. The exochelin contains 3 amino acid moieties - 2 N-hydroxylysines (A and C) and 1 serine (D). moiety F is a saturated alkyl chain which terminates with a methyl ester.
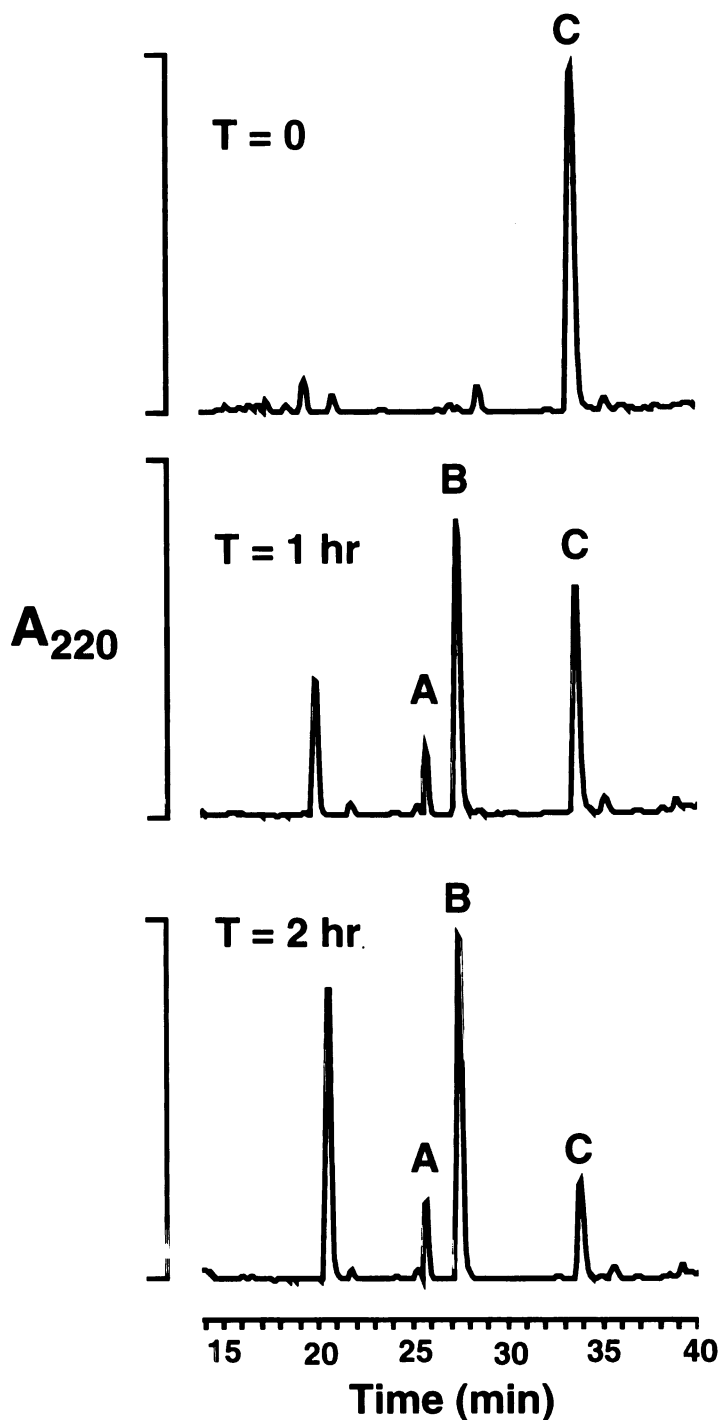
Figure 4.2 HPLC analysis of exochelin rat liver microsome incubations. Synthetic exochelin 720SM was incubated with rat liver microsomes and NADPH for 2 hours. HPLC analysis of small aliquots of the incubations at (A) T = 0, (B) T = 1 hrs, and (C) T = 2 hrs, monitored at 220 nm, revealed 2 metabolites (peaks A and B) not present in the control. Peak C is the unreacted starting material.

116

form $(M + H)^+$ and the iron $(M - 2H + Fe^{III})^+$ adducts of the same molecular ion species (see Fig 4.3). Metabolites A and B and the unchanged exochelin starting material C (see Fig 4.2) were found to have $(M + H)^+$ at m/z 780, 706, and 720, respectively.

All three exochelins were analyzed by MALDI-PSD to characterize their structures further. Fragment ions were assigned to one of six structural moeities (A - F) within the exochelin, arising from one or more cleavages about the amide or ester bonds (see Fig 4.1). Many lower mass peaks were identical for all 3 exochelins, such as peaks at m/z 100, 145, and 171, which correspond to fragments C-CO-OH+2H, C+2H, and A+CO, respectively. The core structure (A - E) of all three exochelins remained unchanged, with the structural differences all occuring in the R_1 alkyl chain (moiety F) (see Fig 4.1).

PSD analysis of peak C showed it to be the unreacted exochelin starting material (with methyl ester still intact). Metabolite B, the major exochelin metabolite, is the free acid form of the exochelin resulting from hydrolysis of the methyl ester at the end of the R_1 alkyl chain (moiety F) (see Table 4.1). The existence of the exochelin as a free acid is supported by the presence of a $(M + H)^+$-18 Da fragment at m/z 688 Da, denoting loss of H_2O, and the absence of $(M + H)^+$-32 Da fragment, a loss of CH_3OH which is characteristic of methyl ester exochelins.

Exochelin A was the most polar of the metabolites, with a $(M + H)^+$ at m/z 780 (see Fig 4.3 and 4.4). Its production is cytochrome P450 dependent since, unlike metabolite B, it was not formed in the incubation which lacked NADPH. A fragment ion at m/z 688 [(M + H)$^+$ - 92 Da], analogous to the loss of CH_3OH in exochelin C or H_2O in exochelin B, suggested that the modification occurred at the end of the R_1 chain in moiety **F** (see Fig 4.4). However, consideration of possible common cytochrome P450 modifications did not reveal a likely candidate with a mass of 91 Da. Since the microsomes had been stored at -80°C in a 20% glycerol solution, it is highly probable that metabolite A was an exochelin whose R_1 alkyl chain terminated with a glycerol ester. This accounts for both the increased polarity of the

Figure 4.3. MALDI mass spectrum of peak A from the rat liver microsome incubations. The two most prominent ions at *m/z* 833.3 amd 780.4 correspond to the singly charged molecular ion for the iron-bound state and the iron-free state, respectively. Both of these ions are further substituted with sodium and/or magnesium.
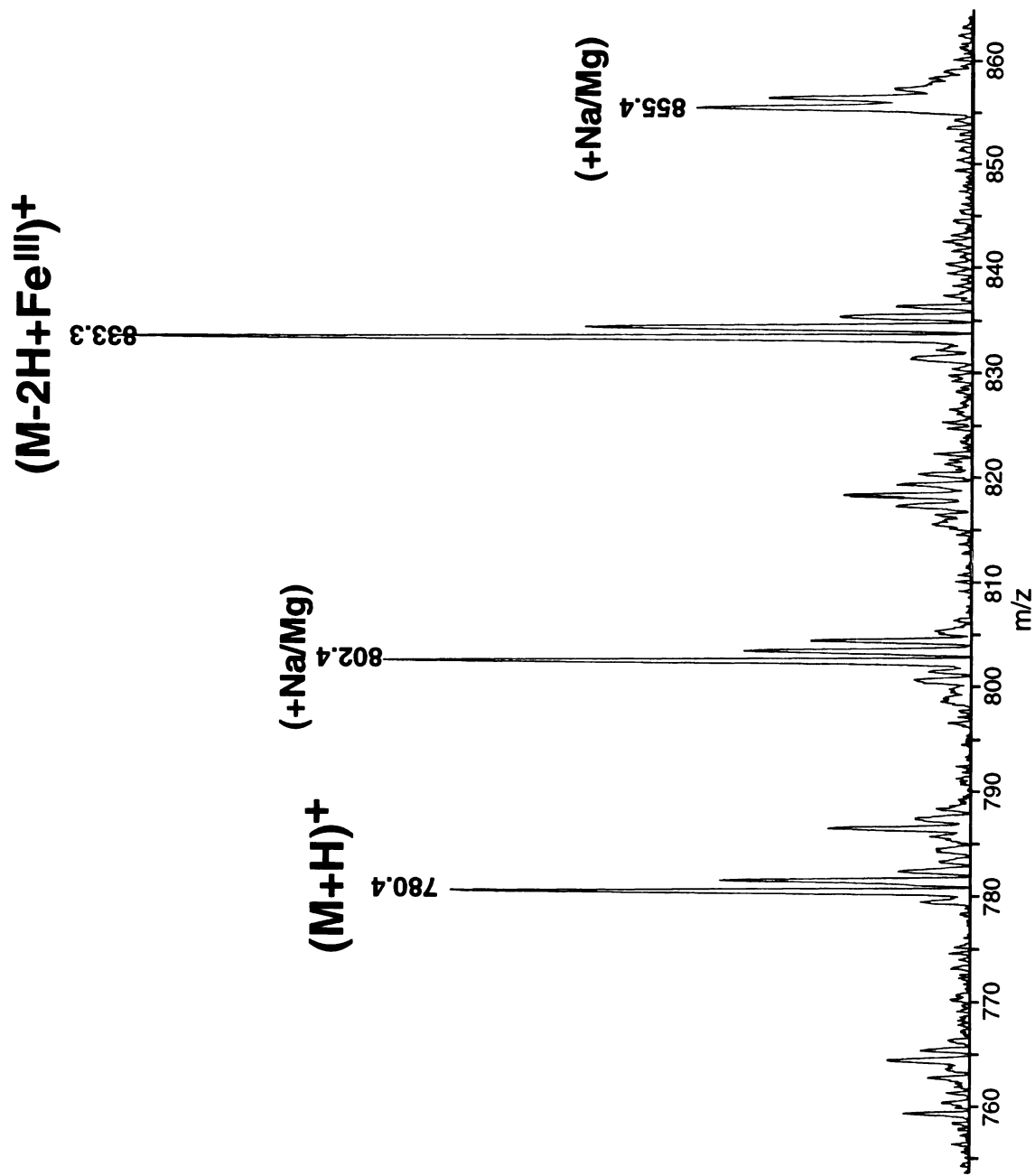
Table 4.1. Fragment ions (Da) of exochelin metabolites from rat liver microsome incubations

Fragment	Peak A $(M+H)^+$ 780	Peak B $(M+H)^+$ 706	Peak C $(M+H)^+$ 720
C-CO-OH+2H	100	100	100
C+2H	145	145	145
DE-CO	162	162	162
A+CO	171	171	171
DE+NH+2H	207	207	207
AB-O	213	213	213
AB+2H	231	231	231
CD+2H		242	
AB+CO			257
CDE+H	334	334	334
CDE+O+3H	352	352	352
BCDE+H	420	420	420
BCDE+NH+2H	437	437	437
CDEF-CO	522	448	462
CDEF	550	476	490
CDEF+O+2H	568	494	508
ABCF+2H	591		
BCDEF+H	637	563	
ABCDE+2H	564	564	564
BCDEF+NH+2H	653	579	593
MH^+-$C_3O_3H_7$	688		
MH^+-H_2O		688	
MH^+-CH_3OH			688
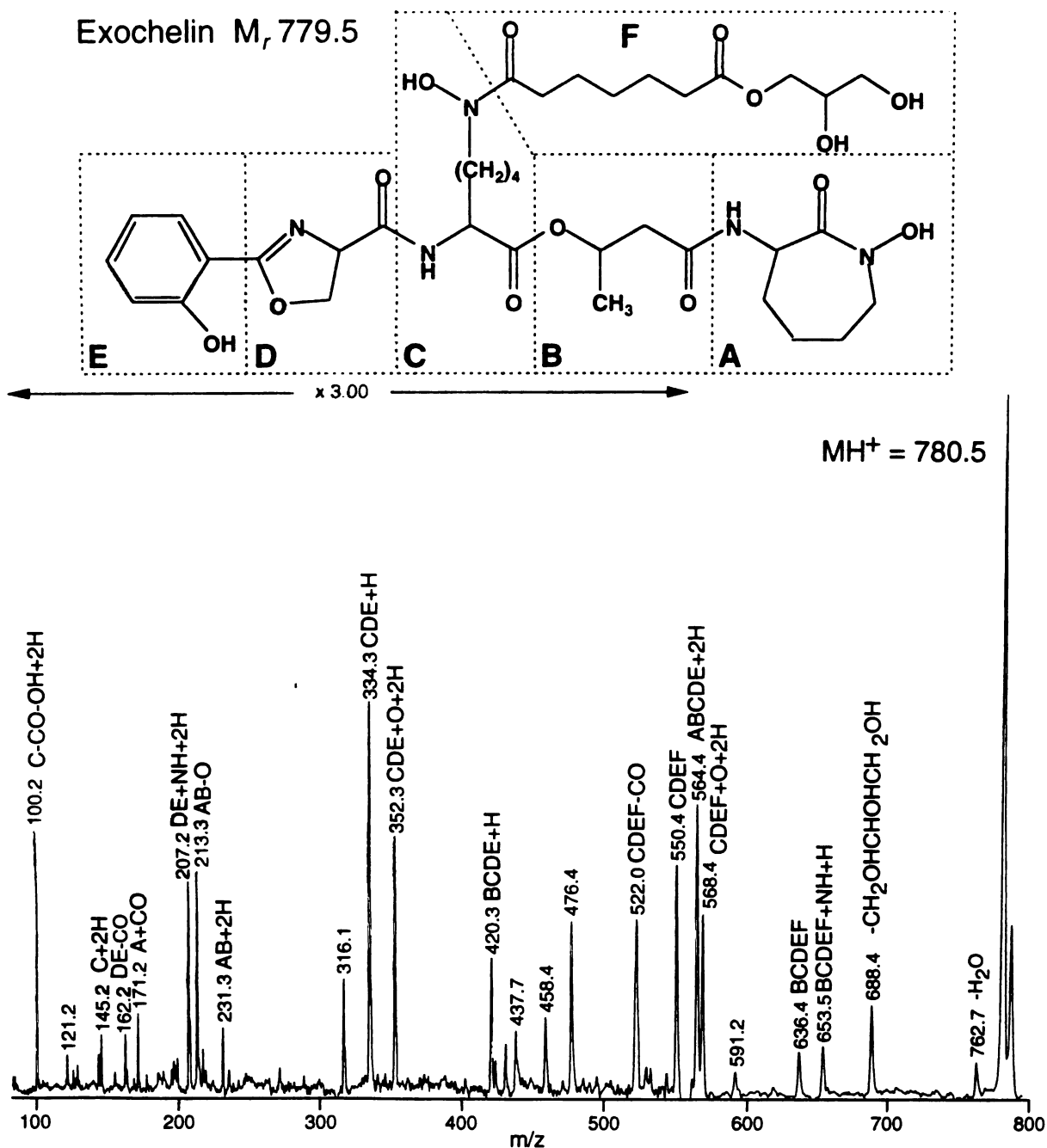
Figure 4.4 MALDI-PSD spectrum of exochelin metabolite A with (M+H)⁺
at *m/z* 780.4. Fragment ions of the exochelin are assigned to 1 of 6 structural moieties
(A - F) resulting from cleavages of amide and/or ester bonds. On the mass spectrum,
hydrogen transfers are indicated by +1, +2, and +3. All fragment ions containing moiety F
are shifted up in mass by 60 units relative to the starting material (see Fig 4.6).

metabolite and the mass increase. In this case, the glycerol may be acting as a trap for a more reactive P-450-derived exochelin metabolite, such as a peroxide intermediate.

4.3.2 Rat hepatocyte incubations

HPLC analysis of incubations of synthetic exochelin with freshly isolated rat hepatocytes revealed the formation of seven different exochelin metabolites over a period of two hours. Time points were taken at 0, 30 min, 1 hr, and 2 hrs. Analysis of individual HPLC peaks by MALDI revealed metabolites to have a $(M + H)^+$ at m/z 706 (one peak), 722 (four peaks), and 736 (two peaks) (see Fig 4.5). As with the rat liver microsome incubations, the major exochelin metabolite found in the hepatocyte studies was the free acid exochelin with $(M + H)^+$ at m/z 706, as confirmed by MALDI-PSD. However, unlike in the microsome studies, which only yielded one modified exochelin (glycerol ester), six new exochelin metabolites were characterized. Mass spectrometric analysis using MALDI-PSD of all the metabolites proved very useful in distinguishing the differences between the isobaric metabolites. As with the other exochelin metabolites, some lower mass peaks such as m/z 100, 145, and 171, corresponding to conserved, unmodified structural units A and C were present. The first 4 metabolites, all with $(M + H)^+$ at m/z 722, resulted from hydroxylation of the free acid form of the exochelin [$(M + H)^+$ at m/z 706]. Hydroxylation of the methyl ester exochelin [$(M + H)^+$ at m/z 720] at different positions in the molecule, resulted in two metabolites, both with $(M + H)^+$ at m/z 736. The site of hydroxylation in the exochelin can be localized to a specific portion of the molecule (moieties A - F) through examination of the fragment ions of the MALDI-PSD spectrum. In comparison to the spectrum of the unmodified methyl ester exochelin (see Fig 4.6), peaks which increase in mass by 16 Da relative to the parent ion are indicative of hydroxylation in one of these moieties. These shifts are highlighted in **bold** in table 4.2. For example, in the unmodified exochelin, fragment ions at m/z 334 and 564 correspond to **CDE + H** and **ABCDE + 2H**, respectively. In exochelin metabolite 6, the corresponding fragments have
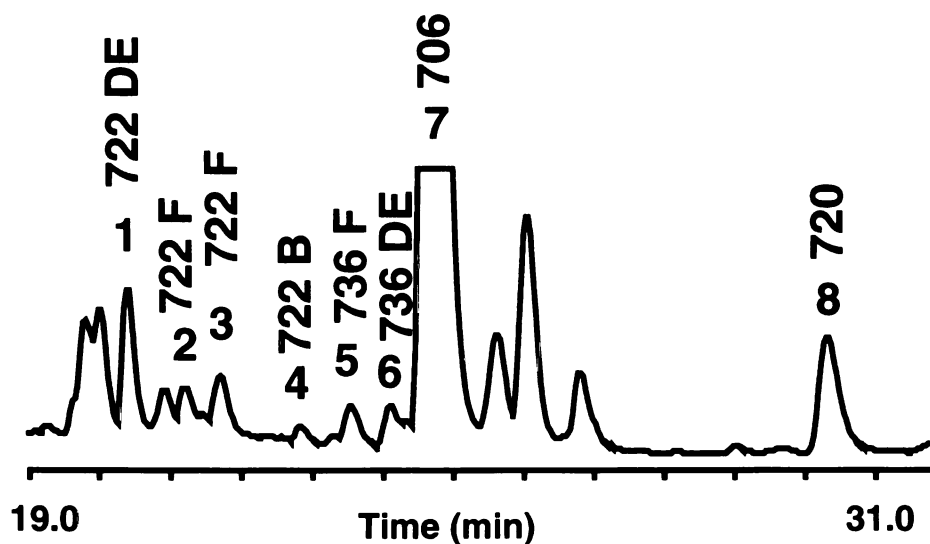
Figure 4.5 HPLC analysis of exochelin hepatocyte incubations at T = 2 hrs.

The synthetic exochelin was incubated with rat hepatocytes for 2 hrs. HPLC analysis,

monitoring at 220 nm, revealed several peaks (1 - 8) not present in the control (no

exochelin added). Subsequent mass spectrometric analysis of the HPLC peaks

revealed masses of the exochelin metabolites [desferri molecular ion $(M+H)^+$] and

the site, if any, of hydroxylation, as indicated above the peak numbers. For instance,

'736F' denotes an exochelin metabolite with $(M+H)^+$ at m/z 736 which is

hydroxylated in the F portion of the molecule. Peaks 7 and 8 were identified as the

free acid and methyl ester forms of the exochelin, respectively, and were not found to

be hydroxylated. Note: peak 7 is off scale.

Figure 4.6. MALDI-PSD mass spectrum of exochelin 720SM (HPLC peak 8). Fragment ions of the exochelin are assigned to 1 of 6 structural moieties (A - F) resulting from cleavages of amide and/or ester bonds. This spectrum confirmed the identity of peak 8 as unreacted starting material, with the methyl ester still intact.

MH$^+$ = 720.5

688.4 -CH$_3$OH

593.7 BCDEF+NH+2H

564.8 ABCDE+2H

509.1 CDEF+O+3H

490.2 CDEF

476.3

437.2 BCDE+NH+2H

420.5 BCDE+H

405.8

363.7

352.6 CDE+O+3H

334.2 CDE+H

271.4

256.4 AB+CO

231.1 AB+2H

213.1 AB-O

207.2 DE+NH+2H

171.3 A+CO

162.0 DE-CO

145.1 C+2H

100.1 C-CO-OH+2H

m/z

100   200   300   400   500   600   700

A

B

C

D

E

F

OCH$_3$

CH$_3$

(CH$_2$)$_4$

OH

HO

OH
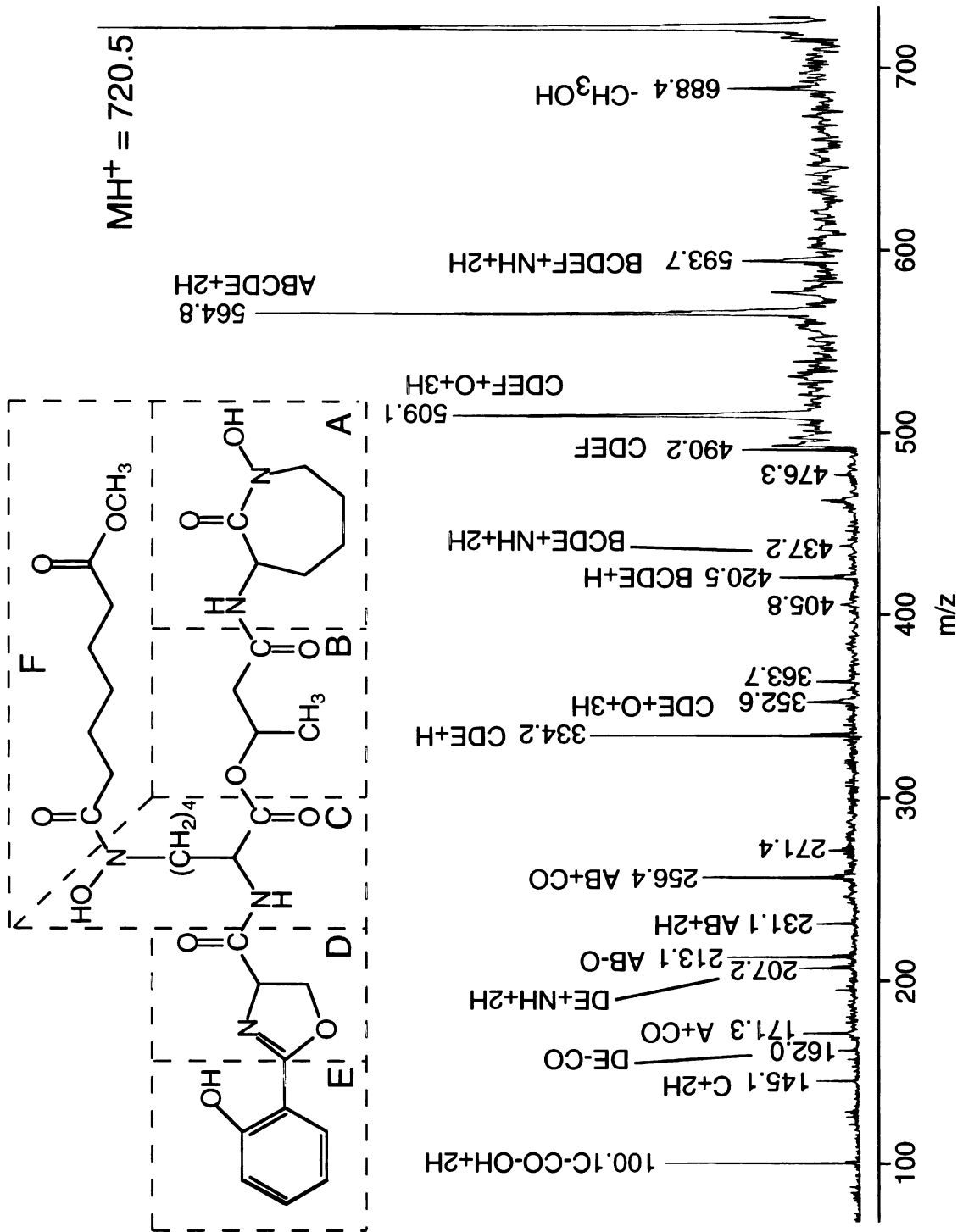
also increased in mass by 16 Da to m/z 350 and 580, respectively. In addition, fragment ions derived from C and A (peaks at m/z 100 and 171), remained unchanged, indicating that these portions of the molecule were not hydroxylated (see Fig 4.7). Since only one oxygen was added to the intact molecule, this data shows that the modification must have occurred in either the **D** or **E** moieties. Analysis of the PSD spectrum of metabolite 5 revealed that hydroxylation must have occurred in the R_1 alkyl chain of moiety **F**. When comparing metabolite 5 with the methyl ester exochelin, peaks corresponding to fragment **CDEF** shifted from m/z 490 to 506, yet those corresponding to CDE + H (m/z at 334), CDE + O + 3H (m/z at 352), and BCDE + H (m/z at 420) remained unchanged (see Fig 4.8).

The 3 metabolites with (M + H)$^+$ at m/z 722 refer to exochelins resulting from hydroxylation at different positions in the free acid exochelin. Exochelin 1 was hydroxylated in the **DE** moiety as supported by mass shifts of fragment ions containing the **DE** portions of the molecule. For example, **CDE + H** shifted up from m/z 334 in the free acid exochelin to m/z 350, while the fragment ion corresponding to C alone, remained unchanged. Both exochelins 2 and 3 were found to be modified in the **F** portion of the molecule, presumably at different positions on the alkyl chain as they elute at different retention times from the reverse phase-HPLC column. For both of these exochelins, fragments corresponding to **CDEF + O + 2H** shifted from m/z 495 to 511 while ABCDE + 2H (m/z 564) remained unchanged between the starting material and the metabolite. Hydroxylation occurred in portion **B** of exochelin metabolite 4. This is clearly evident in the PSD spectrum since fragments for **AB - O** and **AB + 2H** were both shifted up by 16 units to m/z 229 and 247, respectively, while the fragment ion for A + CO at m/z 171 remained the same. All of these fragment ions are listed in Table 4.2, with the mass shifts (indicating hydroxylation) highlighted in **bold**.

126

Table 4.2. Fragment ions (Da) of exochelin metabolites from rat hepatocyte incubations

Fragment	Peak 1 Exo 722 DE	Peak 2 Exo 722 F	Peak 3 Exo 722 F	Peak 4 Exo 722 B	Peak 5 Exo 736 F	Peak 6 Exo 736 DE	Peak 7 Exo 706	Peak 8 Exo 720
C-CO-OH+2H	100	100	100	100	100	100	100	100
C+2H	145		145		145	145	145	145
DE-CO					162		162	162
A+CO	171	171	171	171	171	171	171	171
DE+NH+2H		207	207	207	207	**223**	207	207
AB-O	213	213	213	229	213	213	213	213
AB+2H		231		**247**	231	231	231	
CD+2H	242						242	
AB+CO						257		256
CDE-O+H						334		
CDE+H	**350**ᵃ	334	334	334	334	**350**	334	334
CDE+O+3H	**368**	352	352	352	352	**368**	352	352
BCDE+H	**436**	420	420		420	**436**	420	420
BCDE+NH+2H							437	437
CDEF-CO	**464**							
CDEF	**492**	492		476	**506**		476	490
CDEF+O+2H	**510**	**510**	**510**		**524**	**524**	496	
BCDEF+H					**593**			
ABCDE+2H	**580**	564	564	**580**	564	**580**	564	564
BCDEF+NH+2H								594
MH⁺-H₂O			718					
MH⁺-CH₃OH								688

ᵃ fragment ions in bold indicate a shift in mass of 16 Da, relative to the unhydroxylated form of the exochelin

127

Figure 4.7. MALDI-PSD mass spectrum of exochelin metabolite 6. The

fragment ions in this spectrum demonstrated that this exochelin, with $(M + H)^+$ at m/z 736,

was hydroxylated in either the D or E moieties. Fragment ions containing these 2 portions

are shifted up in mass by 16 Da relative to the unmodified exochelin starting material (see

Fig 4.6). For instance, the ion corresponding to **CDE + H** has shifted from m/z 334 to

350.

$(M+H)^+ = 736.4$

580.7 ABCDE+2H
524.9 CDEF+O+3H
507.1 CDEF
463.4 BCDE+H
368.6 CDE+O+3H
350.1 CDE+H
334.2 CDE-O+H
256.6 AB+CO
231.1 AB+2H
223.1 DE+NH+2H
213.2 AB-O
171.0 A+CO
145.1 C+2H
128.1
100.1 C-CO-OH+2H
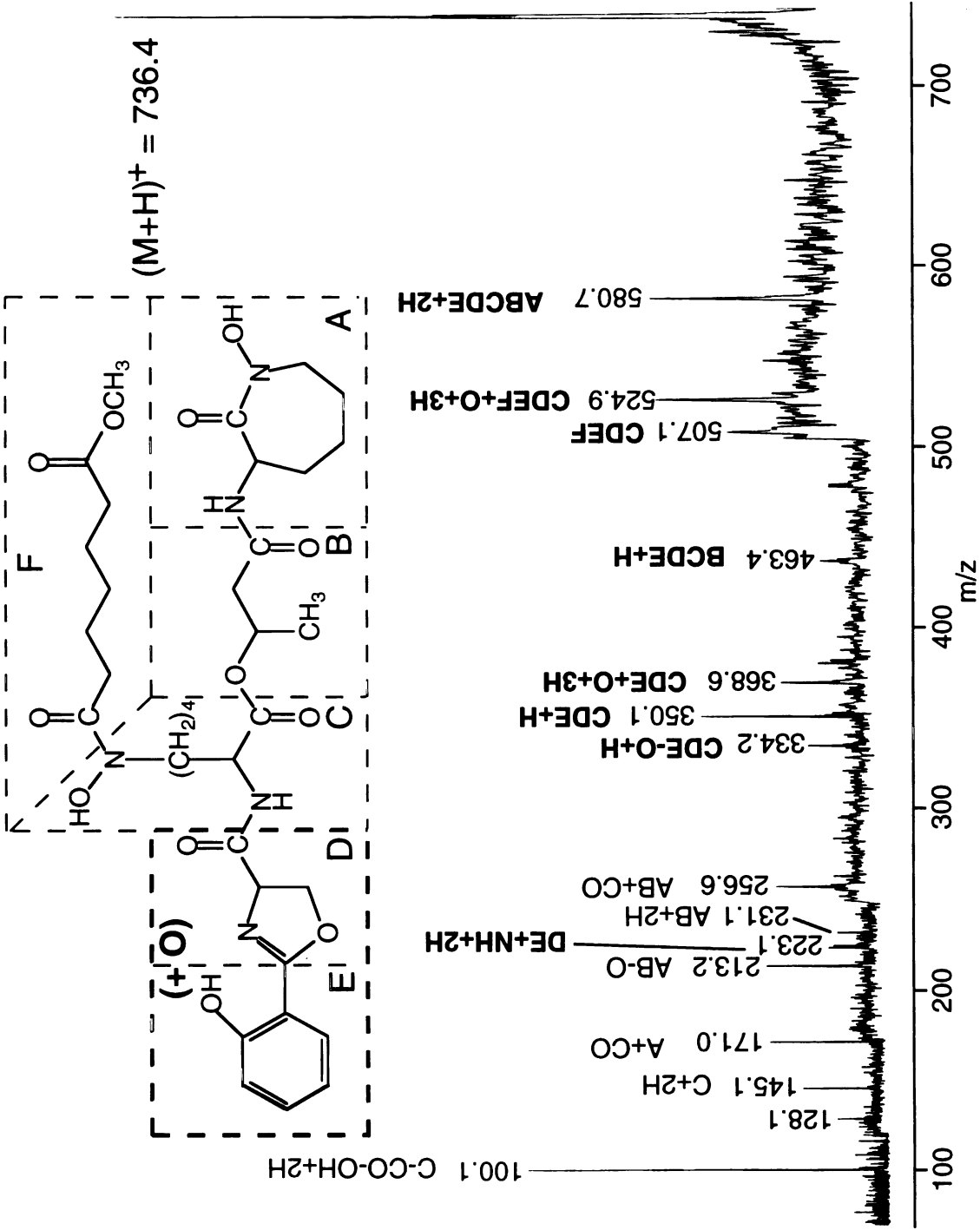
Figure 4.8. MALDI-PSD mass spectrum of exochelin metabolite 7. This exochelin metabolite, with $(M + H)^+$ at m/z 736, was hydroxylated in the R_1 alkyl chain (moiety F) of the molecule. This is apparent in the observed mass shifts of fragments **CDEF**, **CDEF** + O + 3H, and **BCDEF**, while the fragment corresponding to ABCDE + 2H remained unchanged.

$(M+H)^+ = 736.3$

718.3 $-H_2O$

592.7 BCDEF

564.8 ABCDE+2H

525.0 CDEF+O+3H

506.9 CDEF

420.3 BCDE+H

352.1 CDE+O+3H

334.1 CDE+H

231.1 AB+2H

213.1 AB-O

207.1 DE+NH+2H

171.0 A+CO

162.1 DE-CO

145.1 C+2H

100.1 C-CO-OH+2H

m/z

131

4.4 DISCUSSION

In this study, 7 exochelin metabolites were detected in the extracts from the rat hepatocytes. Hepatocytes are a good system to study *in vitro* metabolism since the permeability of the plasma membrane is maintained. Therefore, these intact cells are able to retain all of the enzymes (membrane-bound and soluble) and necessary cofactors. This allows for both phase 1 and phase 2 metabolic reactions to occur (Perotti et al. 1994), making the hepatocyte system most similar to an *in vivo* system. Measurements of cell viability, as determined by trypan blue exclusion, showed that the exochelin was not cytotoxic after 2 hours of incubation. The viability of the cells was shown to be 75%, which was identical to the cell viability in control incubations.

As stated previously, the fragment ions revealed in the MALDI-PSD spectra of the metabolites does not allow for the detection of the exact site of hydroxylation in the exochelin, only for the localization of the oxidation site to a portion of the molecule. The major metabolite (see Fig 4.5, peak 7) represented roughly 88% of the total metabolites and was formed by hydrolysis of the methyl ester in the R_1 alkyl chain of the exochelin (moiety F), as revealed by MALDI-PSD analysis. Mass spectrometric analysis of exochelin metabolites revealed that the free acid was the substrate for further metabolic reactions, as several hydroxylated forms of this exochelin were detected in the incubations (see Fig 4.5, peaks 1, 2, 3 and 4). In addition, the methyl ester form of the exochelin was also a substrate for P450 enzymes as two hydroxylated methyl ester exochelins were found (see Fig 4.5, peaks 5 and 6). Two of the metabolites were found to be oxidized in the R_1 alkyl chain while the other was hydroxylated in moiety B, 3-hydroxybutyric acid.

In the rat liver microsome system, cofactors that are necessary for both P-450 (NADPH) and glucuronidation [uridine 5'-diphosphoglucuronic acid (UDPGA)] reactions are required to be added to the incubations. Two metabolites were found when NADPH was added to the rat liver microsome incubations, a free acid (metabolite B) and a glycerol ester (metabolite A) exochelin. Hydrolysis of the methyl ester accounted for the majority of

132

the metabolic reactions, with metabolite B accounting for approximately 82% of the total. As stated previously, we postulate the glycerol in which the microsomes were stored is acting to trap a more reactive exochelin metabolite. Not surprisingly, this glycerol ester was not detected in the hepatocyte studies since the hepatocytes were freshly isolated and were not stored in a glycerol solution. In addition, none of the hydroxylated exochelin metabolites that were found in the hepatocyte studies were detected in any of the microsome incubations. This may be a result of a decreased level of enzyme activity in that preparation of microsomes.

Other routes of exochelin metabolism were also investigated. Many drugs and endogenous substances containing hydroxyls or carboxylic acids are modified with glucuronic acid to form ether and acyl glururonides, respectively (Dutton 1980). After the exochelin was deesterified, it was thought that this free acid form may be a substrate for glucuronidation. Therefore, *in vitro* experiments with rat liver microsomes, in which UDPGA was added to the incubation, were performed. However, beyond the formation of the free acid form, the exochelin did not appear to be metabolized further (data not shown). In addition, chain shortening of the R_1 alkyl group of the exochelin was expected as similar long alkyl chains in other molecules like prostaglandins (Galli et al. 1997; Hankin et al. 1997) and arachidonic acid (Retterstol et al. 1996; Luthria et al. 1997), are substrates for β-oxidation reactions. However, there were no detectable forms of exochelins with truncated alkyl side chains in the hepatocyte studies.

It should be noted that in our HPLC assay of the exochelin metabolites, we are only able to detect the biotransformation of intact exochelins. Hydrolysis of internal ester and amide bonds resulting in exochelin fragments may also be occurring in the incubations, yet those fragments may go undetected during the HPLC purification process due to their enhanced polarity (early eluting) and decreased UV absorbance character.

Metabolic studies of other compounds have shown that rat hepatocytes and rat liver microsomes are excellent predictors of primary routes of metabolism *in vivo* (Jajoo et al.

133

1990; Berry et al. 1997; von Moltke et al. 1998). These *in vitro* studies on the biotransformation of the exochelins from *M. tuberculosis* will hopefully provide a good starting point for our future *in vivo* studies and may also serve as a basis for the design and production of monoclonal antibodies specific for the metabolites identified in this study.

Chapter 5. Identification of Fur, aconitase, and other proteins expressed by *Mycobacterium tuberculosis* under conditions of low and high iron by combined two dimensional gel electrophoresis and mass spectrometry

5.1 INTRODUCTION

The *M. tuberculosis* genome sequencing project has provided information on sequences of hundreds of new proteins encoded by this pathogen's DNA. The availability of this information provides new opportunities for increasing our understanding of the pathophysiology of *M. tuberculosis* in the human host. Toward this end, a major next step is to determine the function of the proteins revealed by the genome project and their interplay under different physiological conditions in the host.

One physiological condition in the host known to be important in *M. tuberculosis* infection is the concentration of iron. Iron is an essential nutrient for all pathogens, but this element appears to play an especially critical role in the pathogenesis of tuberculosis. For example, serum containing poorly saturated transferrin, such as human serum, is tuberculostatic, an effect neutralized by the addition of iron (Kochan 1969; Kochan et al. 1971).

Iron is severely limited in the host at sites of *M. tuberculosis* replication. A facultative intracellular parasite, *M. tuberculosis* multiplies within macrophages in the lung and elsewhere. Within the macrophage, iron is limited as a result of the effects of the immunomodulator interferon gamma. This cytokine depletes iron in the labile iron pool of the cell by downregulating transferrin receptor expression and the intracellular concentration of ferritin (Byrd and Horwitz 1989; Byrd and Horwitz 1993). *M. tuberculosis* also multiplies extracellularly in lung cavities. In the extracellular space, iron is severely limited owing to the high affinity with which it is bound by the host iron-binding proteins transferrin and lactoferrin.

One measure of the importance of iron to *M. tuberculosis* is the degree to which it goes to obtain this element. The pathogen is known to produce at least two high affinity iron siderophores in great abundance - exochelins and mycobactins (Snow 1965; Macham et al. 1975; Gobin et al. 1995). Exochelins are released extracellularly and may be the most abundant molecule exported by *M. tuberculosis*. On a molar basis, the concentration of exochelins in *M. tuberculosis* culture filtrates (~ 5 µM) is 150-fold that of the 30 kDa (antigen 85b) major secretory protein of *M. tuberculosis* (~ 30 nM), the most abundant protein exported by this organism (Wiker and Harboe 1992; Leao et al. 1993; Gobin et al. 1995; Harth et al. 1996). It has been proposed by Macham and colleagues that exochelins bind iron in the aqueous extracellular milieu of the mycobacterium and transfer it to mycobactins in the cell wall for subsequent internalization into the bacterial cytoplasm (Wheeler and Ratledge 1994). Consistent with this hypothesis, we have demonstrated that exochelins remove iron from human transferrin and lactoferrin and transfer it to mycobactins in the cell wall of live *M. tuberculosis* (Gobin and Horwitz 1996).

To learn more about the role of iron in the physiology of *M. tuberculosis*, we have been investigating iron-regulated proteins of *M. tuberculosis*. In this study, we have taken advantage of three major scientific or technological advances to gain a more complete picture of how *M. tuberculosis* responds to changes in the iron concentration in its environment. The first advance, already noted, is the database generated by the *M. tuberculosis* genome sequencing project (Philipp et al. 1996). The second advance is the development of high resolution two-dimensional (2-D) gel electrophoresis allowing greatly enhanced separation of proteins. The third advance is the development of mass spectrometric methods for the low level detection and identification of proteins and peptides. In an effort to learn about cellular components affected by iron levels, we used these three modalities - 2-D gel electrophoresis, mass spectrometry (MS), and database searching - to identify proteins expressed under conditions of low- or high-iron concentration. We report the identification of 10 proteins from 11 different gel spots

whose expression levels were markedly affected by low- or high-iron conditions. These include two proteins already known to be affected by environmental iron levels in other bacteria, Fur and aconitase, as well as several mycobacterial antigens and enzymes not previously known to be affected by environmental iron levels.

5.2 MATERIALS AND METHODS

5.2.1 Materials

5.2.1.1 *Bacteria*

M. tuberculosis Erdman strain (ATCC no. 35801) was obtained from the lungs of guinea pigs infected with the bacteria by aerosol. Frozen bacterial stocks for use in iron studies were prepared from 7H11 agar plates as described (Horwitz et al. 1995).

5.2.1.2 *Medium*

Iron-deficient Sauton's broth was prepared by subjecting the broth to a chelating resin as described (Calder and Horwitz 1998). Briefly, 5 g/L of Chelex 100 resin (Bio-Rad, Hercules, CA) was added to Sauton's medium prepared without ferric ammonium citrate and magnesium sulfate (Eidus and Hamilton 1964), and the medium was stirred at 4°C overnight. The Chelex-treated medium was passed through a 0.2 μm filter into an acid-washed glass flask. Magnesium sulfate (250 mg/L) and trace amounts of metals including zinc (2 mg/L $ZnSO_4 \bullet 7H_2O$) and copper (0.5 mg/L $CuSO_4$) were added. This iron-deficient medium was then supplemented with ferric ammonium citrate to the desired iron concentration (1, 15, or 70 μM). The iron concentration in the medium was routinely checked by the ferrozine assay (Fish 1988).

5.2.1.3 *Cultures*

Bacteria from frozen stocks were cultured on 7H11 agar plates at 37°C in 5% CO_2 for 3 weeks, inoculated into Sauton's medium containing 15 μM Fe at an initial optical density at 540 nm (OD_{540}) of 0.05, and cultured for 3 weeks at 37°C in 5% CO_2 without shaking to a final OD_{540} of approximately 1.0. The bacteria were then subcultured into Sauton's medium containing either 1 μM or 70 μM Fe at an initial OD_{540} of 0.05, grown for 3 weeks to an OD_{540} of 0.7 to 1.0, harvested, and stored at -20°C until use.

5.2.2 Methods

5.2.2.1 *Sample preparation and 2-D gel electrophoresis*

Approximately 20 ml wet volume of bacteria were suspended in 80 ml phosphate buffer containing 100 μM PMSF, 100 μM benzamidine, and 0.5 mM EDTA. The bacterial suspension was sonicated 4 times for 10 min on an ice bath using a 1 cm diameter probe attached to a sonicator set at 50% duty cycle, strength 5 with pulse (W-375, Heat System-Ultrasonics, Inc., Farmingdale, NY) and centrifuged at 10,000 x g for 30 minutes to pellet unbroken bacteria and bacterial cell walls. The supernatant was passed sequentially through a 0.45 μm and a 0.2 μm filter, further clarified by centrifugation at 40,000 x g for 2 hr, and fractionated by ammonium sulfate precipitation. Protein concentration was determined by the BCA protein assay (Pierce, Rockford, IL). Two-dimensional gel electrophoresis was performed as described (Lee and Horwitz 1995) with modifications. Protein samples of 300 μg were dissolved in sample buffer containing 2% sodium dodecyl sulfate, 5% 2-mercaptoethanol, and 10% glycerol and heated at 95°C for 5 min. The samples were centrifuged at 100,000 x g for 10 min to remove any insoluble material and loaded onto 2.4 mm (internal diameter) x 16 cm isoelectric focusing tube gels with the ratio of ampholytes pH 3-10: pH 5-7 = 1:4. The samples were focused at 200 V for 2 hr; 500 V

for 2 hr; and 800 V for 16 hr. The second dimension gels were 10% to 20%

polyacrylamide linear gradient gels of size 20 cm x 16 cm x 1.5 mm.

5.2.2.2 In-Gel Digestion with Trypsin

The in-gel digestion procedure was similar to the methods of Rosenfeld *et al.*

(Rosenfeld et al. 1992) and Sheer (Sheer 1994) with modifications as described below (K.

Clauser personal communication). Protein spots of interest were cut out of the gel and

diced into small pieces with a stainless-steel scalpel or a vortex mixer and placed in

siliconized microfuge tubes. The gel was destained and dehydrated by washing 3 times

(~10 minutes) with 25 mM NH_4HCO_3/50 % acetonitrile (or until the Coomassie stain was

no longer visually detectable). The destained gel particles were then dried under vacuum

for 30 minutes. After rehydrating the particles with a minimal amount of 25 mM

NH_4HCO_3 with 0.1 µg/µl trypsin, the protein was digested overnight at 37°C. Recovery

of the peptides was accomplished by extracting the digestion mixture 3 times with 50%

acetonitrile/ 5% trifluoroacetic acid (TFA). In an effort to reduce the amount of volatile

salts (eg. TFA and NH_4HCO_3), the recovered peptides were concentrated in a Speed-Vac

(to a final volume of ~ 5 µl) and rehydrated at least 3 times. Control digestions were

performed on gel slices that did not contain any protein and revealed trypsin autoproteolysis

products and keratin contaminants that were readily identified in the subsequent mass

spectrometric analyses (see below).

5.2.2.3 MALDI-TOF MS of the Unseparated Digests

As described in Matsui *et al.*(Matsui et al. 1997), portions (approximately 1/10th)

of the unseparated tryptic digestion mixture were mixed 1:1 v/v with an α-cyano-4-

hydroxycinnamic acid matrix (Hewlett Packard) and analyzed on a ToFSpec SE

(Micromass Inc., Manchester, UK) matrix-assisted laser desorption ionization time-of-

flight (MALDI-TOF) mass spectrometer with a nitrogen laser and operated in reflectron

mode (Karas et al. 1991). A standard peptide mixture was used to externally calibrate all mass spectra. Post-source decay (PSD) sequencing (Kaufmann et al. 1993) involved gating a precursor ion to selectively transmit an individual peptide and its metastable fragment ions to the reflectron. The PSD experiments were carried out varying the reflectron voltage in 9-11 steps, with the voltage at each step being reduced to 75% of the previous step. The complete PSD spectrum was produced by stitching the segments from individual steps together. Calibration in PSD mode was done using the fragment ions from a standard peptide, ACTH 18-39.

5.2.2.4 *MALDI-CID MS*

Small aliquots of unseparated digestion mixture (1 µl, approximately 1/10th of the total) were mixed 1:1 with the matrix (saturated solution of 2,5-dihydroxybenzoic acid (Aldrich) in acetone). Samples were analyzed by collision-induced dissociation (CID) on a Micromass Autospec orthogonal acceleration TOF mass spectrometer (Micromass Inc., Manchester, UK) equipped with a N_2 laser (337 nm). After the MS-1 was tuned manually to transmit the ^{12}C monoisotopic ion of the precursor mass, a two stage deceleration electrostatic lens focused the ions into an approximately parallel beam before they entered the gas collision cell (Bateman et al. 1995). The collision cell was filled with Xe gas with a collision energy of 800 eV. Voltage applied periodically from a "push-out" electrode extracted the precursor and product ions into a linear TOF mass analyzer. All spectra were recorded with a microchannel plate detector using a time-to-digital converter (Precision Instruments, Knoxville, TN) (Medzihradszky et al. 1997).

5.2.2.5 *Database searches for protein identification*

A program available via the internet (http://prospector.ucsf.edu) and developed in the UCSF Mass Spectrometry Facility (Clauser *et al.*, manuscript in preparation) was used to search genomic databases. MS-Tag uses fragment ion masses (generated by MALDI-

PSD or -CID MS) to search the databases for matches to peptides from known proteins. The following parameters were used in the searches: no errors mode, *Mycobacterium* species, protein molecular mass range 1,000 - 120,000 Da, trypsin digest (one missed cleavage allowed), parent ion mass tolerance of ± 1.5 Da, fragment ion mass tolerance of ± 1.5 Da, and allowed fragment ion types a, b, y, a-NH_3, b-NH_3, y-NH_3, b-H_2O, and internal. The protein sequences found using MS-Tag were used to search protein databases for homologous proteins using NCBI's Basic Local Alignment Search Tool (BLAST). Basic BLAST searches using the blastp program were performed on the nonredundant database (Altschul et al. 1990). The Wisconsin Sequence Analysis Package, version 8.0 (Genetics Computer Group, Inc., Madison, WI) was used to perform sequence alignments (PILEUP) and identity calculations (DISTANCES).

5.3 RESULTS

Proteins of M. tuberculosis modulated by iron

Proteins of *M. tuberculosis* cultured in Sauton's medium containing low (1 μM) or high (70 μM) iron were sequentially fractionated by ammonium sulfate precipitation (0%-20%, 20%-55%, and 55%-95%) and analyzed by 2-D gel electrophoresis. With increasing amounts of ammonium sulfate, improved resolution of protein spots was obtained on 2-D gels. Heavy vertical and horizontal streaks were seen on 2-D gels with samples precipitated with 0-20% ammonium sulfate and these streaks severely interfered with analysis of protein spots. Although Triton X-114 extraction improved the resolution of samples precipitated with 20-55% ammonium sulfate, the best comparison of protein spots between high-iron and low-iron cultures was obtained from samples precipitated with 55-95% ammonium sulfate. Of more than 250 protein spots revealed by 2-D gel electrophoresis of samples precipitated with 55-95% ammonium sulfate, the expression of at least 15 proteins was induced and the expression of at least 12 proteins was decreased by

low iron (see Fig 5.1). The protein spots with differential expression under low-iron and high-iron conditions were further analyzed by MALDI mass spectrometry.

Protein spots from single (spots 1, 2, 15, 18, 21, 22-25) or several (spots 4, 11, 21) 2-D gels were removed and digested with trypsin. The resulting digestion mixture was analyzed by MALDI mass spectrometry to determine the molecular masses of the tryptic peptides (see Figs 5.2A and 5.3A). To obtain sequence information, masses of the fragment ions of selected tryptic peptides were obtained using MALDI-PSD (see Figs 5.3B-D) or MALDI-CID (see Fig 5.2B) mass spectrometry. MS-Tag fragment ion searches using minimally restricted search parameters (*Mycobacterium* species, 1,000-120,000 Da) of the NCBI protein database offered possible matches to peptide sequences of *M. tuberculosis* proteins. This information, in conjunction with the mass fingerprints of the proteins obtained by MALDI-TOF MS analysis, allowed for the matching of 11 protein spots to *M. tuberculosis* proteins in the database. BLAST searches of these protein sequences yielded possible identities and functional roles of many of these proteins as summarized below and in Table 5.1.

As noted above, the MS-Tag searches were restricted to searching *Mycobacterium* sequences only and were not intended as homology searches. In some of the searches, the fragmentation data was also found match the identitcal peptide in the same protein in another *Mycobacterium* species (aconitase and EF-Tu see Table 5.1).

5.4 DISCUSSION

5.4.1 *Regulators*

5.4.1.1 *Fur*

Protein gel spot #25, whose expression was upregulated under high-iron conditions and virtually absent under low-iron conditions, was taken from a single 2-D gel. The gel

Figure 5.1. Two-dimensional gel analysis of proteins of *M. tuberculosis* cultured in medium containing a (A) high (70 µM) or (B) low (1 µM) concentration of iron. Equal amounts of proteins precipitated by 55%-95% ammonium sulfate were separated by isoelectric focusing (pH 4-7 from right to left) in the first dimension and by linear gradient SDS-PAGE (10%-20% from top to bottom) in the second dimension. The second dimension gels were stained with Coomassie blue. Open circles and open squares represent protein spots with increased or decreased expression under the indicated condition, respectively.

(A)70 μM Fe

(kDa)

66 –

45 –

36 –

29 –

24 –

20 –

14 –

(B) 1 μM Fe
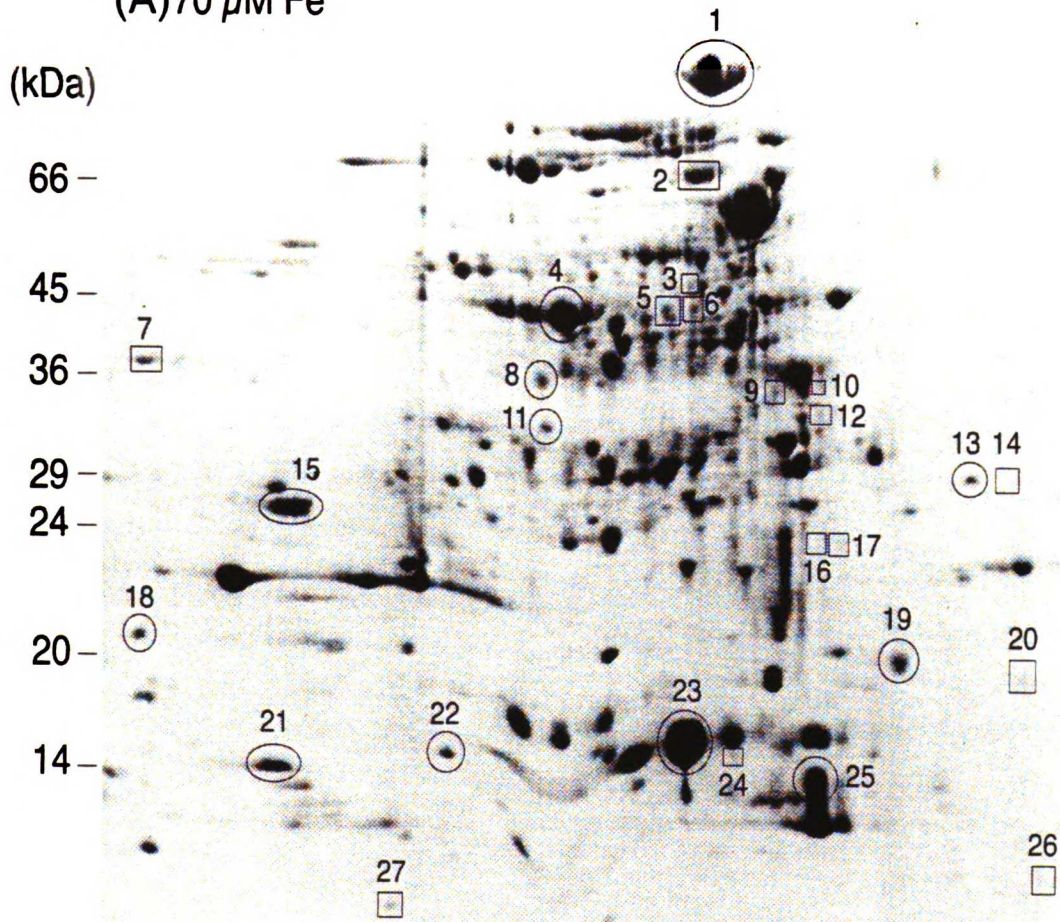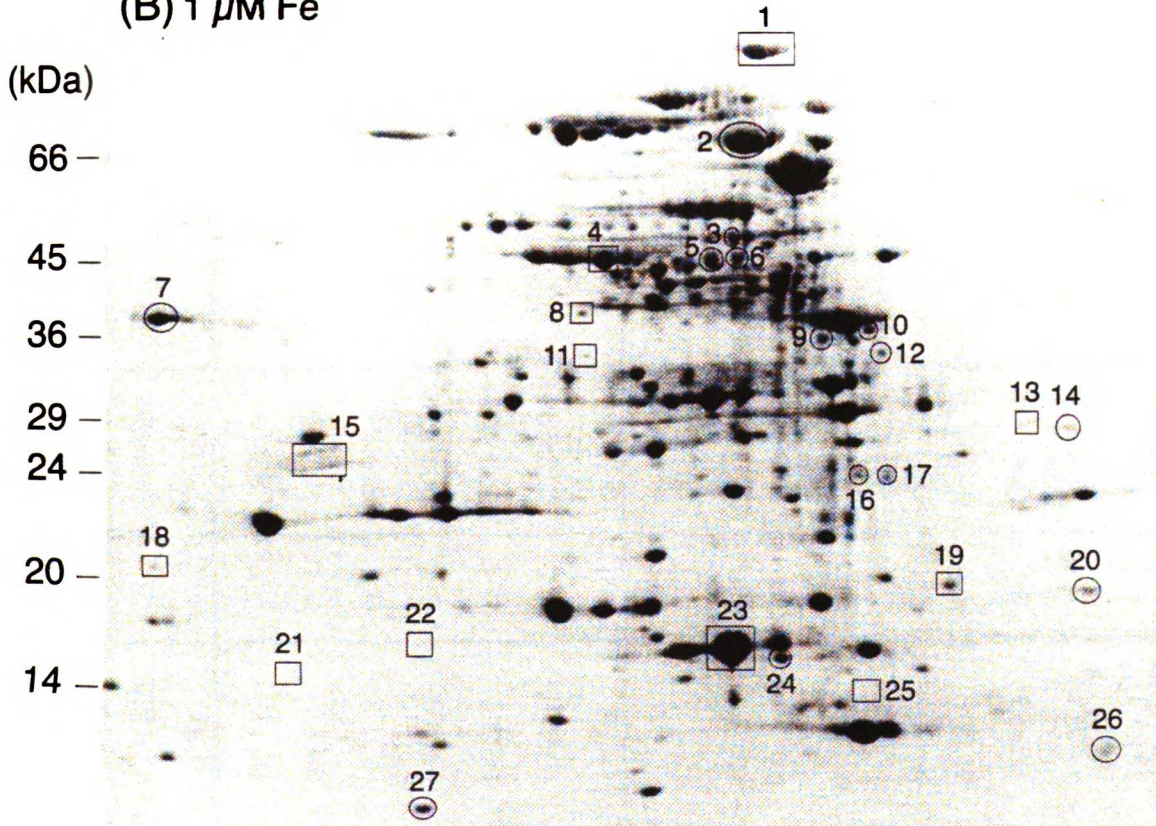
TABLE 5.1. Summary of proteins identified from 2-D gels of *M. tuberculosis* cell extracts

Spot #	Name NCBI Accession No.	Peptide MH[+] (Da)	Δ Mass	Start-End Position	Sequence[b]
1	Aconitase (NCBI# 2791409) MW 102449.6 Da	927.9	0.3	42-49	VLAENLLR
		845.6	0.2	747-754	DYNSFGSR
		1021.8	0.3	839-847	AVIAESFER
		1349.9	0.2	904-916	GDGATIEFDAVVR
		1438.1	0.4	773-785	NQLLDDVSGGYTR
		1897.0	0.5	278-294	*FVEFYGEGVAEVPLANR*[c]
		2297.3[a]	0.8	667-686	NLPTPSGNTFEWDPNSTYVR
2	Phosphoenolpyruvate Carboxykinase (NCBI# 1871584) MW 67253.5 Da	688.3	0	524-528	WIVDR
		957.6	0.2	371-377	**GNDWYFR**
		1086.7	0.1	423-432	TTVPLVTEAR
		1114.7	0.1	496-503	VFFVNWFR
		1163.7	0.1	203-211	**YITHFPETR**
		1310.4	0.8	510-520	FLWPGFGENSR
		1377.8	0.2	290-301	AETLGDDIAWMR
		1544.1	0.4	165-178	AALEKMGDDGFFVK[c]
		1544.1	0.3	110-121	SIMKDLYRGCMR

146

		Mass		Residues	Peptide
4	Elongation Factor Tu (NCBI# 399422) MW 43593.8	837.5	0	120-126	EHVLLAR
		1140.5	0.07	256-265	TTVTGVEMFR
		1343.2	1.5	365-376	LIQPVAMDEGLR
		1405.6	1	48-59	AFDQIDNAPEER [f]
		1682.6	0.7	267-282	**LLDQGQAGDNVGLLLR** [f]
		1802.8 [a]	0.2	158-173	**ELLAAQEFDEDAPVVR** [f]
		2077.2 [a]	0.9	140-157	ADAVDDEELELVEMEVR
		2156.8 [a]	1.3	236-255	GVINVNEEVEIVGIRPSTTK
		2197.1 [a]	0.6	207-225	ETDKPFLMPVEDVFTITGR
		2538.0 [a]	1.9	233-255	VERGVINVNEEVEIVGIRPSTTR
		2732.9 [a]	1.7	93-119	NMITGAAQMDGAILVVAATDGPMPQTR
11	Oxidoreductase (NCBI# 2072661) MW 29814.6	970.3	0.8	7 - 15	TMFISGASR
		1193.5	0.9	113 - 122	**FDLMNGIQVR**
		1209.5	0.9	113 - 122	FDLMNGIQVR [c]
		1768.7 [a]	0.7	55 - 71	ELEEAGGQALPIVGDOR
		2037.7 [a]	1.4	194 - 213	TMVATAAVQNLLGGDEAMAR [c]
		2530.6 [a]	1.7	216 - 238	KPEVYADAAYVIVNKPATEYTGK

15	hypothetical 21.5 kD protein (NCBI# 1731190) MW 21534.6	866.3	0.3	75-81	FTAEELR
		922.3	0.1	95-101	YNELVER
		1239.5	0.9	83-94	AAEGYLEAATSR
		1584.6 ^{a}	0.2	60-72	**LQEDLPEQLTELR**
		1648.2 ^{a}	0.6	95-108	**YNELVERGEAALER**
		2538.7 ^{a}	0.9	122-145	AEGYVDQAVELTQEALGTVASQTR
18	Peptidyl-prolyl cis-trans isomerase (NCBI# 1552563) MW 19239.5	1602.7	0	141-154	**HTIFGEVIDAESQR**
		2203.8 ^{a}	1.4	162-182	**TATDGNDRPTDPVVIESITIS**
		2431.2 ^{a}	0.3	51-73	DYSTQNASGGPSGPFYDGAVFHR
21	Lsr 2 (NCBI# 2113979) MW 12098.5	770.5	0.1	50-56	QWVAAGR [d]
		787.5	0.1	50 - 56	**QWVAAGR**
		884.6	0.2	90-97	NGHNVSTR
		1040.7	0.2	89-97	RNGHNVSTR
		1286.8	0.1	73-84	GAIDREQSAAIR
		1570.4	0.6	98-112	**GRIPADVIDAYHAAT**

148

22	hypothetical 15.9 kD protein (NCBI# 2113920) MW 15312.4	1113.0	0.4	124-134	**LLGSVPANVSR**
		1629.4 [a]	0.5	60-74	VTGTAPIYEILHDAK
		1656.1 [a]	0.2	107-123	ADLLVVGNVGLSTIAGR
		1698.0 [a]	0.1	34-48	**LIIASAYLPQHEDAR**
		2478.7 [a]	0.1	84-106	NVEERPIVGAPVDALVNLADEEK
23, 24	HSP 16.3 (α-crystallin) (NCBI# 231343) MW 16227.4	1163.0	0.5	91-100	**SEFAYGSFVR**
25	Fur (NCBI# 231343) MW 15892.0	1410.9	1.2	1-12	*MSSIPDYAEOLR*
		1450.1	0.4	72-84	IQPSGSVARYESR
		1577.1	0.7	71-84	KIQPSGSVARYESR

[a] Molecular weights indicate average masses (all other masses are monoisotopic)

[b] Sequences in BOLD were determined by MALDI-PSD. Seqeuences in ITALICS were determined by MALDI-CID.

[c] 1 Met-ox

[d] 1 pyro-Glu

[e] MS-Tag search using this sequence found *M. tuberculosis* and *M. avium* aconitase proteins containing this peptide.

[f] MS-Tag searches using these sequences found *M. tuberculosis* and *M. leprae* EF-Tu proteins containing these peptide.

plug was subjected to in-gel digestion with trypsin and the extracts were analyzed by MALDI-TOF mass spectrometry to obtain molecular masses of the tryptic peptides. Analysis of the peptide with MH$^+$ at *m/z* 1410.8 by MALDI-CID MS and subsequent searching of the protein sequence databases using MS-Tag identified spot #25 as a *M. tuberculosis* Fur homolog. Fur (or ferric uptake regulator) proteins are a family of iron-responsive DNA-binding proteins. Subsequent review of the MALDI mass spectrum of the unseparated digestion mixture revealed two other tryptic peptides belonging to the *M. tuberculosis* Fur protein.

The level of iron in the environment is known to regulate the expression of genes encoding many high affinity bacterial iron uptake pathways. Under iron rich conditions, the Fur protein is activated when it binds Fe(II) as a cofactor. This activated repressor is then able to bind the "Fur box", a consensus sequence located in the promoter region of many bacterial genes. In conditions of iron deprivation, the Fur protein does not bind to the promoter sequence, allowing for the transcription of the genes (Ochsner et al. 1995). Homologs of the Fur repressor have been found in many gram-negative bacteria. Their sequences appear to be fairly well conserved with a high degree of homology with the first-discovered *E. coli* Fur protein, ranging from 49% homology for *Neisseria gonorrhoeae* Fur (Berish et al. 1993) to 76% for *Vibrio vulnificus* Fur (Litwin and Calderwood 1993). The Fur homolog of *M. tuberculosis* shows less identity to the Fur proteins of *E. coli* (22.9%), *Legionella pneumophila* (28.4%), and *N. gonorrhoeae* (25.4%). Originally thought of as only a negative repressor, it is now known that Fur also positively regulates many genes in *E. coli* and *Salmonella typhimurium* (Foster and Hall 1992; Stojiljkovic and Hantke 1995). Fur may also act as a global regulator affecting gene expression in response to signals besides iron levels. In addition, Fur may be part of a cascade of control elements in which it regulates the expression of secondary regulatory elements (Foster and Hall 1992).

5.4.1.2 *Aconitase*

Protein gel spot #1, expressed at a higher level under conditions of high iron, was excised from a single 2-D gel and subjected to in-gel digestion with trypsin. MALDI-TOF MS analysis of the digestion extracts yielded molecular masses of several tryptic peptides (see Fig 5.2A). The peptide with MH^+ at m/z 1897.0 (monoisotopic) was analyzed by MALDI-CID MS to obtain additional s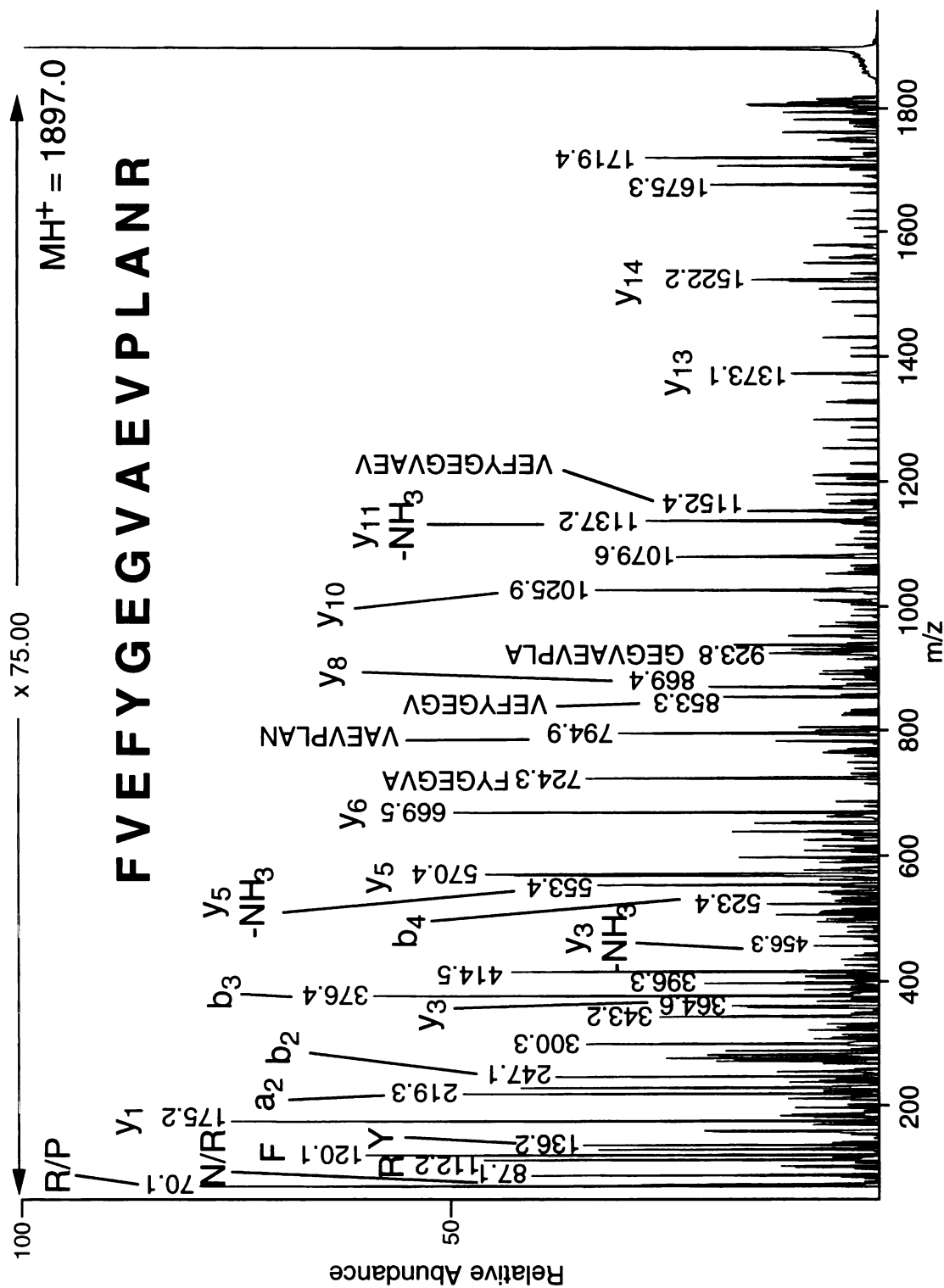equence information (see Fig 5.2B). The resultant fragment ion data were used to search the protein databases using MS-Tag and the peptide was originally matched to a portion of a *Mycobacterium avium* protein (MW 104,025.7 Da). A subsequent BLAST search of the non-redundant protein database with the *M. avium* peptide sequence revealed the protein to be an aconitase. The tight correlation of the fragmentation data with the *M. avium* aconitase peptide suggested that spot #1 was a *M. tuberculosis* aconitase protein whose sequence had yet to be entered into the database. Subsequent to our initial identification of this protein as an aconitase homolog, the sequence for the *M. tuberculosis* aconitase protein (MW 102,449.6 Da) was entered and it contains a peptide (FVEFYGEGVAEVPLANR) whose sequence is identical to that of the *M. avium* peptide that was originally discovered by MS-Tag. A total of 8 tryptic peptides from the *M. tuberculosis* aconitase were detected in the MALDI mass spectrum of the unseparated digest. The *M. tuberculosis* aconitase protein is highly homologous to the *M. avium* aconitase (83.1 % identity) and to a lesser extent to the aconitases from *E. coli* (58.3 % identity) and mouse (51.0% identity).

It is not surprising that an aconitase was identified as one of the iron-regulated proteins in these studies. The cytosolic aconitase is a protein with dual roles. It catalyses the reversible isomerization of citrate and isocitrate via cis-aconitate, as part of the Krebs cycle and serves as an iron-responsive element binding protein (IRE-BP). Aconitases are monomeric proteins that contain a single cubane (4Fe-4S) cluster. In the large family of 4Fe-4S proteins, it is unusual in that only 3 of the irons are directly ligated to the peptide backbone through cysteines. In aconitase, the fourth iron is labile and coordinates the

151

Figure 5.2. Analysis of aconitase homolog by mass spectrometry. (A) MALDI-TOF reflectron peptide mass fingerprint spectrum produced by in-gel tryptic digestion of gel spot #1. Masses outlined by boxes indicate tryptic peptides from the *M. tuberculosis* aconitase protein. Peaks labeled with "T" and "K" indicate trypsin autolytic products and tryptic peptides from human keratin, respectively. (B) MALDI-CID spectrum of a tryptic peptide with MH$^+$ at *m/z* 1897.0 (monoisotopic). Fragment ions referred to as "a" and "b" ions originate from peptide backbone cleavage with the charge retained on the N-terminus and "y" ions refer to peptide fragments with the charge retained on the C-terminus (Biemann 1990). Multiple bond cleavages internal to the peptide are labeled with the corresponding portion of the peptide sequence. All (or a combination) of these fragment ions were used in the MS-Tag database searches.

153

F V E F Y G E G V A E V P L A N R

MH$^+$ = 1897.0

x 75.00

Relative Abundance

R/P

y$_1$ 70.1

N/R 87.1 112.2

F 120.1

R Y 136.2

y$_1$ 175.2

a$_2$ b$_2$ 219.3

247.1

300.3

y$_3$ 343.2

364.6

b$_3$ 376.4

396.3

414.5

y$_3$ -NH$_3$ 456.3

b$_4$ 523.4

553.4

y$_5$ 570.4

y$_5$ -NH$_3$

y$_6$ 669.5

FYGEGVA 724.3

VAEVPLAN 794.9

VEFYGEGV 853.3

y$_8$ 869.4

GEGVAEVPLA 923.8

y$_{10}$ 1025.9

1079.6

y$_{11}$ -NH$_3$ 1137.2

VEFYGEGVAEV 1152.4

y$_{13}$ 1373.1

y$_{14}$ 1522.2

1675.3

1719.4

100

50

200 400 600 800 1000 1200 1400 1600 1800

m/z

154

atoms of the cluster along with a water molecule and the substrate. The instability of the cluster is exploited as a molecular switch, enabling cells to reciprocally regulate the aconitase and RNA binding activity of the protein in response to changes in iron levels. Under conditions of iron deprivation, the apo form (no 4Fe-4S cluster) of the protein is inactive as an aconitase but active for RNA binding. The IRE-binding function of the protein results in a tight interaction with the IREs contained in the mRNAs of molecules involved in iron storage in mammalian cells, like transferrin receptor and ferritin. Binding of the protein to IREs located in the 5' untranslated region (UTR) of mRNAs prevents translation by inhibiting the binding of initiation factors. However, binding of the protein to IREs in the 3' UTR stimulates mRNA translation by protecting the mRNA against degradation (Melefors and Hentze 1993). When iron levels rise, the protein dissociates from the IRE and is again active as an aconitase. The reason underlying the physiological role of the cytosolic aconitase in iron regulation is still unclear. The fact that citrate, the substrate for the aconitase, is capable of binding iron and has been proposed as a possible transporter of intracellular iron in mammals is very curious. In one model, the increased synthesis of iron storage proteins (ferritin and transferrin) and reduced synthesis of iron uptake proteins (transferrin receptors) in iron-replete conditions, in addition to the reduced levels of citrate (conversion to isocitrate by aconitase), would eventually lead to reduced intracellular iron levels and the subsequent conversion of the protein back to its iron-binding form (Melefors and Hentze 1993).

5.4.1.3 *Elongation Factor Tu*

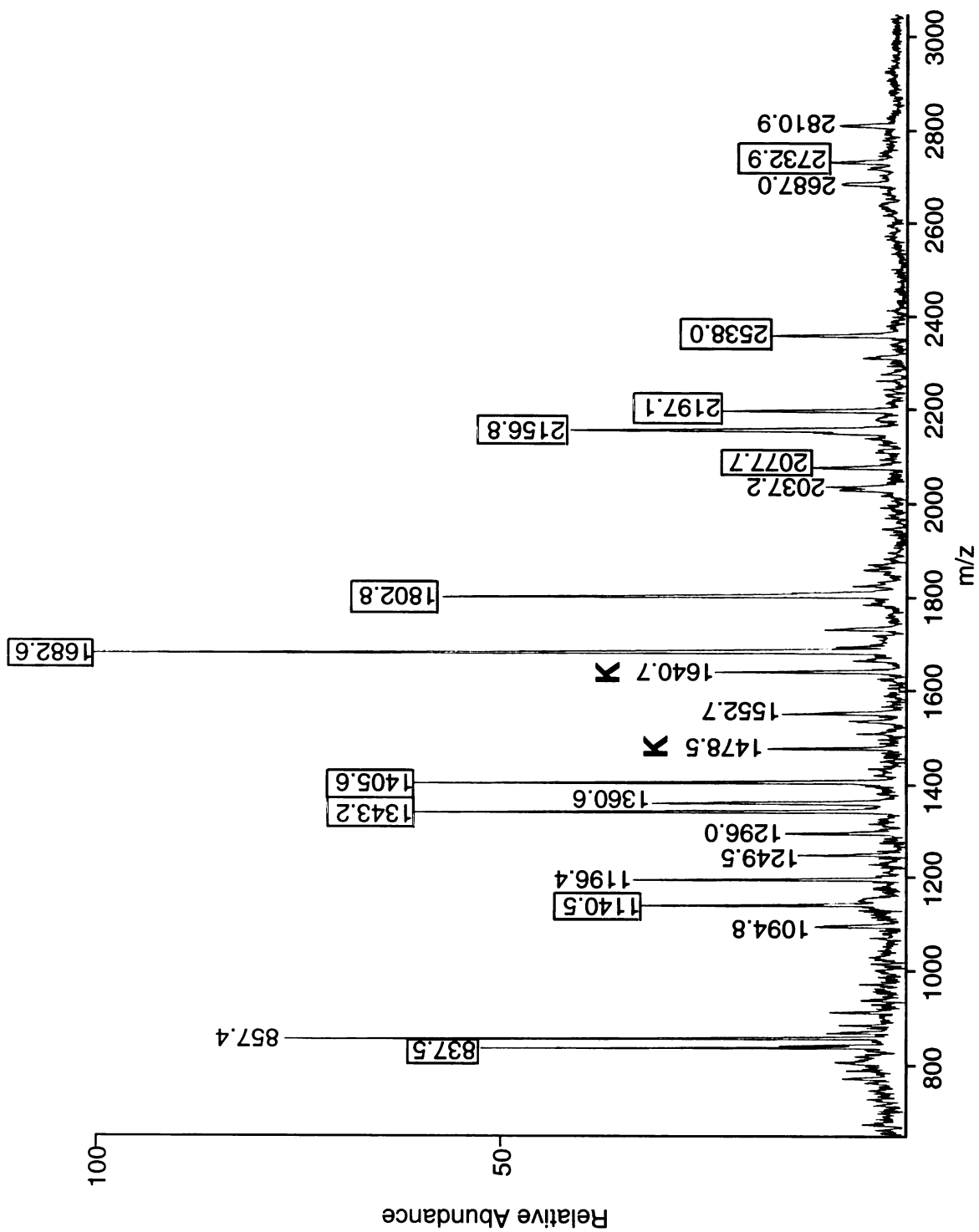Protein gel spot #4, which is expressed at higher levels when grown in the high-iron medium, was excised from four 2-D gels and subjected to in-gel tryptic digestion. The resultant digestion mixture was analyzed by MALDI-TOF mass spectrometry (see Fig 5.3A). The tryptic peptides with MH$^+$ at m/z 1405.6 (see Fig 5.3B), 1682.6 (see Fig 5.3C), and 1802.8 (see Fig 5.3D) were further analyzed by MALDI-PSD MS to obtain
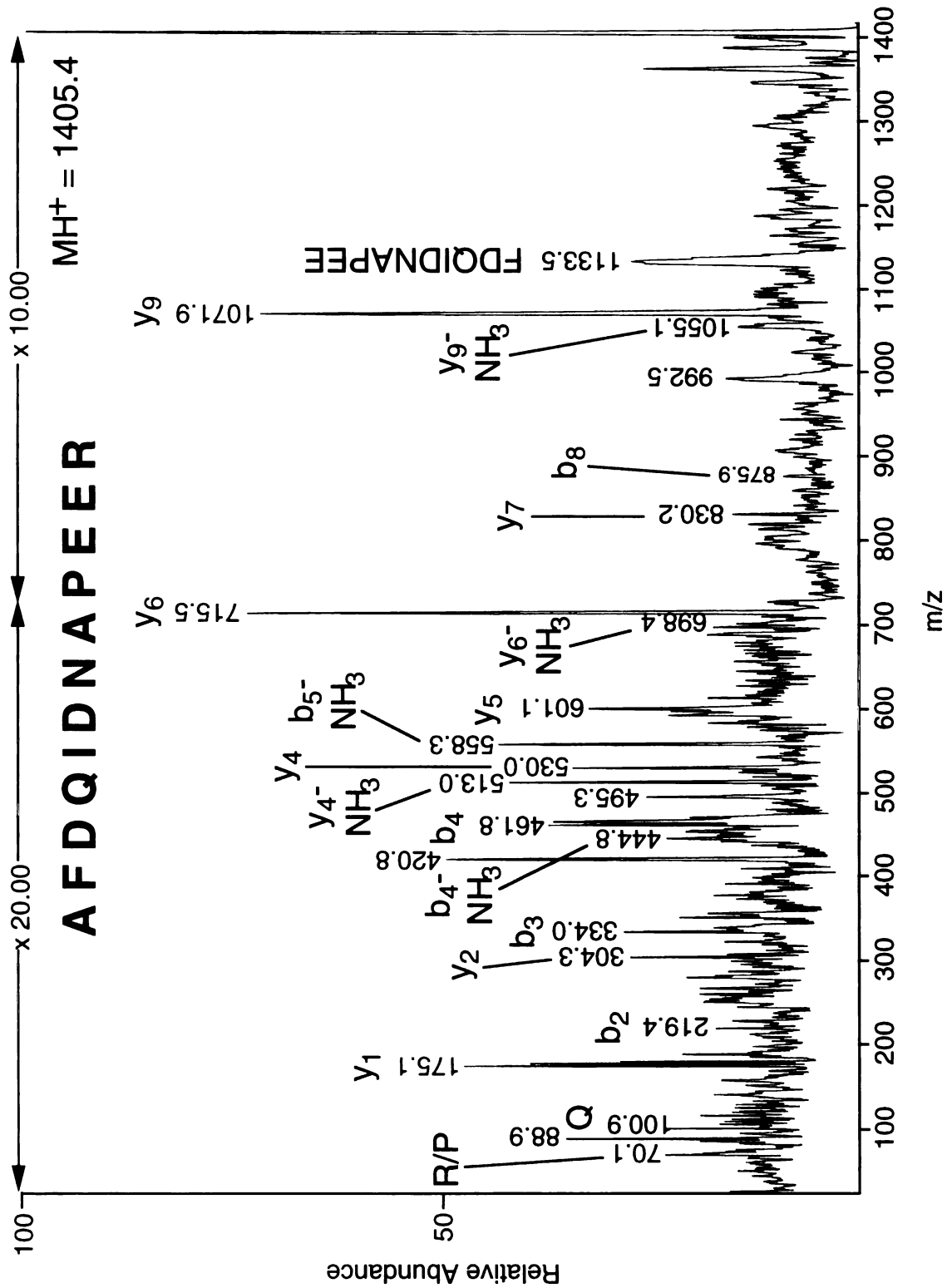
sequence information. Database searching using MS-Tag and BLAST revealed spot #4 to be elongation factor Tu (EF-Tu), a helper protein involved in protein synthesis encoded by the *tuf* gene. A total of 11 tryptic peptides from *M. tuberculosis* EF-Tu was observed and additional sequence information obtained on 3 of the peptides (see Fig 5.3). In addition to identifying spot #4 as a *M. tuberculosis* EF-Tu proteins, MS-Tag searches also found a *M. leprae* EF-Tu protein (MW 43667.9 Da) containing the same 3 peptides. EF-Tu is a GTPase which promotes the binding of aminoacyl-tRNA to ribosomes (Sprinzl 1994). The *tuf* gene of *M. tuberculosis* was discovered when a λgt11 *M. tuberculosis* gene library was screened with monoclonal antibodies raised by immunizing rats with live *Mycobacterium bovis* BCG. The *M. tuberculosis* EF-Tu homolog showed high sequence similarity with EF-Tu proteins from several other organisms including *Mycobacterium leprae* (95.2% identity), *S. typhimurium* (75.1% identity), and *E. coli* (75.1% identity).

Besides its essential role in protein biosynthesis, EF-Tu has been shown by Young *et al.* to be methylated and to become membrane-associated when *E. coli* is starved for glucose, galactose, ammonia, glutamate, or phosphate (Young and Bernlohr 1991). This raises the possibility that EF-Tu may also have roles in the regulation of cell growth and the organism's response to stress. These investigators propose that EF-Tu's membrane association allows for its interaction with receptors or proteins that interact with nutrients in the environment that could regulate its methylation. Conditions of nutrient deprivation would result in EF-Tu hypermethylation and subsequent membrane release, allowing for the possibility that the intracellular EF-Tu assumes multiple regulatory roles. In addition to regulating translation through its interaction with tRNA and ribosomes, enabling it to stop the translation of unnecessary proteins and trigger the synthesis of stress-induced proteins, EF-Tu has also been known to act as a transcriptional activator in the presence of RNA polymerase and the appropriate sigma factor (Travers et al. 1970; Halliday 1983). Therefore, it may be able to regulate both the translation and transcription of starvation-induced proteins. A preliminary report that patients with tuberculosis, but not tuberculin-

Figure 5.3. Analysis of EF-Tu homolog (spot #4) by mass spectrometry.
(A) MALDI-TOF MS peptide mass fingerprint spectrum produced by in-gel tryptic
digestion of gel spot #4, pooled from four 2-D gels. (B-D) MALDI-PSD MS spectrum of
a tryptic peptide with (B) MH$^+$ 1405.4, (C) MH$^+$ 1682.7, and (D) MH$^+$ 1802.7. Fragment
ions detected in the PSD analysis were used to search the protein databases with MS-Tag.
See legend to Figure 5.2 for an explanation of peak labels.

AFDQIDNAPEER

MH⁺ = 1405.4

x 10.00

x 20.00

159

LLDQGQAGDNVGLLLR

x 15.00   x 8.00 MH^+ = 1682.7

Relative Abundance

m/z

Peaks (reading the mass spectrum):

- L   86.2
- R   112.0
- y_1 175.1
- b_2 227.2
- $y_2^-NH_3$ 271.5
- DQG   301.1
- b_3 342.3
- AGDN   358.4
- y_3 388.9
- LDQG   401.1
- 413.6
- GQAGD/DQGQ   429.2
- DQGQA   473.5
- y_4 514.6
- y_5 548.3
- 571.0
- y_6 669.9
- 724.0
- $y_7^-NH_3$ 767.5
- y_7 784.6
- $y_8^-NH_3$ 883.0
- y_8 900.3
- y_9 956.2
- y_{10} 1027.7
- y_{11} 1156.0
- y_{12} 1213.4
- $y_{13}^-NH_3$ 1323.3
- y_{13} 1340.3
- y_{14} 1455.5
- $y_{16}^-NH_3$ 1665.9

100   200   300   400   500   600   700   800   900   1000   1100   1200   1300   1400   1500   1600   1700

MH⁺ = 1802.7

ELLAAQEFDEDAPVVR

negative individuals, develop an antibody response to the protein suggests a potential role for the protein in serodiagnosis of mycobacterial disease (Carlin et al. 1992).

5.4.2 *Antigens*

5.4.2.1 *LSR2*

Protein gel spot #21, expressed at a higher level under high-iron conditions, was excised from four 2-D gels. In-gel tryptic digestion, followed by MALDI mass analysis, revealed gel spot #21 to be a *M. tuberculosis* homolog of LSR2, a protein antigen of *M. leprae*. The digestion mixture was found to contain 6 tryptic peptides. Additional sequence information was obtained using MALDI-PSD MS on 2 of the peptides.

Using polyclonal antibodies from pooled sera of lepromatous patients, Laal *et al.* (Laal et al. 1991) screened a λgt11 DNA expression library in an effort to identify genes involved in the immune response to *M. leprae* infection. These investigators identified LSR2, a dominant T-cell antigen. BLAST searches of this ~10 kD protein revealed that *M. tuberculosis* LSR2 has 92.9% identity with the LSR protein of *M. leprae* but is not homologous to any other known proteins. Analysis of overlapping peptides spanning the *M. leprae* LSR sequence showed that 2 peptides (GVTYEIDLTNKNAA and IDLTNKNAAKLRGD) were recognized by the sera of leprosy patients (Singh et al. 1994). Single residue deletions of the peptides enabled the identification of 3 distinct sequences (GVTY, NAA, and RGD) found to be important for antibody recognition (Singh et al. 1994). Although nothing is yet known of the *M. tuberculosis* homolog's role in the immune response, 2 of the 3 sequences important for antibody recognition in leprosy patients, GVTY and RGD, are present in its sequence.

5.4.2.2 Hsp16.3 (α-crystallin homolog)

Protein gel spot #23, upregulated under conditions of high iron, was taken from a single 2-D gel and subjected to in-gel digestion and MALDI mass analysis. Only one *M. tuberculosis* tryptic peptide was identified in the digestion mixture. MALDI-PSD MS analysis on this peptide (MH⁺ at *m/z* 1163.0) and database searching revealed gel spot #23 to be a small heat shock protein (Hsp16.3) of the α-crystallin family (Verbon et al. 1992). Mass spectrometric analysis showed gel spot #24 also to have tryptic peptides originating from Hsp16.3, possibly a degraded and/or truncated form of the protein. Members of this family of small heat shock proteins (sHSPs) are thought to function as chaperones, acting as molecular surfactants which prevent protein aggregation through non-specific weak interactions with the properly folded proteins (Lindquist 1986; Chang et al. 1996). Hsp16.3 is a major *M. tuberculosis* antigen which can generate a cell-mediated immune response and is thought to be located on the periphery of the cell membrane (Kingston et al. 1987; Lee et al. 1992). When Hsp16.3 was overexpressed in wild-type *M. tuberculosis*, a slower decline in viability after the end of log-phase growth was observed (Yuan et al. 1996). Besides the *M. tuberculosis* Hsp16.3, an α-crystallin homolog has been detected in *M. leprae* (Nerland et al. 1988) and *M. bovis*, but not in *Mycobacterium smegmatis* or the pathogenic species *M. avium* (Yuan et al. 1996).

In investigations into the regulation of Hsp16.3 expression under various stress conditions, carbon starvation, heat and cold shock, and low pH all failed to induce Hsp16.3 expression (Yuan et al. 1996). The only environmental stress shown to significantly upregulate the expression of Hsp16.3 was growth under microaerobic or anaerobic conditions (Yuan et al. 1996; Cunningham and Spreadbury 1998). The environment inside caseous granulomas, where mycobacteria are thought to exist in a dormant state, is unknown. However, many environmental stresses, like oxygen deprivation, may signal mycobacteria to produce proteins like the α-crystallin homolog to aid in the long-term survival of the bacteria. On the other hand, the diversity of this family

of sHSPs suggests that the protective capacity of this protein may be general, not necessarily specific to the pathogenic species *M. tuberculosis* and *M. leprae*.

5.4.3 *Enzymes*

5.4.3.1 *Phosphoenolpyruvate Carboxykinase*

Protein gel spot #2, upregulated under low-iron conditions, was found to be homologous to many GTP-dependent phosphoenolpyruvate carboxykinases (PEPCK) from numerous other species, including *M. leprae* (86.0% identity), *Drosophila melanogastor* (51.3% identity), and *Homo sapiens* (52.5% identity). MALDI mass analysis of the digestion mixture revealed 9 tryptic peptides. Further analysis using MALDI-PSD MS was carried out on two of the peptides to obtain sequence information. PEPCK is part of the gluconeogenic pathway, catalyzing the reversible decarboxylation and mononucleotide-dependent phosphorylation of oxaloacetate (OAA) to phosphoenolpyruvate (PEP) (Matte et al. 1997). Most PEPCKs require two metal cations for activity. One of the cations (Mg^{+2} or Mn^{+2}) must complex with the substrate to form a cation-nucleotide complex. For optimal activity, a second cation (often a transition metal) is required to interact directly with the protein, possibly mediating the interaction of the substrate (OAA or PEP) with the enzyme to facilitate the formation of the active ternary complex (Lee et al. 1981). In GTP-dependent PEPCKs, it has been proposed that the second ion may help position the substrate for catalysis by binding the PEP phosphoryl group and the nucleotide β- or γ-phosphate, either directly (Hebda and Nowak 1982) or through an interaction with water (Lee and Nowak 1984; Duffy and Nowak 1985; Matte et al. 1997).

In early investigations, Fe(II) was found to be the most efficient activator of rat liver cytosolic PEPCK when incubated with the cytosol fraction of the liver homogenate (Bentle et al. 1976). However, studies found a rapid Fe(II)-dependent inactivation after continued incubation with the enzyme in the absence of substrate. This loss of activity is

thought to result from PEPCK oxidative damage caused by the reactive oxygen species formed from Fe(II) autoxidation (Reynolds 1980). The presence of a ferroactivator, a cytosolic protein factor originally identified as glutathione peroxidase in rat liver and thought to act by removing reactive oxygen species, results in the restoration of enzyme activity (Punekar and Lardy 1987). It has been proposed that PEPCK may exist in a dynamic equilibrium between an active and inacitve form [caused by the Fe(II) autoxidation]. If this is the case, the ferroactivator may have a role in shifting the equilibrium towards the active enzyme (Reynolds 1980).

5.4.3.2 *Oxidoreductase*

Protein gel spot #11, down-regulated in low-iron medium, was identified as a homolog of an oxidoreductase. A total of 6 tryptic peptides was detected by MALDI mass analysis of the digestion mixture. The large number of microbial alcohol oxidoreductases can be categorized into 3 major groups: (a) NAD(P)-dependent dehydrogenases, (b) NAD(P)-independent enzymes which use pyrroloquinoline quinone, heme, or cofactor F_{420} as the cofactor, and (c) enzymes that catalyze the essentially irreversible oxidation of alcohols (Reid and Fewson 1994). The *M. tuberculosis* oxidoreductase homolog belongs to a subgroup of the group (a) NAD(P)-dependent dehydrogenases, the short-chain alcohol dehydrogenase (SCAD) superfamily. Members of this subgroup are known to act on a large variety of substrates, including sugars, steroids, prostaglandins, aromatic hydrocarbons, antibiotics, and compounds involved in nitrogen metabolism (Krozowski 1994). The SCAD enzymes do not require any metal ions to function and are typically around 250 amino acids in length. Sequence comparisons between members of the superfamily reveal 6 conserved domains (Krozowski 1994). Among the family members, there is a pattern of 13 largely conserved residues. Alignments between enzyme pairs typically reveal approximately 25% identity, with single forms ranging from 14-58% (Persson et al. 1991). The oxidoreductase of *M. tuberculosis* shows homology to enzymes

165

from *Caenorhabditis elegans* (48% identity), *E. coli* (27.6% identity),and *H. sapiens* (19.5% identity) within this range.

5.4.3.3 *Peptidyl-prolyl   cis-trans   isomerase*

Gel spot #18, whose expression is reduced in a low-iron environment, was removed from a single 2-D gel. MALDI-PSD MS analysis of 2 of the 3 tryptic peptides found in the digestion mixture (MH$^+$ at *m/z* 1602.7 and 2203.8), followed by database searching matched them to a *M. tuberculosis* protein (MW 19,239.5) with significant homology to peptidyl-prolyl cis-trans isomerases.

Immunophilins are housekeeping proteins with many roles, including membrane channeling and protein folding and trafficking (Fischer and Schmid 1990). Besides exhibiting peptidyl-prolyl cis-trans isomerase (PPIase) activity in the unliganded form, immunophilin-drug (cyclophilin or FK506) complexes inhibit clonal expansion of T cells and have toxic effects on numerous other cellular components. Many intracellular pathogens produce proteins with significant homology to immunophilins and have PPIase activity. The role of these proteins in microbial pathogenicity is as yet unclear; the immunophilins may interact with various partner molecules in mammalian cells or may interact with other components through its PPIase activity by interrupting protein folding or altering protein structure dynamics (Hacker and Fischer 1993). Many facultative or obligate intracellular pathogens adapted to mammalian cells, like *L. pneumophila* and *Chlamydia trachomatis*, produce FKBP-like immunophilins, such as the Mip protein ("macrophage infectivity potentiator") of *Legionella*. These proteins have been proposed to aid in intracellular survival. Mip-negative mutants appear to have a reduced ability to initiate intracellular replication (Cianciotto et al. 1990). The site of action of Mip is not known, nor whether it acts by altering the conformation of other *Legionella* proteins (Hacker and Fischer 1993).

The *M. tuberculosis* peptidyl-prolyl cis-trans isomerase shows homology to immunophilins of the cyclophilin family of several other species including *Streptomyces chrysomallus* (61.4% identity), *C. elegans* (48.4% identity), and *H. sapiens* (46.1% identity). Unlike the Mip proteins of the FKBP family, these bacterial proteins have not been extensively characterized. However, the existence of cyclophilin-like proteins in *E. coli*, *S. typhimurium*, and *L. pneumophila* suggests that a large array of these proteins are produced by bacterial species. There is speculation that these proteins have roles in protein folding and secretion (Liu and Walsh 1990).

5.4.4 *Unclassified proteins*

Protein gel spots #15 and #22, both down-regulated in low-iron medium, were matched to protein sequences in the database which did not show sequence homology with any proteins of known function. They would be predicted to encode proteins of 21,534.6 Da and 15,312.4 Da, respectively.

5.5 CONCLUSION

In this study, we have used 2-D gel electrophoresis, MALDI mass spectrometry, and database searching to identify *M. tuberculosis* proteins regulated by extracellular iron levels. Previous studies in our laboratories with 1-D SDS-PAGE (unpublished data) did not allow for the direct identification of iron-regulated proteins since single bands were found to contain multiple co-migrating proteins. However, once we obtained the proper conditions for the separation of complex protein mixtures from *M. tuberculosis* cell lysates by 2-D gel electrophoresis , we were able to analyze and identify single protein-containing gel spots by mass spectrometry. The number of *M. tuberculosis* tryptic peptides detected in digestion mixtures from individual samples varied greatly, ranging from as little as one to as many as 11 peptides (see Table 1). Therefore, in addition to determining the masses of the tryptic peptides, we chose to generate sequence information. In most cases, useful

167

sequence data could be obtained from only the more abundant signals in the MALDI mass spectra of the digestion mixtures by PSD and/or CID analysis. This sequence data provided a higher level of confidence in the identification of proteins than would have been afforded by tryptic peptide masses alone. This was particularly true in cases where only a few peptide molecular masses could readily be observed over background.

2-D gel electrophoresis identified at least 27 proteins whose expression is modulated by iron concentration - 15 proteins are upregulated and 12 proteins are down-regulated under low-iron conditions. Of these proteins, 11 (including 2 forms of 1 protein) were identified by MALDI mass spectrometry and database searching. The identification of 2 of the proteins as Fur and aconitase homologs suggests the possibility that these proteins function as transcriptional regulators in *M. tuberculosis*, as in other bacteria, and that they exert control over the expression of many of the other proteins which show differential expression under low- and high-iron conditions. In future experiments, this may be explored further by comparing the protein expression of Fur or aconitase-deletion mutants with wild-type *M. tuberculosis*, or by analyzing genes with upstream Fur or aconitase binding regions. Elongation factor Tu may also play a role in the organism's response to iron starvation conditions through its ability to regulate protein expression.

Despite the successful identification of 10 proteins in this study, we were unable to obtain sufficient data to identify unambiguously 16 of the proteins that appeared to be under iron-regulation. Further refinements in methodology should allow us to identify these later proteins in addition to other proteins whose expression levels are very low and may only be visible by silver-staining.

Our study demonstrates the feasibility and utility of combining 3 powerful technologies - 2-D gel electrophoresis, mass spectrometry, and database searching - to study how mycobacteria and other pathogens respond to changes in the environment. Studies of this type should help us to take full advantage of the wealth of new data

provided by genomic studies and greatly enhance our understanding of the pathophysiology of *M. tuberculosis* and other human pathogens.

REFERENCES

Abou-Zeid, C., Ratliff, T. L., Wiker, H. G., Harboe, M., Bennedsen, J. and Rook, G. A. (1988). Characterization of fibronectin-binding antigens released by *Mycobacterium tuberculosis* and *Mycobacterium bovis* BCG. *Infect. Immun. 56(12)*, 3046-3051.

Adams, L. B., Fukutomi, Y. and Krahenbuhl, J. L. (1993). Regulation of murine macrophage effector functions by lipoarabinomannan from mycobacterial strains with different degrees of virulence. *Infect. Immun. 61(10)*, 4173-4181.

Alford, R. H. (1990). Antimicrobial agents. Principles and Practice of Infectious Diseases. Mandell, G. L., Douglas, R. G. Jr. and Bennet, J. E. New York, Churchill Livingstone: 350-360.

Altschul, S. F., Gish, W., Miller, W., Myers, E. W. and Lipman, D. J. (1990). Basic local alignment search tool. *J. Mol. Biol. 215(3)*, 403-410.

Archibald, F. (1983). *Lactobacillus planatarum*, an organism not requiring iron. *FEMS Microbiol. Lett. 19*, 29.

Armstrong, J. A. and Hart, P. D. (1971). Response of cultured macrophages to *Mycobacterium tuberculosis*, with observations on fusions of lysosomes with phagosomes. *J. Exp. Med. 134*, 713-740.

Arruda, S., Bomfim, G., Knights, R., Huima-Byron, T. and Riley, L. W. (1993). Cloning of an *M. tuberculosis* DNA fragment associated with entry and survival inside cells. *Science 261(5127)*, 1454-1457.

Bagg, A. and Neilands, J. B. (1987). Molecular mechanism of regulation of siderophore-mediated iron assimilation. *Microbiol. Rev. 51(4)*, 509-518.

Barclay, R., Ewing, D. F. and Ratledge, C. (1985). Isolation, identification, and structural analysis of the mycobactins of *Mycobacterium avium*, *Mycobacterium intracellulare*, *Mycobacterium scrofulaceum*, and *Mycobacterium paratuberculosis*. *J. Bacteriol. 164(2)*, 896-903.

Barclay, R. and Ratledge, C. (1983). Iron-binding compounds of *Mycobacterium avium*, *M. intracellulare*, *M. scrofulaceum*, and mycobactin-dependent *M. paratuberculosis* and *M. avium*. *J. Bacteriol. 153(3)*, 1138-1146.

Barclay, R. and Ratledge, C. (1986). Participation of iron on the growth inhibition of pathogenic strains of *Mycobacterium avium* and *M. paratuberculosis* in serum. *Zentralbl. Bakteriol. Mikrobiol. Hyg. [A] 262(2)*, 189-194.

Barclay, R. and Ratledge, C. (1988). Mycobactins and exochelins of *Mycobacterium tuberculosis*, *M. bovis*, *M. africanum*, and other related strains. *J. Gen. Microbiol. 134*, 771-776.

Barnes, P. F. and Barrows, S. A. (1993). Tuberculosis in the 1990s. *Ann. Intern. Med. 119(5)*, 400-410.

Basus, V. J., Billeter, M., Love, R. A., Stroud, R. M. and Kuntz, I. D. (1988). Structural studies of alpha-bungarotoxin. 1. Sequence-specific ^{1}H NMR resonance assignments. *Biochem. 27(8)*, 2763-2771.

Bateman, R. H., Green, M. R., Scott, G. and Clayton, E. (1995). A combined magnetic sector-time-of-flight mass spectrometer for structural determination studies by tandem mass spectrometry. *Rapid Commun. Mass Spectrom. 9(13)*, 1227-1233.

Bax, A. and Davis, D. G. (1985a). MLEV-17-based two-dimensional homonuclear magnetization transfer spectroscopy. *J. Magn. Reson. 65*, 355-360.

Bax, A. and Davis, D. G. (1985b). Practical aspects of two-dimensional transverse NOE spectroscopy. *J. Magn. Reson. 63*, 207-213.

Bentle, L. A., Snoke, R. E. and Lardy, H. A. (1976). A protein factor required for activation of phosphoenolpyruvate carboxykinase by ferrous ions. *J. Biol. Chem. 251(10)*, 2922-2928.

Berish, S. A., Subbarao, S., Chen, C. Y., Trees, D. L. and Morse, S. A. (1993). Identification and cloning of a Fur homolog from *Neisseria gonorrhoeae. Infect. Immun. 61(11)*, 4599-4606.

Bermudez, L. E. and Young, L. S. (1989). <u>*Mycobacterium avium* complex adherence to mucosal cells: a possible mechanism of virulence</u>. 29th Interscience Conference on Antimicrobial Agents and Chemotherapy, Washington, American Society for Microbiology. : 142.

Bermudez, L. E., Young, L. S. and Enkel, H. (1991). Interaction of *Mycobacterium avium* complex with human macrophages: roles of membrane receptors and serum proteins. *Infect. Immun. 59(5)*, 1697-1702.

Berry, M. N., Grivell, A. R., Grivell, M. B. and Phillips, J. W. (1997). Isolated hepatocytes--past, present and future. *Cell Biol. Toxicol. 13(4-5)*, 223-233.

Biemann, K. (1990). Peptides and proteins: overview and strategy. *Methods Enzymol. 193*, 351-360.

Bliska, J. B., Galan, J. E. and Falkow, S. (1993). Signal transduction in the mammalian cell during bacterial attachment and entry. *Cell 73(5)*, 903-920.

Bloch, A. B., Cauthen, G. M., Onorato, I. M., Dansbury, K. G., Kelly, G. D., Driver, C. R. and Snider, D. E. (1994). Nationwide survey of drug-resistant tuberculosis in the United States. *JAMA 271(9)*, 665-671.

Bloch, H. (1950). Studies on the virulence of tubercle bacilli: isolation and biological properties of a constituent of virulent organisms. *J. Exp. Med. 91*, 197-210.

Bloch, H. and Noll, H. (1953). Studies on the virulence of tubercle bacilli. Variations in the virulence effect elicited by Tween 80 and thiosemicarbazone. *Br. J. Exp. Pathol. 97,* 1-6.

Bloom, B. R., Flynn, J., McDonough, K., Kress, Y. and Chan, J. (1994). Experimental approaches to mechanisms of protection and pathogenesis in *M. tuberculosis* infection. *Immunobiol. 191(4-5),* 526-536.

Bloom, B. R. and Murray, C. J. (1992). Tuberculosis: commentary on a reemergent killer. *Science 257(5073),* 1055-1064.

Boom, W. H. (1996). The role of T-cell subsets in *Mycobacterium tuberculosis* infection. *Infect. Agents Dis. 5(2),* 73-81.

Bothner-By, A. A., Stephens, R. L., Lee, J.-M., Warren, C. D. and Jeanloz, R. W. (1984). Structure determination of a tetrasaccharide: transient nuclear overhauser effects in the rotating frame. *J. Am. Chem. Soc. 106,* 811-813.

Bouvet, E., Casalino, E., Mendoza-Sassi, G., Lariven, S., Vallee, E., Pernet, M., Gottot, S. and Vachon, F. (1993). A nosocomial outbreak of multidrug-resistant *Mycobacterium bovis* among HIV-infected patients. A case-control study. *Aids 7(11),* 1453-1460.

Boyd, J., Oza, M. N. and Murphy, J. R. (1990). Molecular cloning and DNA sequence analysis of a diphtheria tox iron-dependent regulatory element (dtxR) from Corynebacterium diphtheriae. *Proc Natl Acad Sci U S A 87(15),* 5968-72.

Brennan, P. J. and Nikaido, H. (1995). The envelope of mycobacteria. *Annu. Rev. Biochem. 64,* 29-63.

Britton, W. J., Roche, P. W. and Winter, N. (1994). Mechanisms of persistence of mycobacteria. *Trends Microbiol. 2(8),* 284-288.

Brown, K. A. and Ratledge, C. (1975). Iron transport in *Mycobacterium smegmatis*: ferrimycobactin reductase (NAD(P)H:ferrimycobactin oxidoreductase), the enzyme releasing iron from its carrier. *FEBS Lett. 53(2)*, 262-266.

Byers, B. R. and Arceneaux, J. E. (1998). Microbial iron transport: iron acquisition by pathogenic microorganisms. *Met. Ions Biol. Syst. 35*, 37-66.

Byrd, T. F. and Horwitz, M. A. (1989). Interferon gamma-activated human monocytes downregulate transferrin receptors and inhibit the intracellular multiplication of *Legionella pneumophila* by limiting the availability of iron. *J. Clin. Invest. 83(5)*, 1457-1465.

Byrd, T. F. and Horwitz, M. A. (1991). Lactoferrin inhibits or promotes *Legionella pneumophila* intracellular multiplication in nonactivated and interferon gamma-activated human monocytes depending upon its degree of iron saturation. Iron-lactoferrin and nonphysiologic iron chelates reverse monocyte activation against *Legionella pneumophila*. *J. Clin. Invest. 88(4)*, 1103-1112.

Byrd, T. F. and Horwitz, M. A. (1993). Regulation of transferrin receptor expression and ferritin content in human mononuclear phagocytes. Coordinate upregulation by iron transferrin and downregulation by interferon gamma. *J. Clin. Invest. 91(3)*, 969-976.

Calder, K. M. and Horwitz, M. A. (1998). Identification of iron-regulated proteins of *Mycobacterium tuberculosis* and cloning of tandem genes encoding a low iron-induced protein and a metal transporting ATPase with similarities to two-component metal transport systems. *Microb. Pathogen. 24(3)*, 133-143.

Carlin, N. I., Lofdahl, S. and Magnusson, M. (1992). Monoclonal antibodies specific for elongation factor Tu and complete nucleotide sequence of the tuf gene in *Mycobacterium tuberculosis. Infect. Immun. 60(8)*, 3136-3142.

Carter, G. R. (1975). *Mycobacterium*. Diagnostic procedures in veterinary microbiology. Carter, G. R. Springfield, Charles C. Thomas: 138-146.

Casanova, J. L., Blanche, S., Emile, J. F., Jouanguy, E., Lamhamedi, S., Altare, F., Stephan, J. L., Bernaudin, F., Bordigoni, P., Turck, D., Lachaux, A., Albertini, M., Bourrillon, A., Dommergues, J. P., Pocidalo, M. A., Le Deist, F., Gaillard, J. L., Griscelli, C. and Fischer, A. (1996). Idiopathic disseminated bacillus Calmette-Guerin infection: a French national retrospective study. *Pediatrics 98(4 Pt 1)*, 774-778.

Chan, J., Fan, X. D., Hunter, S. W., Brennan, P. J. and Bloom, B. R. (1991). Lipoarabinomannan, a possible virulence factor involved in persistence of *Mycobacterium tuberculosis* within macrophages. *Infect. Immun. 59(5)*, 1755-1761.

Chang, Z., Primm, T. P., Jakana, J., Lee, I. H., Serysheva, I., Chiu, W., Gilbert, H. F. and Quiocho, F. A. (1996). *Mycobacterium tuberculosis* 16-kDa antigen (Hsp16.3) functions as an oligomeric structure in vitro to suppress thermal aggregation. *J. Biol. Chem. 271(12)*, 7218-7223.

Chatterjee, D., Roberts, A. D., Lowell, K., Brennan, P. J. and Orme, I. M. (1992). Structural basis of capacity of lipoarabinomannan to induce secretion of tumor necrosis factor. *Infect. Immun. 60(3)*, 1249-1253.

Cianciotto, N. P., Eisenstein, B. I., Mody, C. H. and Engleberg, N. C. (1990). A mutation in the mip gene results in an attenuation of *Legionella pneumophila* virulence. *J. Infect. Dis. 162(1)*, 121-126.

Clark-Curtiss, J. E. (1998). Identification of virulence determinants in pathogenic mycobacteria. *Curr. Top. Microbiol. Immunol. 225*, 57-79.

Clemens, D. L. and Horwitz, M. A. (1995). Characterization of the *Mycobacterium tuberculosis* phagosome and evidence that phagosomal maturation is inhibited. *J. Exp. Med. 181(1)*, 257-270.

Colditz, G. A., Brewer, T. F., Berkey, C. S., Wilson, M. E., Burdick, E., Fineberg, H. V. and Mosteller, F. (1994). Efficacy Of BCG Vaccine In the Prevention Of Tuberculosis - Meta-Analysis Of the Published Literature. *JAMA 271(9),* 698-702.

Cole, S. T., Brosch, R., Parkhill, J., Garnier, T., Churcher, C., Harris, D., Gordon, S. V., Eiglmeier, K., Gas, S., Barry, C. E., Tekaia, F., Badcock, K., Basham, D., Brown, D., Chillingworth, T., Connor, R., Davies, R., Devlin, K., Feltwell, T., et al. (1998). Deciphering the biology of *Mycobacterium tuberculosis* from the complete genome sequence. *Nature 393(6685),* 537-544.

Collazos, J., Mayo, J. and Martinez, E. (1995). The chemotherapy of tuberculosis--from the past to the future. *Respir. Med. 89(7),* 463-469.

Collins, F. M. (1989). Mycobacterial disease, immunosuppression, and acquired immunodeficiency syndrome. *Clin. Microbiol. Rev. 2(4),* 360-377.

Committee, T. C. T. (1952). Interim report to the Medical Research Council: the treatment of pulmonary tuberculosis with isoniazid. *B. M. J. 2,* 735-746.

Connell, N. D. and Nikaido, H. (1994). Membrane permeability and transport in *Mycobacterium tuberculosis*. Tuberculosis: Pathogenesis, Protection, and Control. Bloom, B. R. Washington, D.C., American Society for Microbiology Press: 333-352.

Cornelissen, C. N., Biswas, G. D., Tsai, J., Paruchuri, D. K., Thompson, S. A. and Sparling, P. F. (1992). Gonococcal transferrin-binding protein 1 is required for transferrin utilization and is homologous to TonB-dependent outer membrane receptors. *J. Bacteriol. 174(18),* 5788-5797.

Cowart, R. E. and Foster, B. G. (1985). Differential effects of iron on the growth of *Listeria monocytogenes*: minimum requirements and mechanism of acquisition. *J. Infect. Dis. 151(4),* 721-730.

Crowle, A. J., Dahl, R., Ross, E. and May, M. H. (1991). Evidence that vesicles containing living, virulent *Mycobacterium tuberculosis* or *Mycobacterium avium* in cultured human macrophages are not acidic. *Infect. Immun. 59(5)*, 1823-1831.

Cunningham, A. F. and Spreadbury, C. L. (1998). Mycobacterial stationary phase induced by low oxygen tension: cell wall thickening and localization of the 16-kilodalton alpha-crystallin homolog. *J. Bacteriol. 180(4)*, 801-808.

Dannenberg, A. M. J. and Rook, G. A. W. (1994). Pathogenesis of pulmonary tuberculosis: an interplay of tissue-damaging and macrophage-activating immune responses - dual mechanisms that control bacillary multiplication. <u>Tuberculosis: pathogenesis, protection, and control</u>. Bloom, B. R. Washington, ASM Press: 459-483.

Davidson, P. T. and Hanh, L. Q. (1986). Respiratory pharmacology. Antituberculosis drugs. *Clin. Chest Med. 7(3)*, 425-438.

Day, M. and Kuntz, I. D. (1993). Sparky: NMR Display and analysis program. San Francisco, University of California, San Francisco.

de Lorenzo, V., Giovannini, F., Herrero, M. and Neilands, J. B. (1988). Metal ion regulation of gene expression. Fur repressor-operator interaction at the promoter region of the aerobactin system of pColV-K30. *J. Mol. Biol. 203(4)*, 875-84.

Dean, C. R. and Poole, K. (1993). Expression of the ferric enterobactin receptor (PfeA) of *Pseudomonas aeruginosa*: involvement of a two-component regulatory system. *Mol. Microbiol. 8(6)*, 1095-1103.

Doi, T., Ando, M., Akaike, T., Suga, M., Sato, K. and Maeda, H. (1993). Resistance to nitric oxide in *Mycobacterium avium* complex and its implication in pathogenesis. *Infect. Immun. 61(5)*, 1980-1989.

Dolin, P. J., Raviglione, M. C. and Kochi, A. (1994). Global tuberculosis incidence and mortality during 1990-2000. *Bull. WHO 72(2)*, 213-220.

Doukhan, L., Predich, M., Nair, G., Dussurget, O., Mandic-Mulec, I., Cole, S. T., Smith, D. R. and Smith, I. (1995). Genomic organization of the mycobacterial sigma gene cluster. *Gene 165(1)*, 67-70.

Duffy, T. H. and Nowak, T. (1985). ^{1}H and ^{31}P relaxation rate studies of the interaction of phosphoenolpyruvate and its analogues with avian phosphoenolpyruvate carboxykinase. *Biochem. 24(5)*, 1152-1160.

Dussurget, O., Rodriguez, M. and Smith, I. (1996). An ideR mutant of *Mycobacterium smegmatis* has derepressed siderophore production and an altered oxidative-stress response. *Mol. Microbiol. 22(3)*, 535-544.

Dutton, G. J. (1980). Glucuronidation of Drugs and Other Compounds. Boca Raton, FL. CRC Press, Inc.

Edlin, B. R., Tokars, J. I., Grieco, M. H., Crawford, J. T., Williams, J., Sordillo, E. M., Ong, K. R., Kilburn, J. O., Dooley, S. W., Castro, K. G. and et al. (1992). An outbreak of multidrug-resistant tuberculosis among hospitalized patients with the acquired immunodeficiency syndrome [see comments]. *N. Engl. J. Med. 326(23)*, 1514-1521.

Eidus, L. and Hamilton, E. J. (1964). In vitro test with 4,4'-dilsoamyloxythiocarbanilide. *Am. Rev. Resp. Dis. 90*, 258-260.

Ellner, J. J., Hinman, A. R., Dooley, S. W., Fischl, M. A., Sepkowitz, K. A., Goldberger, M. J., Shinnick, T. M., Iseman, M. D. and Jacobs, W. R., Jr. (1993). Tuberculosis symposium: emerging problems and promise. *J. Infect. Dis. 168(3)*, 537-551.

Falkinham, J. O. r. (1996). Epidemiology of infection by nontuberculous mycobacteria. *Clin. Microbiol. Rev. 9(2)*, 177-215.

Filley, E. A., Bull, H. A., Dowd, P. M. and Rook, G. A. (1992). The effect of *Mycobacterium tuberculosis* on the susceptibility of human cells to the stimulatory and toxic effects of tumour necrosis factor. *Immunology 77(4)*, 505-9.

Filley, E. A. and Rook, G. A. (1991). Effect of mycobacteria on sensitivity to the cytotoxic effects of tumor necrosis factor. *Infect Immun 59(8)*, 2567-72.

Fischer, G. and Schmid, F. X. (1990). The mechanism of protein folding. Implications of *in vitro* refolding models for *de novo* protein folding and translocation in the cell. *Biochem. 29(9)*, 2205-2212.

Fischer, L. J., Quinn, F. D., White, E. H. and King, C. H. (1996). Intracellular growth and cytotoxicity of *Mycobacterium haemophilum* in a human epithelial cell line (Hec-1-B). *Infect. Immun. 64(1)*, 269-276.

Fischl, M. A., Daikos, G. L., Uttamchandani, R. B., Poblete, R. B., Moreno, J. N., Reyes, R. R., Boota, A. M., Thompson, L. M., Cleary, T. J., Oldham, S. A. and et al. (1992). Clinical presentation and outcome of patients with HIV infection and tuberculosis caused by multiple-drug-resistant bacilli. *Ann. Intern. Med. 117(3)*, 184-190.

Fish, W. W. (1988). Rapid colorimetric micromethod for the quantitation of complexed iron in biological samples. *Methods Enzymol. 158*, 357-364.

Foster, J. W. and Hall, H. K. (1992). Effect of *Salmonella typhimurium* ferric uptake regulator (fur) mutations on iron- and pH-regulated protein synthesis. *J. Bacteriol. 174(13)*, 4317-4323.

Frieden, T. R., Sterling, T., Pablosmendez, A., Kilburn, J. O., Cauthen, G. M. and Dooley, S. W. (1993). The emergence of drug-resistant tuberculosis in New York City. *N. Engl. J.f Med. 328(8)*, 521-526.

Galli, C., Rise, P., Marangoni, F., Petroni, A. and Visioli, F. (1997). Manipulation of the fate of long chain polyunsaturated fatty acids in cultured cells. *Prostaglandins Leukot. Essent. Fatty Acids 57(1)*, 23-26.

Gobin, J. and Horwitz, M. A. (1996). Exochelins of *Mycobacterium tuberculosis* remove iron from human iron-binding proteins and donate iron to mycobactins in the *M. tuberculosis* cell wall. *J. Exp. Med. 183(4)*, 1527-1532.

Gobin, J., Moore, C. H., Reeve, J. R., Jr., Wong, D. K., Gibson, B. W. and Horwitz, M. A. (1995). Iron acquisition by *Mycobacterium tuberculosis*: isolation and characterization of a family of iron-binding exochelins. *Proc. Natl. Acad. Sci. USA 92*, 5189-5193.

Gobin, J., Wong, D. K., Gibson, B. W. and Horwitz, M. A. (1998). Characterization of Exochelins of *Mycobacterium bovis* and *M. bovis* BCG. *Infect. Immun. (submitted)*

Goble, M., Iseman, M. D., Madsen, L. A., Waite, D., Ackerson, L. and Horsburgh, C. R., Jr. (1993). Treatment of 171 patients with pulmonary tuberculosis resistant to isoniazid and rifampin. *N. Engl. J. Med. 328(8)*, 527-532.

Gordon, A. H., Hart, P. D. and Young, M. R. (1980). Ammonia inhibits phagosome-lysosome fusion in macrophages. *Nature 286(5768)*, 79-80.

Gordon, S. and Andrew, P. W. (1996). Mycobacterial virulence factors. *Soc. Appl. Bacteriol. Symp. Ser. 25*, 10S-22S.

Goren, M. B. and Brennan, P. J. (1979). Mycobacterial lipids: chemistry and biological activities. Tuberculosis. Youmans, G. P. Philadelphia, Saunders: 63-193.

Goren, M. B., Brokl, O. and Schaefer, W. B. (1974). Lipids of putative relevance to virulence in *Mycobacterium tuberculosis*: correlation of virulence with elaboration of sulfatides and strongly acidic lipids. *Infect. Immun. 9(1)*, 142-149.

Goren, M. B., Brokl, O. and Schaefer, W. B. (1974). Lipids of putative relevance to virulence in *Mycobacterium tuberculosis*: phthiocerol dimycocerosate and the attenuation indicator lipid. *Infect. Immun. 9(1)*, 150-158.

Goren, M. B., Grange, J. M., Aber, V. R., Allen, B. W. and Mitchison, D. A. (1982). Role of lipid content and hydrogen peroxide susceptibility in determining the guinea-pig virulence of *Mycobacterium tuberculosis*. *Br. J. Exp. Pathol. 63(6)*, 693-700.

Goren, M. B., Hart, D. P., Young, M. R. and Armstrong, J. A. (1976). Prevention of phagosome-lysosome fusion in cultured macrophages by sulfatides of *Mycobacterium tuberculosis*. *Proc. Natl. Acad. Sci. USA 73(7)*, 2510-2514.

Grange, J. M. (1989). Mycobacterial disease in the world. The biology of the mycobacteria. Ratledge, C., Stanford, J. and Grange, J. M. New York, Academic. *3*: 3-36.

Grange, J. M., Aber, V. R., Allen, B. W., Mitchison, D. A. and Goren, M. B. (1978). The correlation of bacteriophage types of *Mycobacterium tuberculosis* with guinea-pig virulence and in vitro-indicators of virulence. *J. Gen. Microbiol. 108(1)*, 1-7.

Greatbanks, D. and Bedford, G. R. (1969). Identification of mycobactins by nuclear-magnetic-resonance spectroscopy. *Biochem. J. 115(5)*, 1047-1050.

Guengerich, F. P. (1989). Analysis and characterization of enzymes. Principles and Methods of Toxicology. Hayes, A. W. New York, Raven Press: 777-814.

Guerinot, M. L. and Yi, Y. (1994). Iron - nutritious, noxious, and not readily available. *Plant Physiol. 104(3)*, 815-820.

Gunter-Seeboth, K. and Schupp, T. (1995). Cloning and sequence analysis of the *Corynebacterium diphtheriae* dtxR homologue from *Streptomyces lividans* and *S. pilosus* encoding a putative iron repressor protein. *Gene 166(1)*, 117-119.

Gupta, K. N. N. S. (1909). The ayurvedic system of medicine. Calcutta, Chatterjee.

Hacker, J. and Fischer, G. (1993). Immunophilins: structure-function relationship and possible role in microbial pathogenicity. *Mol. Microbiol. 10(3)*, 445-456.

Hall, R. M. and Ratledge, C. (1987). Exochelin-mediated iron acquisition by the leprosy bacillus, *Mycobacterium leprae. J. Gen. Microbiol. 133(Pt 1)*, 193-199.

Hall, R. M., Sritharan, M., Messenger, A. J. M. and Ratledge, C. (1987). Iron transport in *Mycobacterium smegmatis*: occurrence of iron-regulated envelope proteins a potential receptors for iron uptake. *J. Gen. Microbiol. 133(8)*, 2107-2114.

Halliday, K. R. (1983). Regional homology in GTP-binding proto-oncogene products and elongation factors. *J. Cyclic Nucleotide Protein Phosphor. Res. 9(6)*, 435-448.

Hancock, D. K., Coxon, B., Wang, S. Y., White, E., Reeder, D. J. and Bellama, J. M. (1993). L-Threo-beta-hydroxyhistidine, an unprecedented iron(III) ion-binding amino acid in a pyoverdine-type siderophore from *Pseudomonas fluorescens* 244. *J. Chem. Soc., Chem. Commun (5)*, 468-470.

Hankin, J. A., Wheelan, P. and Murphy, R. C. (1997). Identification of novel metabolites of prostaglandin E2 formed by isolated rat hepatocytes. *Arch. Biochem. Biophys. 340(2)*, 317-330.

Hantke, K. (1981). Regulation of ferric iron transport in *Escherichia coli* K12: isolation of a constitutive mutant. *Mol Gen Genet 182(2)*, 288-92.

Hantke, K. (1984). Cloning of the repressor protein gene of iron-regulated systems in *Escherichia coli* K12. *Mol. Gen. Genet. 197(2)*, 337-341.

Hart, P. D., Young, M. R., Gordon, A. H. and Sullivan, K. H. (1987). Inhibition of phagosome-lysosome fusion in macrophages by certain mycobacteria can be explained by

inhibition of lysosomal movements observed after phagocytosis. *J. Exp. Med. 166(4)*, 933-946.

Harth, G., Lee, B. Y., Wang, J., Clemens, D. L. and Horwitz, M. A. (1996). Novel insights into the genetics, biochemistry, and immunocytochemistry of the 30-kilodalton major extracellular protein of *Mycobacterium tuberculosis* [published erratum appears in Infect. Immun. 1997 Feb;65(2):852]. *Infect. Immun. 64(8)*, 3038-3047.

Hassett, D. J., Sokol, P. A., Howell, M. L., Ma, J. F., Schweizer, H. T., Ochsner, U. and Vasil, M. L. (1996). Ferric uptake regulator (Fur) mutants of *Pseudomonas aeruginosa* demonstrate defective siderophore-mediated iron uptake, altered aerobic growth, and decreased superoxide dismutase and catalase activities. *J. Bacteriol. 178(14)*, 3996-4003.

Hebda, C. A. and Nowak, T. (1982). Phosphoenolpyruvate carboxykinase. Mn^{2+} and Mn^{2+} substrate complexes. *J. Biol. Chem. 257(10)*, 5515-5522.

Henderson, D. P. and Payne, S. M. (1993). Cloning and characterization of the *Vibrio cholerae* genes encoding the utilization of iron from haemin and haemoglobin. *Mol. Microbiol. 7(3)*, 461-469.

Hines, M. E. n., Kreeger, J. M. and Herron, A. J. (1995). Mycobacterial infections of animals: pathology and pathogenesis. *Lab. Anim. Sci. 45(4)*, 334-351.

Hirsch, C. S., Ellner, J. J., Russell, D. G. and Rich, E. A. (1994). Complement receptor-mediated uptake and tumor necrosis factor-alpha-mediated growth inhibition of *Mycobacterium tuberculosis* by human alveolar macrophages. *J. Immunol. 152(2)*, 743-753.

Holzberg, M. and Artis, W. M. (1983). Hydroxamate siderophore production by opportunistic and systemic fungal pathogens. *Infect. Immun. 40(3)*, 1134-1139.

Horwitz, M. A., Lee, B. W., Dillon, B. J. and Harth, G. (1995). Protective immunity against tuberculosis induced by vaccination with major extracellular proteins of *Mycobacterium tuberculosis*. *Proc. Natl. Acad. Sci. USA 92(5)*, 1530-1534.

Hough, E. and Rogers, D. (1974). The crystal structure of ferrimycobactin P, a growth factor for the Mycobacteria. *Biochem. Biophys. Res. Commun. 57(1)*, 73-77.

Inderlied, C. B., Kemper, C. A. and Bermudez, L. E. (1993). The *Mycobacterium avium* complex. *Clin. Microbiol. Rev. 6(3)*, 266-310.

Iseman, M. D. (1993). Treatment of multidrug-resistant tuberculosis [published erratum appears in N Engl J Med 1993 Nov 4;329(19):1435]. *N. Engl. J. Med. 329(11)*, 784-791.

Iwatsubo, T., Hirota, N., Ooie, T., Suzuki, H., Shimada, N., Chiba, K., Ishizaki, T., Green, C. E., Tyson, C. A. and Sugiyama, Y. (1997). Prediction of *in vivo* drug metabolism in the human liver from *in vitro* metabolism data. *Pharmacol. Ther. 73(2)*, 147-171.

Iwatsubo, T., Suzuki, H., Shimada, N., Chiba, K., Ishizaki, T., Green, C. E., Tyson, C. A., Yokoi, T., Kamataki, T. and Sugiyama, Y. (1997). Prediction of *in vivo* hepatic metabolic clearance of YM796 from *in vitro* data by use of human liver microsomes and recombinant P-450 isozymes. *J. Pharmacol. Exp. Ther. 282(2)*, 909-919.

Jackett, P. S., Aber, V. R. and Lowrie, D. B. (1978). Virulence of *Mycobacterium tuberculosis* and susceptibility to peroxidative killing systems. *J. Gen. Microbiol. 107(2)*, 273-278.

Jackett, P. S., Aber, V. R., Mitchison, D. A. and Lowrie, D. B. (1981). The contribution of hydrogen peroxide resistance to virulence of *Mycobacterium tuberculosis* during the first six days after intravenous infection of normal and BCG-vaccinated guinea-pigs. *Br. J. Exp. Pathol. 62(1)*, 34-40.

Jacobs, W. R. J. and Bloom, B. R. (1994). Molecular genetic strategies for identifying virulence determinants of *Mycobacterium tuberculosis*. Tuberculosis: Pathogenesis, Protection, and Control. Bloom, B. R. Washington, D.C., American Society for Microbiology Press: 253-268.

Jajoo, H. K., Blair, I. A., Klunk, L. J. and Mayol, R. F. (1990). *In vitro* metabolism of the antianxiety drug buspirone as a predictor of its metabolism *in vivo*. *Xenobiotica 20(8)*, 779-786.

Jindal, S., Dudani, A. K., Singh, B., Harley, C. B. and Gupta, R. S. (1989). Primary structure of a human mitochondrial protein homologous to the bacterial and plant chaperonins and to the 65-kilodalton mycobacterial antigen. *Mol. Cell. Biol. 9(5)*, 2279-2283.

Johnsson, K., King, D. S. and Schultz, P. G. (1995). Studies on the mechanism of action of isoniazid and ethionamide in the chemotherapy Of tuberculosis. *J. Am. Chem. Soc. 117(17)*, 5009-5010.

Karas, M., Bahr, U. and Giessmann, U. (1991). Matrix-assisted laser desorption ionization mass spectrometry. *Mass Spectrom. Rev. 10(5)*, 335-357.

Kato, L. (1985). Absence of mycobactin in *Mycobacterium leprae*; probably a microbe dependent microorganism. *Int. J. Lepr. 57*, 58-70.

Kaufmann, R., Spengler, B. and Lutzenkirchen, F. (1993). Mass spectrometric sequencing of linear peptides by product-ion analysis in a reflectron time-of-flight mass spectrometer using matrix-assisted laser desorption ionization. *Rapid Commun. Mass Spectrom. 7(10)*, 902-910.

King, C. H., Mundayoor, S., Crawford, J. T. and Shinnick, T. M. (1993). Expression of contact-dependent cytolytic activity by *Mycobacterium tuberculosis* and isolation of the genomic locus that encodes the activity. *Infect. Immun. 61(6)*, 2708-2712.

Kingston, A. E., Salgame, P. R., Mitchison, N. A. and Colston, M. J. (1987). Immunological activity of a 14-kilodalton recombinant protein of *Mycobacterium tuberculosis* H37Rv. *Infect. Immun. 55(12)*, 3149-3154.

Kneller, D. and Kuntz, I. D. (1993). Striker. San Francisco, University of California, San Francisco.

Kochan, I. (1969). Mechanism of tuberculostasis in mammalian serum. I. Role of transferrin in human serum tuberculosis. *J. Infect. Dis. 119*, 11-18.

Kochan, I., Pellis, N. R. and Golden, C. A. (1971). Mechanism of tuberculostasis in mammalian serum. III. Neutralization of serum tuberculostasis by mycobactin. *Infect. Immun. 3*, 553-558.

Krozowski, Z. (1994). The short-chain alcohol dehydrogenase superfamily: variations on a common theme. *J. Steroid Biochem. Mol. Biol. 51(3-4)*, 125-130.

Laal, S., Sharma, Y. D., Prasad, H. K., Murtaza, A., Singh, S., Tangri, S., Misra, R. S. and Nath, I. (1991). Recombinant fusion protein identified by lepromatous sera mimics native *Mycobacterium leprae* in T-cell responses across the leprosy spectrum. *Proc. Natl. Acad. Sci. USA 88(3)*, 1054-8.

Lambrecht, R. S. and Collins, M. T. (1993). Inability to detct mycobactin in mycobacteria-infected tissues suggests an alternative iron acquisition mechanism by mycobacteria *in vivo. Microb. Pathogen. 14*, 229-238.

Lane, S. J., Marshall, P. S., Upton, R. J., Ratledge, C. and Ewing, M. (1995). Novel extracellular mycobactins, the carboxymycobactins from *Mycobacterium avium. Tetrahed. Lett. 36(23)*, 4129-4132.

Le Cam, E., Frechon, D., Barray, M., Fourcade, A. and Delain, E. (1994). Observation of binding and polymerization of Fur repressor onto operator-containing DNA with electron and atomic force microscopes. *Proc. Natl. Acad. Sci. USA 91(25)*, 11816-11820.

Leao, S. C., Lopes, J. D. and Patarroyo, M. E. (1993). Immunological and functional characterization of proteins of the *Mycobacterium tuberculosis* antigen-85 complex using synthetic peptides. *J. Gen. Microbiol. 139(Jul)*, 1543-1549.

Leao, S. C., Rocha, C. L., Murillo, L. A., Parra, C. A. and Patarroyo, M. E. (1995). A species-specific nucleotide sequence of *Mycobacterium tuberculosis* encodes a protein that exhibits hemolytic activity when expressed in *Escherichia coli. Infect. Immun. 63(11)*, 4301-4306.

Lee, B. Y., Hefta, S. A. and Brennan, P. J. (1992). Characterization of the major membrane protein of virulent *Mycobacterium tuberculosis. Infect. Immun. 60(5)*, 2066-2074.

Lee, B. Y. and Horwitz, M. A. (1995). Identification of macrophage and stress-induced proteins of *Mycobacterium tuberculosis. J. Clin. Invest. 96(1)*, 245-249.

Lee, M. H., Hebda, C. A. and Nowak, T. (1981). The role of cations in avian liver phosphoenolpyruvate carboxykinase catalysis. Activation and regulation. *J. Biol. Chem. 256(24)*, 12793-12801.

Lee, M. H. and Nowak, T. (1984). Phosphorus-31 nuclear relaxation rate studies of the nucleotides on phosphoenolpyruvate carboxykinase. *Biochem. 23(26)*, 6506-6513.

Lehker, M. W. and Alderete, J. F. (1992). Iron regulates growth of *Trichomonas vaginalis* and the expression of immunogenic trichomonad proteins. *Mol. Microbiol. 6(1)*, 123-132.

Lindquist, S. (1986). The heat-shock response. *Annu. Rev. Biochem. 55*, 1151-1191.

Litwin, C. M. and Calderwood, S. B. (1993). Cloning and genetic analysis of the *Vibrio vulnificus* Fur gene and construction of a Fur mutant by in vivo marker exchange. *J. Bacteriol. 175(3)*, 706-715.

Litwin, C. M. and Calderwood, S. B. (1993). Role of iron in regulation of virulence genes. *Clin Microbiol Rev 6(2)*, 137-49.

Liu, J. and Walsh, C. T. (1990). Peptidyl-prolyl cis-trans-isomerase from *Escherichia coli*: a periplasmic homolog of cyclophilin that is not inhibited by cyclosporin A. *Proc. Natl. Acad. Sci. USA 87(11)*, 4028-4032.

Lotte, A., Wasz-Hockert, O., Poisson, N., Dumitrescu, N., Verron, M. and Couvet, E. (1984). BCG complications. Estimates of the risks among vaccinated subjects and statistical analysis of their main characteristics. *Adv. Tuberc. Res. 21*, 107-193.

Lowrie, D. B., Jackett, P. S. and Ratcliffe, N. A. (1975). *Mycobacterium microti* may protect itself from intracellular destruction by releasing cyclic AMP into phagosomes. *Nature 254(5501)*, 600-602.

Lurie, M. B. (1964). Resistance to tuberculosis: experimental studies in native and acquired defensive mechanisms. Cambridge, Harvard University Press.

Luthria, D. L., Chen, Q. and Sprecher, H. (1997). Metabolites produced during the peroxisomal beta-oxidation of linoleate and arachidonate move to microsomes for conversion back to linoleate. *Biochem. Biophys. Res. Commun. 233(2)*, 438-441.

Macham, L. P. and Ratledge, C. (1975). A new group of water-soluble iron-binding compounds from mycobacteria: the exochelins. *J. Gen. Microbiol. 89*, 379-382.

Macham, L. P., Ratledge, C. and Nocton, J. C. (1975). Extracellular iron acquisition by mycobacteria: role of the exochelins and evidence against the participation of mycobactin. *Infect. Immun. 12*, 1242-1251.

Marion, D. and Wuthrich, K. (1983). Application of phase sensitive two-dimensional correlated spectroscopy (COSY) for measurements of ^{1}H-^{1}H spin-spin coupling constants in proteins. *Biochem. Biophys. Res. Commun. 113(3)*, 967-974.

Marshall, B. J. and Ratledge, C. (1972). Salicylic acid biosynthesis and its control in *Mycobacterium smegmatis. Biochim Biophys Acta 264(1)*, 106-16.

Masur, H., Ognibene, F. P., Yarchoan, R., Shelhamer, J. H., Baird, B. F., Travis, W., Suffredini, A. F., Deyton, L., Kovacs, J. A. and Falloon, J. (1989). CD4 counts as predictors of opportunistic pneumonias in human immunodeficiency virus (HIV) infection. *Ann. Intern. Med. 111(3)*, 223-231.

Matsui, N. M., Smith, D. M., Clauser, K. R., Fichmann, J., Andrews, L. E., Sullivan, C. M., Burlingame, A. L. and Epstein, L. B. (1997). Immobilized pH gradient two-dimensional gel electrophoresis and mass spectrometric identification of cytokine-regulated proteins in ME-180 cervical carcinoma cells. *Electrophoresis 18(3-4)*, 409-417.

Matte, A., Tari, L. W., Goldie, H. and Delbaere, L. T. (1997). Structure and mechanism of phosphoenolpyruvate carboxykinase. *J. Biol. Chem. 272(13)*, 8105-8108.

Matzanke, B. F. (1991). Structures, coordination chemistry, and functions of microbial iron chelates. <u>CRC handbook of microbial iron chelates</u>. Winkelmann, G. Boca Raton, Fla, CRC Press: 15-65.

Maurer, P. J. and Miller, M. J. (1983). Total synthesis of a mycobactin: mycobactin S2. *J. Am. Chem. Soc. 105*, 240-245.

McCready, K. A. and Ratledge, C. (1979). Ferrimycobactin reductase activity from *Mycobacterium smegmatis. J. Gen. Microbiol. 113*, 67-72.

McCullough, W. G. and Merkal, R. S. (1982). Structure of mycobactin J. *Curr. Microbiol. 7*, 337-341.

McDonough, K. A. and Kress, Y. (1995). Cytotoxicity for lung epithelial cells is a virulence-associated phenotype of *Mycobacterium tuberculosis. Infect. Immun. 63(12)*, 4802-4811.

McDonough, K. A., Kress, Y. and Bloom, B. R. (1993). Pathogenesis of tuberculosis: interaction of *Mycobacterium tuberculosis* with macrophages. *Infect. Immun. 61*(*7*), 2763-2773.

Medzihradszky, K. F., Maltby, D. A., Qiu, Y., Yu, Z., Hall, S. C., Chen, Y. and Burlingame, A. L. (1997). Protein sequence and structural studies employing matrix-assisted laser desorption ionization-high energy collision-induced dissociation. *Int. J. of Mass Spectrom. Ion Processes 160*, 357-369.

Mehta, P. K., King, C. H., White, E. H., Murtagh, J. J., Jr. and Quinn, F. D. (1996). Comparison of *in vitro* models for the study of *Mycobacterium tuberculosis* invasion and intracellular replication. *Infect. Immun. 64*(*7*), 2673-2679.

Melefors, O. and Hentze, M. W. (1993). Iron regulatory factor--the conductor of cellular iron regulation. *Blood Rev. 7*(*4*), 251-258.

Melefors, O. and Hentze, M. W. (1993). Translational regulation by messenger RNA protein interactions in eukaryotic cells - ferritin and beyond. *Bioessays 15*(*2*), 85-90.

Middlebrook, G., Dubos, R. J. and Pierce, C. H. (1947). Virulence and morphological characteristics of mammalian tubercle bacilli. *J. Exp. Med. 86*, 175-184.

Mitchison, D. A. and Nunn, A. J. (1986). Influence of initial drug resistance on the response to short-course chemotherapy of pulmonary tuberculosis. *Am. Rev. Respir. Dis. 133*(*3*), 423-430.

Mitchison, D. A., Selkon, J. B. and Lloyd, J. (1963). Virulence in guinea pigs, susceptibility to hdrogen peroxide and catalase activity of isoniazid sensitive tubercle bacilli from South Indian and British patients. *J. Pathol. Bacteriol. 86*, 377-386.

Moldéus, P., Hogberg, J. and Orrenius, S. (1978). Isolation and use of liver cells. *Methods Enzymol. 52*, 60-71.

Moore, C. H., Foster, L. A., Gerbig, D. G., Jr., Dyer, D. W. and Gibson, B. W. (1995). Identification of alcaligin as the siderophore produced by *Bordetella pertussis* and *B. bronchiseptica*. *J. Bacteriol. 177(4)*, 1116-1118.

Morse, D. R., Brothwell, D. R. and Ucko, P. J. (1964). Tuberculosis in ancient Egypt. *Am. Rev. Respir. Dis. 90*, 534-541.

Myrvik, Q. N., Leake, E. S. and Wright, M. J. (1984). Disruption of phagosomal membranes of normal alveolar macrophages by the H37Rv strain of *Mycobacterium tuberculosis*. A correlate of virulence. *Am. Rev. Respir. Dis. 129(2)*, 322-328.

Nair, C. N., Mackay-Scollay, E. M., Ramachandran, K., Selkon, J. B., Tripathy, S. P., Mitchison, D. A. and Dickinson, J. M. (1964). Virulence in the guinea pig and susceptibility to hydrogen peroxide of isoniazid-sensitive tubercle bacilli from South Indian patients. *Tubercle 45*, 345-353.

Neilands, J. B. (1981). Iron absorption and transport in microorganisms. *Annu. Rev. Nutr. 1*, 27-46.

Neilands, J. B. (1995). Siderophores: structure and function of microbial iron transport compounds. *J. Biol. Chem. 270(45)*, 26723-26726.

Nerland, A. H., Mustafa, A. S., Sweetser, D., Godal, T. and Young, R. A. (1988). A protein antigen of *Mycobacterium leprae* is related to a family of small heat shock proteins. *J. Bacteriol. 170(12)*, 5919-5921.

Newman, R., Doster, B. E., Murray, F. J. and Woolpert, S. F. (1974). Rifampin in initial treatment of pulmonary tuberculosis. A U.S. Public Health Service tuberculosis therapy trial. *Am. Rev. Respir. Dis. 109(2)*, 216-232.

Niederhoffer, E. C., Naranjo, C. M., Bradley, K. L. and Fee, J. A. (1990). Control of *Escherichia coli* superoxide dismutase (sodA and sodB) genes by the ferric uptake regulation (fur) locus. *J. Bacteriol. 172(4)*, 1930-1938.

Nikaido, H. (1993). Uptake of iron-siderophore complexes across the bacterial outer membrane. *Trends Microbiol.* *1(1)*, 5-8.

Nikaido, H. and Saier, M. H., Jr. (1992). Transport proteins in bacteria: common themes in their design. *Science* *258(5084)*, 936-942.

Noronha-Dutra, A. A., Epperlein, M. M. and Woolf, N. (1993). Reaction of nitric oxide with hydrogen peroxide to produce potentially cytotoxic singlet oxygen as a model for nitric oxide-mediated killing. *FEBS Lett.* *321(1)*, 59-62.

O'Brien, L., Carmichael, J., Lowrie, D. B. and Andrew, P. W. (1994). Strains of *Mycobacterium tuberculosis* differ in susceptibility to reactive nitrogen intermediates *in vitro*. *Infect. Immun.* *62(11)*, 5187-5190.

Obach, R. S., Baxter, J. G., Liston, T. E., Silber, B. M., Jones, B. C., MacIntyre, F., Rance, D. J. and Wastall, P. (1997). The prediction of human pharmacokinetic parameters from preclinical and *in vitro* metabolism data. *J. Pharmacol. Exp. Ther.* *283(1)*, 46-58.

Ochsner, U. A., Vasil, A. I. and Vasil, M. L. (1995). Role of the ferric uptake regulator of *Pseudomonas aeruginosa* in the regulation of siderophores and exotoxin A expression: purification and activity on iron-regulated promoters. *J. Bacteriol.* *177(24)*, 7194-7201.

Oguiza, J. A., Marcos, A. T., Malumbres, M. and Martin, J. F. (1996). Multiple sigma factor genes in *Brevibacterium lactofermentum*: characterization of sigA and sigB. *J. Bacteriol.* *178(2)*, 550-553.

Organization, W. H. (1994). Zoonotic tuberculosis (Mycobacterium bovis): memorandum from a WHO meeting (with the participation of FAO). *Bull World Health Organ* *72(6)*, 851-857.

Pal, P. G. and Horwitz, M. A. (1992). Immunization with extracellular proteins of Mycobacterium tuberculosis induces cell-mediated immune responses and substantial

protective immunity in a guinea pig model of pulmonary tuberculosis. *Infect. Immun.* *60(11)*, 4781-4792.

Payne, S. M. (1993). Iron acquisition in microbial pathogenesis. *Trends Microbiol. 1(2)*, 66-69.

Payne, S. M. and Lawlor, K. M. (1990). The Bacteria: Molecular Basis of Bacterial Pathogenesis. Iglewski, B. H. and Clark, V. L. Academic Press. *VI*: 225-248.

Pearson, M. L., Jereb, J. A., Frieden, T. R., Crawford, J. T., Davis, B. J., Dooley, S. W. and Jarvis, W. R. (1992). Nosocomial transmission of multidrug-resistant *Mycobacterium tuberculosis*. A risk to patients and health care workers. *Ann. Intern. Med. 117(3)*, 191-196.

Perotti, B. Y., Prueksaritanont, T. and Benet, L. Z. (1994). HPLC assay for FK 506 and two metabolites in isolated rat hepatocytes and rat liver microsomes. *Pharm. Res. 11(6)*, 844-847.

Persson, B., Krook, M. and Jornvall, H. (1991). Characteristics of short-chain alcohol dehydrogenases and related enzymes. *Eur. J. Biochem. 200(2)*, 537-543.

Peterson, T., Falk, K. E., Leong, S. A., Klein, M. P. and Neilands, J. B. (1980). Structure and behavior of spermidine siderophores. *J. Am. Chem. Soc. 102*, 7715-7718.

Philipp, W. J., Poulet, S., Eiglmeier, K., Pascopella, L., Balasubramanian, V., Heym, B., Bergh, S., Bloom, B. R., Jacobs, W. R., Jr. and Cole, S. T. (1996). An integrated map of the genome of the tubercle bacillus, *Mycobacterium tuberculosis* H37Rv, and comparison with *Mycobacterium leprae. Proc. Natl. Acad. Sci. USA 93(7)*, 3132-3137.

Portnoy, D. A., Jacks, P. S. and Hinrichs, D. J. (1988). Role of hemolysin for the intracellular growth of *Listeria monocytogenes. J. Exp. Med. 167(4)*, 1459-1471.

Postle, K. (1990). TonB and the gram-negative dilemma. *Mol. Microbiol. 4(12)*, 2019-2025.

Punekar, N. S. and Lardy, H. A. (1987). Phosphoenolpyruvate carboxykinase ferroactivator 1. Mechanism of action and identity with glutathione peroxidase. *J. Biol. Chem. 262(14)*, 6714-6719.

Quinn, F. D., Newman, G. W. and King, C. H. (1996). Virulence determinants of *Mycobacterium tuberculosis. Curr. Top. Microbiol. Immunol. 215*, 131-156.

Rance, M., Sorensen, O. W., Bodenhausen, G., Wagner, G., Ernst, R. R. and Wuthrich, K. (1983). Improved spectral resolution in cosy ^{1}H NMR spectra of proteins via double quantum filtering. *Biochem. Biophys. Res. Commun. 117(2)*, 479-485.

Ratledge, C. (1984). Metabolism of iron and other metals by mycobacteria. The Mycobacteria: A Sourcebook (Part A). Kubica, G. P. and Wayne, L. G. NY, Marcel Dekker, Inc. *15*: 603-627.

Ratledge, C., Macham, L. P., Brown, K. A. and Marshall, B. J. (1974). Iron transport in *Mycobacterium smegmatis*: a restricted role for salicylic acid in the extracellular environment. *Biochim. Biophys. Acta 372(1)*, 39-51.

Ratledge, C., Patel, P. V. and Mundy, J. (1982). Iron transport in *Mycobacterium smegmatis*: the location of mycobactin by electron microscopy. *J. Gen. Microbiol. 128(7)*, 1559-1565.

Ratledge, C. and Winder, F. G. (1962). The accumulation of salicylic acid by mycobacteria during growth on an iron-deficient medium. *Biochem. J. 84*, 501-506.

Ratliff, T. L., Palmer, J. O., McGarr, J. A. and Brown, E. J. (1987). Intravesical Bacillus Calmette-Guerin therapy for murine bladder tumors: initiation of the response by fibronectin-mediated attachment of Bacillus Calmette-Guerin. *Cancer Res. 47(7)*, 1762-1766.

Redfield, A. G. and Kuntz, S. D. (1975). *J. Magn. Reson. 19*, 250.

Reid, M. F. and Fewson, C. A. (1994). Molecular characterization of microbial alcohol dehydrogenases. *Crit. Rev. Microbiol. 20(1)*, 13-56.

Retterstol, K., Woldseth, B. and Christophersen, B. O. (1996). The metabolism of 22:5(-6) and of docosahexaenoic acid [22:6(-3)] compared in rat hepatocytes. *Biochim. Biophys. Acta 1303(3)*, 180-186.

Retzlaff, C., Yamamoto, Y., Hoffman, P. S., Friedman, H. and Klein, T. W. (1994). Bacterial heat shock proteins directly induce cytokine mRNA and interleukin-1 secretion in macrophage cultures. *Infect. Immun. 62(12)*, 5689-5693.

Reynolds, C. H. (1980). Activation and inactivation of phosphoenolpyruvate carboxykinase by ferrous ions. *Biochem. J. 185(2)*, 451-454.

Reyrat, J. M., Berthet, F. X. and Gicquel, B. (1995). The urease locus of *Mycobacterium tuberculosis* and its utilization for the demonstration of allelic exchange in *Mycobacterium bovis* bacillus Calmette-Guerin. *Proc. Natl. Acad. Sci. USA 92(19)*, 8768-8772.

Riley, R. L., Mills, C. C., O'Grady, F., Sultan, L. U., Wittstadt, F. and Shivpuri, D. N. (1962). Infectiousness of air from a tuberculosis ward. Ultraviolet irradiation of infected air: comparative infectiousness of different patients. *Am. Rev. Respir. Dis. 85*, 511-525.

Roach, T. I., Barton, C. H., Chatterjee, D. and Blackwell, J. M. (1993). Macrophage activation: lipoarabinomannan from avirulent and virulent strains of *Mycobacterium tuberculosis* differentially induces the early genes c-fos, KC, JE, and tumor necrosis factor-alpha. *J. Immunol. 150(5)*, 1886-96.

Roach, T. I., Barton, C. H., Chatterjee, D., Liew, F. Y. and Blackwell, J. M. (1995). Opposing effects of interferon-gamma on iNOS and interleukin-10 expression in lipopolysaccharide- and mycobacterial lipoarabinomannan-stimulated macrophages. *Immunol. 85(1)*, 106-113.

Roberts, G. D., Koneman, E. W. and Kim, Y. K. (1991). Manual of clinical microbiology. Manual of clinical microbiology. Balows, A., Hauser, W. R. Jr., Herrmann, K. L., et al. Washinton, D.C., American Society for Microbiology: 304-339.

Rook, G. A. W. and Bloom, B. R. (1994). Mechanisms of pathogenesis in tuberculosis. Tuberculosis: Pathogenesis, Protection, and Control. Bloom, B. R. Washington, D.C., American Soceity of Microbiology Press: 485-501.

Rosenfeld, J., Capdevielle, J., Guillemot, J. C. and Ferrara, P. (1992). In-gel digestion of proteins for internal sequence analysis after one- or two-dimensional gel electrophoresis. *Anal. Biochem. 203(1)*, 173-179.

Samper, S., Martin, C., Pinedo, A., Rivero, A., Blazquez, J., Baquero, F., van Soolingen, D. and van Embden, J. (1997). Transmission between HIV-infected patients of multidrug-resistant tuberculosis caused by *Mycobacterium bovis*. *Aids 11(10)*, 1237-1242.

Sansonetti, P. J. (1991). Genetic and molecular basis of epithelial cell invasion by *Shigella* species. *Rev. Infect. Dis. 13(Suppl 4)*, S285-S292.

Schlesinger, L. S. (1996). Role of mononuclear phagocytes in *M. tuberculosis* pathogenesis. *J. Investig. Med. 44(6)*, 312-323.

Schlesinger, L. S., Bellinger-Kawahara, C. G., Payne, N. R. and Horwitz, M. A. (1990). Phagocytosis of *Mycobacterium tuberculosis* is mediated by human monocyte complement receptors and complement component C3. *J. Immunol. 144(7)*, 2771-2780.

Schlesinger, L. S. and Horwitz, M. A. (1991). Phagocytosis of *Mycobacterium leprae* by human monocyte-derived macrophages is mediated by complement receptors CR1 (CD35), CR3 (CD11b/CD18), and CR4 (CD11c/CD18) and IFN-gamma activation inhibits complement receptor function and phagocytosis of this bacterium. *J. Immunol. 147(6)*, 1983-1994.

Schlesinger, L. S., Hull, S. R. and Kaufman, T. M. (1994). Binding of the terminal mannosyl units of lipoarabinomannan from a virulent strain of *Mycobacterium tuberculosis* to human macrophages. *J. Immunol. 152(8)*, 4070-4079.

Schmitt, M. P. and Holmes, R. K. (1991). Iron-dependent regulation of diphtheria toxin and siderophore expression by the cloned Corynebacterium diphtheriae repressor gene dtxR in C. diphtheriae C7 strains. *Infect Immun 59(6)*, 1899-904.

Schmitt, M. P., Predich, M., Doukhan, L., Smith, I. and Holmes, R. K. (1995). Characterization of an iron-dependent regulatory protein (IdeR) of *Mycobacterium tuberculosis* as a functional homolog of the diphtheria toxin repressor (DtxR) from *Corynebacterium diphtheriae. Infect. Immun. 63(11)*, 4284-4289.

Schryvers, A. B. (1988). Characterization of the human transferrin and lactoferrin receptors in *Haemophilus influenzae. Mol. Microbiol. 2(4)*, 467-472.

Sharman, G. J., Williams, D. H., Ewing, D. F. and Ratledge, C. (1995). Determination of the structure of exochelin MN, the extracellular siderophore from *Mycobacterium neoaurum. Chem. Biol. 2*, 553-561.

Sharman, G. J., Williams, D. H., Ewing, D. F. and Ratledge, C. (1995). Isolation, purification, and struture of exochelin MS, the extracellular siderophore from *Mycobacterium smegmatis. Biochem. J. 305*, 187-196.

Sheer, D. G. (1994). Protein and peptide recovery from polyacrylamide gels. Techniques in protein chemistry V. Crabb, J. W. San Diego, Academic Press: 243-248.

Sibley, L. D., Hunter, S. W., Brennan, P. J. and Krahenbuhl, J. L. (1988). Mycobacterial lipoarabinomannan inhibits gamma interferon-mediated activation of macrophages. *Infect. Immun. 56(5)*, 1232-1236.

Silva, C. L., Ekizlerian, S. M. and Fazioli, R. A. (1985). Role of cord factor in the modulation of infection caused by mycobacteria. *Am. J. Pathol. 118(2)*, 238-247.

Singh, S., Jenner, P. J., Narayan, N. P., Ramu, G., Colston, M. J., Prasad, H. K. and Nath, I. (1994). Critical residues of the *Mycobacterium leprae* LSR recombinant protein discriminate clinical activity in erythema nodosum leprosum reactions. *Infect. Immun. 62(12)*, 5702-5705.

Singh, S., Narayanan, N. P., Jenner, P. J., Ramu, G., Colston, M. J., Prasad, H. K. and Nath, I. (1994). Sera of leprosy patients with type 2 reactions recognize selective sequences in *Mycobacterium leprae* recombinant LSR protein. *Infect. Immun. 62(1)*, 86-90.

Snow, G. A. (1965). Isolation and structure of mycobactin T, a growth factor from *Mycobacterium tuberculosis. Biochem. J. 97*, 166-175.

Snow, G. A. (1969). Metal complexes of mycobactin P and of desferrisideramines. *Biochem. J. 115(2)*, 199-205.

Snow, G. A. (1970). Mycobactins: iron-chelating growth factors from mycobacteria. *Bacteriol. Rev. 34*, 99-125.

Sprinzl, M. (1994). Elongation factor Tu: a regulatory GTPase with an integrated effector. *Trends Biochem. Sci. 19(6)*, 245-250.

Sritharan, M. and Ratledge, C. (1989). Co-ordinated expression of components of iron transport (mycobactin, exochelin and envelope proteins) in *Mycobacterium neoaurum. FEMS Microbiol. Lett. 60*, 183-186.

Sritharan, M. and Ratledge, C. (1990). Iron-regulated envelope proteins of mycobacteria grown *in vitro* and their occurrence in *Mycobacterium avium* and *Mycobacterium leprae* grown *in vivo. Biol. Met. 2(4)*, 203-208.
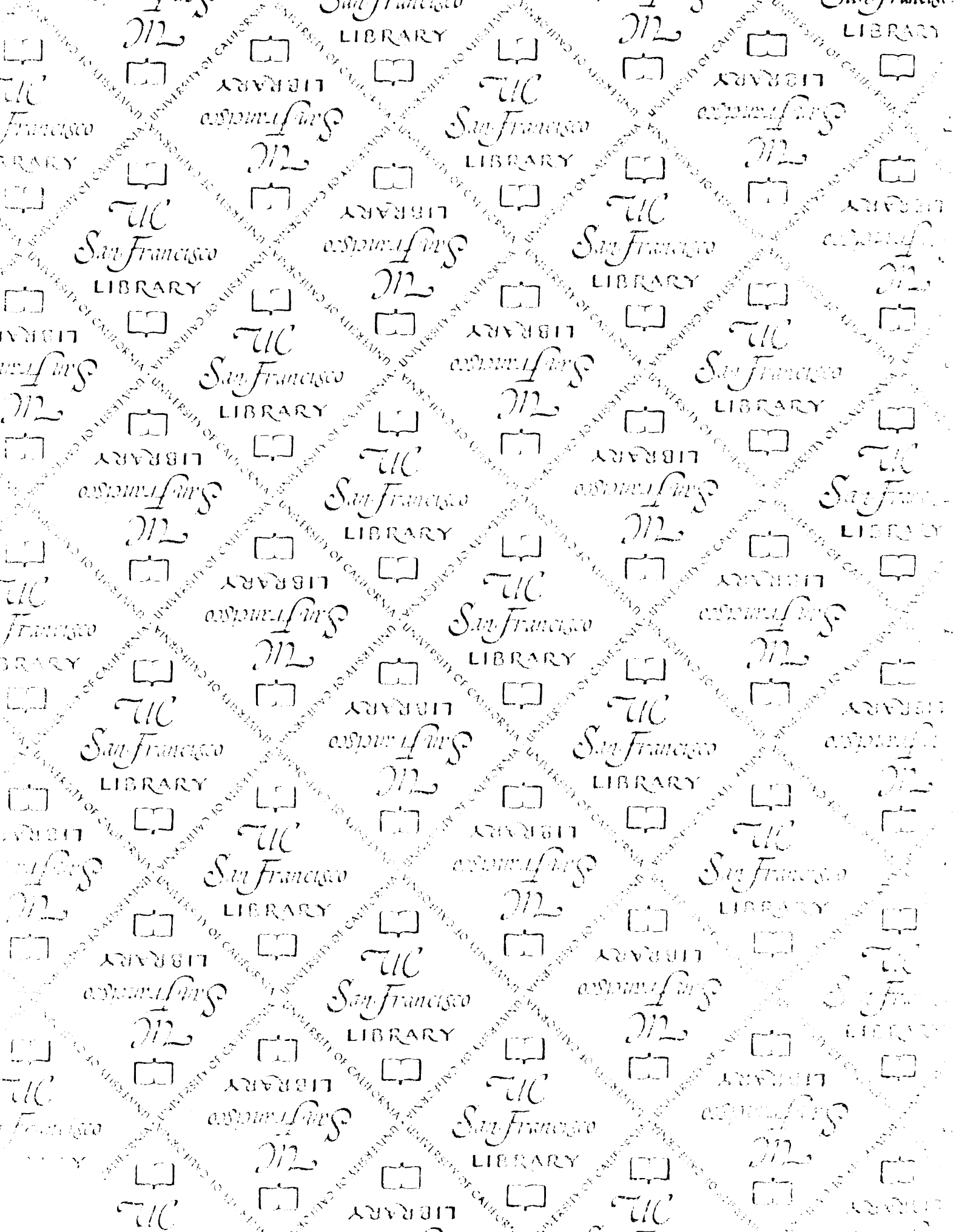
States, D. J., Haberkorn, R. A. and Ruben, D. J. (1982). *J. Magn. Reson. 48*, 286-292.

Stoebner, J. A. and Payne, S. M. (1988). Iron-regulated hemolysin production and utilization of heme and hemoglobin by *Vibrio cholerae*. *Infect. Immun. 56(11)*, 2891-2895.

Stojiljkovic, I. and Hantke, K. (1995). Functional domains of the *Escherichia coli* ferric uptake regulator protein (Fur). *Mol. Gen. Genet. 247(2)*, 199-205.

Sturgill-Koszycki, S., Schlesinger, P. H., Chakraborty, P., Haddix, P. L., Collins, H. L., Fok, A. K., Allen, R. D., Gluck, S. L., Heuser, J. and Russell, D. G. (1994). Lack of acidification in *Mycobacterium* phagosomes produced by exclusion of the vesicular proton-ATPase [see comments] [published erratum appears in Science 1994 Mar 11;263(5152):1359]. *Science 263(5147)*, 678-681.

Thummel, K. E., Shen, D. D., Podoll, T. D., Kunze, K. L., Trager, W. F., Hartwell, P. S., Raisys, V. A., Marsh, C. L., McVicar, J. P., Barr, D. M., Perkins, J. D. and Carithers, R. L., Jr. (1994). Use of midazolam as a human cytochrome P450 3A probe: I. *In vitro-in vivo* correlations in liver transplant patients. *J Pharmacol Exp Ther 271(1)*, 549-56.

Travers, A. A., Kamen, R. I. and Schleif, R. F. (1970). Factor necessary for ribosomal RNA synthesis. *Nature 228(273)*, 748-751.

Advisory Council for the Elimination of Tuberculosis. (1993). Initial therapy for tuberculosis in the era of multidrug-resistance. M. M. W. R. **42:** 1-8.

National action plan to combat multidrug- resistant tuberculosis. (1992). Meeting the challenge of multidrug-resistant tuberculosis - summary of a conference. Management of persons exposed to multidrug-resistant tuberculosis. *M. M. W. R. 41(RR-11)*, 1-71.

Udou, T. (1994). Extracellular hemolytic activity in rapidly growing mycobacteria. *Can. J. Microbiol. 40(4)*, 318-321.

199

Van Scoy, R. E. and Wilkowske, C. J. (1992). Antituberculous agents. *Mayo Clin. Proc.* 67(2), 179-187.

van Soolingen, D., de Haas, P. E., Haagsma, J., Eger, T., Hermans, P. W., Ritacco, V., Alito, A. and van Embden, J. D. (1994). Use of various genetic markers in differentiation of *Mycobacterium bovis* strains from animals and humans and for studying epidemiology of bovine tuberculosis. *J. Clin. Microbiol.* 32(10), 2425-2433.

Verbon, A., Hartskeerl, R. A., Schuitema, A., Kolk, A. H., Young, D. B. and Lathigra, R. (1992). The 14,000-molecular-weight antigen of *Mycobacterium tuberculosis* is related to the alpha-crystallin family of low-molecular-weight heat shock proteins. *J. Bacteriol.* 174(4), 1352-1359.

Vestal, M. L., Juhasz, P. and Martin, S. A. (1995). Delayed extraction matrix-assisted laser desorption time-of-flight mass spectrometry. *Rapid Commun. Mass Spectrom.* 9(11), 1044-1050.

von Moltke, L. L., Greenblatt, D. J., Schmider, J., Wright, C. E., Harmatz, J. S. and Shader, R. I. (1998). *In vitro* approaches to predicting drug interactions *in vivo*. *Biochem. Pharmacol.* 55(2), 113-122.

Walls, F. C., Baldwin, M. A., Falick, A. M., Gibson, B. W., Kaur, S., Maltby, D. A., Gillece-Castro, K. F., Medzihradsky, K. F., Evans, S. and Burlingame, A. L. (1990). Experience with multichannel array detection in tandem mass spectrometric characterization of biopolymers at the picomole level. Biological Mass Spectrometry. Burlingame, A. L. and McCloskey, J. A. Amsterdam, Elsevier: 197-216.

Wayne, L. G. (1976). Dynamics of submerged growth of *Mycobacterium tuberculosis* under aerobic and microaerophilic conditions. *Am. Rev. Respir. Dis.* 114(4), 807-811.

Wayne, L. G. (1977). Synchronized replication of *Mycobacterium tuberculosis*. *Infect. Immun.* 17(3), 528-530.

Wayne, L. G. (1984). Mycobacterial Speciation. The Mycobacteria: A Sourcebook. Kubica, G. P. and Wayne, L. G. New York, Dekker. *Part A*: 25-65.

Wayne, L. G. and Lin, K. Y. (1982). Glyoxylate metabolism and adaptation of *Mycobacterium tuberculosis* to survival under anaerobic conditions. *Infect Immun 37(3)*, 1042-9.

Wheeler, P. R. and Ratledge, C. (1994). Metabolism of *Mycobacterium tuberculosis*. Tuberculosis: Pathogenesis, Protection, and Control. Bloom, B. R. Washington, D.C., American Society for Microbiology: 353-385.

WHO (1996). Report on the tuberculosis epidemic. Geneva, World Health Organization.

Wiker, H. G. and Harboe, M. (1992). The antigen 85 complex: a major secretion product of *Mycobacterium tuberculosis*. *Microbiol. Rev. 56(4)*, 648-661.

Wong, D. K., Gobin, J., Horwitz, M. A. and Gibson, B. W. (1996). Characterization of exochelins of *Mycobacterium avium*: evidence for saturated and unsaturated and for acid and ester forms. *J. Bacteriol. 178(21)*, 6394-6398.

Wong, K. C. and Wu, L. T. (1932). The history of Chinese medicine. Tientsin, Tientsin Press.

Wooldridge, K. G., Morrissey, J. A. and Williams, P. H. (1992). Transport of ferric-aerobactin into the periplasm and cytoplasm of *Escherichia coli* K12: role of envelope-associated proteins and effect of endogenous siderophores. *J. Gen. Microbiol. 138(Pt 3)*, 597-603.

Young, C. C. and Bernlohr, R. W. (1991). Elongation factor Tu is methylated in response to nutrient deprivation in *Escherichia coli*. *J. Bacteriol. 173(10)*, 3096-3100.

Young, D. B. and Duncan, K. (1995). Prospects for new interventions in the treatment and prevention of mycobacterial disease. *Annu. Rev. Microbiol. 49*, 641-673.

Yuan, Y., Crane, D. D. and Barry, C. E. r. (1996). Stationary phase-associated protein expression in *Mycobacterium tuberculosis*: function of the mycobacterial alpha-crystallin homolog. *J. Bacteriol. 178(15)*, 4484-4492.

Zhang, L., English, D. and Andersen, B. R. (1991). Activation of human neutrophils by *Mycobacterium tuberculosis*-derived sulfolipid-1. *J. Immunol. 146(8)*, 2730-2736.

Zhang, L., Goren, M. B., Holzer, T. J. and Andersen, B. R. (1988). Effect of *Mycobacterium tuberculosis*-derived sulfolipid I on human phagocytic cells. *Infect. Immun. 56(11)*, 2876-83.

Zhang, Y., Garcia, M. J., Lathigra, R., Allen, B., Moreno, C., van Embden, J. D. and Young, D. (1992). Alterations in the superoxide dismutase gene of an isoniazid-resistant strain of *Mycobacterium tuberculosis*. *Infect. Immun. 60(6)*, 2160-2165.

Zhang, Y., Heym, B., Allen, B., Young, D. and Cole, S. (1992). The catalase-peroxidase gene and isoniazid resistance of *Mycobacterium tuberculosis*. *Nature 358(6387)*, 591-593.

Zhou, X. H. and van der Helm, D. (1993). A novel purification of ferric citrate receptor (FecA) from *Escherichia coli* UT5600 and further characterization of its binding activity. *Biometals 6(1)*, 37-44.